PART I: APPLICATION OF Pd-PEPPSI COMPLEXES IN REGIOSELECTIVE CROSS-COUPLING AND NATURAL PRODUCT TOTAL SYNTHESIS

PART II: ROOM TEMPERATURE, ADDITIVE-FREE CARBON-SULFUR COUPLING USING NOVEL NHC-Pd COMPLEXES

JENNIFER LYN FARMER

A DISSERTATION SUBMITTED TO THE FACULTY OF GRADUATE STUDIES
IN PARTIAL FULFILMENT OF THE REQUIREMENTS
FOR THE DEGREE OF
DOCTOR OF PHILOSOPHY

GRADUATE PROGRAM IN CHEMISTRY
YORK UNIVERSITY
TORONTO, CANADA

DECEMBER, 2015

ABSTRACT

The first part of this research is focused on the development of an efficient method for the regioselective Suzuki-Miyaura cross-coupling of allylboronic acid pinacol ester derivatives with aryl and heteroaryl halides using *Pd-PEPPSI-IPent* (**P**yridine **E**nhanced **P**re-catalyst **P**reparation **S**tabilization and **I**nitiation) that would be selective for the linear product. *Pd-PEPPSI-IPent* showed high selectivity (>97%) at the α–carbon of the allylboron reagent to generate the desired linear isomer under mild reaction conditions (i.e., THF, 70 °C, 5M KOH). In the case of trisubstituted allylboronates with different substituents on the olefin, minor olefin geometry isomerization was observed (*E/Z* ≈ 80/20). Using this method, isoprenylated natural products methylated cathafuran A and lakoochin A were synthesized. Although the prenyl and geranyl side chains could be installed onto advanced 2-arylbenzofuran building blocks with high α–selectivity, significant amounts of an unwanted side product were observed.

A dramatic solvent effect on the selectivity for the Directed *ortho* Metalation (DoM) of 1,5-dichloro-2,4-dimethoxybenzene, a key building block in our synthetic strategy to cathafuran A and lakoochin A, was observed. A series of time-course and labelling studies has revealed that deprotonation occurs exclusively at C3 followed by isomerization of the anion to C6 in THF. In contrast, when DoM was performed in Et_2O, deprotonation again occurred selectively at C3, but now no isomerization occurs. Labeling studies also revealed that deuterium has an enormous kinetic isotope effect

(KIE) that suppresses not only the original DoM reaction at C3 when deuterium is present there, but also suppresses isomerization to C6 when the label is at that site.

The second part of this research focused on the development and application of new, easily activated NHC–Pd^{II} pre-catalysts featuring a *trans*-oriented morpholine ligand in carbon-sulfur cross-coupling chemistry. [(*IPent*)$PdCl_2$(morpholine)] was identified as the most active pre-catalyst, effectively coupling a variety of deactivated aryl halides with aryl, alkyl, and silyl thiols at ambient temperature. Mechanistic studies revealed that, in contrast to other common NHC–Pd^{II} pre-catalysts, these complexes are rapidly reduced to the active NHC–Pd^0 species in the presence of KO*t*Bu, thus avoiding the need for additives, external activators, or cumbersome pre-activation steps.

DEDICATION

This dissertation is dedicated to my late grandparents: Norma Farmer, Margaret and Henry Russell. Thank you for teaching me the value of hard work and that if you beilieve in yourself you can accomplish great things.

ACKNOWLEDGEMENTS

This thesis would not have been possible without the help and support of many people. First, I would like to express my deepest gratitude to my supervisor, Professor Michael G. Organ, for his continuous encouragement, advice, patience, and support throughout my graduate studies. I will never forget the lessons learned under his guidance, both professional and personal. I would also like to extend thanks to my research committee advisors: Prof. Arturo Orellana for teaching me the importance of designing experiments smartly and for his constructive criticism; and Prof. William Pietro for always encouraging me to think outside the box. In addition, I would like to thank my internal and external examiners, Prof. Barry Loughton and Prof. Kalman Szabó, respectively, for agreeing to examine this thesis. A special thanks to Dr. Howard Hunter, not only for his assistance with the NMR spectroscopy studies, but also for his willingness to share his immense knowledge of NMR spectroscopy.

Next, I would like to thank all past and present members of the Organ group. Each and every one of you made my experience as a graduate student an enjoyable one. Thank you for all your help, friendship and unforgettable memories both in and outside of the laboratory.

Finally, I would like to thank my friends and family for all their love and support throughout the years. Thank you mom, dad, sister, step parents, and the MacMillan's for all your encouragement and free meals! A special thanks to my partner, David, for enduring my unpredictable working hours, endless conversations about my research, and always believing in me even at times when I did not believe in myself.

TABLE OF CONTENTS

LIST OF TABLES

Part I: Application of Pd-PEPPSI Complexes in Regioselective Cross-Coupling and Natural Product Total Synthesis

Part II: Room Temperature, Additive-Free Carbon-Sulfur Coupling Using Novel NHC-Pd Complexes

LIST OF FIGURES

Part I: Application of Pd-PEPPSI Complexes in Regioselective Cross-Coupling and Natural Product Total Synthesis

Part II: Room Temperature, Additive-Free Carbon-Sulfur Coupling Using Novel NHC-Pd Complexes

LIST OF SCHEMES

Part I: Application of Pd-PEPPSI Complexes in Regioselective Cross-Coupling and Natural Product Total Synthesis

LIST OF ABBREVIATIONS

Ac	Acetyl
BINAP	2,2'-bis(diphenylphosphino)-1,1'-binaphthyl
Bn	benzyl
BHE	β-hydride elimination
BHY	Buchwald-Hartwig Yagupol'skii
BPPFA	1-[2,1'-bis(diphenylphosphino)ferrocenyl] ethylamine
BuLi	*n*-Butyl lithium
*t*Bu	tert-butyl
BrettPhos	2-(Dicyclohexylphosphino)3,6-dimethoxy-2′,4′,6′-triisopropyl-1,1′-biphenyl
*t*Bu	tert-butyl
Conv.	conversion
COSY	correlation spectroscopy
cPent	1,3-bis(2,6-dicyclopentylphenyl)imidazole-2-ylidine
Cy	cyclohexyl
CyOct	cyclooctyl
DavePhos	2-Dicyclohexylphosphino-2′-(N,N-dimethylamino)biphenyl
dba	dibenzylideneacetone
DCM	dichloromethane
DFT	density functional theory
DIE	deuterium isotope effect

DIOP	2,3-*O*-isopropylidene-2,3-dihydroxy-1,4-bis(diphenylphosphino)butane
DiPPF	bis(diisopropylphosphino)ferrocene
DME	dimethoxylethane
DMF	dimethylformamide
DMG	Directing Metalating Group
DMSO	dimethyl sulfoxide
DoM	Directed Ortho Metalation
DPEphos	2,2'-oxybis(2,1-phenylene)bis(diphenylphosphine)
dppb	1,4-bis(diphenylphosphino)butane
dppe	1,2-bis(diphenylphosphino)ethane
dppf	1,1'-bis(diphenylphosphino)ferrocene
dppm	bis(diphenylphosphino)methane
dppp	1,3-bis(diphenylphosphino)propane
D-*t*-BPF	1,1′-bis(di-*tert*-butylphosphino)ferrocene
Et	ethyl
EI	electron impact
equiv.	equivalent
ESI	electronspray impact
Et_2O	diethyl ether
EtOAc	ethyl acetate
GC/MS	Gas Chromatography/Mass Spectrometry
HMBC	heteronuclear multiple-bond correlation

HMPA	hexamethylphosphoramide
HPLC	High-performance liquid chromatography
HRMS	high-resolution mass-spectrometry
HSQC	heteronuclear single-quantum correlation
Hz	Hertz
IAd	1,3-diadamantylimidazol-2-ylidine
IBiox	Bisoxazolinium derived NHC
IBX	2-iodoxybenzoic acid
IC_{50}	half maximal inhibitory concentration
IEt	1,3-bis(2,6-diethylphenyl)imidazol-2-ylidine
IHept	1,3-bis(2,6-di(4-hepty)phenyl)imidazole-2-ylidine
$IHept^{Cl}$	1,3-bis(2,6-di(4-hepty)phenyl)-4,5-dichloroimidazol-2-ylidine
IMes	1,3-bis(2,4,6-trimethylphenyl)imidazol-2-ylidine
IPent	1,3-bis(2,6-di(3-pentyl)phenyl)imidazol-2-ylidine
$IPent^{Cl}$	1,3-bis(2,6-di(3-pentyl)phenyl)-4,5-dichloroimidazol-2-ylidine
IPr	1,3-bis(2,6-diisopropylphenyl)imidazole-2-ylidine
IPr^{*}	1,3-bis(2,6-bis(di-para-tolylmethyl)phenyl)imidazol-2-ylidine
IPr^{*OMe}	1,3-bis(2,6-bis(diphenylmethyl)-4-methoxyphenyl)imidazol-2-ylidene
IPr^{Cl}	1,3-bis(2,6-diisopropylphenyl)-4,5-dichloroimidazol-2-ylidine
IPr^{Me}	1,3-bis(2,6-diisopropylphenyl)-4,5-dimethylimidazol-2-ylidine
JosiPhos	(R)-1-[(S_P)-2-(Diphenylphosphino)ferrocenyl]ethyldicyclohexylphosphine
KIE	kinetic isotope effect

LAH	lithium aluminium hydride
LDA	lithium diisopropylamide
LG	leaving group
LiHMDS	lithium bis(trimethylsilyl)amide
MHE	Metal Halogen Exchange
Me	methyl
MOM	methoxymethyl ether
Mp	melting point
NHC	N-heterocyclic carbene
NMP	N-methyl-2-pyrrolidone
NMR	nuclear magnetic resonance
NOESY	nuclear overhauser effect spectroscopy
Nu	nucleophile
OA	oxidative addition
ox.	oxidation
PCC	Pyridinium chlorochromate
PDC	Pyridinium dichromate
PEPPSI	pyridine enhanced precatalyst preparation, stabilization and initiation
Ph	phenyl
PHOX	phosphinooxazoline
QPhos	1,2,3,4,5-Pentaphenyl-1′-(di-tert-butylphosphino)ferrocene
RE	reductive elimination

RDS	rate determining step
rt	room temperature
RuPhos	dicyclohexyl(2',6'-diisopropoxybiphenyl-2-yl)phosphine
S_E2	electrophilic aliphatic substitution
SIMes	1,3-bis(2,4,6-trimethylphenyl)imidazolidine-2-ylidine
SIPr	1,3-bis(2,6-diisopropylphenyl)imidazolidine-2-ylidine
SPhos	2-Dicyclohexylphosphino-2′,6′-dimethoxybiphenyl
TBAF	tetrabutylammonium fluoride
TBDPS	*tert*-butyldiphenylsilyl
TBS	*tert*-butyldimethylsilyl
TEP	Tolman's electronic parameter
THF	tetrahydrofuran
TIPS	triisopropylsilyl
TLC	thin-layer chromatography
TM	transmetallation
TMS	trimethylsilyl
TMEDA	tetramethylethylenediamine
TS	transition state
Xantphos	(9,9-dimethyl-9H-xanthene-4,5-diyl)bis(diphenylphosphine)
XPhos	2-Dicyclohexylphosphino-2′,4′,6′-triisopropylbiphenyl

PUBLICATIONS

Some portions of this work and other related research contributions appear in the following publications:

1) Farmer, J. L.; Froese, R. D. J.; Lee-Ruff, E.; Organ, M. G. *Chem. Eur. J.* **2015**, *21*, 1888-1893. Solvent Choice and Kinetic Isotope Effects (KIE) Dramatically Alter Regioselectivity in the Directed Ortho Metallation (DoM) of 1,5-Dichloro-2,4-dimethoxybenzene.

2) Farmer, J. L.; Pompeo, M.; Lough, A. J.; Organ, M. G. *Chem. Eur. J.* **2014**, *20*, 15790-15798. [(IPent)PdCl2(morpholine)]: a readily activated precatalyst for room-temperature, additive-free carbon-sulfur coupling.

3) Farmer, J. L.; Hunter, H. N.; Organ, M. G. *J. Am. Chem. Soc.* **2012**, *134*, 17470−17473. Regioselective Cross-Coupling of Allylboronic Acid Pinacol Ester Derivatives with Aryl Halides via Pd-PEPPSI-IPent.

PART I: APPLICATION OF Pd-PEPPSI COMPLEXES IN REGIOSELECTIVE CROSS-COUPLING AND NATURAL PRODUCT TOTAL SYNTHESIS

CHAPTER 1 – Introduction

1.1 The Importance of Isoprenylated Arenes

Aromatic compounds possessing one or more isoprenyl units, commonly referred to as isoprenylated arenes, are found in the structure of many natural products, several of which demonstrate significant biological and pharmacological activities (Figure 1).[1] In particular, isoprenylated phenols play an important role in facilitating many biological processes. For example, arnebinol (**1**), a prenylated phenol isolated from the root of *Arnebia euchroma*, displays important anti-inflammatory activity by inhibiting the biosynthesis of prostaglandins (IC_{50} 29.5 μm), which are implicated in the inflammation process.[2] 1,4-anthraquinones, such as kengaquinone 'B' (**2**), which is isolated from the stem bark of *Harungana madagas*, demonstrates α–glucosidase inhibitory activity (IC_{50} 6.3 μm).[3] Prenylated napthaquinones possess anti-bacterial, anti-viral, and anti-inflammatory activities.[4] For example, shikonin (**3**), which is the major chemical component extracted from Zicao (purple gromwell) the dried root of *Lithospermum erythrorhizon*, is commonly used in Chinese herbal medicine to treat inflammation of the kidney caused by autoimmune disease, systemic lupus erythematosus (also known as lupus).[5] In addition, isoprenylated phenols, can serve as valuable intermediates for the synthesis of other aromatic natural products, such as chromenes (**4**) and chromans (**5**) (Figure 1).

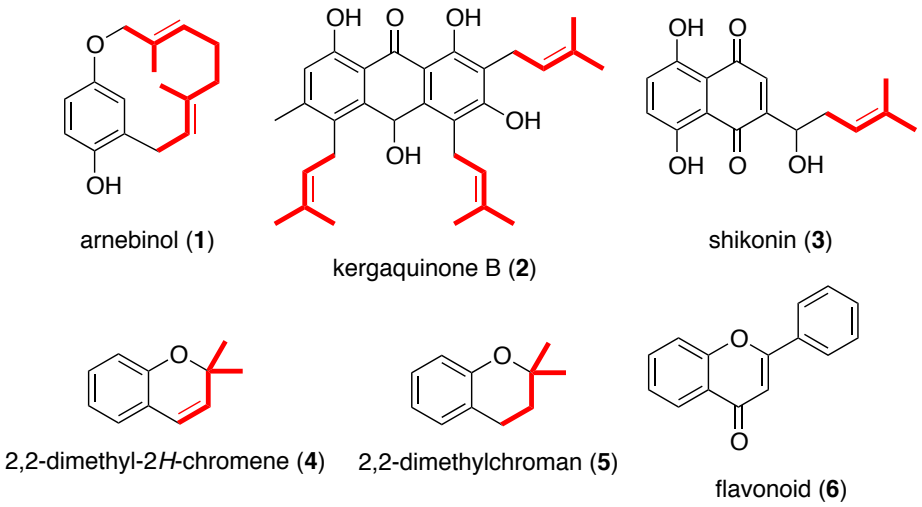

Figure 1: Structures of natural products containing prenyl side chains, natural products derived from prenylated arenes, and the core structure of flavonoids.

Prenylation of aromatic ring systems plays a vital role in the diversification of aromatic natural products. For example, ca. 1000 different prenylated flavonoids exist in plants as a result of prenylation at different positions on the flavonoid ring system, use of various lengths of prenyl side chains, and further modification of the prenyl moiety after prenylation (i.e., cyclization).[6] Studies have also shown that introducing prenyl and related 3,3–disubstituted allyl groups onto functionalized aromatic systems often increases the lipophilicity of the natural product, and as a result, enhances their bioactivity and bioavailability.[7] Traditionally, the pharmaceutical industry has been reluctant to synthesize molecules with structural complexity, especially those possessing stereodefined alkyl moieties, due to the challenges associated with their synthesis. As a result, medicinal chemists have focused much of their efforts on developing libraries of compounds comprised largely of achiral, flat molecules (e.g., biaryls). Unfortunately, many of these compounds show non-specific target binding, lower bioavailability, and

increased toxicity.[8] To address these difficulties, there is a growing interest among medicinal chemists to synthesize compounds with higher alkyl content that would enhance the three-dimensional topology and increase the structural complexity of their molecular libraries.[9]

In nature, prenylation of aromatic ring systems occurs by enzymatic reactions, which are mediated by substrate-specific prenyltransferases (PTases).[1b,6, 10] These enzymes catalyze the transfer of C5 (dimethyl allyl), C10 (geranyl), or C15 (farnesyl) prenyl groups derived from the corresponding isoprenyl diphosphate units onto electron-rich aromatic systems, producing the prenylated natural products (i.e., α– or γ–products) in a highly regioselective manner (Figure 2). Given the importance of isoprenylated arenes, a significant amount of research has gone into developing synthetic methods to facilitate the selective formation of these aryl-prenyl carbon–carbon (C–C) bonds (Figure 2). While various methods have been developed for the prenylation of aromatic rings, in general, the ability of synthetic chemists to develop methodologies that mimic the efficiency of nature's biosynthetic machinery to generate either the corresponding α– or γ–product in a highly regioselective manner remains a challenge. Here, a brief overview of traditional prenylation methods (i.e., transition metal free processes) of aromatic ring systems is first presented, followed the development of Pd-catalyzed prenylation reactions.

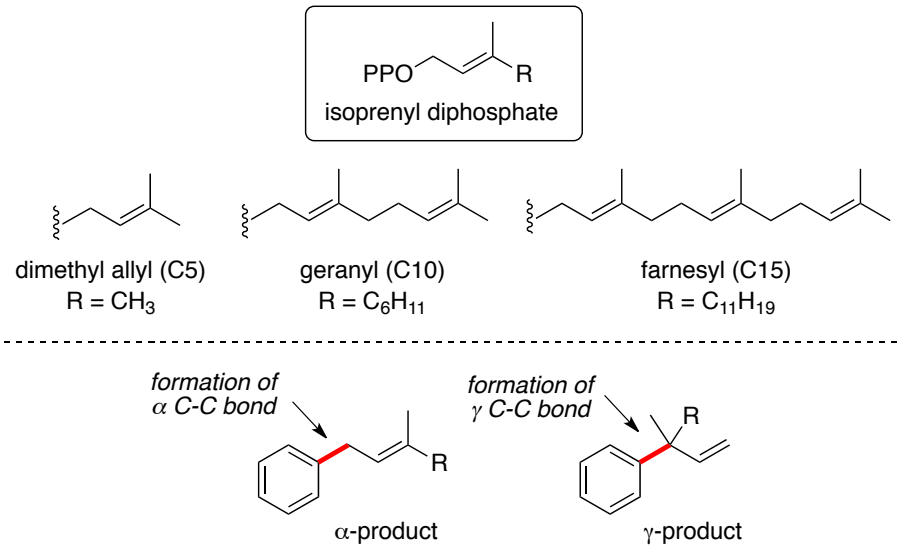

Figure 2: Structures of isoprenyl diphosphates (e.g., geranyl) chains and isoprenylated arenes containing α and γ C-C bonds.

1.2 Traditional Prenylation Methods

Direct prenylation of aromatic compounds can be achieved by electrophillic aromatic substitution. For example, the Friedel-Crafts-type prenylation of electron rich arenes has been used to synthesize various isoprenylated arenes.[11] In the presence of a Lewis acid catalyst, the prenyl electrophile, such as halide, alcohol, or acetate is converted to a prenyl cation, which reacts with the aromatic ring, forming a σ–complex. Subsequent regeneration of aromaticity via deprotonation, produces the prenylated product and regenerates the Lewis acid catalyst (Figure 3). As depicted in Figure 3, the reaction typically occurs at the least substituted carbon of the prenyl cation and the least hindered, most nucleophilic position on the aromatic ring.

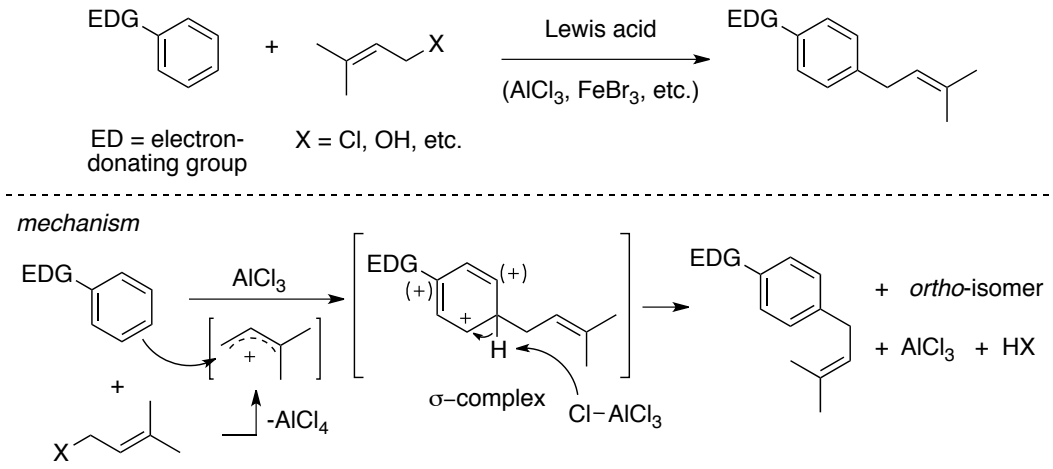

Figure 3: General mechanism for Friedel-Crafts-type prenylation.

As with all Friedel-Crafts alkylations, one major drawback of this reaction is over-prenylation. Since addition of a prenyl group further activates the aromatic ring, the prenylated products are more reactive than the reactants. As a result, the products are more likely to undergo further reaction with the prenyl cation compared to the reactants, leading to low yields of the mono-prenylated products. The problem of over-prenylation can be avoided by using a large excess of the aromatic compound. For example, Kodomari and coworkers demonstrated that using a 10:1 ratio of *para*–xylene to crotyl chloride in the presence of $ZnCl_2/SiO_2$ and K_2CO_3/Al_2O_3, significantly minimized over-allylation and the mono-prenylated compound was obtained as the major product in good yield (Scheme 1).[12] The supported $ZnCl_2/SiO_2$–K_2CO_3/Al_2O_3 complex was also found to help minimize the formation of compounds **7** and **8**, which are common by-products resulting from the addition of hydrogen chloride to the double bond of the product.

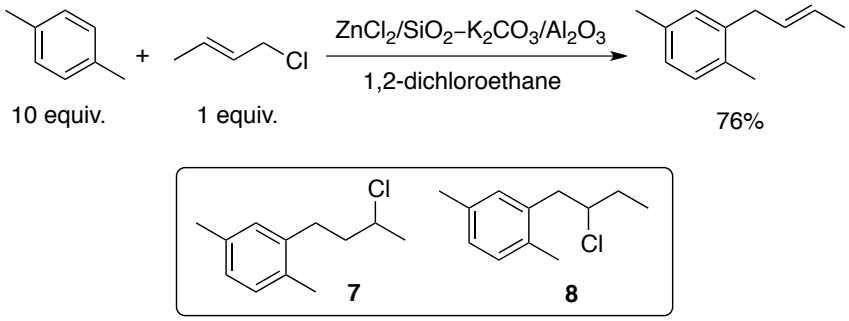

Scheme 1: Friedel-Crafts-type prenylation using weakly acid conditions.

While using a large excess of starting material helps minimize over-prenylation this strategy is unattractive, especially when starting materials are expensive or difficult to access. Controlling the regioselectivity of this transformation can also be problematic when one electron-donating group is present on an aromatic ring as both the *ortho*– and *para*–position are activated, leading to a mixture of products. While *para*-prenylation is generally observed as the major product, selective *ortho*–prenylation can be achieved by blocking the *para*–position on the aromatic ring as illustrated in Scheme 1.[12] To date, only a few Friedel-Crafts-type prenylation reactions have been reported in the total synthesis of isoprenylated natural products. In 2003, Koo and co-workers reported the total synthesis of coenzyme Q-10 (**12a**) and vitamin $K_{2(20)}$ (**12b**) using a Friedel-Crafts-type prenylation reaction as the key step for installing the isoprenyl group on protected dihydroquinone core **9** (Scheme 2).[13] Using the conditions outlined in Scheme 2, selective prenylation of dihydroquinone **9a**/**b** with C_5 allylic sulfone **10a**/**b** gave key intermediates **11a** and **11b** in 89% (*E/Z* ratio 10:1) and 72% (*E* only) yield, respectively.

Intermediates **11a** and **11b** were then carried on to synthesize compounds **12a** and **12b** in **42%** and **62%** overall yield, respectively, over 3 steps.

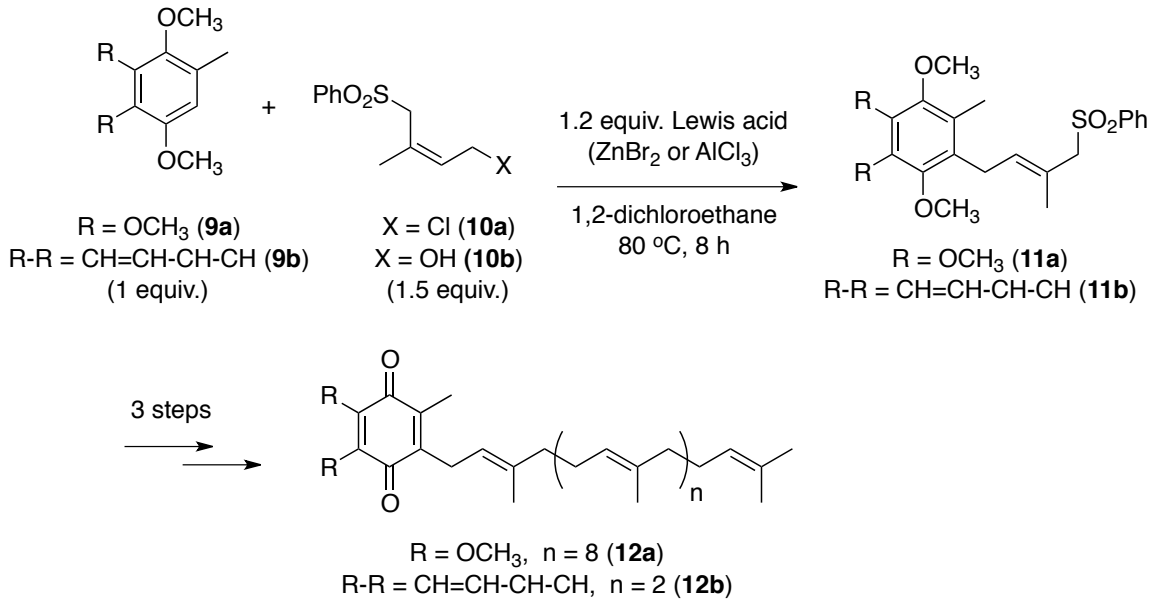

Scheme 2: Synthesis of coenzyme Q-10 (**12a**) and vitamin $K_{2(20)}$ (**12b**) via Friedel-Crafts-type prenylation of **9a** and **9b**.

Directed *ortho*-metalation (DoM) is another powerful method for accessing substituted aromatic systems in a highly regioselective manner that are otherwise difficult to prepare by electrophilic substitution reactions.[14] The DoM prenylation strategy works well for synthesizing *ortho*-prenylated phenols (Scheme 3, path a). Both symmetric and asymmetric phenol derivatives containing two or fewer oxygen substituents work well with this protocol, however aromatics containing more than two oxygen substituents can be a challenge as they are more difficult to deprotonate. Often a proton transfer can take place from the neighbouring protecting group (i.e., OBn or OMOM), quenching the newly formed aryl anion.[15] The regioselectivity of the metalation reaction is controlled by

the directing ability of the phenol protecting group, also referred to as the directing metalating group (DMG). For an in depth review of DoM see Chapter 4, Section 1.4.

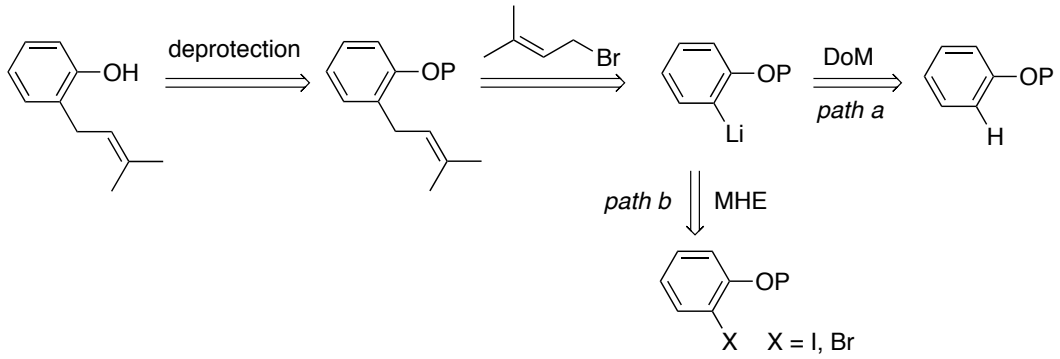

Scheme 3: General retro-synthetic approach using DoM (*path a*) and MHE (*path b*) strategies for the prenylation of phenols.

In 2005, Neighbors and co-workers used the DoM alkylation protocol to access key building block **17** in the total synthesis of pawhuskin C (**16**) (Scheme 4), an opioid receptor modulator isolated from *Dalea purpurea*, a flowering plant found in central North America.[16] Deprotonation of **13** was carried out at −20 °C with *sec*-butyllithium (*sec*-BuLi) in the presence of tetramethylethylenediamine (TMEDA) and subsequent addition of geranyl bromide **14** to the aryl lithium afforded **15** in 73% yield.

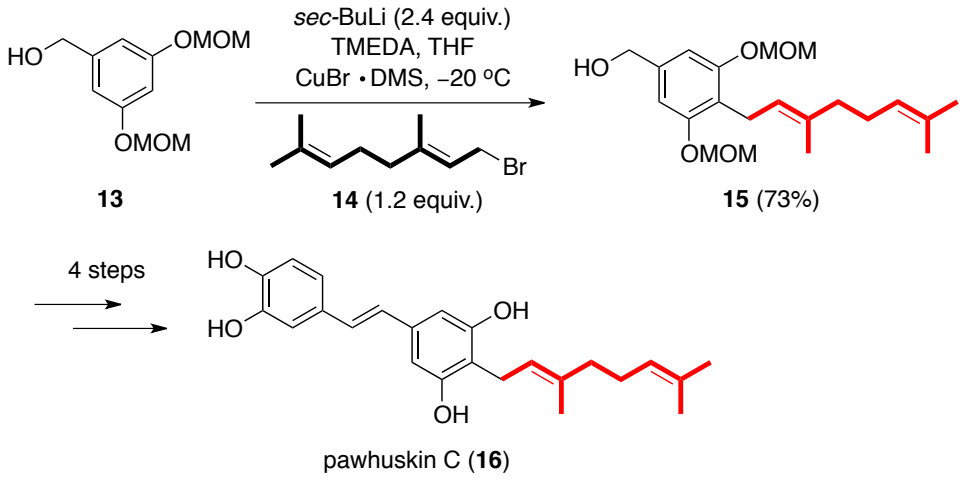

Scheme 4: Synthesis of pawhuskin C (**16**) using the DoM prenylation strategy.

Metal Halogen Exchange (MHE) has also proven to be a useful transformation for accessing isoprenylated arenes (Scheme 3, path b). Here, the halogen atom on the aromatic ring and not the DMG dictates the regioselectivity of the metalation step. Thus, isoprenylated arenes other than *ortho*–prenylated arenes may be generated. In 2006, Neighbors and co-workers demonstrated the use of the MHE prenylation strategy in the total synthesis of schweinfurthin B analog **19** (Scheme 5).[17] These compounds belong to a small set of natural stilbenes isolated in the late 1990s from the African tree *Macaranga schweinfurthii*.[18] Lithium-halogen exchange of aryl bromide **17** at –78 °C in THF, followed by the addition of **14** to the resulting aryl lithium affords geranylated intermediate **18** in 70% yield. The resulting geranylated arene **18** was then carried on to synthesize schweinfurthin B analog **19** in 41% yield over 4 steps.

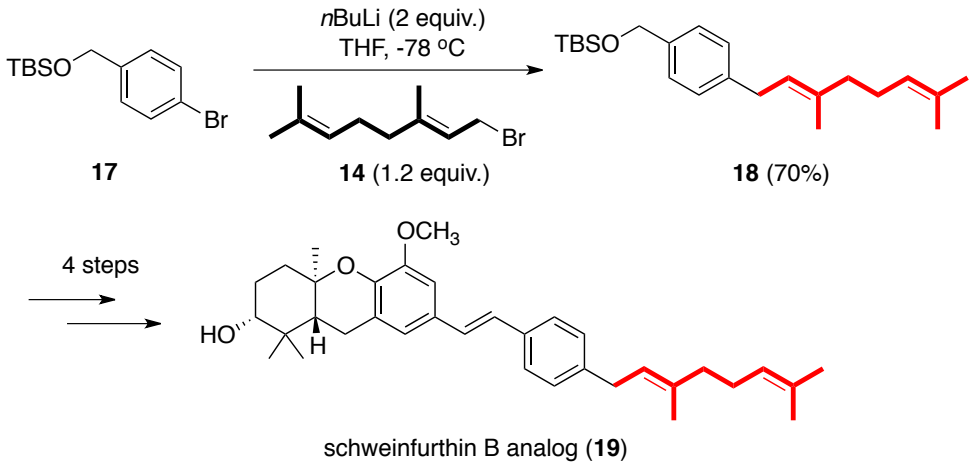

Scheme 5: Synthesis of schweinfurthin B analog (**19**) using the MHE prenylation strategy.

While both DoM and MHE have proven to be useful synthetic strategies for introducing prenyl side chains onto aromatic compounds there are some limitations. The highly basic and nucleophilic character of organolithium reagents significantly limits the substrate scope of this methodology. Typically, phenols must be protected prior to the metalation step and then deprotected after the installation of the prenyl side chain, adding to the overall step count. Further, the desymmetrization of multi-hydroxy aromatics is not a trivial process and if not readily accessible, substantial amounts of material can be lost during the production of these protected phenols. Lastly, majority of reports using DoM and MHE methodologies to generated prenylated arenes have only been demonstrated on specific systems, thus lacking general substrate scope applicability. Recently, prenylation using transition metal-catalyzed cross-coupling methodology has been able to address some of these limitations.

1.3 Palladium-Catalyzed Allylation Reactions

Transition metal-catalyzed cross-coupling reactions have emerged as a more mild and general protocol for selective C–C bond formation. Since Kharash[19] discovered that small quantities of transition metal salts could catalyze the formation of C–C bonds between Grignard reagents and organic halides in 1941, numerous cross-coupling methodologies have been developed with a variety of transition metals, ancillary ligands, and organometallic reagents.[20] Of the transition metals explored, palladium has proven to be the most versatile and robust, coupling a wide variety of substrates with high functional-group tolerance under the mildest conditions. The value of Pd-catalyzed cross-coupling reactions in organic synthesis was recognized in 2010, with the Nobel Prize in Chemistry awarded to Ei-ichi Negishi, Richard Heck, and Akira Suzuki for their pionerering work in this area.

The general mechanism of a cross-coupling reaction typically features at least three elementary steps: oxidative addition (OA), transmetallation (TM), and reductive elimination (RE).[21] With respect to Pd-catalyzed allylic substitution reactions, two different mechansims can operate depending on the electronic nature of the allylic substrate.

1.3.1 Prenyl Electrophiles

When the allylic substrate is the electrophile the reaction is referred to as an allylic substitution and proceeds through the mechanism outlined in Figure 4.[22] The catalytic cycle begins with a coordination event between a zerovalent Pd-catalyst and the

double bond of an allylic halide or pseudo-halide, forming (η^2-allyl)Pd^0 complex (**20**) which then undergoes OA, expelling the leaving group and forming (η^3–allyl)-palladium (II) complex (**21**). This process is also referred to as ionization and occurs with inversion of configuration (Figure 5). The next step in the catalytic cycle can proceed by two different pathways (*path a* or *b*) depending on the type of nucleophile.

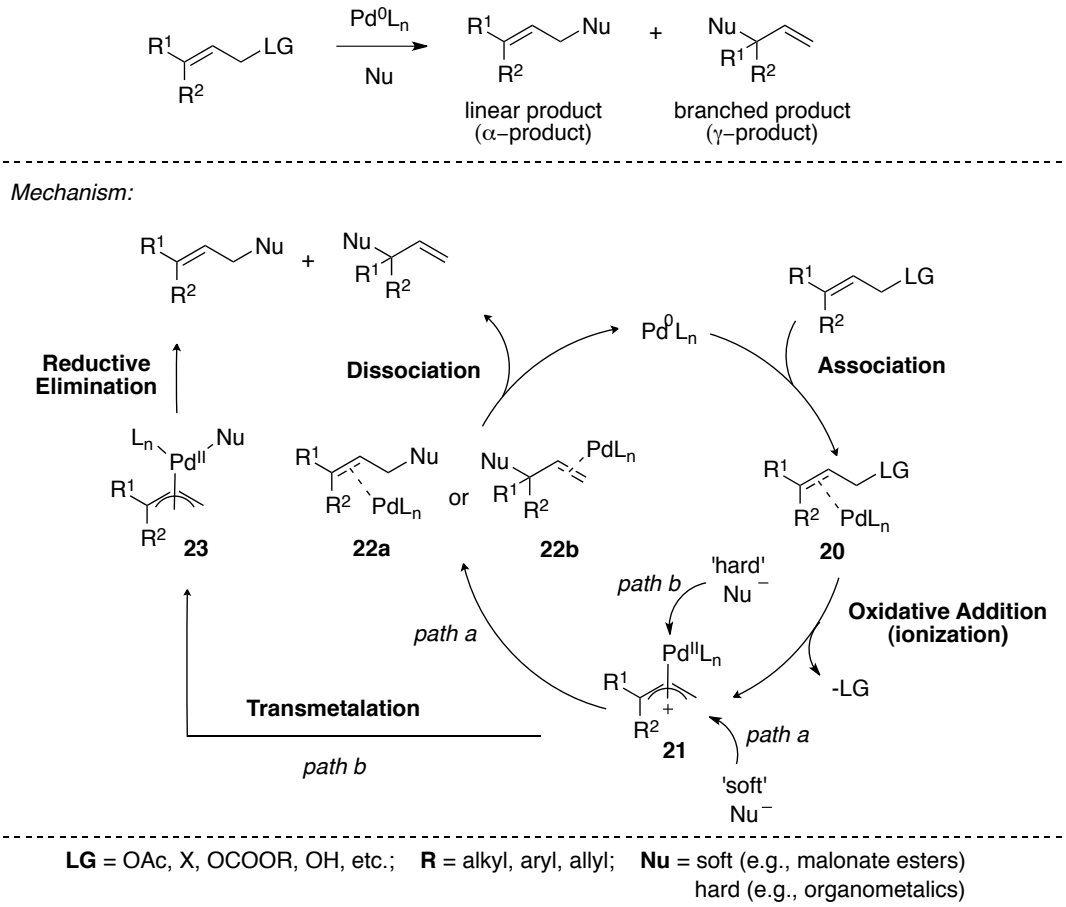

Figure 4: Proposed catalytic cycle for Pd-catalyzed allylic substitution reactions using 3,3-disubstituted allyl electrophiles.

'Soft' carbon nucleophiles, defined as those derived from conjugate acids with a pka < 25 (e.g., malonate-type nucleophiles), generally react directly with the carbon of the allyl

group, forming intermediates **22a** or **22b**, depending on where the nucleophile attacks. Subsequent dissociation from the double bond yields the prenylated product and regenerates the active catalyst. The reaction with 'soft' nucleophiles occurs with an overall retention of configuration since nucleophilic attack also proceeds with inversion (Figure 5). Conversely, 'hard' carbon nucleophiles, derived from conjugate acids with a pka > 25 (e.g., organometallic reagents), tend to react first with the metal centre via transmetallation, followed by reductive elimination (RE) to yield the desired prenylated products. Reactions with 'hard' nucleophiles retain the stereochemistry of the (η^3–allyl)-Pd^{II} complex (**23**), resulting in net inversion of configuration (Figure 5).

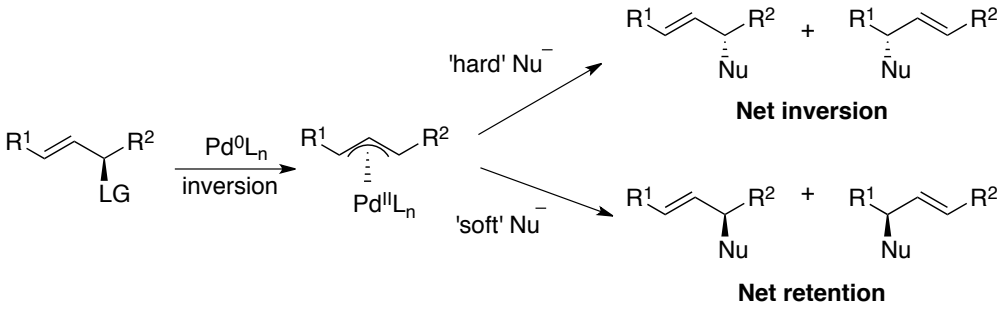

Figure 5: The stereochemical outcome with 'soft' and 'hard' nucleophiles.

Since its introduction nearly 50 years ago,[23] Pd-catalyzed allylic substitution reactions have been extensively studied and the regiochemical outcome has been shown to depend on several factors, including the leaving group, the alkene substitution pattern (e.g., symmetrical vs unsymmetrical), ancillary ligand, and nucleophile (hard vs soft). The most commonly employed electrophiles for this transformation are allylic acetates, however a number of other leaving groups, such as alcohols, halides, and carbamates can serve as electrophiles.[24] Mono- and disubstituted allylic substrates usually undergo

substitution with both 'soft' and 'hard' nucleophiles at the least hindered allylic terminus (i.e., α–position) to give the linear product (Figure 4).[25] However, substitution at the more hindered allylic terminus (i.e., γ–position), which generates the branched product, has attracted more interests since, not only is a new C–C bond formed, but also a new stereogenic centre when $R^1 \neq R^2$.

Since Pd-catalyzed allylic substitution reactions proceed via a (η^3–allyl)-Pd^{II} complex, isomerization of the allylic substrate is often observed, resulting in the formation of stereoisomers of the final product. This occurs through a process known as η^3–η^1–η^3 isomerization or *syn–anti* isomerization.[26] The palladium can be coordinated to the allyl substrate at all three allylic carbons (i.e., (η^3–allyl)-Pd^{II}) or to one allylic carbon (i.e., (η^1–allyl)-Pd^{II}) (Scheme 6). Substituents on allylic substrates are named according to their position relative to the C2 carbon substituent. Thus, substituents *syn* to the C2 hydrogen shown in Scheme 6 are labelled as *syn* and substituents *anti* to the C2 hydrogen are labeled as *anti*. It is important to note that these π-allyl Pd^{II} complexes are often in a state of dynamic equilibrium and on the time scale of the catalytic cycle, the *syn/anti* substituents can exchange positions much more rapidly than alkylation of the allylic substrate.[25] Thus, controlling both the regio- and stereochemical outcome of these reactions remains a challenge.

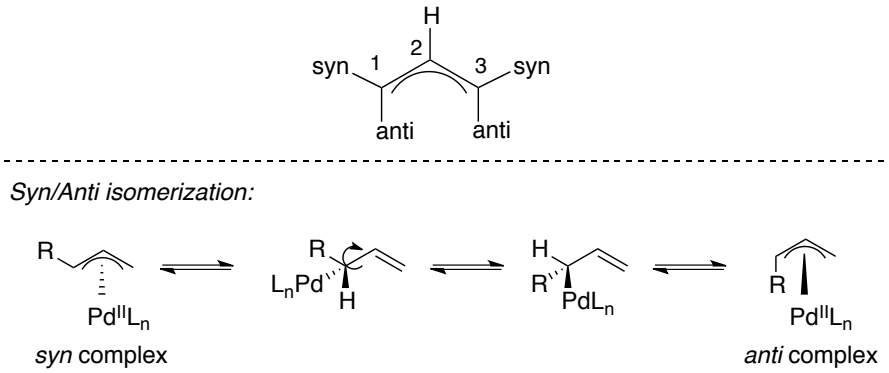

Scheme 6: Nomenclature of allyl ligands and the *syn–anti* isomerization pathway for η^3-allyl Pd^{II} complexes.

Similar to other Pd-catalyzed cross coupling reactions, much effort has focused on ligand design to improve the regio- and stereoselectivity of Pd-catalyzed allylations.[23,27] Ancillary ligands on the Pd-centre impart important electronic and steric properties that help facilitate cross-coupling reactions (see Section 1.4). To date, phosphine ligands have been the most widely used ancillary ligands not only in this transformation but in Pd-catalyzed cross-couplings generally. Since the discovery by Trost [28] that triphenylphosphine (PPh_3) could significantly improve the reactivity of an allylpalladium chloride dimer in the alkylation of diethyl malonate, numerous phosphine ligands have been developed and investigated. Bulky mono- and bidentate phosphine ligands typically yield the linear product due to steric interactions between the ligand and the nucleophile as well as the ligand and the allyl substrate. It is important to note that steric interactions between the nucleophile and ligand will vary depending on the type of nucleophile. Whereas soft nucleophiles directly attack the allylic terminus of complex **21**, hard nucleophiles attack the Pd-centre first resulting in a direct interaction with the ligands in the metal coordination sphere. This information becomes more relevant when designing

chiral phosphine ligands since interactions between the incoming nucleophile, chiral ligand, and allyl moiety will vary during the C-C bond forming event depending on the nature of the substrates employed.[27c,29] In recent decades, numerous chiral ligands have been developed for enantioselective Pd-catalyzed allylic substitution reactions, with some selected examples shown in Figure 6. Ligands can be categorized based on their chiral topology. For example, the (*R*)-BINAP,[30] Trost,[29,31] and (*S,S*)-DIOP[31] ligand are C_2-symmetric ligands, whereas ferrocene based ligands, such as (*R,S*)-BPPFA[32] possess planar chirality. Phosphinooxazoline ligands, such as (*S*)-PHOX[33] are classified as non-symmetrical chiral ligands and induce chirality through the substituent located on the oxazoline ring. Unfortunately, no one ligand has been developed that facilitates excellent enantioselectivity across a broad range of substrates.

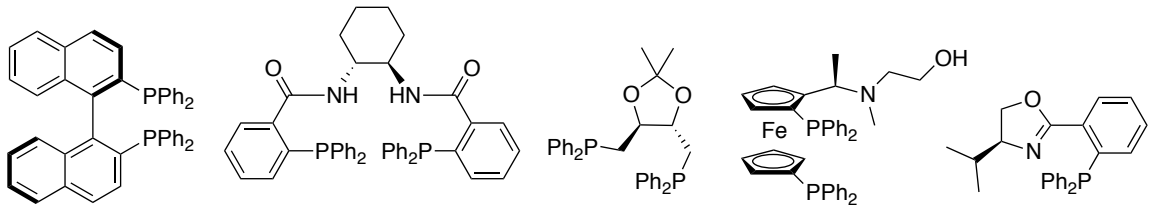

Figure 6: Examples of chiral ligands used in Pd-catalyzed allylic substitution reactions.

Pd-catalyzed allylic arylation reactions typically employ organometallic reagents as the 'hard' nucleophiles, such as organometallic reagents, and have been less developed with 'soft' nucleophiles. The choice of the transmetalating reagent is important and can affect various aspects of the reaction, such as chemoselectivity and rate of transmetallation.[20] While organomagnesium (Grignard) reagents are easy to prepare, are highly nucleophilic, and have shown success in Pd-catalyzed allylic arylations[34] they

suffer from poor chemoselectivity and have low functional group tolerance. Less reactive organometallic reagents, such as organozinc (Zn),[35] organostannane (Sn),[36] and organoboron (B)[37] have proven to be useful alternatives to Grignard reagents in this reaction as they offer better chemoselectivity, greater functional group compatibility, and enhanced stability.[35] Unfortunately, organometallic reagents of more electronegative metals are typically more reluctant to engage in transmetallation, which can have a negative impact on both the regio- and stereoselectivity. For example, boron and carbon have similar electronegativities (B = 2.04 and C = 2.55), which makes the C–B bond relatively non-polar, rendering the transmetalating agent (i.e., the organoborane) a poor nucleophile. This allows sufficient time for η^3–η^1–η^3 isomerization to occur and when the allyl substrate is unsymmetrical (i.e., $R^1 \neq R^2$) scrambling of the olefin geometry can be observed (Scheme 7).

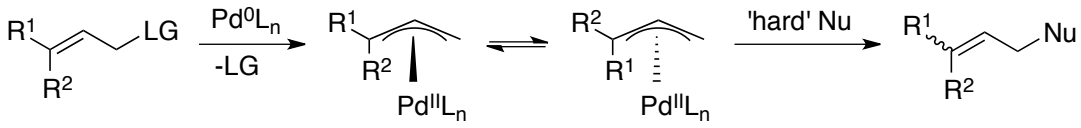

Scheme 7: Isomerization of the olefin geometry for unsymmetrical allyl substrates.

Although Pd-catalyzed allylations using allylic electrophiles is a viable method when coupling a variety of prenyl or 3,3–disubstituted allyl electrophiles with a limited set of aryl nucleophiles, it becomes less practical when a library of prenylated arenes containing the same 3,3–disubstituted allyl substrate with different aryl rings is required. Thus, another approach to prenylated arenes via Pd-catalyzed allylations would be to

switch the electrophile to an aryl halide or pseudohalide, as these are more readily available, and the nucleophile to a prenyl or 3,3−disubstituted allyl substrate.

1.3.2 Prenyl Nucleophiles

The mechanism for Pd-catalyzed cross-coupling of 3,3−disubstituted allyl nucleophiles with aryl halides is shown in Figure 7. When Pd(II) complexes are used, the first step is reduction to the catalytically active Pd(0) species, a process commonly referred to as "catalyst activation." This is typically achieved by double transmetallation of the nucleophile followed by reductive elimination. The next step is oxidative addition (OA) of Pd(0) to the aryl halide or pseudohalide, producing intermediate **24**. The order of reactivity of the halide leaving group decreases in the following order I > OTf > Br > CI and can be correlated with R-X bond dissociation energies.[38] Although organochlorides are much less reactive than their bromide or iodide analogues, their low cost, stability, and ready accessibility make them more attractive and thus, much research has gone into improving their reactivity.[21] The next step in the catalytic cycle is transmetallation. Here, intermediate **24** undergoes metal/metal exchange with 3,3−disubstituted allyl **25**, generating an inorganic salt by-product in the process. Depending on the nature of the transmetalating agent used, several cross-coupling protocols have been developed and the names of these reactions are directly linked to the chemists that either discovered them or developed their use: the Kumada-Tamao-Corriu reaction (Mg), the Negishi reaction (Zn), the Suzuki-Miyaura reaction (B), the Hiyama reaction (Si), the Stille-Migita reaction (Sn).[20]

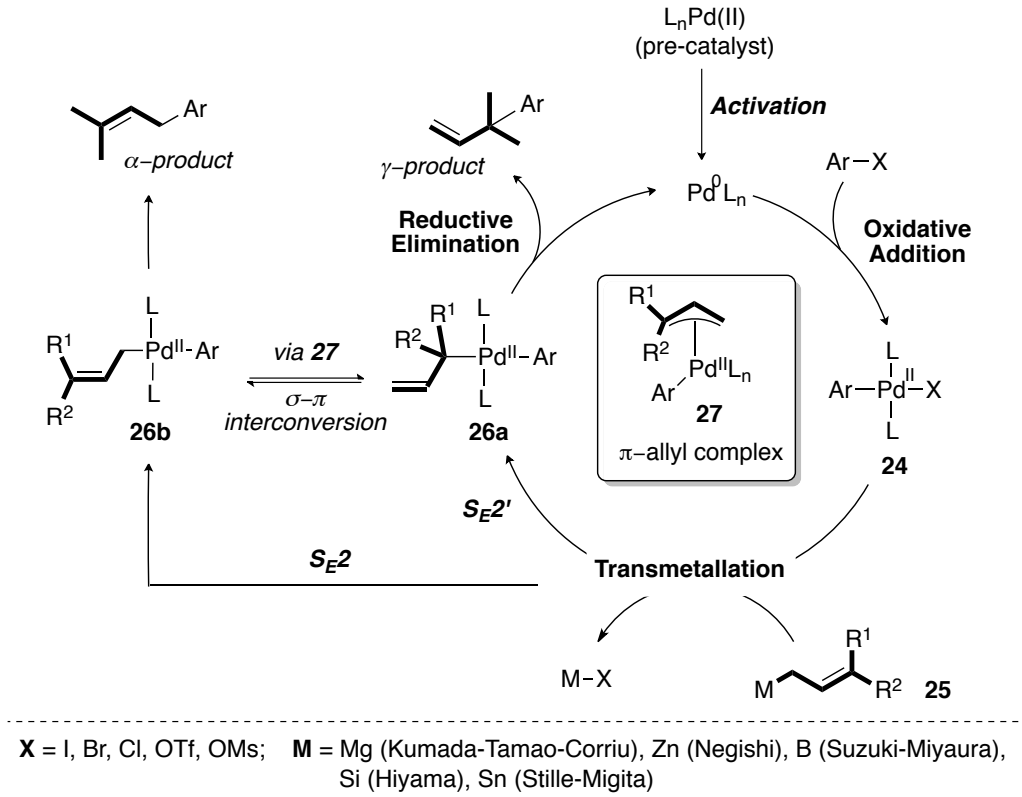

Figure 7: Proposed Pd-catalytic cross-coupling of 3,3-disubstituted ally metals.

The mechanism of transmetallation can be composed of a single elementary step, as is the case when pre-formed organometallic reagents are used (e.g., organozincs) or may be composed of two or more elementary reactions and require the presence of a base additive, as is the case when organoboron reagents are used in Suzuki-Miyaura cross-coupling.[24] The last step in the catalytic cycle is reductive elimination (RE), where the desired prenylated arene is released from the cycle and the active Pd(0) catalyst is regenerated.

While Pd-catalyzed cross-coupling of 3,3-disubstituted allyl metals has proven to be one of the most powerful methods for introducing prenyl and related allyl side chains

onto functionalized aromatic ring systems, achieving adequate regiocontrol has been challenging. The main difficulty in this transformation lies in controlling the regioselectivity that the allyl organometallic fragment couples during TM as two different pathways are possible (S_E2 or S_E2'). Another challenge is the rate of RE. If RE is slow, the linear (σ–allyl)Pd complex (**26b**) could isomerize to the corresponding branched (σ–allyl)Pd complex (**26a**), or the reverse depending on the mechanism of TM, via (η^3–π–allyl)Pd complex **27**, leading to the formation of undesired regioisomers (i.e., γ–product or α–product) (Figure 7, *vide supra*).[27] The ancillary ligand as well as the type of the organometallic reagent employed impacts this selectivity.[39,40,41,42,43,44]

Unsymmetrical allyl zinc and magnesium reagents (Figure 8, $R^1 \neq R^2$) are known to interconvert rapidly between the α– and γ–allyl metal in solution, forming constitutional isomers that can both undergo TM.[45] To date, prenylation of aryl halides with prenyl-type zinc or Gignard reagents remains rare.[46] Organometallic reagents with less electronegative metals, such as Sn, Si, and B do not undergo this interconversion process given the stronger C-M bond and as a result, have been more frequently employed in this cross-coupling reaction. While organostannane reagents are reported to proceed through an undergo S_E2 mechanism with high α–selectivity,[40] organosilanes and organoboranes are believed to transmetalate by an S_E2' process, resulting in γ–regioselectivity.[39,41a-c]

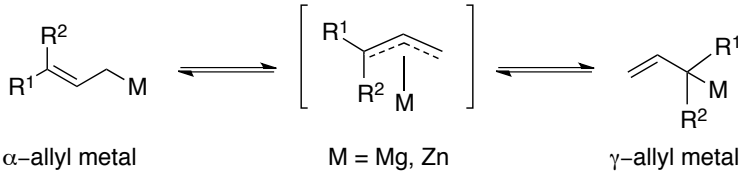

Figure 8: Simplified representation of the isomerization pathway for 3,3-disubstituted allyl zincs and Grignard reagents.

The strategy for imparting better regiocontrol in this reaction has largely focused on the development of improved ancillary ligands. To date, sterically hindered mono- and bidentate phosphine ligands have been the most widely employed ancillary ligands in Pd-catalyzed cross-coupling of 3,3-disubstituted allyl metals. Bulky phosphine ligands have been shown to facilitate rapid RE, resulting in improved regioselectivities for either isomer. Hiyama and co-workers were the first to realize the influence of bulky phosphines in Pd-catalyzed cross-coupling of allyltrifluorosilanes with organic halides or triflates.[39] They reported that γ-selectivity occurred when PPh_3 or bisphosphine ligands with large bite angles, such as dppb were employed, whereas bisphosphine ligands with small bite angles, such as dppp, gave mostly the α-product (Figure 9). Mechanistic studies revealed that TM occurrs exclusively at the γ–carbon of the anionic allylsilicate, forming (σ–allyl)Pd complexes, such as **26a**, leading the authors to conclude that bulky phosphine ligands facilitate rapid RE to give the observed γ–selectivity. Conversely, less bulky ligands suffer from slow RE, allowing isomerization to the less sterically crowded (σ–allyl)Pd complex, such as **26b**, which gives the α–coupled product. A similar trend was also observed by Tsuji in Stille coupling of aryl halides and $Me_3SiCH{=}CHCH_2SnBu_3$.[40c] Unfortunately, the efficiency and generality of both these

reactions are unsatisfactory as they require harsh conditions, such as temperatures well in excess of 100°C for Hiyama coupling, the use of toxic organometallic reagents (e.g. Sn), and have limited substrate scope with respect to the aryl oxidative addition partner. Despite the many advantages of organoboron reagents, including air and moisture stability and low toxicity, few studies have yielded reliably high regioselectivity with allylic derivatives. While Miyaura[41a-c] and Szabó[41f] have developed conditions for high selectivity for the branched product (i.e., the γ-isomer) with allyltrifluoroborates and allylboronic acids, respectively, (Figure 9), very few catalyst systems have been developed that are broadly selective for the linear product (i.e., the α-isomer). This is unfortunate since many natural products and compounds of medicinal interest contain prenyl and geranyl side chains attached at the α-carbon.

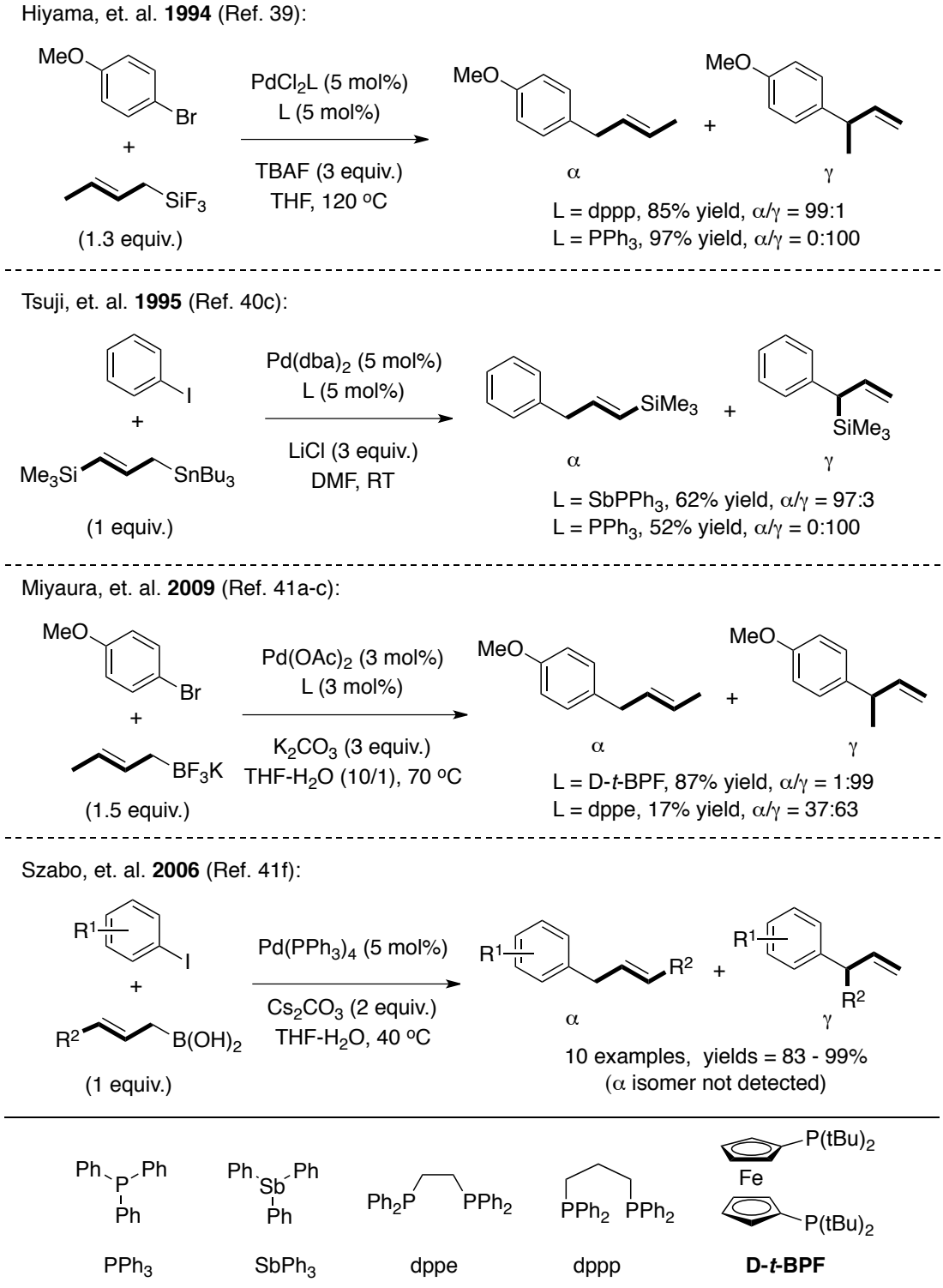

Figure 9: Selected examples demonstrating the effects of bulky phosphine ligands in the Pd-catalyzed cross-coupling of unsymmetrical allyl metals.

1.4 Ancillary Ligands

Ancillary ligands are important in Pd-catalyzed cross-coupling as they are responsible for transmitting key steric and electronic properties to the metal centre that are essential for enabling catalysis. It is now well accepted that OA into the C-X bond is enhanced by an electron-rich Pd-centre whereas RE is promoted by an electron-deficient and sterically crowded Pd-centre. In addition, ligands capable of strongly coordinating to the metal will also lead to a more stable complex in solution during the reaction. Consequently, ligand design has focussed on developing ligand systems that contain a balance between steric bulk and favourable electronic properties essential for each elementary step in the catalytic cycle. To date, the two most studied ancillary ligands for Pd-catalysis are phosphine and N-heterocyclic carbene (NHC) ligands.

1.4.1 Phosphine Ligands

Phosphine ligands are an important class of ligands whose steric and electronic properties can be altered in a systematic and predictable way by changing the substituents attached to phosphorus. In 1970, Tolman developed a reliable method for measuring both the steric property and electron-donating ability of various phosphine ligands.[47,48] The Tolman cone angle (θ) is the steric parameter used to quantify the steric topography of monodentate tertiary phosphine ligands around the metal centre. It is obtained by measuring the angle of a cone that has the metal at its apex with a metal-phosphorous (M-P) distance of 2.28 Å and extends to the van der Waals radii of the outermost ligand atoms. The steric topography of bidentate phosphine ligands is quantified using bite

angles, which describe the preferred chelation angle (P-M-P bond angle) of the bidentate phosphine ligand backbone to the metal centre (Figure 10).[49]

(a)

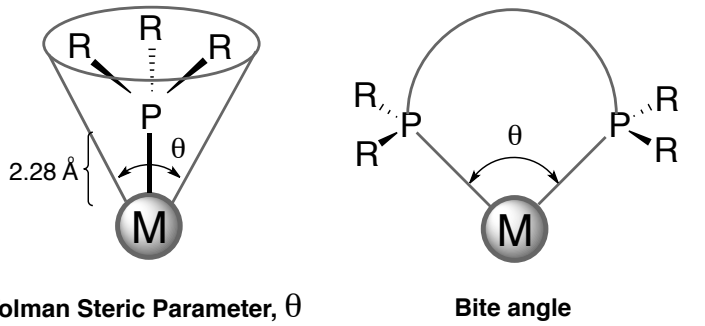

Tolman Steric Parameter, θ **Bite angle**

(b)

Ligand	Cone and bite angle (θ)
$P(OMe)_3$	107
PMe_3	118
PEt_3	132
PPh_3	145
$P(tBu)_3$	182
dppp	91
dppf	99

Figure 10: (a) Simplified schematic of the cone and bite angle for mono- and bidentate phosphine ligands; and (b) Cone and bite angles for selected phosphine ligands.

As seen in Figure 10, increasing the size of the substituent on phosphorus (R=Ph vs R=Et) increases the Tolman cone angle. As the Tolman cone angle increases so does the steric influence of the ligand on the metal centre and this increase has been shown to have a positive affect on catalyst activity. For example, Negishi and coworkers demonstrated that $Pd(PR_3)_2X_2$ complexes containing bulky phosphine ligands (i.e., PPh_3) undergo faster RE than those containing less bulky ligands (i.e., PEt_3).[50] Since alkyl phosphines are more Lewis basic than aryl phosphines, this result also suggests that an electronic effect could be at play.

The electronic properties of phosphine ligands can be assessed independently of the steric parameter using the Tolman electronic parameter (TEP). This is done by measuring the A1 stretching frequency (ν) of the carbonyl ligands in $Ni(CO)_3L$ ($L = PR_3$) complexes. When ligated to a metal centre, phosphine ligands can act as both σ–donors and π–acceptors, depending on the substituents attached to phosphorus. Electron-rich

phosphine ligands, such as alkyl phosphines, are strong σ–donors, dontating electron density to the metal through the σ orbital whereas electron-deficient phosphine ligands, such as $P(OR)_3$ act as both σ–donors and π–acceptors, accepting electron density from the metal into the σ^* orbital of the $P(OR)_3$ (Figure 11). Both of these interactions effect the ν(CO) stretching frequency in the $Ni(CO)_3L$ complex as illustrated in Figure 11.

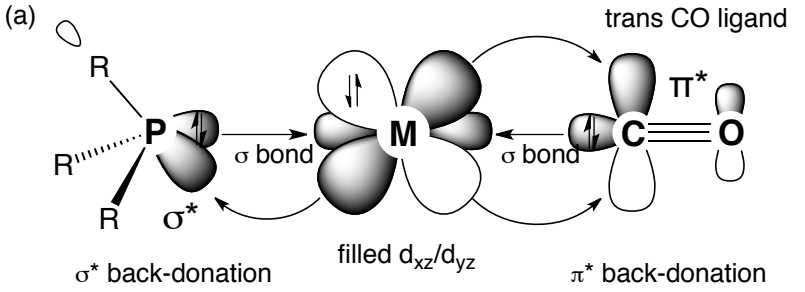

(b)

Ligand	υ(CO) cm^{-1}
$P(tBu)_3$	2056.1
PMe_3	2064.1
PPh_3	2068.9
$P(OEt)_3$	2076.3
PF_3	2110.8

Figure 11: (a) Schematic of phosphine-metal-CO bonding highlighting σ-donation, σ^* back-donation and π^* back donation; and (b) selected ν(CO) stretching frequencies for $[Ni(CO)_3L]$ complexes.[48,51]

Strong σ–donor ligands increase the electron density on Ni, resulting in π–back-donation from the metal to the carbonyl ligand anti-bonding orbital (π^*), which in turn lowers the ν(CO) stretching frequency. As a result, the M-L bond becomes stronger and the C-O triple bond becomes weaker. Conversly, strong π–acceptors lead to higher ν(CO) stretching frequencies since the phosphine ligand is able to accept electron density from the metal into its σ^* orbital.[48,52]

Using these steric and electronic parameters, numerous mono- and bidentate phosphine ligands have been developed for Pd-catalyzed cross-coupling (Figure 12). Historically, ligand modification focused on optimizing the three identical substituents on phosphorus (e.g., triphenylphosphine (PPh_3) or tricyclohexylphosphine (PCy_3)). For

years, PPh_3 was considered the ligand of choice due to its low cost, ease in preparation, and versatility. However, bidentate ligands, such as dppf started to gain popularity once they were shown to supress β–hydride elimination in the coupling of alkyl substrates.[53] Bidentate phosphine ligands with wide bite angles have also been shown to facilitate fast RE,[54] presumably by binding to the metal in a *cis* configuration, forcing the remaining two ligands to adopt a *cis* orientation which is the correct orientation for RE.[55,56] Trialkyl phosphines received little attention until the mid 1990s, when Fu and co-workers demonstrated that P(*t*-Bu)$_3$ could be used in the Suzuki-Miyaura cross-coupling of aryl chlorides (Ar-Cl).[57] The strong electron-donating ability of the alkyl groups was found to help facilitate OA of the Pd(0) species into the Ar-Cl bond while the large cone angle enhanced the rate of RE. More recently, considerable effort has been spent in the preparation of more architecturally complex phosphine ligands, including mixed alkyl/aryl phosphines such as Buchwald's dialkyl biaryl phosphines (e.g., XPhos).[58]

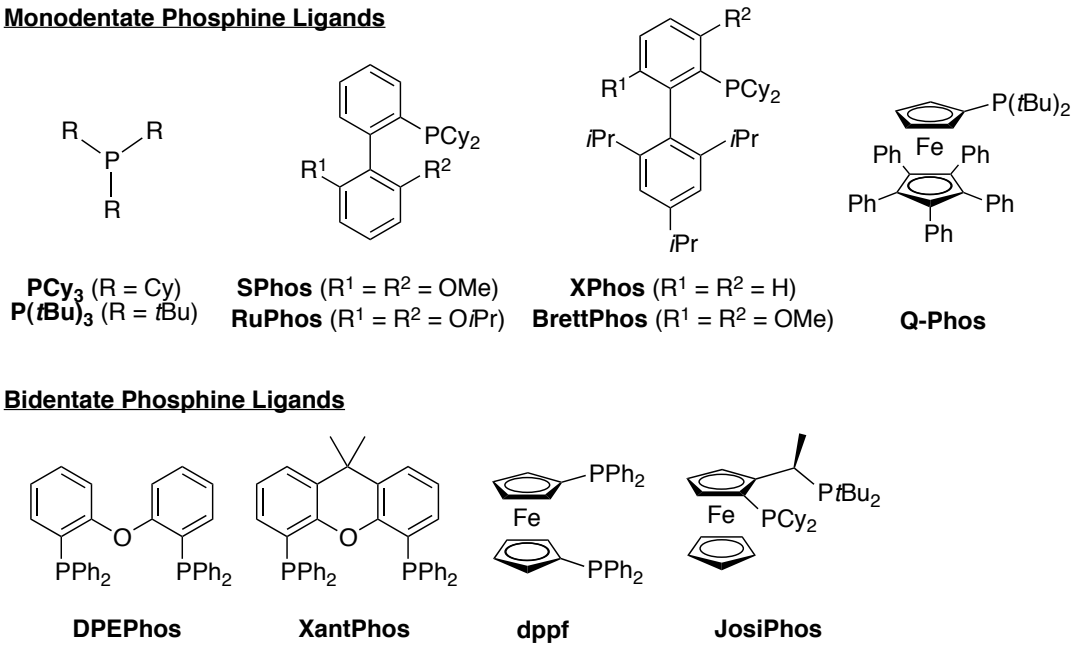

Figure 12: Selected examples of common mono- and bidentate phosphine ligands.[53,57,58,59]

While phosphines have been demonstrated to be good ancillary ligands for Pd-catalysis, there are a number of limitations associated with their use. First, trialkyl phosphines and, to a lesser extent, triaryl phosphines are sensitive to air and often require handling in an inert-atmosphere glovebox to avoid oxidation. Next, phosphines are subject to degradation at high temperatures, therefore an excess amount of ligand is usually required. Lastly, the steric bulk of triaryl and trialkyl phosphines is projected away from the metal centre, limiting the influence of the steric bulk on the metal centre during catalysis. Although phosphine ligands have been the most widely used, N-heterocyclic carbenes (NHCs) been gaining popularity due to their high thermal stability and ease in tunability of steric and electronic properties.[60]

1.4.2 N-Heterocyclic Carbene (NHC) Ligands

NHCs were first synthesized and characterized in 1968 independnently by Wanzlick[61] and Öfele[62] as free salts and as mercury and chromium complexes. However, it was not until 1991 when Arduengo[63] reported the isolation of the first stable free carbene (**28**) that these compounds started to receive wider attention. Subsequently in 1995, Herrmann and co-workers first demonstrated that NHCs could be used as ligands in Pd-catalysis instead of phosphine ligands.[64] Since then, many different NHCs have been synthesized and with an increasing number of available NHCs, wider interest in their use as ligands in transition metal catalyzed reactions began to develop.[65] The most commonly employed NHC ligands in Pd-catalyzed cross-coupling are derived from imidazole and imidazolidine rings and a selection of important NHCs is given in Figure 13. Arduengo's IMes (**30**) and IPr (**34**) ligands were some of the first NHCs synthesized and were found to be among the most electron-donating NHCs, which is one of the reasons why they are "go-to" ligands in cross-coupling, along with their unsaturated analogues SIMes (**29**) and SIPr (**33**).[66] More recently, Glorius (**31**, **32**),[67] Organ (**40**, **41**, **43**),[68] Dorta (**44**-**47**), Markó (**38**),[69] Nolan (**39**),[70] and Lavigne (**36**)[71] have developed more sterically demanding NHC ligands that have proven to be very efficient in Pd-catalyzed C-C and C-heteroatom bond formations.

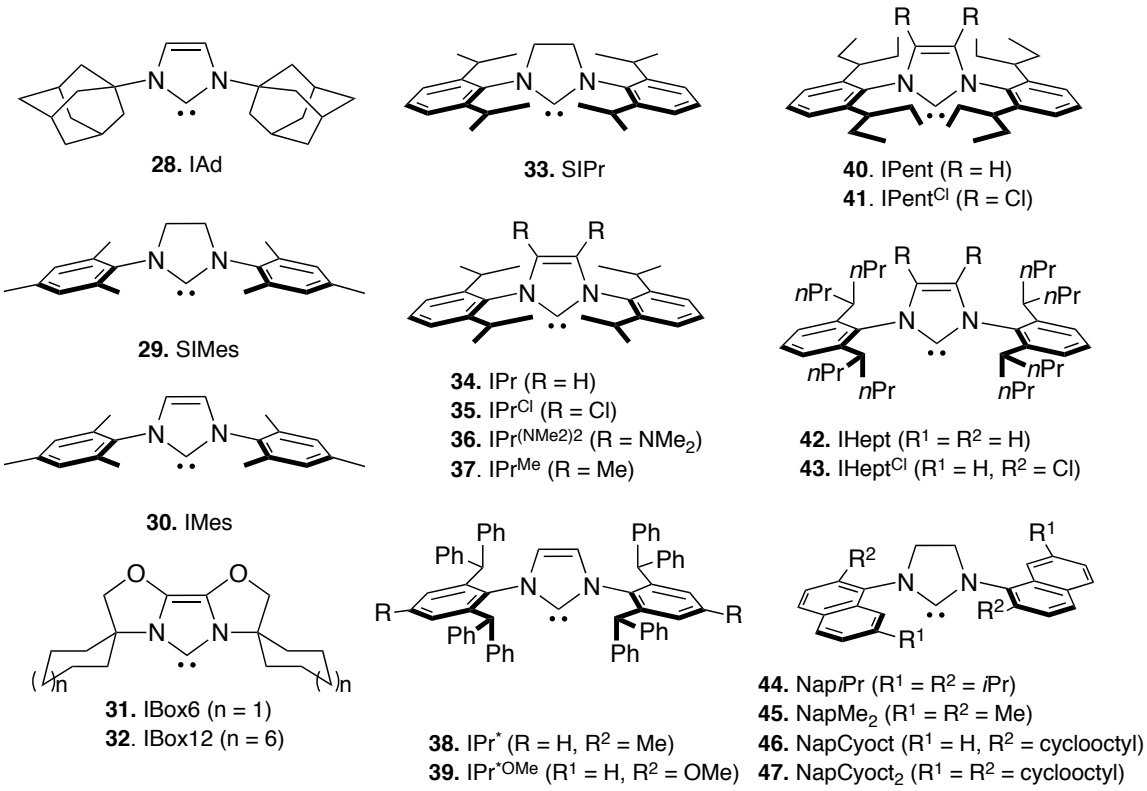

Figure 13: Selected examples of five-membered imidazoline and imidazolidine-based N-heterocyclic carbene (NHC) ligands used in cross-coupling.

Much effort has gone into understanding the key structural features of the NHC core that lead to improved catalytic performance. Similar to phosphine ligands, the σ–donating ability of the NHC ligand can be quantified using the TEP. Crabtree[72] and Nolan[73] developed a series of [(L)Ir(CO)$_2$Cl] complexes [L = NHC, PR$_3$, P(OR)$_3$] in order to compare the electron donating ability of phosphine and NHCs, without having to use the extremely toxic Ni(CO)$_4$ precursor. From these studies they found that imidazolium NHCs are far better σ–donors than even the most electron-rich trialkyl phosphines, implying a stronger M-L bond for NHCs relative to phosphines. These studies also showed that the nature of the *ortho*-substiuents on the N-aryl ring did not

significantly affect the donating ability of the carbene carbon. Unlike phosphine ligands, where varying the substituents on the phosphine not only affects its donor abilities but its steric properties as well, the electronic and steric properties of NHCs can be more independently tuned. This is because the substituents on the imidazole ring are not directly attached to the carbene carbon whereas in phosphines, the substituents are directly bonded to the phosphorus atom.

The steric bulk of NHC ligands also differs from phosphines. While the three substituents on phosphines are projected away from the metal centre, NHCs project the N-aryl subsituents towards the metal centre (Figure 14a). Therefore, Tolman's cone angle is no longer applicable to measure the steric properties of NHCs. To quantify the steric properties of NHC ligands, Nolan and Cavallo developed a new steric parameter called percent buried volume, $\%V_{Bur}$, which is defined as the percentage of total volume of a sphere around a metal occupied by a given ligand.[74] The sphere has a defined radius and the volume of the sphere represents the potential coordination sphere around the metal that a ligand can occupy (Figure 14b). The value of this parameter can be calculated using crystallographic data from $[(NHC)Ir(CO)_2Cl]$ complexes. In general, the bulkier the NHC ligand, the greater the $\%V_{Bur}$. Since the $\%V_{Bur}$ model was found to correlate well with the Tolman cone angle, it has also been extended to include phosphines.

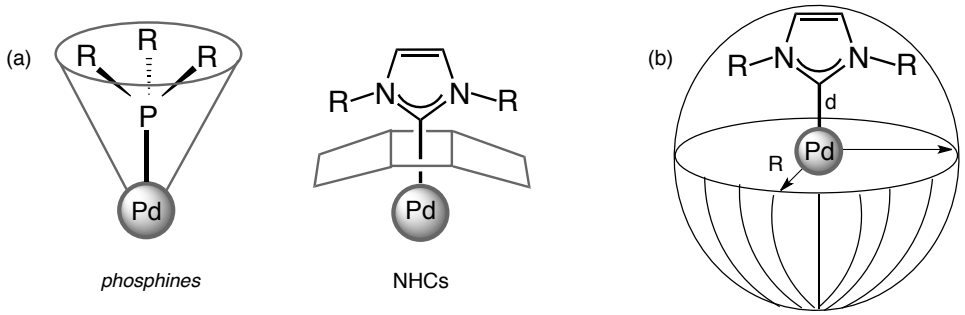

Figure 14: (a) Steric topology of phosphine and NHC ligands; and (b) Simplified representation of the sphere used for the $\%V_{Bur}$ calculation.

1.5 Pd-PEPPSI Pre-catalysts

Compared to phosphine ligands, NHCs are much stronger σ–donors and upon complexation, generate a more electron rich metal centre. As a result, stronger bonds are formed between palladium and the NHC, forming complexes with greater thermal stability that are resistant to ligand dissociation.[75] While Pd-NHC complexes can be formed *in situ* by mixing the NHC salt with a palladium source (e.g., $Pd(OAc)_2$), the stability of the Pd-NHC bond has allowed for the preparation of pre-formed Pd-NHC complexes.[65] Perhaps the most popular Pd-NHC pre-catalysts used in cross-coupling to date are those developed by Organ and co-workers. Coined PEPPSI (Pyridine Enhanced Pre-catalyst, Preparation, Stabilization, and Initiation), these complexes feature a Pd-NHC complex with a *trans*-ligated 3-chloropyridine ligand (i.e., throw-away ligand) (Figure 15). These pre-catalysts are air and moisture-stable and reduce readily to the active Pd(0) species under typical cross-coupling conditions. Over the past decade, the Organ group has developed a variety of Pd-NHC pre-catalysts with some notable examples shown in Figure 15.

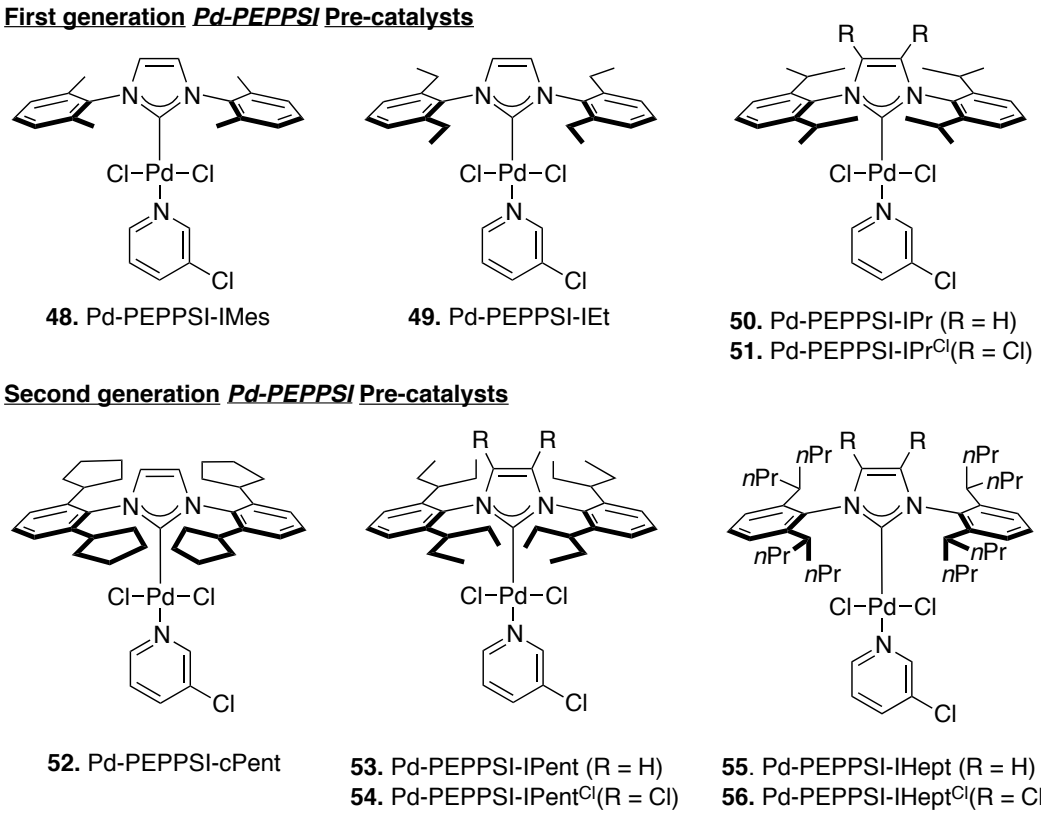

Figure 15: Structures of selected *Pd-PEPPSI* pre-catalysts used in cross-coupling.

The most reactive catalyst from the first generation of *Pd-PEPPSI* complexes was *Pd-PEPPSI-IPr* (**50**). In a series of publications, **50** was found to outperform the less bulky IMes (**48**) and IEt (**49**) analogues in a variety of cross-coupling reactions, including Negishi,[76] Suzuki-Miyaura,[77] Kumada-Tamao-Corriu (KTC),[78] and Buchwald-Hartwig-Yagupol'skii (BHY) amination.[79] Since the σ–donor abilities of IMes and IPr carbenes are similar, improvements in catalyst performance were attributed to the increased steric bulk around the metal centre.[80] This led to the development of a second generation of *Pd-PEPPSI* complexes featuring more sterically bulky *ortho*-substituents on the N-aryl rings of the NHC (**52**, **53**, **55**).[81] These complexes were screened in the Suzuki-Miyaura

coupling of tetra-*ortho* substituted biaryls and *Pd-PEPPSI-IPent* (**53**) was found to be the most acitve. These results highlighted the importance of "flexible-steric-bulk"[82] around the metal centre necessary to promote this challenging reaction. Since 2009, **53** has proven to be an excellent pre-catalyst for Negishi,[83] Suzuki-Miyaura,[68,84] Stille-Migita,[85] BHY amination,[86] and C-S coupling.[87] More recently, Organ and co-workers have developed complexes **54** and **56**, which have shown to be highly reactive in the Negishi coupling of secondary organozinc reagents.[88]

1.6 Plan of Study

Given the importance of isoprenylated arenes in nature, specifically those containing prenyl and geranyl side chains attached at the α–carbon, it would be desirable to develop a method for introducing these side chains in a highly regioselective manner. Compared to traditional or non-catalytic methods, Pd-catalyzed cross-coupling of 3,3-disubstituted allyl metals has emerged as the most direct method for introducing these side chains onto functionalized arenes. While the Suzuki-Miyaura cross-coupling of 3,3-disubstituted allylboronates is an attractive alternative to reactions employing other organometallic reagents (e.g., organostannanes), the majority of these protocols are typically selective for the branched isomer (i.e., γ–product) when employing bulky phosphine ligands. While NHC ligands have emerged as useful alternatives to phosphine ligands, their use in Pd-catalyzed allylation has not been explored. Therefore, the first objective of this project was to develop a mild set of Pd-catalyzed Suzuki-Miyaura coupling conditions that make use of Pd-NHC pre-catalysts, in particular *Pd-PEPPSI-IPent* (**53**), and that would be highly selective for the linear isomer (i.e., α–product).

Specifically, 3,3-disubstituted allylboronic acid pinacol esters were investigated since these organoboron reagents are known to be easier to prepare, handle, and purify compared to their boronic acid congeners.[89] Such a methodology would have significant synthetic value because it would allow for the selective construction of α–products. This is important as isomeric allylated products are typically very difficult to separate from one another. Once a set of conditions had been developed that were highly selective for the linear product, the second objective of this project was to apply the methodology to the total synthesis of a prenylated natural product. Recently, cathafuran A and lakoochin A were isolated by the Yu[90] and Kitakoop[91] groups, respectively (Figure 16). The structural features of these compounds combined with their biological and pharmacological activities (e.g., antimicrobial, antioxidative, anti-inflammation, and cytotoxic) makes them interesting synthetic targets. To date, no total synthesis has been reported for these compounds.

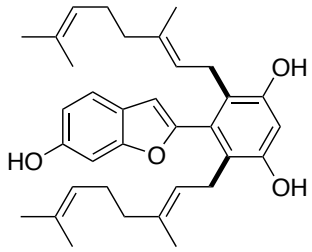

cathafuran A (**58**)

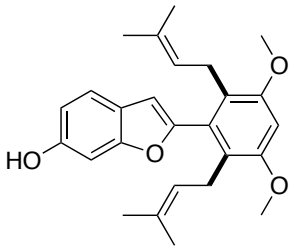

lakoochin A (**59**)

Figure 16: Structures of isoprenylated natural products cathafuran A (**58**) and lakoochin A (**59**).

CHAPTER 2 – Regioselective Coupling of 3,3-Disubstituted Allylboronic Acid Pinacol Ester Derivatives onto Aromatic Rings using *Pd-PEPPSI IPent (53)*

2.1 Background

In 2009, Podestá and co-workers reported conditions for α-selective allylation using $Pd(PPh_3)_4$ for the cross-coupling of aryl iodides with prenyl boronic acid pinacol ester (**60a**) (Scheme 8).[92] Using this as a starting point, *Pd-PEPPSI-IPent* (**53**) was evaluated in this reaction as it had demonstrated excellent reactivity in sp^2-sp^2 and sp^3-sp^3 Suzuki-Miyaura[84a] and Negishi[83a,b] cross-coupling reactions. However, its reactivity in sp^2-sp^3 coupling reactions involving allylic metals with aryl and/or alkenyl electrophiles had not yet been explored despite the fact that this reaction could provide access to an important substitution pattern found in isoprenylated natural products. When investigating both catalysts in the reaction outlined in Scheme 8, we were surprised to find that $Pd(PPh_3)_4$ was highly selective for the branched (γ) product instead of the expected linear (α) product (8:92). Conversely, *Pd-PEPPSI-IPent* (**53**) exhibited almost exclusive selectivity for the linear product (98:2). Based on these promising results, **53** was investigated for the α-selective cross coupling of prenylboronic acid pinacol ester **60a**, along with other 3,3-disubstituted allylboronate derivatives, with a variety of hetero(aryl) halides before applying this protocol towards the total synthesis of isoprenylated natural products, such as cathafuran A.

While the selectivity was high with aryl iodide **59**, side reactions leading to reduction and homocoupling were significant, leading to a low yield of allylated products

(**61**). The reaction between 1-bromo-4-(*tert*-butyl)benzene (**62**) and prenylboronic acid pinacol ester (**60a**) was chosen to optimize reaction conditions and to study the kinetics for this transformation since **62** showed minimal steric or electronic bias[93] and was suitable for analysis by GC/MS. However, before optimization could take place, a calibration curve needed to constructed, in which all possible products resulting from the reaction could be accounted for and quantified.

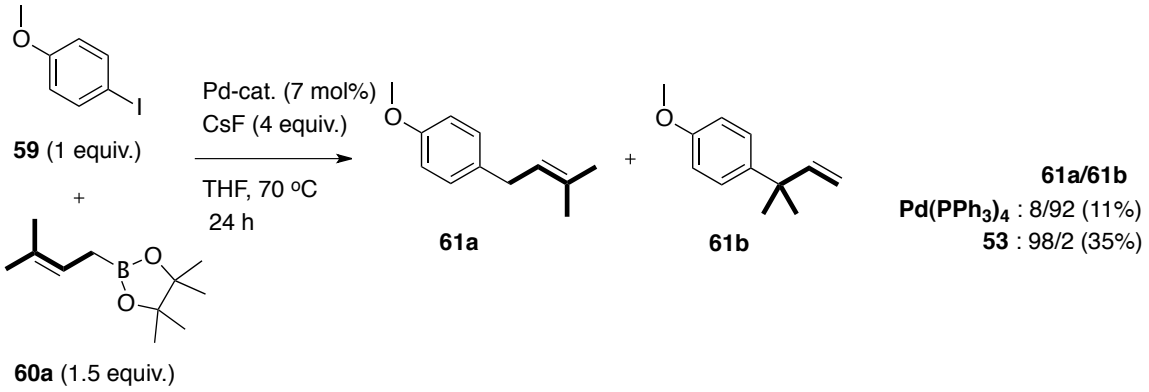

Scheme 8: Comparison of $Pd(PPh_3)_4$ and *Pd-PEPPSI-IPent* (**53**) in the Pd-catalyzed allylation of **59** with **60a**.

2.2 Preparation of Regioisomers 61a and 61b.

While some of the side products arising from this attempted coupling are commercially available, α- and γ-isomers (**68a** and **68b**) are not, thus a synthetic route for each isomer had to be developed. Close inspection of the two isomers revealed a Wittig disconnection, which led to reaction Scheme 9, outlined below.

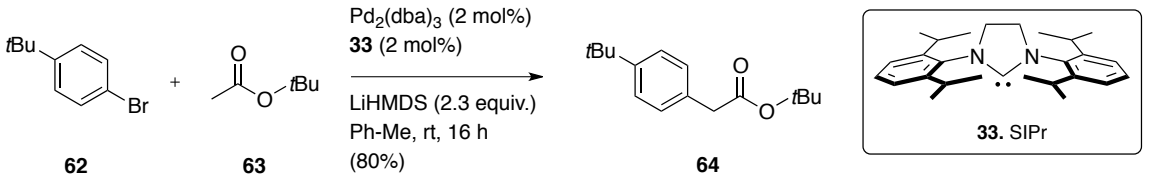

*A: Synthesis of α–isomer (**68a**).*

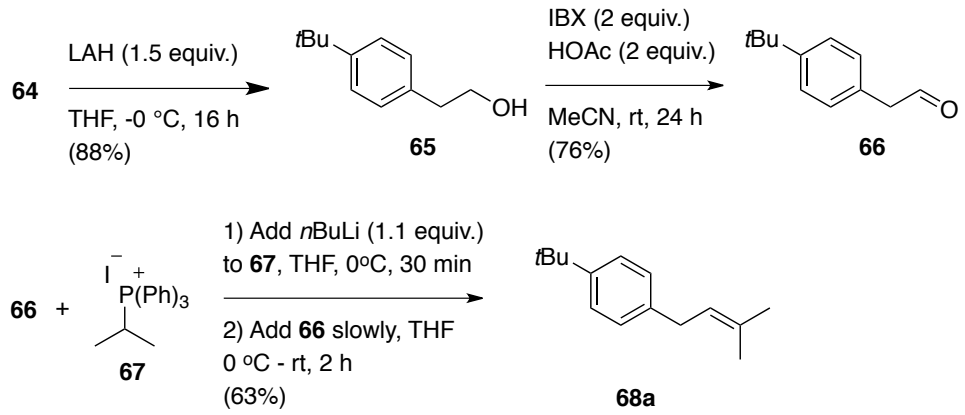

*B: Synthesis of γ–isomer (**68b**).*

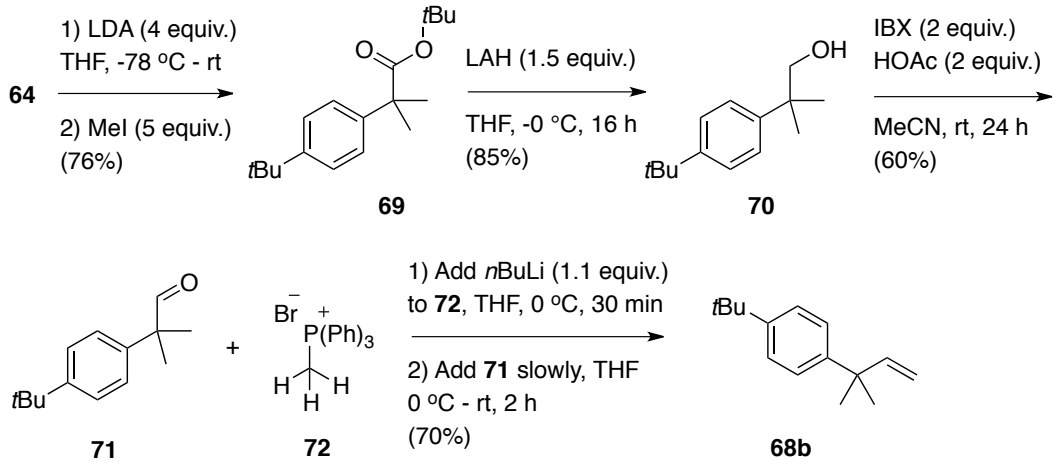

Scheme 9: Preparation of α– and γ–isomers (**68a** and **68b**) via Wittig Reaction.

Using a protocol established by Hartwig and co-workers, the lithium enolate of *tert*-butyl acetate (**63**) was cross-coupled with aryl halide **62** using 2 mol% Pd_2dba_3 and ligand precursor **33**, to afford **64** in 80% yield.[94] Next, compound **64** could either be reduced with LAH to give **65** (Route A) or undergo double methylation and then reduction to give **69** (Route B) to make the α- and γ-isomer, respectively. Both reactions proceeded smoothly, yielding **65** and **69** in 88% and 76% yield, respectively. Interestingly, oxidation

of **65** with IBX, PCC, and PDC afforded a mixture of 2-(4-*tert*-butylphenyl)acetaldehyde **66** and 4-*tert*-butylbenzaldehyde (**73**).

Table 1: Screening different oxidation conditions.

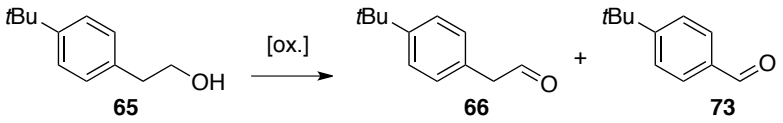

65 **66** **73**

Entry	Oxidation Method	Conv. (%)[a]	Product Ratio **66/73**
1	IBX	100	90/10
2	Swern[b]	-	-
3	PCC	100	75/25
4	PDC	85	60/30
8	IBX/HOAc	80	1/0 (76%)

[a] Conversions and product ratios were determined by ^{1}H-NMR spectroscopy of the crude reaction mixture. [b] Significant decomposition and/or polymerization observed.

After screening several oxidation conditions, it was found that oxidation with IBX in the presence of acetic acid, afforded **66** exclusively (Table 1, Entry 8). Using these conditions, oxidation of alcohols **65** and **70**, followed by a standard Wittig reaction, afforded **68a** and **68b**. With these compounds in hand, optimization of the regioselective Suzuki-Miyaura cross-coupling reaction conditions could be undertaken and a calibration curve was made for GC/MS analysis of the reaction mixtures.

2.3 Optimization Study for the Regioselective Suzuki-Miyaura Cross-coupling of Prenylboronic Acid Pinacol Ester 60a

Table 2 shows the results from the initial base screening for the coupling between prenylboronic acid pinacol ester **60a** and aryl bromide **62** conducted in tetrahydrofuran (THF). Aqueous 5 M potassium hydroxide (KOH) (4 equiv.) provided optimal results

whereas under anhydrous conditions, poor conversions were observed (Table 2, Entries 5 and 8). Although cesium fluoride (CsF) generated better conversions than potassium fluoride (KF), switching to tetrabutylammonium fluoride (TBAF), an organic-soluble fluoride source, led to lower conversions (Table 2, Entries 1-2). Interestingly, K_2CO_3, one of the most commonly used bases in Suzuki-Miyaura cross-coupling reactions, led to lower conversions both with and without added water (Entries 7 and 4, respectively).

Table 2: Optimization study – Base screen.[a]

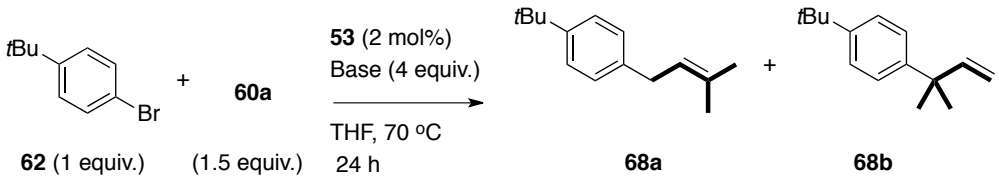

Entry	Base	Conv. (%)[b]	**68a/68b**[b]
1	KF	0	0
2	CsF	42.5	98/2
3	TBAF	< 4	100/0
4	K_2CO_3	< 4	100/0
5	KOH	10	100/0
6	KO^{t}Bu	0	0
7	2 M K_2CO_3	18.5	96/4
8	5 M KOH	81	97/3

[a] Reactions were conducted with 0.5 mmol of substrate **62** at 0.25 M concentration in THF; reactions were performed in duplicate [b] Determined by GC/MS using a calibrated internal standard (undecane).

While 5 M aqueous KOH proved to be an effective base system for this reaction, the concentration and amount of base was investigated in order to arrive at milder reaction conditions (Table 3). Decreasing the concentration of base appeared to have no affect on the conversion or selectivity (Entries 8-11), whereas lowering the equivalents of base appeared to significantly reduce conversion to the allylated products (Entries 2-5). Similar trends were also observed when the concentration or equivalents of KOH_{aq} were

increased (Entries 1, 6, and 7). Therefore, 5 M KOH (4 equiv.) was found to be the best base system for this transformation.

Table 3: Optimization study – KOH aqueous base screen.[a]

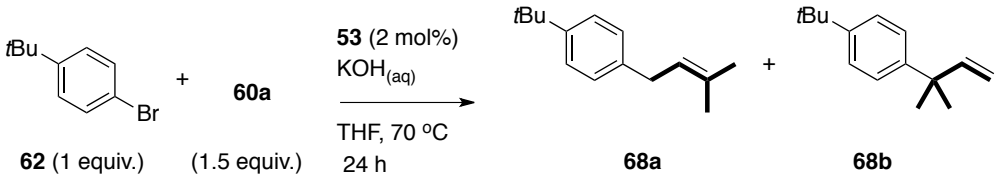

Entry	Conc.	Equiv.	Conv. (%)[b]	**68a/68b**[b]
1	5 M	5	79	96/4
2	5 M	4	81	97/3
3	5 M	3	72	97/3
4	5 M	2	68	97/3
5	5 M	1	39	97/3
6	10 M	4	74	96/4
7	7 M	4	82	96/4
8	4 M	4	73	97/3
9	3 M	4	73	97/3
10	2 M	4	72	97/3
11	1 M	4	72	97/3

[a] Reactions were conducted with 0.5 mmol of substrate **62** at 0.25 M concentration in THF; reactions were performed in duplicate [b] Determined by GC/MS using a calibrated internal standard (undecane).

Having arrived at the optimal base system, the reaction conditions were further refined by performing a solvent screen (Table 4). Ethereal solvents exhibited high α–selectivity (Entries 1-3), with THF providing the best conversion (Entry 3). While toluene also showed good conversion to allylated products **68a** and **68b** (Entry 4), selectivity for the α-isomer was slightly diminished (Entries 1-3).

Table 4: Optimization study – Solvent screen.[a]

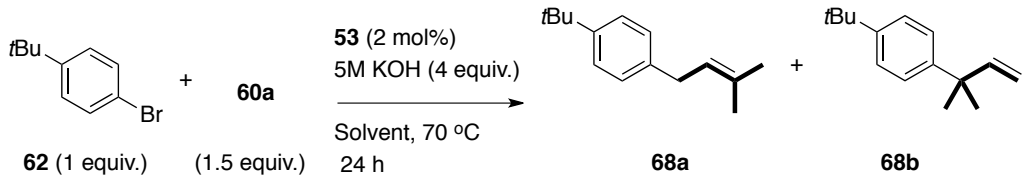

Entry	Solvent	Conv. (%)[b]	**68a/68b**[b]
1	1,4-Dioxane	58	97/3
2	DME	72	97/3
3	THF	81	97/3
4	Toluene	71	94/6

[a] Reactions were conducted with 0.5 mmol of substrate **62** at 0.25 M concentration in THF; reactions were performed in duplicate [b] Determined by GC/MS using a calibrated internal standard (undecane).

Next, other phosphine ligands reported to selectively produce the α-isomer were screened against **53** (Table 5). Both dppe and dppp were found to be unselective despite their difference in bite angles (86° vs. 91°) (Entries 1-2). This was surprising since other research has shown a significant difference between the two ligands in other Pd-catalyzed allylation reactions, albeit under different reaction conditions.[39-41] Once again, $Pd(PPh_3)_4$ showed high selectivity for the γ-isomer. Other sterically bulky NHC ligands were also investigated. While both the IPr and IPent ligands displayed high selectivity for the α-isomer, IPent provided slightly higher α-selectivity over IPr. Interestingly, both IPr^{Cl} and $IPent^{Cl}$ showed much diminished selectivity for the α-isomer compared to their non-chlorinated backbone congeners (Entries 4 and 6 vs Entries 5 and 7, respectively).

Table 5: Optimization study – Effects of ligands.[a]

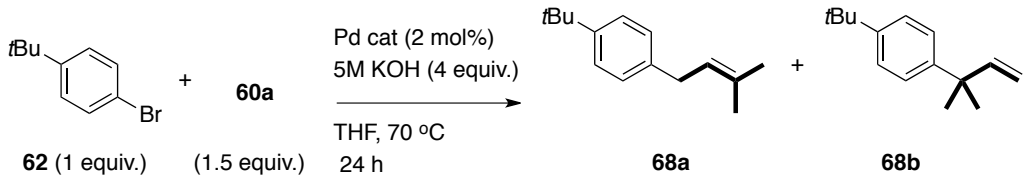

62 (1 equiv.) (1.5 equiv.) **68a** **68b**

Entry	Catalyst	Conv. (%)[b]	**68a/68b**[b]
1	$Pd(OAc)_2$/dppe	90	56/44
2	$Pd(OAc)_2$/dppp	76	54/46
3	$Pd(PPh_3)_4$	90	5/95
4	*Pd-PEPPSI-IPr* (**50**)	86	93/7
5	*Pd-PEPPSI-IPr*^{Cl} (**51**)	86	65/35
6	*Pd-PEPPSI-IPent* (**53**)	81	97/3
7	*Pd-PEPPSI-IPent*^{Cl} (**54**)	67	78/22

[a] Reactions were conducted with 0.5 mmol of substrate **62** at 0.25 M concentration in THF; reactions were performed in duplicate [b] Determined by GC/MS using a calibrated internal standard (undecane).

2.4 Substrate Study

With optimization completed, **53** was evaluated in the allylation of a variety of aryl and heteroaryl halides with **60a** (Table 6). Exclusive α-selectivity was observed in almost all cases. The reactions proceeded smoothly under these conditions regardless of how sterically or electronically deactivated the aryl halide. Compound **60a** could be coupled in the presence of a carbonyl group, albeit in low yield, with no significant sign of the addition product (i.e. nucleophilic attack at the ketone) observed. With the aryl bromides showing good reactivity, attention was then focused on aryl chlorides, as they are more readily available and much less expensive than their bromide congeners. Also, there are very few reports of this coupling in the literature. Again, the reactions proceeded smoothly and in most cases were higher yielding than the corresponding aryl bromide, which was attributed to less reduction. In all cases, heterocyclic halides also coupled well. The reaction conditions could also be extended to dihaloarenes, with only trace

amounts of the mono-coupled product observed and **85** isolated as the major product. This was extremely promising as **85** is similar to the key, core structure (2-arylbenzofurans; **91** and **93**) in our synthetic pathway towards natural products **58** and **59** (Scheme 12, Chapter 3). Interestingly, when 1.1 equiv. of **60a** was used to couple only one of the chlorines, formation of the di-coupled product was observed as the major product.[95]

Table 6: Substrate scope study of prenylboronic acid pinacol ester (**60a**) and with *Pd-PEPPSI-IPent* (**53**).[a,b]

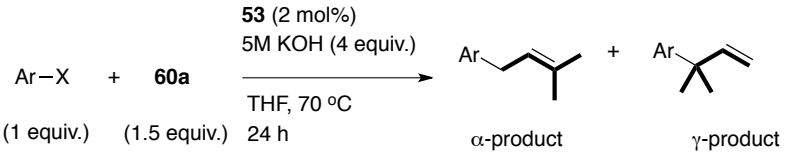

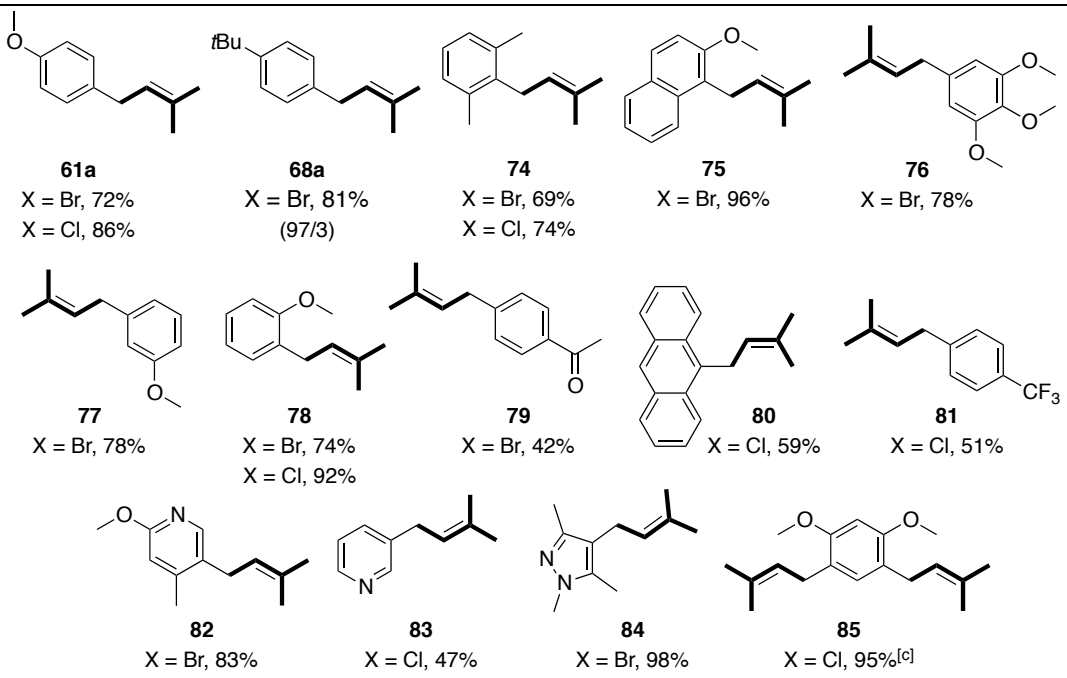

[a] Yields of isolated products following silica gel chromatography (averages of two runs) are reported. [b] Product ratios were determined by ^{1}H-NMR spectroscopy of the crude reaction mixtures and were >99/1 (**α/γ**) unless otherwise indicated. [c] 3 equiv. of **60a** and 8 equiv. of 5 M KOH were used.

2.5 Regioselective Suzuki-Miyaura Cross-coupling Reaction – Mechanism of Transmetallation

Allylborates are believed to transmetalate by an inversion (S_E2') process,[41c] however there is evidence to also support an addition-elimination[41f] process. Both pathways lead to the γ–product (Figure 7). An S_E2' mechanism would be promoted by bulky phosphine ligands that could facilitate fast reductive elimination for the observed γ-regioselectivity. In both the addition-elimination or inversion process, formation of a π–allyl-Pd^{II} intermediate (e.g., **27**, Figure 7) leading to α-coupling, was ruled out.

To examine the possible formation of **27**, a classical allylic substitution reaction was carried out with prenylbromide (**86**) with **87** in the presence of $Pd(PPh_3)_4$ (Scheme 10a). Both catalysts provided nearly no regioselectivity, which was surprising since other Suzuki-type allylations proceeding through (π–allyl)palladium intermediates were reported to couple at the unsubstituted allylic terminus preferentially to give the linear product.[37] The results in Scheme 10a suggest that after OA, the less hindered σ-complex is slightly favoured in the equilibrium due to steric interactions with the ligands and the metal centre. Assuming RE is relatively fast with both catalysts, the α- and γ-isomers are produced in the same ratio as their corresponding Pd σ-complexes. In other words, while after OA there is σ–π–σ interconversion, there is not such interconversion following TM. This would be consistent with the proposals by Miyaura[41c] and Szabó.[41f] However, coupling **88** with **60a** under the same reaction conditions (Scheme 10b) gave similar regioselectivities as shown in Scheme 8. Here $Pd(PPh_3)_4$ gave primarily the γ-product (**61b**) while **53** gave exclusively the α-product (**61a**). These results suggest that RE from

σ-complexes (**26a** and **26b**) must be faster than σ–π–σ interconversion via **27**, to explain the high regioselectivities observed (Scheme 10b).

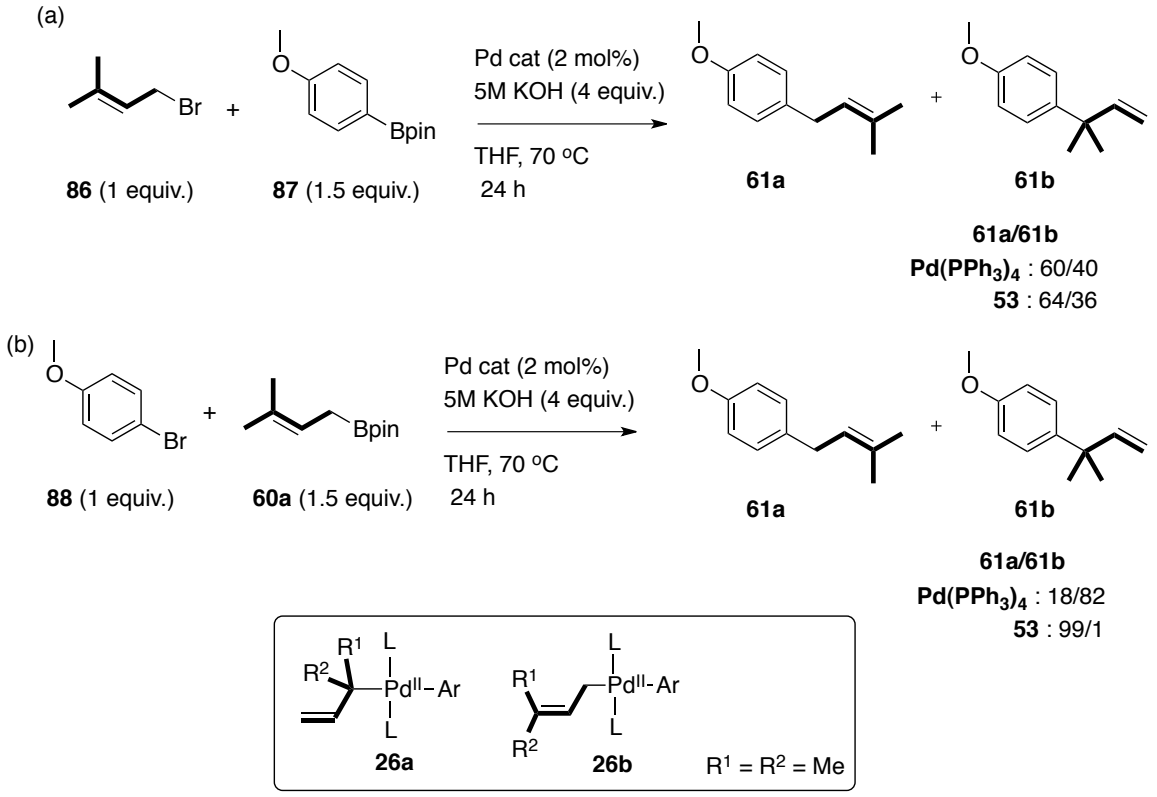

Scheme 10: Investigation into the formation of (π–allyl)Pd^{II} intermediates using: (a) Classical Pd-catalyzed allylic substitution reaction; and (b) Pd-catalyzed Suzuki-Miyaura cross-coupling reaction. Structures of intermediates **26a** and **26b**.

Before this methodology could be used towards the total synthesis of cathafuran A and lakoochin A, the existence of a post-transmetallation π-allyl complex resembling **27** needed to be further investigated to determine whether trisubstituted allylboroates, such as **60b** could be coupled with retention of configuration as well as high α-selectivity. Therefore, different trisubstituted allylboranes were synthesized where one of the methyl groups on **60a** was substituted with different groups and different olefin

geometry to look for scrambling of the olefin stereochemistry (Table 7).[96] From these results, there seems to be a small amount of scrambling of olefin stereochemistry, which must have taken place through the formation of a Pd–π–allyl complex.

Table 7: Allylation of **62** with allylboronic acid pinacol ester derivatives catalyzed by **53**.[a,b]

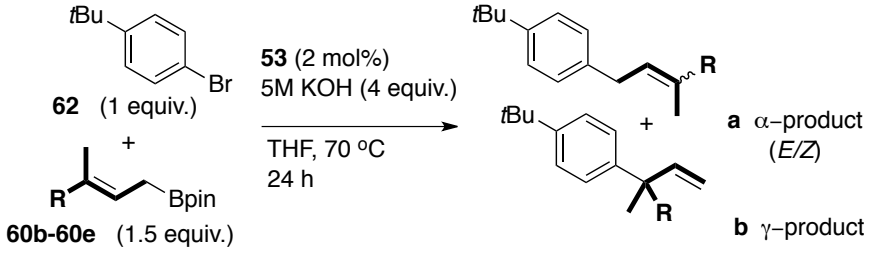

Entry	Boronic Ester (**60b-60e**)	α–product (*E/Z*)
1	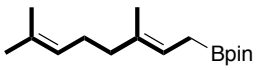 **60b** *E-geometry*	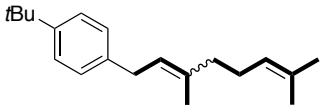 **89a** 92%, *E/Z* = 80/20
2	**60b** *E-geometry*	**89a** 19%, *E/Z* = 80/20; **89b** 81%[c]
3	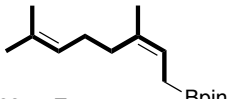 **60c** *Z-geometry*	**89a** 62%, *E/Z* = 45/55
4	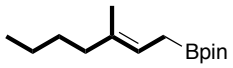 **60d**	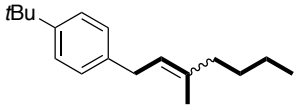 **90a** 80%, *E/Z* = 80/20
5	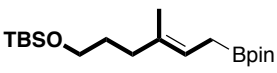 **60e**	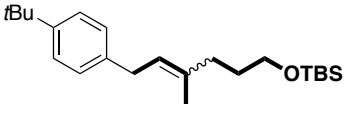 **91a** 76%, *E/Z* = 80/20

[a] Yields are reported on isolated products following silica gel chromatography; isolated yields are the average of two runs. [b] Product ratios determined by ^{1}H-NMR spectroscopy of the crude reaction mixture and are >99/1 (α/γ) unless otherwise indicated. [c] The yields and isomer ratios produced by $Pd(PPh_3)_4$. Yield of combined products was 93%.

In general, the same 80/20 *E/Z* ratio was observed in all cases where the (*E*)-allylboronate was used (Entries 1, 4 and 5). However, when the *Z* isomer **60c** was used, only 45% scrambling of the *Z* stereochemistry (i.e. *Z* to *E*) was observed (Entry 3), despite leading to a more stable Pd–π–allyl complex. These results demonstrate that limited σ–π–σ interconversion occurs via π-allyl complex **27** with catalyst **53**, as the two different boronate isomers do not reach equilibrium before RE occurs. This experiment also confirms that RE with catalyst **53** is relatively fast. Furthermore, the results from Table 7 again highlight the high α–selectivity observed with catalyst **53**, as none of the branched isomer was observed, even in the presence coordinating functional groups (Entry 4). This was nicely demonstrated in Entries 1 and 2, where **62** was reacted with **60b** in the presence of both **53** and $Pd(PPh_3)_4$, respectively. While the major product formed with $Pd(PPh_3)_4$ was the γ–isomer (**89b**), **53** showed complete selectivity for the α–isomer (**89a**).

The connectivity for products **89-91** was assigned using ^1H-^1H COSY, ^1H-^{13}C HSQC and ^1H-^{13}C HMBC and the olefin geometry was assigned by evaluating the proton interactions at the vinylic center using 2D ^1H-^1H gradient NOESY spectroscopy. As seen in Figure 17, there are two resonances that are partially overlapping at 5.4 ppm (i.e., H-8). The larger component is on the left hand side of the resonance and the smaller component is on the right hand side, which is consistent with the 2D HSQC (not shown here). The smaller component on the right hand side of H-8 appears to have a correlation to H-10 but not H-11. Conversely, the larger component on the left hand side of H-8

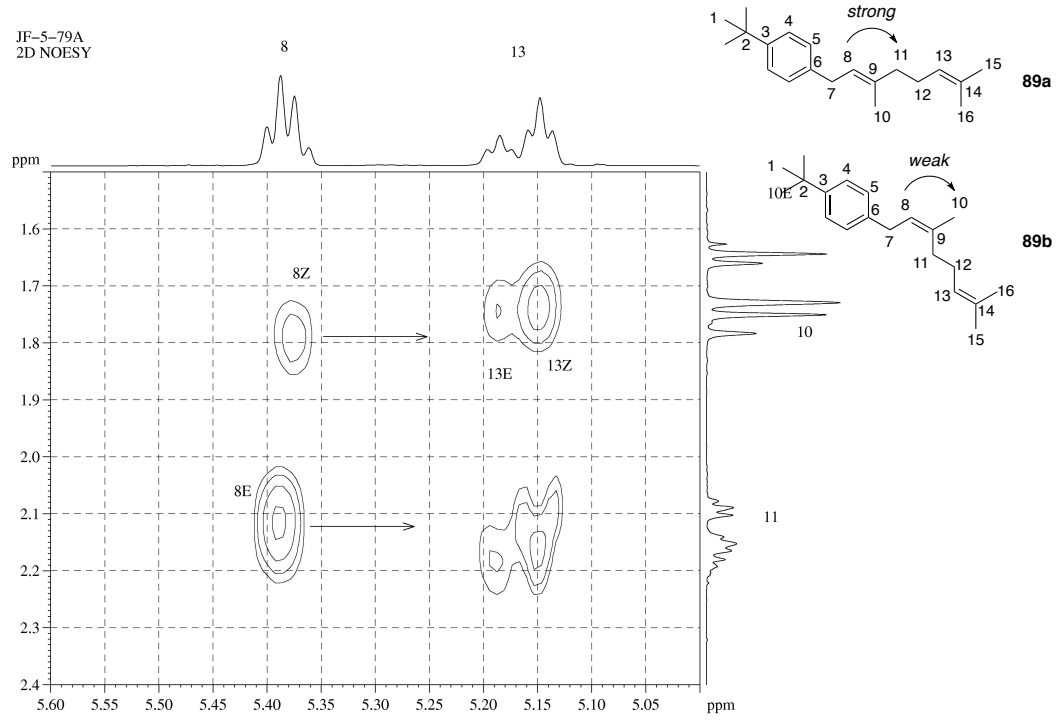

Figure 17: Representative example for the assignment of *E/Z* stereochemistry in product **89a**.

appears to have a stronger correlation between H-8 and H-11 but not H-8 and H-10. Therefore, it was concluded that the correlation between H-8 and H-11 was the result of *E*-stereochemistry while the correlation between H-8 and H-10 was the result of *Z*-stereochemistry. Compound **89a** was also used as a model substrate for quantitative proton NMR spectroscopy. The *E/Z* components were overlapped in the 1D ^{1}H spectrum at 600 MHz and the *E/Z* ratio was determined using the volume integration of the 2D ^{1}H-^{13}C HSQC pulse program as provided by the Bruker pulse program library. Fortunately, the proton resonances used in the *E/Z* isomer ratio determination in compounds **89-91** were all found to have similar $^{1}J_{13C\text{-}1H}$ coupling values, T_1 values and chemical shifts.

This volume integration HSQC method was found to be accurate to within 3% error by comparing the resolvable proton integrations and the 2D HSQC volumes of the other *E/Z* isomers.

The last thing to clarify was the mechanism of TM itself. The difference in observed regioselectivities between the two catalysts suggested a different mechanism of TM. Since **53** has been shown to facilitate fast RE in other cross-coupling reactions due to its bulky nature,[81] it was believed that TM must proceed without allylic transposition (S_E2) (Scheme 8). To investigate this, **60f**[97] and **62** were reacted in the presence of both $Pd(PPh_3)_4$ and **53** (Eq. 3). While $Pd(PPh_3)_4$ showed high regioselectivity for the γ–isomer, albeit with low conversion, very little product was obtained for **53** (Eq. 1). This suggests that TM, at least with the IPent ligand on Pd, does not proceed by an S_E2' mechanism. If TM first involves olefin coordination then one might expect **60f** to transmetallate faster, or at least as fast as **60a** since it is sterically less hindered. That it barely reacted suggests that with **53**, TM proceeds via S_E2 and that the borane may be too hindered to allow it to be activated.

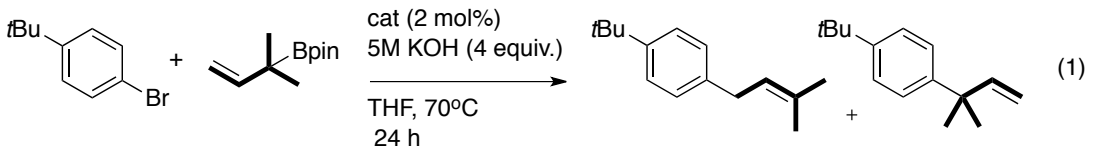

62 (1 equiv.) **60f** (1.5 equiv.) **68a** **68b**

(69a/68b)
53 : 100/0 (6% conv.)
$Pd(PPh_3)_4$: 30/70 (30% conv.)

2.6 Conclusion

Sterically bulky *Pd-PEPPSI-IPent* **53** has been shown to be extremely reactive in metal-catalyzed allylation. The high α–selectivity demonstrated by **53** over all other Pd-catalysts in the Suzuki-Miyaura coupling of prenylboronic ester **60a** with a variety of arylhalides was the first of its kind. Since then, Buchwald and co-workers reported a phosphine based catalyst system, generated by mixing *t*-BuPhos and $Pd(allyl)Cl_2$, to be highly selective for the α–product.[98] In the case of trisubstituted allylboronates with different substituents on the olefin, minor olefin geometry isomerization is observed with **53** (*E/Z* ~ 80/20*)*. The results shown in Scheme 10 and Eq. 1 suggest that TM with **53** does work by an S_E2 mechanism, whereas with $Pd(PPh_3)_4$, it may well proceed by an S_E2' mechanism. The high α–selectivity (>97%) and stereoselectivity demonstrated by **53** over all other Pd-catalysts can be attributed to both the significant steric bulk of the NHC ligand and the substitution of the allylboronic ester. The high linear selectivity demonstrated by **53** relative to other common Pd-catalysts has significant synthetic value as this process can now be used with high reliability to selectively produce such allylated aromatics. This is especially important since these isomeric allylated products typically cannot be separated.

CHAPTER 3 – Application of Regioselective Suzuki-Miyaura Coupling using *Pd-PEPPSI-IPent* in Total Synthesis.

3.1 Background

Morus, also known as mulberry, is a genus of flowering plants belonging to the Moraceae family. *Morus* consists of 10-16 species of deciduous trees native to warm, temperate, and subtropical regions of Asia, Africa, and the Americas. Mulberry trees have been important in China for thousands of years for both agricultural and medicinal purposes. The leaves of mulberry have been used as a feedstock for silk worms and other livestock while its bark roots have been used to treat various illnesses, including asthma, bronchitis, and hypertension as part of traditional Chinese medicine.[99] Another tree of the Moraceae family displaying important medicinal value is *Artocarpus lacucha (A. lacucha)*, a tropical evergreen tree native to the Indian Subcontinent and Southeast Asia. The wood from *A. lacucha* has been used in traditional Thai medicine to treat tapeworms.[91,100]

The constituents of the bark from *Morus* and *A. lakoocha* have been studied in depth and as a result, numerous isoprenylated phenolic compounds have been isolated. Many of these phenolic compounds have showed significant antimicrobial, antioxidative, anti-inflammatory, and cytotoxic activities. Among these compounds are cathafurans A (**58**) and lakoochin A (**59**) (Figures 16). Compound **58** was isolated recently by the Yu group in 2009, along with three other cathafurans (B-C) from the stem bark of *Morus cathayana,* one of the 16 species of *Morus* found in China.[90] Compound **59** was isolated along side lakoochin B by Kittakoop and co-workers from the roots of *Artocarpus*

lakoocha in 2004.[91] The structure of these compounds was established by spectroscopic techniques. Each compound contains a 2-arylbenzofuran core with either an attached 5-carbon prenyl (lakoochin A) or 10-carbon geranyl group (cathafuran A) on the phenolic ring. To date, no total synthesis has been reported for cathafurans A-D and lakoochins A and B. However, in 1991, Mann and Widdowson reported the synthesis of a similar isoprenylated natural product, moracin I (Scheme 11).[101] The prenyl group was introduced onto the protected 1,3,5-trihydroxybenzene ring by DoM and the key 2-arylbenzofuran core was constructed through Stille coupling of the benzofuran stannane and the aryl triflate. While this procedure affords moracin I in 9 steps with an overall yield of 32% (from 1,3,5-trihydroxybenzene), the use of organostannanes in the last step of a total syntesis is not appealing as these compounds are toxic and are generally difficult to separate from the desired cross-coupled product. However, the disconnections made by Mann and Widdowson are appealing as they allow for different analogues of the isoprenylated natural products to be constructed by simply changing either the 3,3-disubstituted allyl group or the 2-arylbenzofuran.

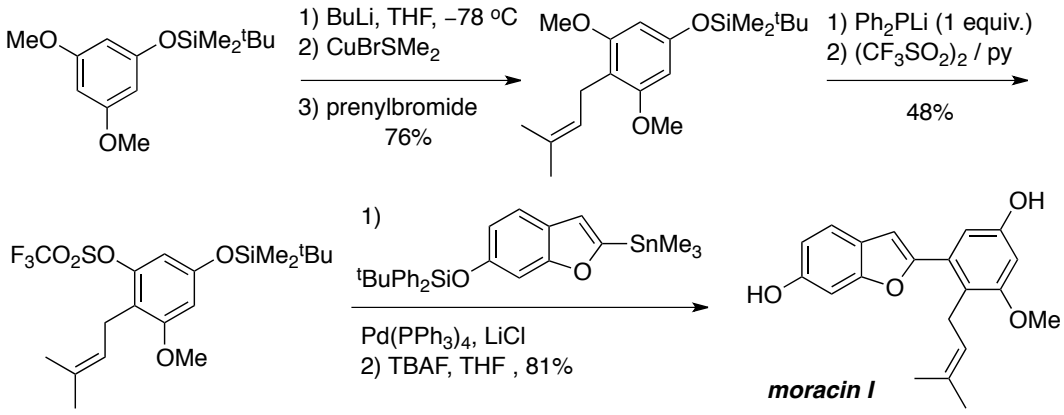

Scheme 11: Mann and Widdowson's approach to the total synthesis of moracin I.

3.2 Overview of Synthetic Approach

Inspired by work of Mann and Widdowson, the retrosynthetic route developed to prepare cathafuran A and lakoochin A was based on a sequential Pd-catalyzed Suzuki-Miyaura/Negishi cross-coupling sequence (Scheme 12). Advanced benzofuran building block (**93**) could be prepared by Directed Ortho Metallation (DoM) of **96** at C6 to provide the lithium salt of **95** selectively, which following TM to the corresponding boron or zinc derivatives would be open for selective Pd-catalyzed cross-coupling with heteroaryl iodide (**94**). Subsequent stereo- and regioselective Suzuki-Miyaura cross-coupling with the requisite terprenylborate and *Pd-PEPPSI-IPent* (see Chapter 2), followed by demethylation would then give the desired final targets. In the course of these studies, a dramatic solvent effect on the selectivity of the DoM process was uncovered, which in turn revealed some interesting insights into the creation of kinetic and thermodynamic aryl anions. To better understand the kinetic and thermodynamic profile of this selective deprotonation a number of experiments were designed and the

results from those experiments are described in Chapter 4.

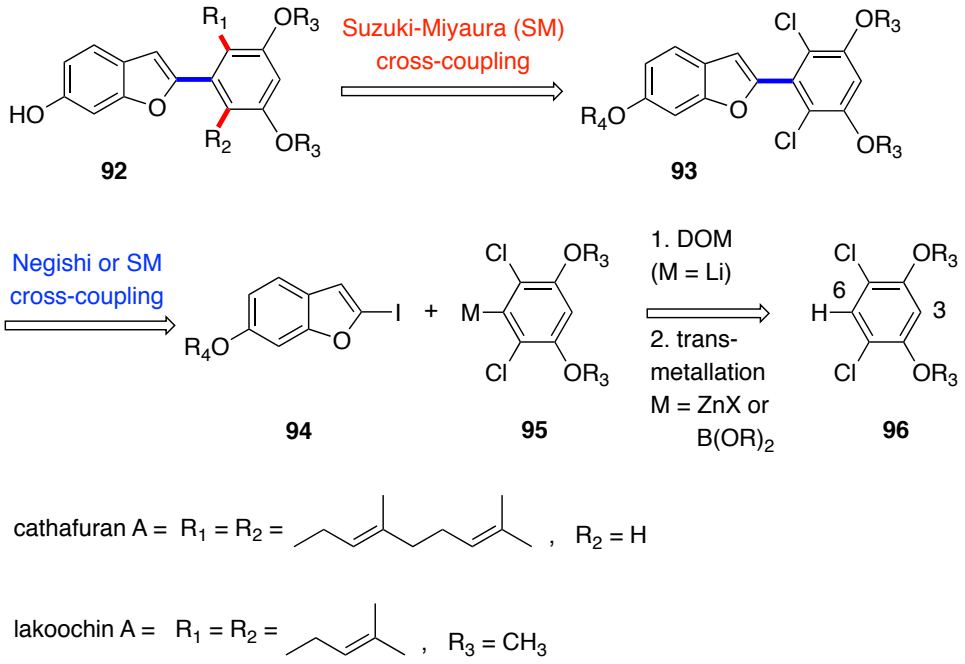

Scheme 12: Retrosynthetic analysis of cathafuran A and lakoochin A.

3.3 Construction of 2-arylbenzofuran core

The construction of the key 2-arylbenzofuran core started with the preparation of 2-halogentated benzofurans. Perhaps the most direct and widely used method for accessing 2-halogenated benzofurans is by α–lithiation of benzofuran substrates with an organolithium reagent (typically alkyl lithiums) followed by trapping with an electrophilic halogen source. Therefore, this method was first investigated for the synthesis of 2-halogenated benzofurans. 2-Idodobenzofuran (**98**) was prepared directly from **97** via lithiation with *t*BuLi in Et_2O at –78 °C (Scheme 13, Reaction A). When the same reaction was carried out using *n*BuLi, no reaction occurred and only starting material was recovered. Compound **98** was prepared to use as a model substrate for

developing cross-coupling conditions for the constructuion of 2-arylbenzofurans since **98** is easier to prepare than 2-iodobenzofuran **102**.

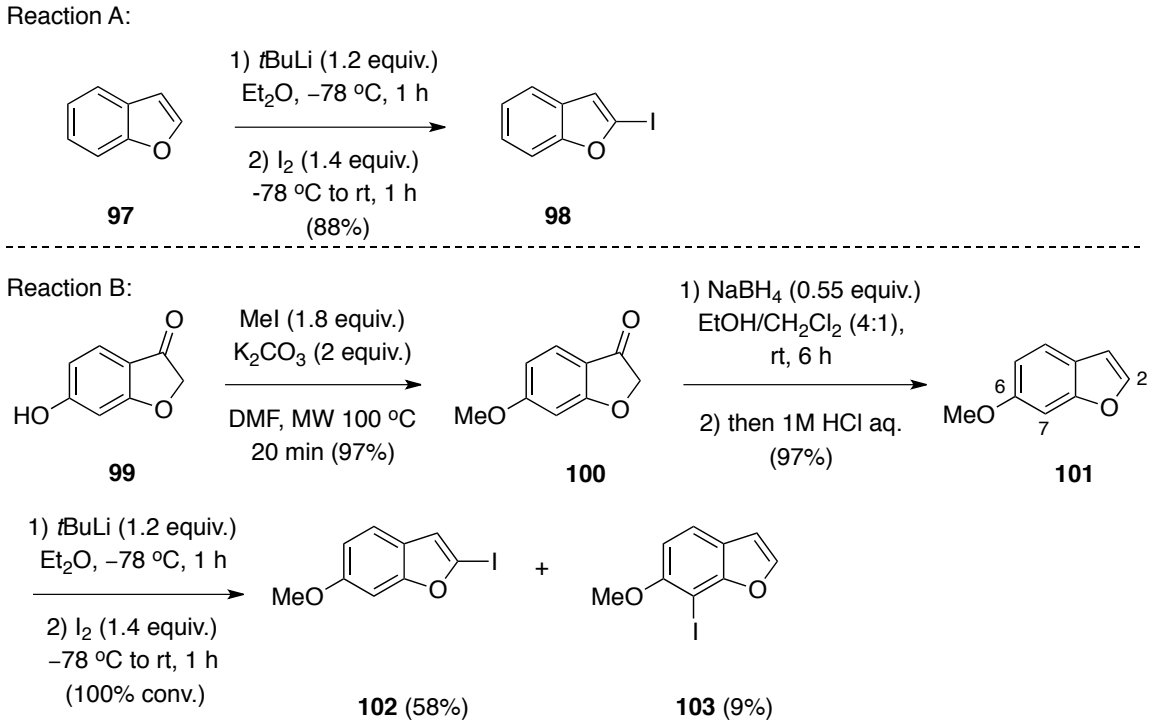

Scheme 13: Synthesis of 2-iodobenzofurans **98** and **102**.

Compound **102** was prepared from commercially available 6-hydroxy-3-coumaranone (**99**) over three steps. First, **99** was methylated with MeI under standard conditions using microwave irradiation as the heating source. While methyl ethers require harsh reaction conditions for their removal, protection as the methyl ether was chosen for a number of reasons. Firstly, to increase the solubility of the benzofuran for subsequent reactions. Secondly, many naturally-occurring compounds contain methylated moieties. Lastly, other bulkier protecting groups such as trialkylsilyl protecting groups, are easily removed by aqueous acids/bases and fluoride salts. That last point is extremely important since the

methodology developed for introducing prenyl and geranyl groups (see Chapter 2) onto aromatic rings operates under strongly basic conditions (5M KOH). Reduction of **100** to **101** was achieved using $NaBH_4$ followed by hydrolysis of the resulting alcohol with 1 M HCl aqueous. Lastly, deprotonation with *t*BuLi and quenching with a slight excess of iodine gave iodinated compound **102** in 58% yield, with 7-iodo-6-methoxybenzofuran (**103**) also being observed (Scheme 13, Reaction B).

While C-2 functionalization of benzofuran (**97**) itself can be achieved readily by lithiation at the benzylic position (i.e., the α-position), the analogous reaction with **101** to give **102** is not so straightforward. The methoxy group at C-6 introduces competitive deprotonation at C-7 by acting as a directing group for DoM and by acidifying the proton. This leads to the formation of 2- and 7-iodo-6-methoxybenzofuran in a 2.3:1 ratio (Table 8, Entry 1). Under similar reaction conditions, Widdowson and co-workers observed the same selectivity issue when trying to synthesize **102** and its organostanane analogue from **101**.[102] However, increasing the temperature from −78 °C to room temperature they were able to increase selectivity for the 2-substituted products from 1:1 to 4:1 (C-2:C-7-substituted). Unfortunately, increasing the temperature from −78 °C to room temperature here did not improve selectivity for the 2-lithio species (Table 8, Entry 1 vs 3). Additionally, changing the alkyllithium from *n*BuLi to *t*BuLi was examined at −78 °C (Entry 2). As was seen with benzofuran no reaction occurred (Scheme 13). It has been well established that the coordinating ability of an organolithium to a directing group (i.e., heteroatom) on a substrate can be greatly altered by introducing strongly coordinating solvents, such as THF or TMEDA into the reaction mixture.[103] Once

coordinated to the basic solvent, the Lewis acidity of the organolithium decreases as well as the coordinating ability of the directing group. As a result, the metalation is directed less by coordination and more by the acidifying effects of the heteroatom. Therefore, in an attempt to favour metalation at the α-position (i.e., the more acidic proton) over DoM, the solvent was switched from Et_2O to THF (Table 8, Entry 4). Unexpectedly, this led to the formation of more DoM product (i.e., **103**) than the product resulting from α-lithiation (i.e., **102**). While DoM can be avoided by bulking up the hydroxy-protecting group, for example to *t*-butyldiphenysilyl ether, this was not a viable option in our synthetic strategy for reasons stated previously. Although the selectivity for compound **102** was low using this procedure, compounds **102** and **103** can be separated by column chromatography.

Table 8: Optimization of α–lithiation reaction conditions – Organolithium and solvent study.

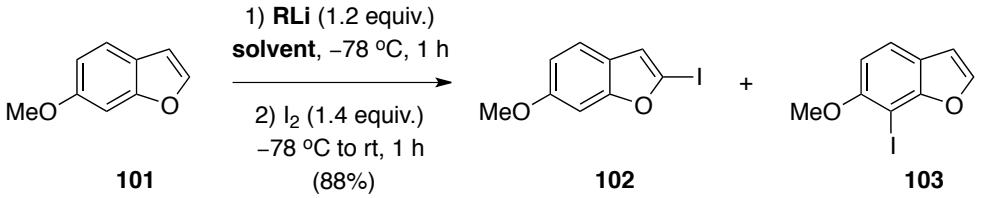

101 **102** **103**

Entry	Solvent	RLi	Temp (°C)	Conv (%)	Product Ratio (**102**:**103**)[a]
1	Et_2O	*t*BuLi	–78	100	2.3:1
2	Et_2O	*n*BuLi	–78	0	-
3	Et_2O	*n*BuLi	25	100	1.9:1
4	THF	*t*BuLi	–78	100	1:1.4

[a] Ratios were determined by ^{1}H-NMR spectroscopy on crude reaction mixtures.

With the α-lithiation procedure proving non-selective for the preparation of 2-halogenated benzofurans, alternative methods were investigated for preparing these substrates. In 2009, Lautens and co-workers reported the synthesis of a wide range of 2-

halogenated benzofurans from *gem*-dibromoolefins using an intramolecular Ullmann cross-coupling procedure (Scheme 14).[104] Intramolecular cross-coupling reactions using palladium catalysts proved unsuccessful, often providing complex mixtures of products or recovered starting material. The authors also report a protocol for preparing *gem*-dibromoolefin precursors from commercially available salicylaldehyde derivatives using a protecting group free Ramirez olefination procedure (Scheme 14).

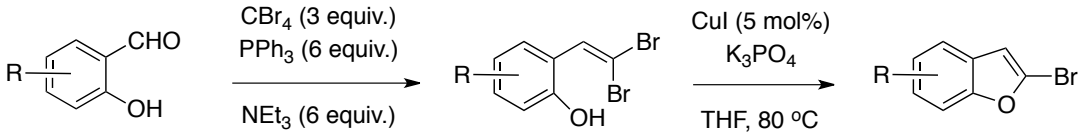

Scheme 14: Synthesis of 2-bromo benzofurans by intramolecular Ullmann coupling from *gem*-dibromovinyl phenols.

Intrigued by this study, the synthesis of *gem*-dibromoelfin (**104**) was attempted using the conditions outlined in Scheme 15. Unfortunately, conversion to the desired product was low with mostly starting material recovered, which proved difficult to separate and isolate by silica gel chromatography (Scheme 15). Although the authors note that the use of excess ylide and slow addition of reagents were necessary for high yields, these claims could not be reproduced.

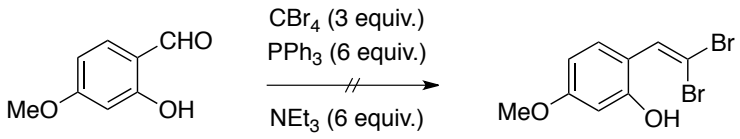

104

Scheme 15: Attempted synthesis of *gem*-dibromovinyl phenol (**104**).

Since 2-bromobenzofurans proved more challenging to prepare than their 2-iodo analogues, this route was abandoned and 2-iodobenzofurans **98** and **102** were used to

investigate Pd-catalyzed cross-coupling conditions for the synthesis of the advanced 2-arylbenzofuran core (**93**).

With compounds **98** and **102** in hand, attention was focused on preparing organometallic reagent **95**, where M = $B(OR)_2$ or ZnX. As previously mentioned, it was envisioned that **95** could be prepared by selective deprotonation at C6 (i.e., between the two chlorides) affording the lithium salt of **95**, which following transmetallation to the corresponding boron or zinc derivative could then be cross-coupled with heteroaryl iodides **98** and **102** yielding compound **93** and its derivatives (Scheme 12). Based on a report by Kraus and Zeng,[105] compound **105** was selectively lithiated between the two chlorides with *n*BuLi in THF at −78 °C for 1 hour and then quenched with deuterated methanol (CD_3OD). As was observed by Kraus and Zeng, the only product obtained was that resulting from substitution at C6 (Figure 18). Compound **107** was characterized by ^{1}H-, ^{2}H- and ^{13}C-NMR spectroscopy and High Resolution Mass Spectrometry (HRMS). ^{1}H-NMR showed only one signal in the aromatic region at 6.55 ppm, which corresponds to the proton at C3 and ^{2}H-NMR showed one signal at 6.36 ppm, which corresponds to deuterium at C6 (Figure 18). This information led to the conclusion the deprotonation did indeed occur exclusively at C6 and was further supported by ^{13}C-NMR spectroscopy and HRMS (see Chapter 5).

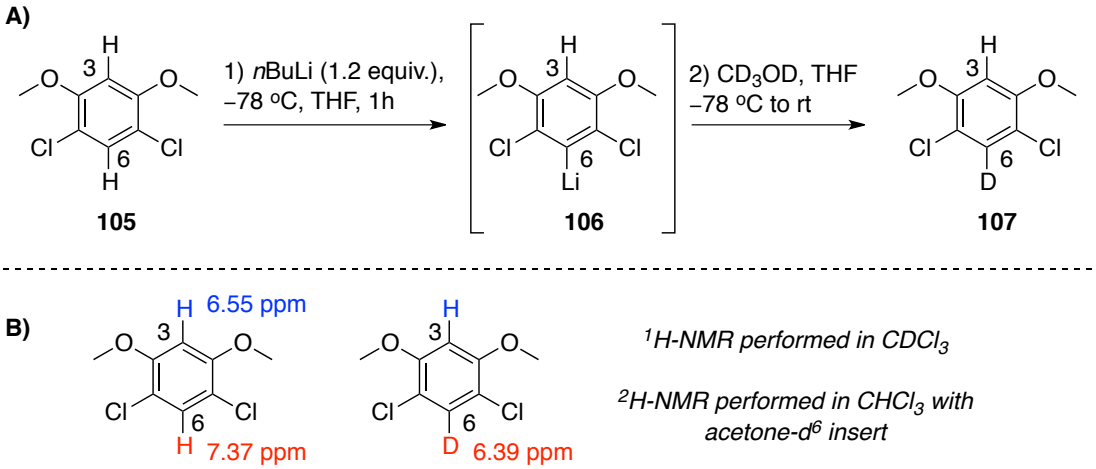

Figure 18: (A) Preparation of 2,4-dichloro-3-deuterium-1,5-dimethoxybenzene (**105**); and (B) key proton and deuterium signals of compounds **105** and **107** observed by ^{1}H- and ^{2}H-NMR spectroscopy.

With this knowlegde, attention was then focused on converting the lithium salt (**106**) to the corresponding organo-boron and -zinc reagents. TM to boron was investigated first as these organometallic reagents are generally more stable and easier to store and handle than organozinc reagents. Aryllithiums, such as **106** can be converted to arylboronic acids by treatment with a trialkylborate reagent at low temperatures (typically −78 °C), followed by an acidic aqueous workup (Table 9, Entries 1-5). Similarly, **106** can be treated with a more robust trialkyborate, such as 2-isopropoxy-4,4,5,5-tetramethyl-1,3,2-dioxaborolane (*i*Pr-O-Bpin), to give the arylboronic ester **108b** (Table 9, Entry 7). As shown in Table 9, quenching with triethylborate ($B(OEt)_3$) and then hydrolyzing to the boronic acid with 1M HCl (entries 3-5) proved to be more successful than using triisopropylborate ($B(O\text{-}iPr)_3$), as only trace amounts of product were observed (entries 1-2). Although good conversion was observed with $B(OEt)_3$, isolating and purify **108a** was problematic, with **108a** only being isolated once in moderate yield (Entry 3). Other

subsequent reactions contained an unknown impurity seen in the crude ^{1}H-NMR spectra, even when different work-up procedures were used (entries 4 and 5). It was thought the impurity might be some other type of acidic species so D_2O was added to a ^{1}H-NMR sample in DMSO-d[6] and analyzed (Entry 4).

Table 9: Preparation of 2,6-dichloro-3,5-dimethoxyphenylboronic acid (**108a**) and boronic ester (**108b**).

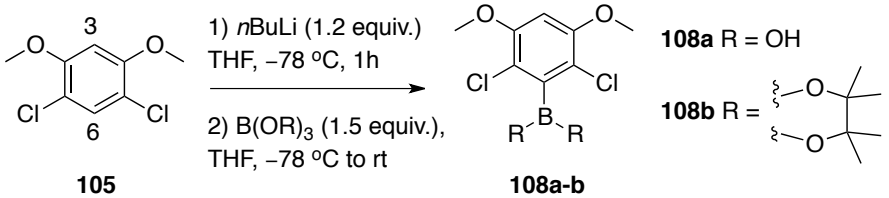

105 **108a-b**

Entry	Boron Reagent	Time (h)[a]	Work-up[b]	Product	Conversion (%)[c]
1	B(O-*i*Pr)$_3$	0.5	1M HCl	**108a**	0
2	B(O-*i*Pr)$_3$	12	1M HCl	**108a**	Traces
3	B(OEt)$_3$	0.5	1M HCl	**108a**	100 (64%)
4[d]	B(OEt)$_3$	0.5	1M HCl	**108a**	97
5[d]	B(OEt)$_3$	0.5	1M HCl[e]	**108a**	86 (0%)
6	*i*Pr-OB(pin)	12	NH_4Cl	**108b**	100 (72%)

[a] Time that solution stirred following addition of the boron reagent and prior to the addition of HCl/NH_4Cl. [b] Reaction acidified to a pH ~2-4. [c] Conversions determined by ^{1}H-NMR spectroscopy of the crude reaction mixtures. Yields are given in parentheses. [d] Crude reaction mixture showed an unknown peak at 6.54 ppm in the ^{1}H-NMR spectrum. [e] Reaction acidified to a pH 1.

Disappearance of both proton signals at 8.50 ppm and 6.54 ppm confirmed the presence of two acidic species. The singlet observed at 6.54 ppm was attributed to the unknown impurity since arylboronic acids typically display singlets between 8-9 ppm. Unfortunately, all attempts to remove the unknown impurity were unsuccessful. Both **108a** and **108b** were fully characterized by ^{1}H-NMR, ^{13}C-NMR, ^{11}B-NMR and HRMS.

With compounds **108a** and **108b** in hand, we then proceeded to test their reactivity in the Suzuki-Miyaura cross-coupling of 2-iodobenzofuran (**98**) using *Pd*-

PEPPSI-IPr (**50**) as the catalyst. Using conditions previously developed by the Organ group,[68] **108a** was reacted with **98** under microwave irradiation as the source of heating (Scheme 16, reaction A). Unfortunately, the reaction did not work and only starting materials were recovered. Following a procedure developed by Yamamoto and co-workers,[106] **98** was reacted with 2 equiv. of **108b** in the presence of **50** (Scheme 16, reaction B). Again, no reaction was observed. With both **108a** and **108b** proving to be unreactive, attention was focused on making the corresponding organozinc reagents and testing their reactivity in Negishi cross-coupling.

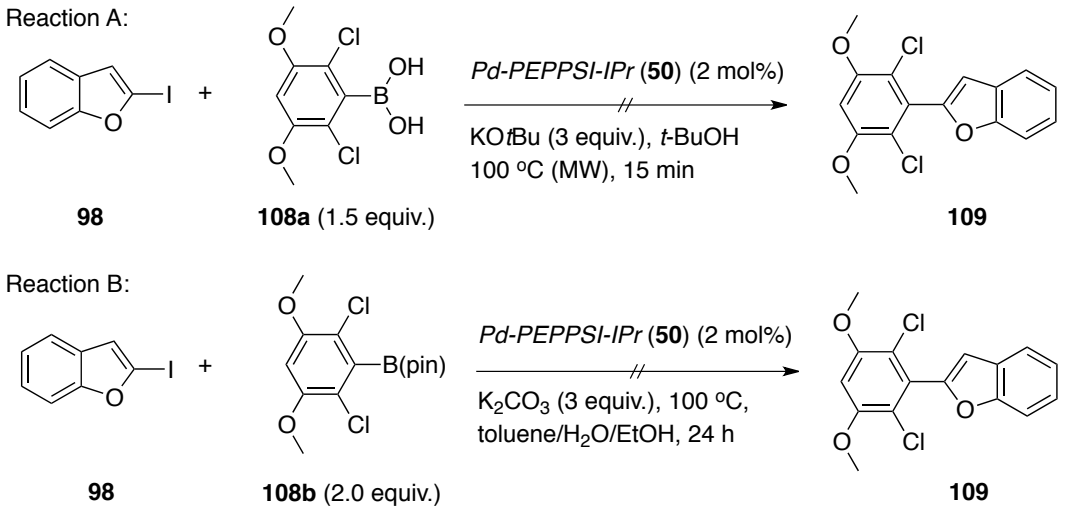

Scheme 16: Attempted synthesis of 2-arylbenzofuran **109** by Pd-catalyzed Suzuki-Miyaura coupling of aryl boronates **108a** and **108b**.

In 2004, Buchwald and co-workers developed a one pot Negishi cross-coupling reaction where organozinc reagents were prepared *in situ* from the corresponding aryllithium salt.[107] In the presence RuPhos (Figure 12, Chapter 1), a range of (hetero)aryl bromides and chlorides were coupled with a variety of challenging arylzincs in good-to-excellent yield. With the knowledge that compound **105** could be selectively

deprotonated between the two chlorine atoms, organozinc **110** was prepared *in situ* using the Buchwald and co-workers DoM protocol by treating **105** with *n*BuLi, followed by addition of zinc chloride ($ZnCl_2$) and allowing the reaction to warm to room temperature (Scheme 17). Unfortunately, quantifying arylzinc **110** was not possible as titration with iodine in THF saturated with LiCl (ca. 0.5M) using Knochel's procedure[108] did not work, thus **110** was carried forward under the assumption that it was formed fully.

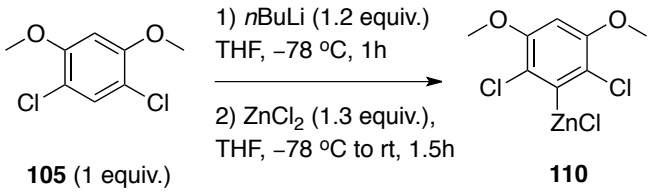

Scheme 17: Preparation of organozinc **110**.

Next, *Pd-PEPPSI-IPr* (**50**) was screened against Buchwald's RuPhos ligand to see if it was a suitable catalyst for this Negishi coupling (Table 10). As shown in Table 10, **50** performed just as well as RuPhos in coupling **110** with **98** and so, **50** was used for further optimization (Entries 1 and 2). The stability of organozinc **110** was also investigated. A stock solution of **110** was prepared in advance and stored at room temperature. After 1 day, conversion of the reaction dropped from 100% to 85% (Entry 3) and after 5 days the conversion further dropped down to 31% (Entry 4). Storing **110** in the fridge did little to improve conversion to product **109**. These results suggest that organozinc **110** is unstable and therefore should be used shortly after preparation. Further optimization showed that the temperature could be lowered from 100 °C to 50 °C with no loss in conversion (Entry 5). Lastly, increasing the amount of $ZnCl_2$ from 1.1 equiv. to 1.5 equiv. (with respect to

105) also improved conversion to product **109** (Entry 10). Under these same conditions (i.e. Entry 10) compound **111** was produced in good yield.

Table 10: Optimization of Negishi reaction conditions for the preparation of 2-arylbenzofurans **110** and **111**.

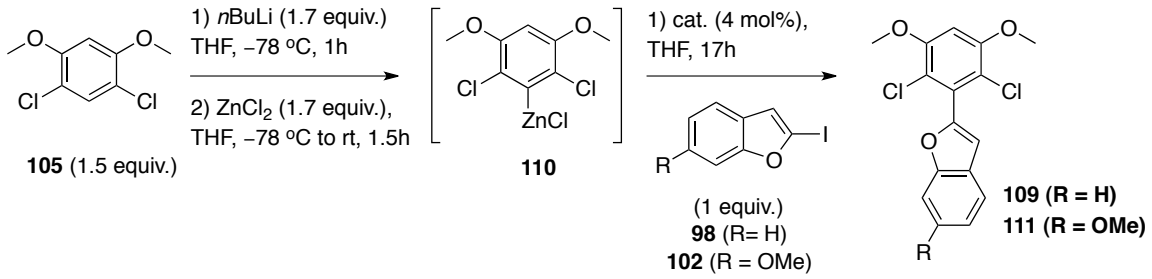

Entry	Aryliodide	Catalyst	Temp. (°C)	Major Products	Conv. (%)[a]	Yield (%)[b]
1	H	Pd_2dba_3/RuPhos	100	**109**, **105**	100	65
2	H	*Pd-PEPPSI-IPr* (**50**)	100	**109**, **105**	100	60
3[c]	H	**50**	100	**109**, **105**	85	58
4[d]	H	**50**	100	**109**, **105**	31	-
5	H	**50**	50	**109**, **105**	100	64
6	H	**50**	25	**109**, **105**	32	-
7[e]	H	**50**	50	**107**	100	98
8[f]	H	**50**	50	**107**	100	96
9[g]	H	**50**	50	**109**, **105**	100	60
10[h]	H	**50**	50	**109**, **105**	100	75
11	OME	**50**	50	**111**, **105**	100	72

[a] Conversions determined by ^{1}H-NMR spectroscopy of the crude reaction mixtures and are relative to residual starting material **98**/**102**. [b] Yields are reported on isolated products (**93-94**) following silica gel chromatography. [c] Stock solution of organozinc **110** was prepared prior to the reaction, stored at room temperature and used 1 day later. [d] Stock solution of organozinc **110** was prepared prior to the reaction, stored at room temperature and used 5 day later. [e] Aryllithium **106** quenched with CD_3OD. [e] Organozinc **110** quenched with CD_3OD. [f] The crude reaction mixture was quenched with CD_3OD at the end of the reaction. [h] $ZnCl_2$ was increased from 1.1-1.5 equiv. with respect to **105**.

While all of **98** is consumed, only 70-80% of the desired product is isolated, the rest being mostly starting material **105** and traces of homocoupled arylhalide. From previous studies, it was established that DoM of **105** goes to completion within an hour so this can't be the reason for the low conversions observed. Perhaps TM with organozinc **110** is

slow and upon reaction workup gets quenched in the process. Therefore, at the end of the reaction deuterated methanol (CD_3OD) was added instead of water. Compound **107** was observed, along with homocoupling of the aryl halide. Since both aryllithium **106** and organozinc **110** can react with CD_3OD (entries 7 and 8), this result suggests that either: 1) TM of **106** to **110** is not complete, which would explain the low reaction yields as **106** won't react under these conditions; or 2) TM with **110** is slow and the reaction isn't being given enough time to go to completion. With a protocol for accessing 2-arylbenzofurans **109** and **111** in hand, attention was focused on developing mild conditions for introducing prenyl and geranyl side chains into aromatic systems that would be highly selective for the linear product, thus providing access to the natural products shown in Scheme 12.

3.4 Introduction of Allylbornic Acid Pinacol Ester Derivatives onto 2-arylbenzofurans 109 and 111.

With a protocol worked out for introducing prenyl and geranyl side chains onto aromatic systems with both high regio- and stereoselectivity, attention was then focused on using this methodology to synthesize the desired natural product targets cathafuran A and lakoochin A.

3.4.1 Optimization Study

Using **109** as a model substrate, the coupling of **60a** was first explored under the optimized conditions, however allowing the reaction to proceed for 48 h (Table 11, Entry 1). This resulted in little formation of the desired dicoupled product (**114**), with mostly starting material recovered. After a short but intensive optimization study, it was found

that increasing the concentration of the reaction mixture, base, and catalyst loading to 0.5 M, 7 M, and 6 mol%, respectively, provided optimal results (Entry 8).

Table 11: Optimization study - Regioselective prenylation of **109** with **60a** catalyzed by **53**.

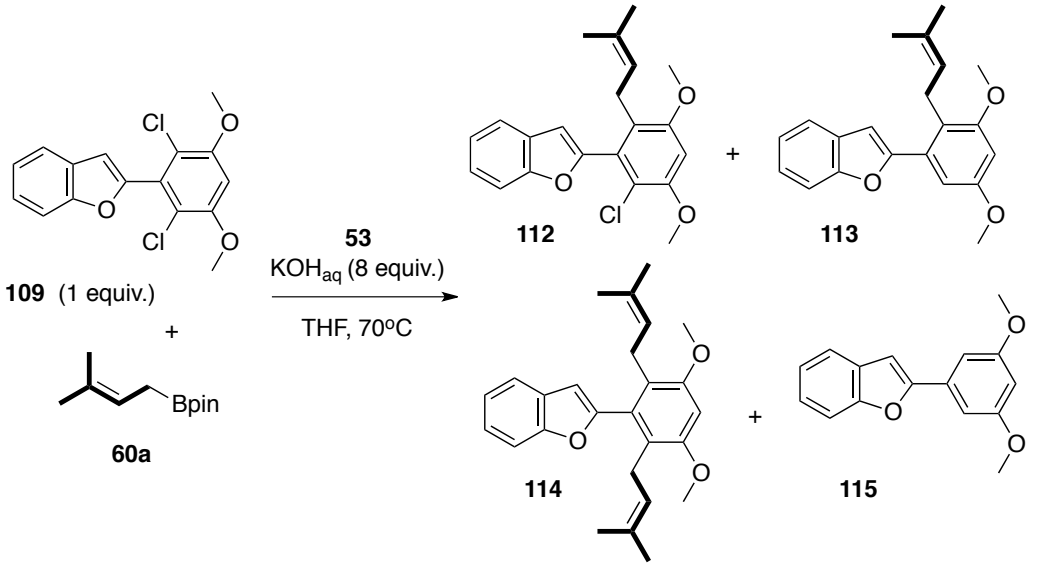

Entry	**60a** (equiv.)	**53** (mol%)	KOH_{aq} (M)	Conc. (M)	Time (h)	Product Conv. (%)[a] **109**	**112**	**113**	**143**	**115**
1	3	2	5	0.25	48	40	27	10	5	18
2	3	3	5	0.25	24	26	35	16	10	13
3	1.5	3	5	0.25	24	35	33	14	6	12
4	3	3	5	0.5	24	6	44	23	23.5	3.5
5	3	3	5	1.0	24	10	49	23	14	4
6	3	3	7	0.5	24	0	25	31	40.5	3.5
7	6	3	7	0.5	24	10	66	17	10	3
8	3	6	7	0.5	24	0	0	39	56	5
9	3	10	7	0.5	24	0	0	41	52	7
10	3	6	10	0.5	24	0	0	42	51.6	6.5

[a] Product ratios were determined by ^{1}H-NMR spectroscopy of the crude reaction mixtures.

As seen in Table 11, it is apparent that reduction of arylchloride **109** is a competing side reaction (i.e. formation of **113** and **115**) that cannot be avoided entirely. Prior to

optimizing the reaction conditions outlined in Table 11, compound **112** was made by reacting **109** with 1.5 equiv. of **60a** (Entry 3). Comparing the results of this reaction to those in Entry 2, essentially no difference is seen to all products. While the formation of **115** can be understood as bis reduction, it was unclear how **112** was being formed. There are two possible explanations: 1) after OA, reduction of **109** is faster than TM, leading to intermediate **116** which can then re-enter the catalytic cycle to go on and form **113**; or 2) **112** is less reactive than **109**, leading to reduction of arylchloride **112** and formation of **113** instead of undergoing TM to give compound **114** (Scheme 18).

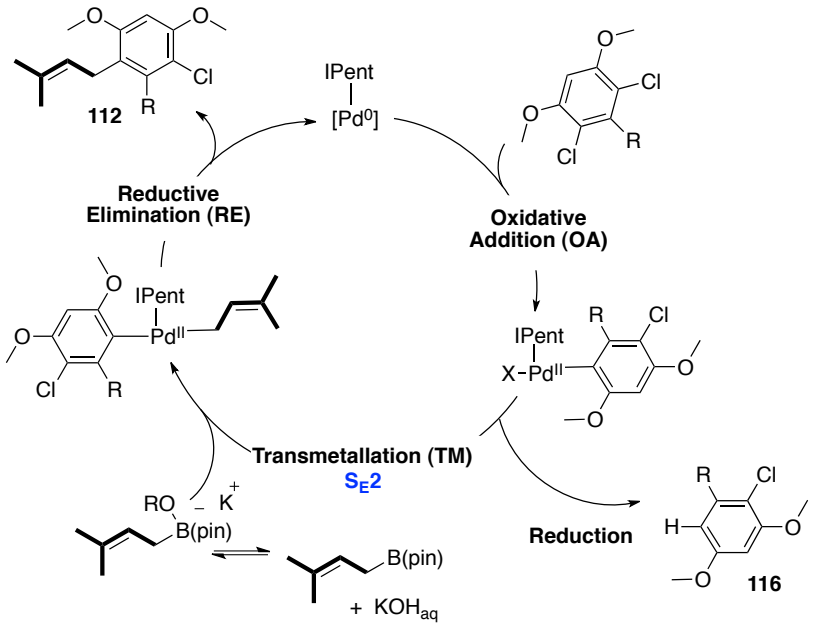

Scheme 18: Proposed mechanism for the formation of **112** and **116**.

The crude reaction mixture from Entry 8 was subjected to silica gel chromatography, eluting with a gradient of pentane/ether (pentane → 5/95 ether/pentane) to obtain compounds **113** and **114** as a mixture due to similar retention factor (R_f) values in addition to another unknown impurity. The mixture was further purified by High

Pressure Liquid Chromatography (HPLC) using a C-18 analytical column and a gradient of MeCN/H_2O eluent system. Unfortunately, due to the small loading volumes of the analytical column only enough sample was collected to run characterization studies (e.g., ^{1}H- and ^{13}C-NMR spectroscopy, HRMS, etc.). Further purification using a C-18 semi-preparative column was attempted using a similar gradient eluent system to the analytical column. Five fractions were collected and analyzed by ^{1}H-NMR spectroscopy. Preliminary analysis of the fractions indicates that this separation method was unsuccessful in separating the compounds as none of the fractions collected match the compounds isolated using the analytical column. Further analysis of the fractions by Gas Chromatography Mass Spectrometry (GC/MS) system confirm that this was the case, therefore, yields for compounds **113** and **114** cannot be reported at this time. Isolated products obtained from the HPLC analytical fractions were fully characterized by 1D and 2D NMR spectroscopy and connectivity was determined using ^{1}H-^{1}H COSY, ^{1}H-^{13}C HSQC and ^{1}H-^{13}C HMBC spectroscopy.

3.4.2 Synthesis of methylated lakoochin A and cathafuran A

The successful synthesis of model substrate **114** encouraged us to apply the optimized conditions to the synthesis of lakoochin A and cathafuran A. Methylated lakoochin A (**116**) was prepared by coupling **111** with **60a** and methylated cathafuran A (**118a**) was prepared by coupling **111** with **60b**. Both reactions proceeded smoothly under the optimized conditions with mono-coupled ($\mathbf{P^M}$) and di-coupled ($\mathbf{P^D}$) products observed as the major products (Table 12).

Table 12: Synthesis of methylated lakoochin A and cathafuran A.

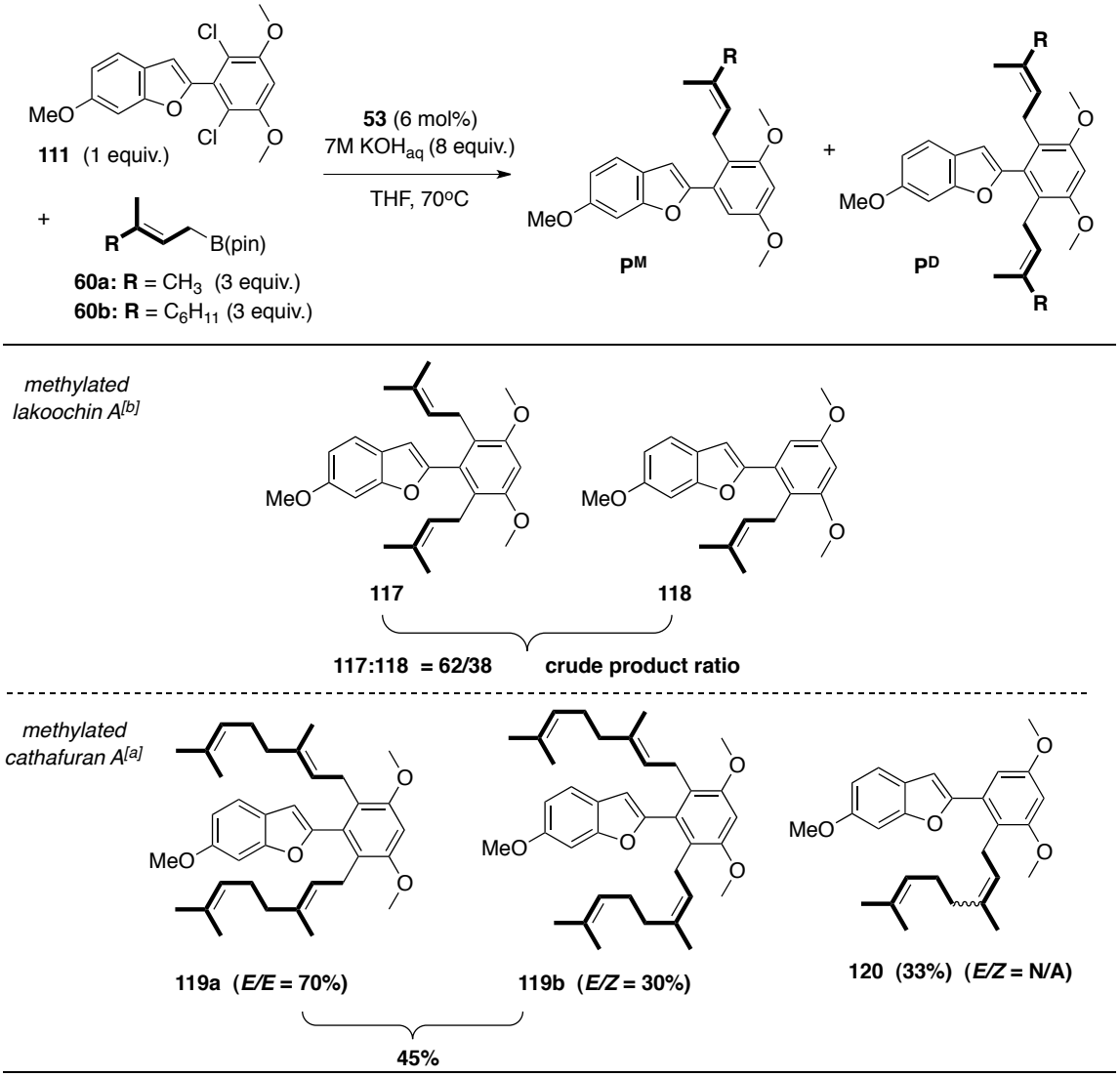

[a] Product ratios were determined by ^{1}H-NMR spectroscopy of either the crude or purified reaction mixtures. [b] Yields of the isolated products following silica gel chromatography are reported. *E/Z* ratios were determined using the volume integration of the 2D ^{1}H-^{13}C HSQC pulse program as provided by the Bruker pulse program library. [c] Product ratios were determined by ^{1}H-NMR spectroscopy of the crude reaction mixtures.

The crude reaction mixture for the synthesis of methylated lakoochin A looked promising with 62% conversion to the desired dicoupled product (**117**) and 38% conversion to the monocoupled product (**118**) observed. Unfortunately, purification by silica gel chromatography proved to be ineffective at separating **117** and **118** from the

rest of the side products in the reaction mixture. Since the HPLC C-18 semi-preparative column did not work well for model substrate **114**, it was decided not pursue this substrate any further.

The crude reaction mixture for the synthesis of methylated cathafuran A showed 60% conversion to the desired dicoupled product (**119**) and 40% conversion to the monocoupled product (**120**). The crude mixture was subjected to silica gel chromatography, eluting with a gradient of toluene/hexane (50% → 75% toluene/hexanes) to obtain two fractions. Fraction 1 was characterized by 1D and 2D NMR spectroscopy on a Bruker AV 400 and DRX 600 NMR spectrometers. Connectivity was determined using ^{1}H-^{1}H COSY, ^{1}H-^{13}C HSQC and ^{1}H-^{13}C HMBC, while assignment of the *E/Z* stereochemistry was completed by evaluating the proton interactions at the vinylic center using 2D ^{1}H-^{1}H gradient NOESY spectroscopy using a similar approach as described in Chapter 2, Section 2.5. Analysis of the correlation between H-1/H-4 in the NOESY spectrum, indicated *E*-stereochemistry whereas the correlation between H-1'/H-5' indicated *Z*-stereochemistry. Lastly, proton integration suggested more than 1 compound. Based on these results the following compounds were proposed (**119a-c**, Figure 19).

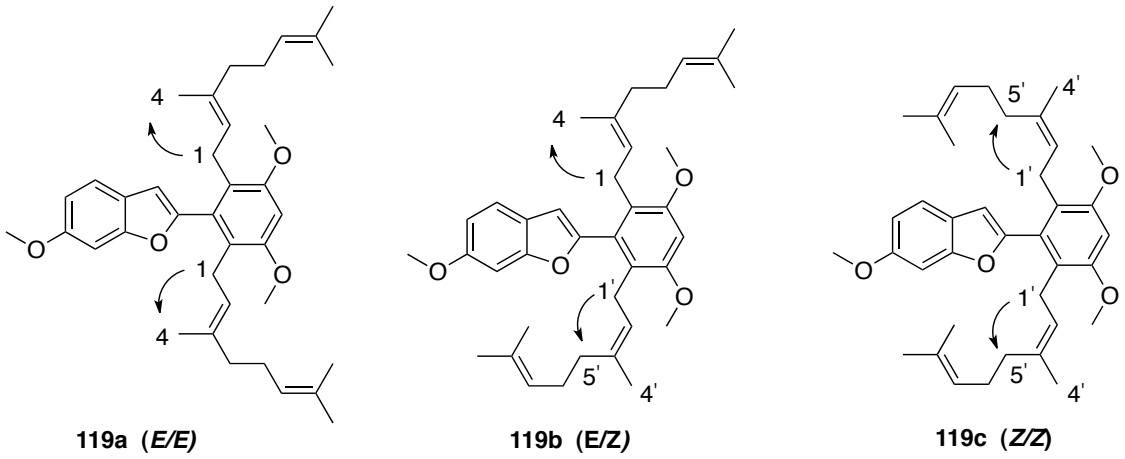

Figure 19: Proposed structures for compounds **119a-c**.

As discussed previously in Chapter 2, **60b** was shown to couple with 1-bromo-4-(*tert*-butyl)benzene (**62**) with 80% retention of *E*-configuration, the remaining 20% was determined to be the *Z*-isomer. Statistically speaking, it seems unlikely that a significant amount of compound **119c** would form. After completion of the first catalytic cycle, the olefin geometry should be 80/20 *E/Z*. For **119c** to form in an appreciable amount, that same 20% (i.e., *Z*-isomer) from the first cross-coupling would need to couple a second time and form the *Z*-isomer, which only has a 20% probability of happening. Therefore, we propose the two compounds in fraction 1 are **119a** and **119b**, as they would have a higher probability of forming. The yield of each compound was determined by integration of the resolved proton signals in the alkyl region (i.e., 0-2 ppm). Fraction 2 contained one major compound corresponding to monocoupled product (**120**) and a small amount of some other unknown impurity.

3.5 Attempted O-dealkylation of Aryl Methyl Ethers

With compound **119** in hand, the next step was O-dealkylation of the methyl ethers to provide the desired final target, cathafuran A. Aryl methyl ethers can be cleaved using a number reagents, including Lewis acids, alkaline reagents, silicon compounds, oxidizing agents, and reducing agents.[109] While a number of these reagents are reported to give monodemethylated products some can perform sequential demethylations in one flask. Using **85** as a model substrate, demethylation with BBr_3 was first investigated as this reagent is commonly used to perform sequential demethylations for dimethoxybenzenes (Table 13, Entry 1). The crude mass for the reaction was extremely low (< 20%) and analysis of the crude reaction mixture by ^{1}H-NMR showed no signs of either demethylated product. Disappearance of the vinylic proton on the prenyl side chain was also observed. One explanation for this observation could be that the bottle of BBr_3 used contained small amounts of HBr, which under the reaction conditions, could affect the integrity of the double bond.

Table 13: Double demethylation – Condition screen.

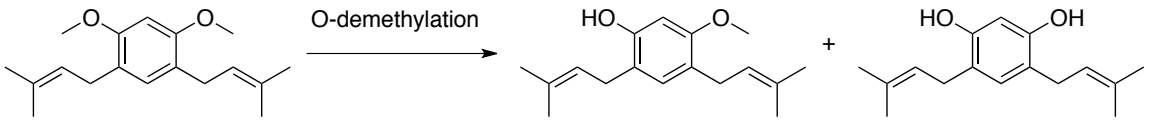

85 **121** **122**

Entry	Reagent	Conditions	Conv. (%)[a]		Yields (%)[b]	
			121	**122**	**121**	**122**
1	BBr_3 (4 equiv.)	DCM, –78 °C to 25 °C, 2 h	-	-	0	0
2	1-octanethiol (3 equiv.)	NaOH (6 equiv.), NMP, 130 °C, 20 h	100	0	85	0
3	Ph_2PH (4 equiv.)	*n*BuLi (4 equiv.), THF, 70 °C, 20 h	45	55	0	0

[a] Product ratios were determined by ^{1}H-NMR spectroscopy of the crude reaction mixtures. [b] Yields are reported on isolated products following silica gel chromatography.

Strongly nucleophillic reagents, such as alkyl thiolates[110] have also been shown to perform sequential demethylations. However, the bad smell and toxic gases that arise during the reaction and work-up with alkyl thiolates make them unpleasant to work with and have limited their use compared to other demethylating reagents. More recently, papers describing the use of long chain thiols have been reported as 'odourless demethylation' reactions.[111,112] Upon work-up with an aqueous base, thiol by-products remain in the organic phase. The product can then be extracted back into the organic phase by adjusting the pH of the aqueous solution to an acidic pH. With this knowledge, **85** was treated with 1-octanethiolate (3 equiv.) and heated to 130 °C in *N*-methyl-2-pyrrolidone (NMP) for 20h (Table 13, Entry 2). While all of **85** was consumed, only one of the methoxy groups was cleaved to give the monodeprotected product (**121**). To see if the olefin on the prenyl side chain was having a negative impact on the reaction, 1,3-dimethoxybenzene was reacted under the same conditions outline in Entry 2. Again, only monodemethylated product was observed. Lastly, deprotection with lithium diphenylphosphide ($LiPPh_2$) was screened as this reagent has been reported to work with a number of prenylated natural products, including compound **118** which gives demethylmoracin I.[40f] After 20 h, the reaction was quenched with aqueous NH_4Cl. Analysis of the crude reaction mixed showed both the monodeprotected (**121**) and double deprotected (**122**) in 55% and 45% conversion, respectively. Another by-product was also observed which could not be completely separated from **122** by column chromatography.

3.6 Conclusion

In conclusion, combining the regioselective lithiation of **105** with Buchwald and co-workers' one pot Negishi cross-coupling protocol, using *Pd-PEPPSI-IPr* (**50**) as the catalyst, was found to be a reliable method for producing 2-arylbenzofurans **109** and **111**. The regio- and stereoselective Suzuki-Miyaura methodology developed with *Pd-PEPPSI-IPent* (**53**) was investigated, and was found to couple prenylboronic acid pinacol ester **60a** with 2-arylbenzofuran **109** with high α–selectivity. After a quick re-optimization study, it was found that a concentration of 0.5M of the reaction mixture, a 6 mol% catalyst load, and 7M KOH was necessary to achieve optimal results. Although these conditions diminished aryl halide reduction, this side reaction was not entirely unavoidable as significant amounts of the mono-coupled product were still observed. Nevertheless, using this method, methylated cathafuran and lakoochin A were sythesized. While the mono- and di-coupled derivatives of lakoochin A (**117** and **118**, respectively) could not be separated from one another, methylated cathafuran A was obtained in 45% yield, with the major product being the desired *E/E* isomer.

Attempts to deprotect model substrate **85** have proven unsuccessful, with only approx. 50-60% of the double deprotected product obtained. Although demethylating conditions screened thus far have proven unsuccessful at cleaving both methoxy groups, other deprotection methods which do not involve Lewis acids could be investigated. Since a suitable deprotection method could not be found for removing multiple methoxy groups, the deprotection of methylated cathafuran A could not be achieved.

CHAPTER 4 – Investigating the Effects of Solvent and Kinetic Isotope Effects (KIEs) in the Directed *Ortho* Metalation (DoM) of 1,5-Dichloro-2,4-dimethoxybenzene

4.1 Directed ortho Metalation (DoM)

DoM is a powerful and efficient method in organic synthesis used for the functionalization of aromatic systems in a highly regioselective manner that are otherwise difficult to prepare by electrophilic substitution reactions. DoM may be viewed as a three step process and the generally accepted mechanism for DoM is depicted in Scheme 19.[15] First, an organolithium coordinates with the lone pairs of the Lewis basic heteroatom of the "directing metalating group" (DMG), forming a pre-lithiation complex. The organolithium used for the deprotonation step is usually *n*-, *s*-, or *t*-BuLi, however for more electron deficient aromatic rings, lithium diisopropylamide (LDA) can be used. Subsequent removal of the proton on the carbon *ortho* to the DMG results in the formation of an *ortho*-lithiated intermediate, which then reacts with a suitable electrophile to yield the 1,2-disubstituted arene. It is generally accepted that the regioselectivity of the reaction is a result of the pre-lithiation complex bringing the lithiating agent in close proximity to the acidic hydrogen on the aromatic ring.[113]

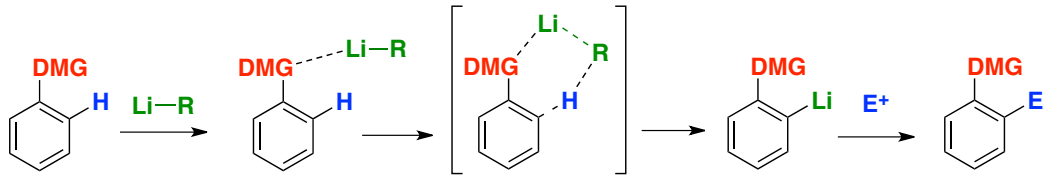

Scheme 19: Proposed mechanism of DoM.

The first example of a DoM reaction was reported independently by Gilman and Wittig, where *n*BuLi was found to deprotonate anisole exclusively at the *ortho* position of the (DMG) (i.e., OMe) (Scheme 19).[15] Since this discovery, over 40 DMGs have been identified and studied, with some DMGs also serving as protecting groups.[114,115] A suitable DMG group should contain the following: a coordination site for the alkyllithium to "dock" onto and no (or very poor) electrophilic sites, so that nucleophilic attack of the DMG instead of deprotonation can be avoided. In 1990, Snieckus divided the various DMGs into 5 main classes and ranked them based on their directing ability towards DoM and their application in synthesis (Figure 20).[15] Carboxylic acid and carbonate-derivatives (i.e., carbamates, oxazolines, amides) were grouped as the "N+O class" and are considered strong DMGs. Not only are these functional groups stongly electron-withdrawing, which significantly acidifies the adjacent protons on the ring, but they can also be transformed into other functional groups. Further, the multiple heteroatoms on these functional groups serve as strong coordination sites for the alkyllithium base. Conversely, halides are considered weak DGMs as these functional groups can only direct the organolithium by induction.

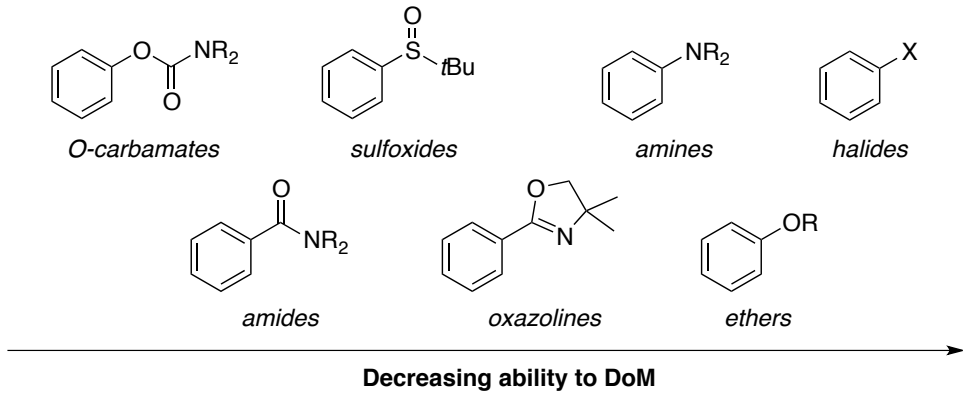

Figure 20: Selected examples for the ranking of DMG towards DoM.

Solvent choice also plays a major role in DoM. The electron-deficient lithium atom in an alkyllithium reagent requires greater stabilization than what can be provided by a simple 2 centre, 2 electron bond between itself and the carbon atom.[116] As a result, multi-centre bonds of lithium are formed with the surrounding solvent. Depending on the coordinating ability of the solvent, different aggregates are formed. For example, *n*BuLi tends to form hexamers in hydrocarbon solvents (e.g., pentane) and tetramers or dimers in etheral solvents (e.g., THF). In general, Lewis bases tend to break down alkyllithium aggregates, which in turn, increases the basicity of the organolithium reagent.[117]

While DoM has been used mainly to trap the resulting aryllithium with electrophiles by nucleophilic substitution, transmetallation has also proven to be an effective pathway into cross-coupling chemistry.[107,118] This approached appealed to us as we considered a general strategy for the preparation of the isoprenylated natural products cathafuran A and lakoochin A shown in Scheme 12 (Chapter 3, Section 3.2). In 2000, Kraus and Zeng reported the regioselective lithiation of **105**, quenching with a few electrophiles, such as primary alkyl halides and aldehydes, to produce a small collection of 5-substituted

resorcinols. This led Kraus and Zeng to conclude that C6 was also the site of deprotonation. Taking advantage of the regioselective metallation of **105**, we were able to combine this with Buchwald and co-workers' one pot Negishi cross-coupling protocol developed in 2004, to gain access to advanced benzofuran building blocks such as **111a**. While this method works well for accessing 2-arylbenzofurans, it was unclear how deprotonation was occurring and why only the formation of **111a** was observed and not its regioisomer (**111b**) (Figure 21). Therefore, a number of experiments were designed to further investigate the regioselective DoM of **105** to better understand the kinetic and thermodynamic profile of this transformation.

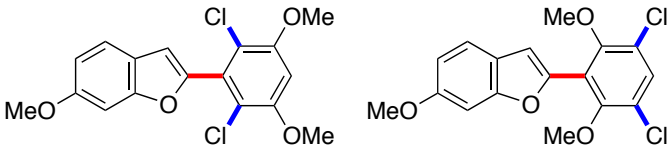

111a **111b**

Figure 21: Regioisomers of 2-arylbenzofurans.

4.2 Regioselective DoM of 1,5-Dichloro-2,4-dimethoxybenzene (105)

As observed by Kraus and Zeng, treatment of **105** with *n*BuLi in THF at −78 °C for 30 min. and then quenching with I_2 or deuterated methanol (CD_3OD) (Table 14, entries 1 and 5) led to the formation of products resulting from substitution at C6 between the two chlorides (e.g., **123**). While *ortho* lithiation between two chlorides is with precedent,[119] ether groups are known to be better directing groups for lithium, yet no products were observed resulting from deprotonation at C3. There are two competing effects here that deserve consideration: coordination and anion stability. The methoxy groups are better

templaters than the chlorine groups and would direct lithiation between them, however the site between the two chlorines is more acidic and would better stabilize the resulting carbanion. Therefore, we wondered if it was not more likely that deprotonation was occurring first at C3 between the methoxy groups and then the resulting anion (e.g., **126**) was isomerizing to the other site (e.g., **106**) to give the more thermodynamically stable anion (Scheme 20).

Table 14: DoM of **105** and electrophile in THF and Et_2O.

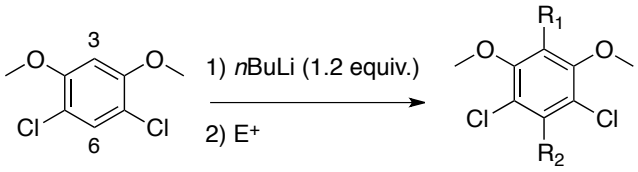

105

Entry	Solvent	Temp. (^oC)	Electrophile (E^+)	R_1	R_2	Product (% Yield)[a]
1	THF	−78	I_2	H	I	**123** (90%)
2	Et_2O	−78	I_2	H	H	**105** (88%)[b]
3	Et_2O	25	I_2	I	H	**124** (66%)
4	Et_2O	25	CD_3OD	D	H	**125** (75%)
5	THF	−78	CD_3OD	H	D	**107** (80%)

[a] Yields are reported on isolated products following silica gel chromatography. [b] Represents recovered starting material (**105**).

To address this, compounds **123** and **124** were prepared and reacted under metal/halogen exchange conditions using *t*BuLi to determine which anion is more thermodynamically stable. *t*BuLi was used instead of *n*BuLi to avoid quenching/alkylation problems associated with the *n*BuI byproduct of the exchange with *n*BuLi. Assuming metal/halogen exchange is significantly faster than deprotonation, it was anticipated that carbanion **106** would be more stable than **126** due to the close

proximity of the electron withdrawing chlorine groups, leading to the formation of **125** when **124** was lithiated. Indeed, this is what was found. Under nearly the same reaction conditions that were used to carry out the DoM reactions, lithiation of **124** (after quenching) led to the formation of **125**, while lithiation of **123** (after quenching) also led to the formation of **125**. These reactions revealed that isomerization of **126** to anion isomer **106** is extensive in THF. These results are also consistent with the idea that in THF anion **106** is the thermodynamic anion and deprotonation between the methoxy groups occurs first.

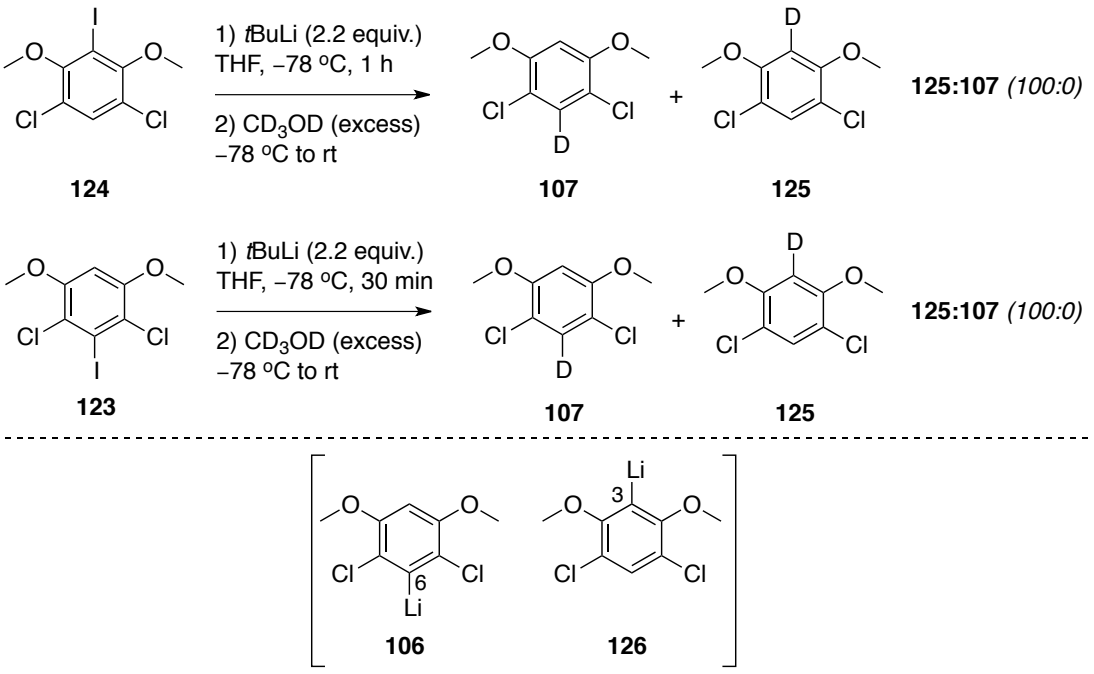

Scheme 20: Determination of the thermodynamic anion of **105** through isomerization studies in THF by Li-I exchange at C3 (**124**) and C6 (**123**).

To better understand the rates involved in the deprotonation and isomerization processes described above, time-course studies were conducted. Deprotonation was

examined first using **105** (Table 15) and was shown to be relatively slow at −78 °C as roughly 20% of **105** remained after 1 min (Entry 4). However, this study did reveal that deprotonation occurs first between the methyl groups at C3 (Entry 1), at least to some extent, and that isomerization of anion **126** to **106** does occur and that it is very fast. For example, the quench with I_2 in Entry 1 was done immediately following the application of the last drop of *n*BuLi. Assuming that deprotonation only occurs at C3, isomerization of **126** to **106** must be very rapid as only small amounts of compound **124** were detected.

Table 15: Regioselective lithiation of 1,5-dichloro-2,4-dimethoxybenezne (**105**) with *n*BuLi – A kinetic study.

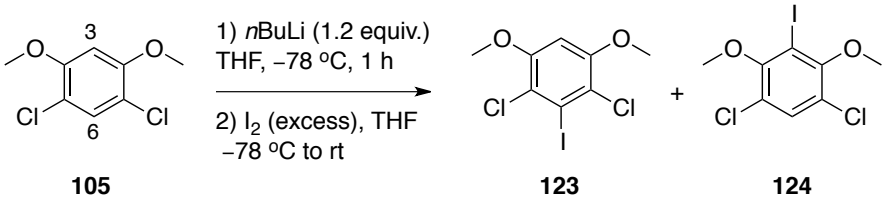

105 **123** **124**

Entry	Time (s)[a]	Product Distribution[b]			**123:124**
		123	**124**	**105**	
1	0.5	30	4	66	88:12
2[c]	0.5	31	6	63	84:14
3	30	59	2	39	96:4
4	60	79	2	19	98:2

[a] Time that solution stirred following addition of *n*-BuLi and prior to the addition of I_2. [b] Product distributions and ratios determined by ^{1}H-NMR spectroscopy on the crude reaction mixtures. [c] TMEDA (1.2 equiv) was mixed with *n*BuLi and stirred for 5 min prior to being added to solution of **105**.

To further examine the rate of isomerization, more time-course studies were conducted, using lithium-halogen exchange conditions since these reactions operate at near diffusion-limited rates (Table 16). Thus, **126** could be generated immediately and completely allowing isomerization to be tracked more meaningfully. When the reaction was quenched, just after the last drop of *t*BuLi was added, all of **124** was consumed and

isomerization to **106**, which leads to product **125**, had proceeded to 70% (Entry 1). While the results from Entry 1 show that isomerization of anion **126** to **106** is very rapid, it clearly slows down over time as it takes approximately one full hour to go to completion (Entries 3, 5, 6), which is suggestive that isomerization occurs by an intermolecular mechanism (See Section 4.2.3 below). Keeping the reaction time the same but lowering the temperature from -78 °C to -100 °C also seems to significantly affect the rate of isomerization. For example, Entry 2 shows that after the last drop of *t*BuLi was added, while all of **124** was still consumed, isomerization to **106** had only proceeded to 50%, whereas at -78 °C, 70% isomerization was observed (Entry 1).

Table 16: Lithium-Halogen exchange of **124** with *t*BuLi – A kinetic study.

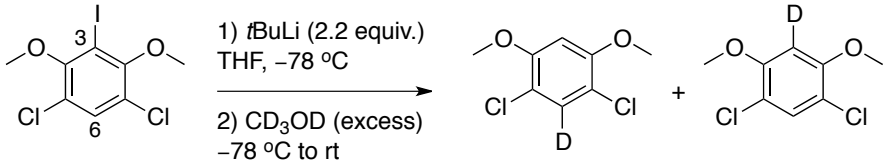

124 **107** **125**

Entry	Time [a]	Product Distribution[b]			**125:107**
		125	**107**	**124**	
1	0.5 s	28	70	1	30:70
2	0.5 s	46	53	1	50:50
3	30 s	20	78	2	20:80
4	30 s	42	57	1	40:60
5	30 min	20	80	0	20:80
6	60 min	0	100	0	0:100

[a] Time that solution stirred following addition of *t*-BuLi and prior to the addition of CD_3OD. [b] Product distributions and ratios determined by ^{1}H-NMR spectroscopy on the crude reaction mixtures. [c] Reactions performed at -100°C.

4.2.1 Solvent Effects

When preparing compounds **107**, **123-125** a dramatic solvent effect was also observed. It was shown that treatment of **105** with *n*BuLi in THF affords **106** and, after

quenching, results in the electrophilic capture at the site between the two chlorides (Table 14, Entry 1). The goal then became making anion **126** selectively. Anion stability is greatly influenced by solvent, therefore the DoM process in a lower dielectric/coordinating solvent was investigated. Since THF is a better coordinating solvent than Et_2O, it was believed switching the solvent from THF to Et_2O would maximize the directing ability of the methoxy groups, affording anion **126**. When **105** was lithiated and quenched at −78 °C in ether, no reaction took place (Table 14, Entry 2). However, when lithiation was conducted at ambient temperature, complete consumption of starting materials was observed and only the quenched products of anion **126** were isolated (entries 3 and 4). These results demonstrate a complete reversal of regioselectivity compared to when the identical reactions were conducted in THF. Although similar changes in DoM regioselectivity have been reported in the literature, they involve highly coordinating solvents and additives, such as hexamethylphosphoramide (HMPA) or TMEDA that significantly alter the organolithium's ability to template the directing groups.[103,120] When TMEDA was added to the DoM reaction of **105** in THF, there was no change in regioselectivity from that observed with THF alone (Table 14, entries 1 vs 2). There was also no change in regioselectivity when TMEDA was added to the DoM reaction in Et_2O (i.e., the product obtained was from the anion at C3). Thus, the DoM selectivity and regiochemical change observed here with two similar ethereal solvents appears to be unique and without precedent when compared with other reports of solvent changes (e.g., TMEDA) in the literature.[103,120]

Although this solvent effect was a very important discovery for synthetic purposes, it also offered an interesting mechanistic puzzle. A few questions come to mind: does the site of deprotonation change in ether, does the thermodynamic anion stability change dramatically in the two solvents, or is it purely a solubility issue as the reaction in Et_2O becomes heterogeneous following deprotonation? To address these questions, deprotonation was first conducted at −78 °C in Et_2O, stirred for 10 min and then warmed to room temperature. After stirring for an additional 30 min. at room temperature the reaction was quenched (with CD_3OD or I_2). The only products isolated were those resulting from electrophilic capture at the site between the two methoxy groups (i.e., C3) (Scheme 21a). Although **105** is insoluble in ether at −78 °C, it is completely soluble at room temperature, enabling deprotonation to occur at C3 (Table 14, entries 2 and 3). Interestingly, the resulting anion that is formed (i.e., **126**), appears to be insoluble in Et_2O at room temperature and precipitates out of solution. This result suggests that the solubility of the anion (i.e., **126**) has a big impact on isomerization, in that isomerization will not occur if anion **126** is not in solution. To address this, the lithium-halogen exchange reaction was revisited since starting material **124** is soluble in both ether and THF at −78 °C. Lithiation of **124** in THF, after quenching with CD_3OD, led mostly the formation of **107** while in ether, **125** was the only product observed (Scheme 21b). It appears that after the lithium-halogen exchange, anion **126** is insoluble in ether and precipitates out of solution while in THF; it is more soluble and remains in solution allowing for the rearrangement to occur.

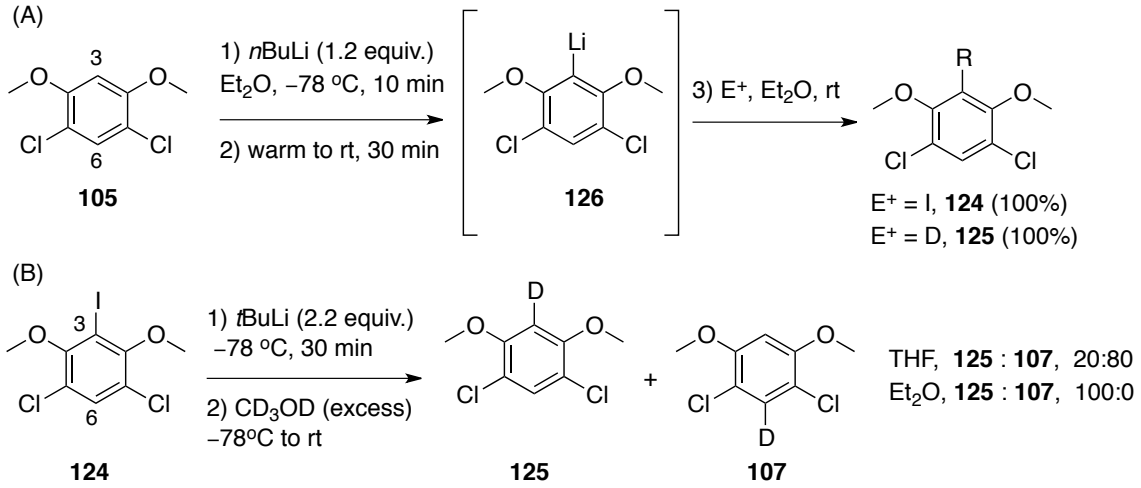

Scheme 21: Investigation of the effects of solvent on the solubility of aryl anion **126** following: (a) the DoM of **105** in Et_2O and (b) MHE of **124** in Et_2O and THF.

To further examine the effects of solvent in the DoM reaction of **105**, deprotonation was first conducted at room temperature in ether, which leads exclusively to anion **126**. Following the normal 30 min. stirring period after the addition of *n*BuLi, the solvent was carefully removed anaerobically, the flask was cooled to −78 °C, and then THF was added. After stirring for an additional 30 min. the reaction was quenched with CD_3OD and the only product obtained was **106** derived from complete isomerization of **126** (Scheme 22). Thus, when anion **126** was formed completely in Et_2O, **105** cannot be involved in the isomerization of **126** to **106** in THF. These results also prove that THF is unquestionably the trigger for isomerization.

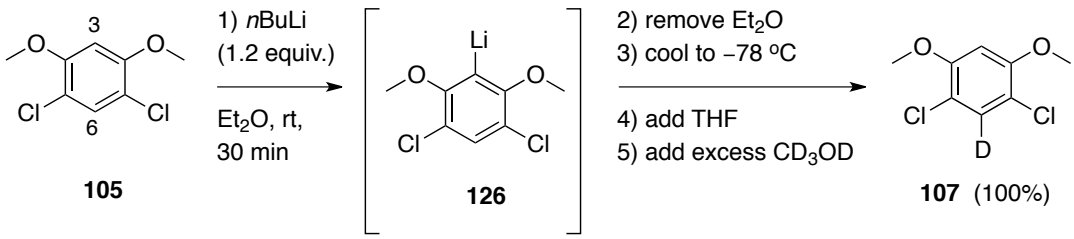

Scheme 22: Exchange of Et_2O for THF following the DoM of **105**.

3.2. Isotope Effects:

In an attempt to learn more details about the mechanism of deprotonation/isomerization sequence, deuterium-labelled starting materials were prepared and used in the DoM reaction (Table 17). When compound **125**, possessing a deuterium between the two methoxy groups, was treated with *n*BuLi at −78 °C in THF and then quenched with methanol after stirring for 30 min., only starting material (i.e. **125)** was recovered (Entry 1). This result suggests that no deprotonation occurred due to a pronounced kinetic isotope effect (KIE) at C3. When compound **107**, possessing a deuterium between the two chloride groups, was reacted under the same reaction conditions, again mostly the starting material was recovered but 15% of **105** was also observed (Entry 2). If deprotonation at C3 in **107** did occur in the usual way, then the results from Entry 2 suggest that the rate of isomerization is now significantly retarded due to another KIE for the deuterium at C6. With this knowledge, we wondered if it was not more likely that compound **125** was being deprotonated but now at C6 instead of at C3 due to this large KIE. To further probe the mechanism, the two reactions were

repeated but this time quenching with a deuterium source instead of hydrogen to more effectively track deprotonation.

Table 17: Effect of deuterium KIE on DoM.

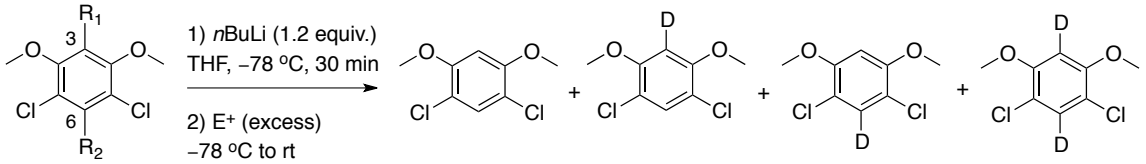

125, R_1 = D, R_2 = H
107, R_1 = H, R_2 = D

105 **125** **107** **127**

Entry	Starting Material	E	Product Distribution[a]			
			105	**125**	**107**	**127**
1	**125**	CH_3OH	0	100	0	0
2	**107**	CH_3OH	15	0	85	0
3	**125**	CD_3OD	0	0	0	100
4	**107**	CD_3OD	0	0	15	85

[a] Product distributions and ratios determined by ^{1}H-NMR spectroscopy on the crude reaction mixtures.

As expected, when the reaction with **125** was quenched with CD_3OD, full incorporation of a second deuterium was observed leading to the isolation of **127**. This reaction confirmed two things: 1) that the deuterium on C3 was acting as a protecting group and 2) that DoM did occur but now selectively at C6 (Entry 3).[121] The complementary experiment was also done on **107** (Entry 4) and as expected, the deuterium at C6 had no effect on the normal DoM at C3, producing compound **127** along with trace amounts of compound **107**. It is difficult to say whether compound **107** recovered at the end of the reaction is recovered starting material or is the result of isomerization.

Interestingly, the large KIE mentioned above (and discussed further below) associated with the deprotonation of the H/D at C3 on compounds **105**/**125** is

dramatically solvent dependent. Although the deuterium at C3 in compound **125** blocked deprotonation at that site, directing deprotonation to C6 in THF (Table 17, Entry 1), the same reaction in ether led to selective deprotonation of the deuterium at C3 (Scheme 23).

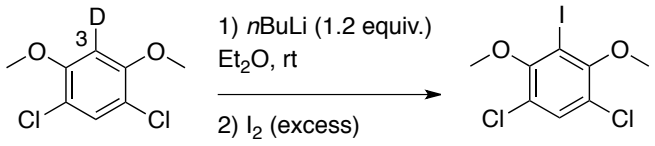

125 **124** (64% conv.)

Scheme 23: Deprotonation of the C3 deuteron in compound **125** by *n*BuLi in ether at RT.

There is only one other example in the literature where despite a large KIE the kinetic DoM site was retained.[120] However, in this example, the unexpected results were attributed to the unique properties of the ethoxyvinyllithium base, compared to more conventional alykyllithium. In the current study, it seems unlikely that two solvents of such similar structure and dielectric (ε values for THF and Et_2O are 7.6 and 4.3, respectably) could have such a drastic effect to overcome the profound KIE at C3 on **125**.[122]

4.2.2 Computational Studies

In an effort to better understand the observed regioselectivites for the DoM reaction of **105,** density functional theory (DFT) calculations were performed by our collaborator Dr. Robert Froese at The Dow Chemical Company. To simplify things, M062X and G3MP2B3 calculations were done using MeLi as a model instead of *n*BuLi to reduce the computational time required to account for the different conformers of *n*BuLi and summarized in Table 18.[123] While Collum and coworkers used Me_2Li in their

computational studies,[124] the data in Table 18 for the deprotonation of **105** were generated using MeLi as the base.[125] Interestingly, when the polarization continuum model (PCM, in THF) was included, MeLi binding to the methoxy groups was found to be enthalpically only slightly exothermic (M062X, -1.4 kcal/mol) compared to the gas phase (-7.7 kcal/mol). Further, while no MeLi binding could be found in solution to the chloride groups, it was found to bind in the gas phase, therefore it was assumed that deprotonation at C6 is not due to a "templating" effect. Lastly, the entropies shown in Table 18 are calculated as bimolecular values (i.e., **105** +MeLi), however the true entropies will depend on the degree of solvation/aggregation. With that said, it is believed that although the absolute barriers may not be accurate, the selectivities and trends should be.

Table 18: Thermodynamic parameters for important structures for the lithiation reaction of **105** at C6 to form **106** and C3 to form **126**.[a]

	M062X/6-311+G** in THF			G3MP2B3 in THF		
Compound	ΔH	ΔS	ΔG	ΔH	ΔS	ΔG
105 + LiMe	0.0	0.0	0.0	0.0	0.0	0.0
105 complex	-1.4	-17.4	3.8	-1.7	-16.0	3.1
TS(**105↔126**)	7.8	-24.1	15.0	10.9	-18.6	16.5
TS(**105↔106**)	10.1	-25.4	17.7	14.4	-20.6	20.5
126 + CH_4	-19.5	-5.0	-18.0	-18.4	-3.3	-17.4
106 + CH_4	-22.6	-3.5	-21.6	-21.0	-2.9	-20.1

[a] Calculations use M062X/6-311+G** and G3MP2B3 with PCM/THF. Enthalpies and free energies (25 °C) are in kcal mol^{-1}, whereas entropies are in cal $mol^{-1}K$ relative to **105**+LiMe.

The data in Table 18 shows that deprotonation favors the site between the two methoxy groups (i.e., C3; organolithium **126**) over the two chloride groups (i.e., C6; organolithium **106**) by 2.7 (M062X) and 4.0 (G3MP2B3) kcal/mol, indicating high kinetic selectivity at C3. The two possible transition states (TSs) (i.e., **105↔126** and

105↔106) for this deprotonation process are shown in Figure 22 along with some of the critical bond parameters. For deprotonation at C3, the TS (**105↔126**) is mostly C-H-C bond breaking/forming with the Li coordinated to one of the oxygen atoms of the methoxy groups. Assuming that MeLi can reversibly bind to the oxygen atom in the complex, which is likely true due to the 11.2 (M062X) or 13.4 (G3MP23) kcal/mol difference between the TS and the complex, then the "templating" effect must be kinetic in nature and due to stabilization of the lithium by the oxygen in the TS. Figure 22 supports this argument.

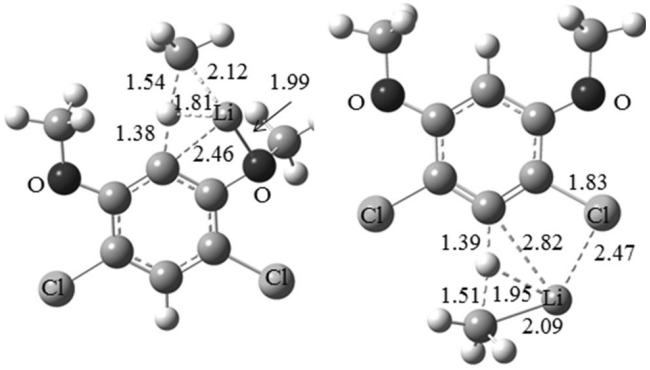

TS(105↔126) **TS(105↔106)**

Figure 22: Important bond-length parameters in the two transition states (TSs) defining the selectivity.

Lastly, two isomers of **126** were computed from the kinetically preferred pathway, one with a distorted Li-O interaction and one without this interaction. The former was found to be lower in energy. However, the geometric isomer with the Li residing between the chlorides (i.e., **106**) was found to be 3.6 (M062X) or 2.7 (G3MP2B3) kcal/mol more stable than **126**. Although no low energy isomerization pathways could be determined,

the thermodynamically more stable anion **106** is opposite of the kinetic anion **126** and coincides with what was found experimentally.

4.2.3 Mechanistic Consideration

Considering only the results from the DoM reaction of **105**, it would appear that starting material (**105**) is deprotonated at C3 by *n*BuLi, that is templated strongly by the methoxy group(s) generating **126**. Knowing that deprotonation is slow and that there is still a significant amount of starting material (**105**) in the reaction mixture (Table 14, Entry 1), anion **126** could deprotonate another molecule of **105**, which would produce **106** and regenerate **105** in the process. This would create a cycle that would systematically work its way through **105** until all of it is consumed and the reaction mixture contains only **106 (**Scheme 24a). The rates from Table 15 suggest that this might be possible as DoM itself is rather slow, thus giving isomerization plenty of time to occur.

However, the metal/halogen exchange results in Table 16 indicate that such a straightforward mechanism for isomerization is not possible or at least not the primary means by which **106** is formed. Here **126** is formed instantaneously from **124** and we know that isomerization is relatively slow as it takes more than 30 min. for full isomerization to occur (entries 5 and 6). The same conclusions can be made from the solvent exchange reaction outlined in Scheme 22. Prior to the removal of ether and switching the solvent to THF, all of **105** has been converted to anion **126**. Thus, there has to be a means by which a complete flask of **126** can be isomerized to **106** without involving **105**, which happens in THF but not in Et_2O (Scheme 24b).

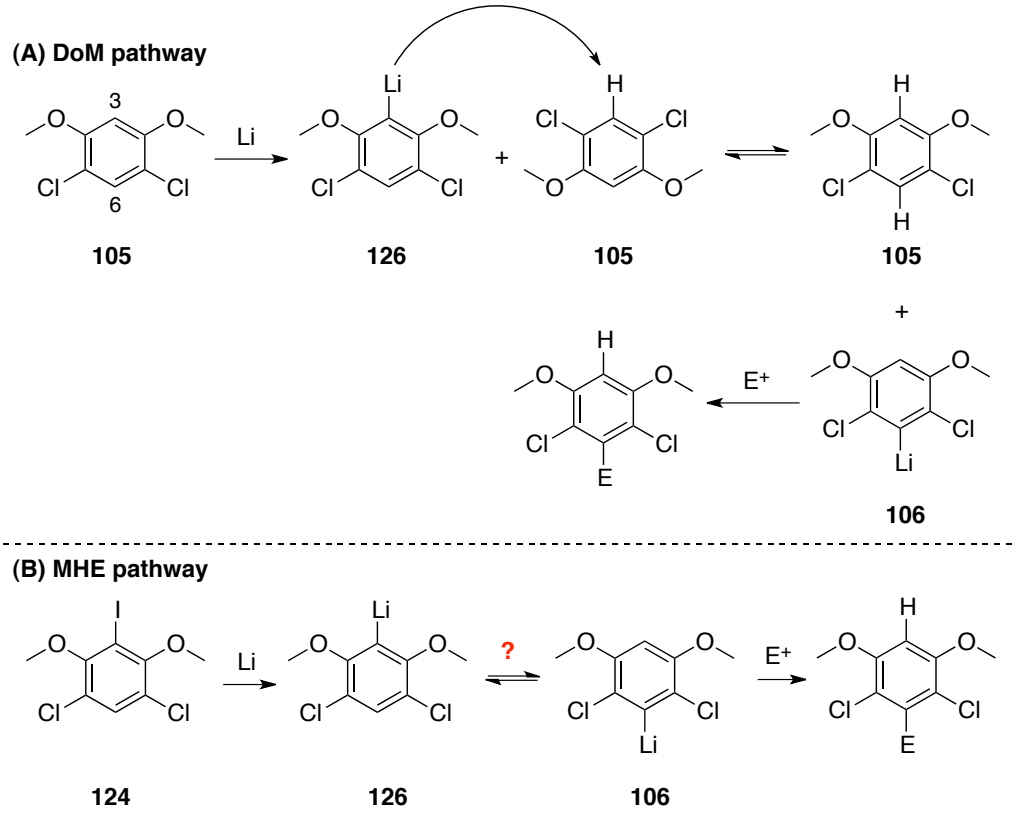

Scheme 24: Possible mechanism of isomerization for: (A) the DoM of **105** in THF and (B) the MHE of **124** in THF.

In a last attempt to determine more details about the mechanism of isomerization, metal/halogen reactions with **124** were reinvestigated, however this time varying the concentration of the reaction mixture, while keeping all other parameters constant (Table 19). All reactions were quenched with CD_3OD immediately following the last drop of *t*BuLi. Considering only the ratios of **107**:**125**, Entries 1-3 show no change in product distribution, indicating that isomerization does not occur by a bimolecular process. While a change in product distribution is seen for Entries 4 and 5, this is most likely the result of the reaction mixture being heterogeneous at these concentrations. Interestingly, as the concentration of the reaction increases, we start to see the formation of compound **123**.

At this time, we do not have a working hypothesis for the formation of **123** or for the mechanism of isomerization.

Table 19: MHE of **124** with *t*BuLi – Investigating an intramolecular process of isomerization.[a]

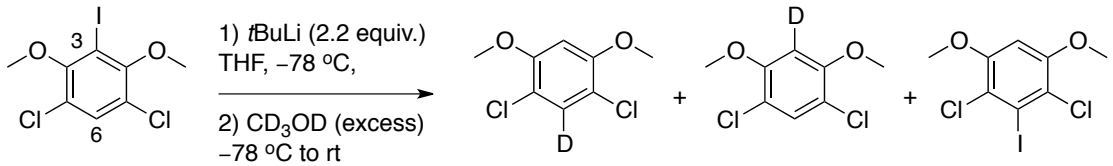

124 **107** **125** **123**

Entry	Conc. (M)	Product Distribution[b]				Ratio
		123	**122**	**107**	**125**	**107**:**125**
1	0.0625	0	0	49	51	1:1
2	0.125	2	0	50	48	1:1
3	0.25	6	4	44	45.5	1:1
4	0.5	6.5	1.5	49	43	1:1[c]
5	1.0	19	5	49	27	1.8:1[d]

[a] *t*BuLi was added dropwise over 20 sec. to a solution of 7 followed immediately by MeOD. [b] Product distributions and ratios were determined by ^{1}H-NMR spectroscopy on the crude reaction mixtures. [c] Reaction was a thick heterogeneous mixture.

Referring back to Table 17, the high selectivity observed for C6 when C3 is deuterated (Entries 1 and 3) can be explained in terms of a rate-determining deprotonation of the complexed lithiated species during the DoM process. Recall that DoM occurs at C3 by a 6-centered TS (Figure 23, TS **106↔126**). The corresponding activated complex for the C3-deuterated species was calculated to lie 0.8 kcal/mol higher in energy, which would predict a normal DIE of 7.9 at –78 °C in contrast to the observed selectivity, where the DIE must be greater than 99 to account for the unusually high selectivity observed. In contrast, deprotonation at C6 does not involve DoM and the difference in activation energies between the C6-deuterated and protonated TSs of 0.9

kcal/mol, leads to a normal DIE of 10.3 at −78 °C, which is more consistent with the observed selectivity.

The exceptionally large DIE (> 99:1) at C3 is consistent with tunneling associated with cyclic (5- or 6-centered) TSs, where small changes in geometry and narrow energy barriers are involved in a chemical reaction. Tunneling occurs when a particle penetrates through a potential energy barrier instead of climbing over it and is most prominent in reactions involving hydrogen atoms (e.g., hydrogen atom- or proton-transfer reactions). There are numerous examples of tunneling reported in the literature, however only ones involving cyclic TSs are included here. For example, Ingold and co-workers reported unusually large DIE values over a range of temperatures (−26 °C to −160 °C) for the isomerization of 2,4,6-tri-*tert*-butylphenyl to 3,5-di-*tert*-butylneophyl.[126] The DIE was found to decrease with increasing temperatures (1400 and 80 at −100 °C and −30 °C, respectively) following non-linear Arrhenius plots, which is typical for processes involving tunneling. Such temperature effects have also been observed in the α−deprotonation of organic phosphates, where the DIE was found to be low at −50 °C (i.e., 6) and very high at −78 °C (i.e., ≥ 100).[127] The corresponding alkyl lithium intermediates were reported to be stable up to −50 °C and rearranged, with retention of configuration, to the corresponding α−hydroxyphosphonates (phosphate-phosphonate rearrangement). In some instances, the large kinetic isotope effects observed have led to the use of deuterium as a "protecting group" in directing regioselectivity, where it is removed at a later stage.[103,128,129]

4.3 Synthetic Utility – Applications in Nucleophilic Additions to Aldehydes and Negishi Cross-Coupling

The solvent effect observed during the DoM of **105** has led to the selective creation of two isomeric aryl lithium species by simply changing the solvent from THF to Et_2O. Using this methodology, regioisomeric products were produced with full and absolute regioselectivity (i.e., Table 14). This is important, as many aromatic isomers are difficult to separate. The ability to selectively form one anion in one solvent and another anion in a different solvent also offers great synthetic opportunities. Taking advantage of this remarkable solvent effect, the substrate scope for the DoM reaction of **105** was expanded to include more challenging electrophiles, as shown in Table 20. Deprotonation of **105** in THF followed by addition of either electron-rich (**128**) or electron-poor (**129**) aldehydes gave selective attack at C6 (Table 20). As expected, switching the solvent from THF to Et_2O, gave only the products of nucleophilic addition to C3 (**130** and **131**).

Table 20: Regioselective DoM of **105** and regioselective nucleophilic additions to aldehydes in ether and THF.

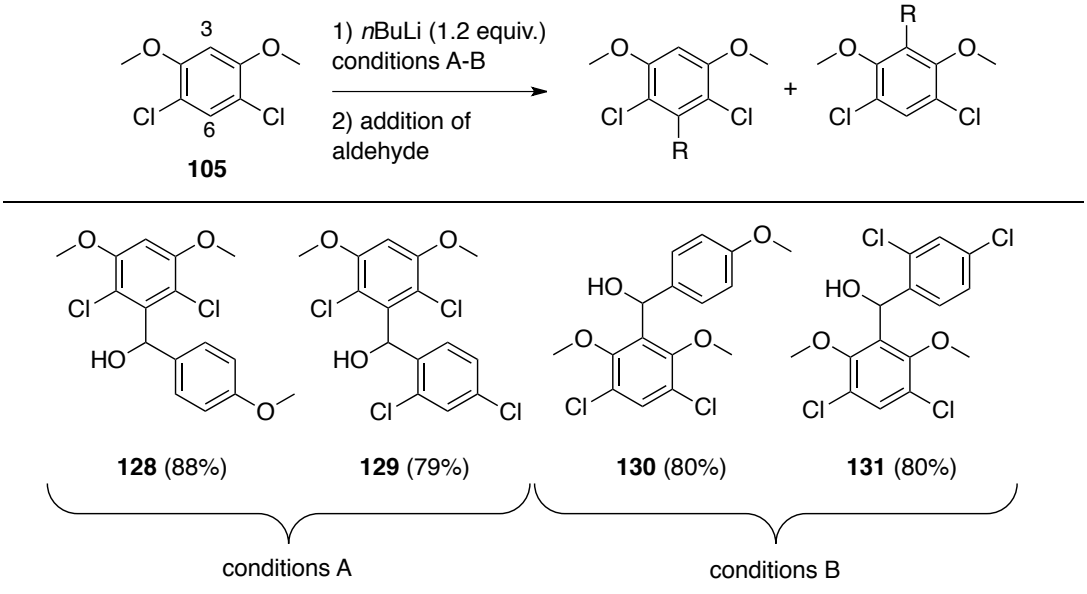

Conditions A: 1) THF, –78 ºC, 2) THF, –78 ºC to rt; Conditions B: 1) Et_2O, rt, 2) Et_2O, rt

The solvent effect could also be applied to the regioselective Negishi cross-coupling of **105**. Recall, lithiation of **105** in THF followed by transmetallation with $ZnCl_2$ gave **110**, which upon addition of the *Pd-PEPPSI-IPr* (**50**) pre-catalyst and oxidative addition partner **98**, led exclusively to the formation of compound **109a** (Scheme 25a). Conducting the DoM in Et_2O, followed by transmetallation with $ZnCl_2$ locks the organometallic at C3 (i.e., **132**). Addition of **50** and **98**, leads exclusively to the formation isomer **109b** (Scheme 25b). It is important to note that zinc derivative (i.e. **132**) does not isomerize once the THF is added that is necessary for the Negishi coupling. Without this unique solvent feature, the direct cross-coupling of these two different sites on **105** would not be possible. Optimization for the DoM reaction of **105** in THF, followed by Negishi cross-coupling can be found in Chapter 3, Section 3.3.

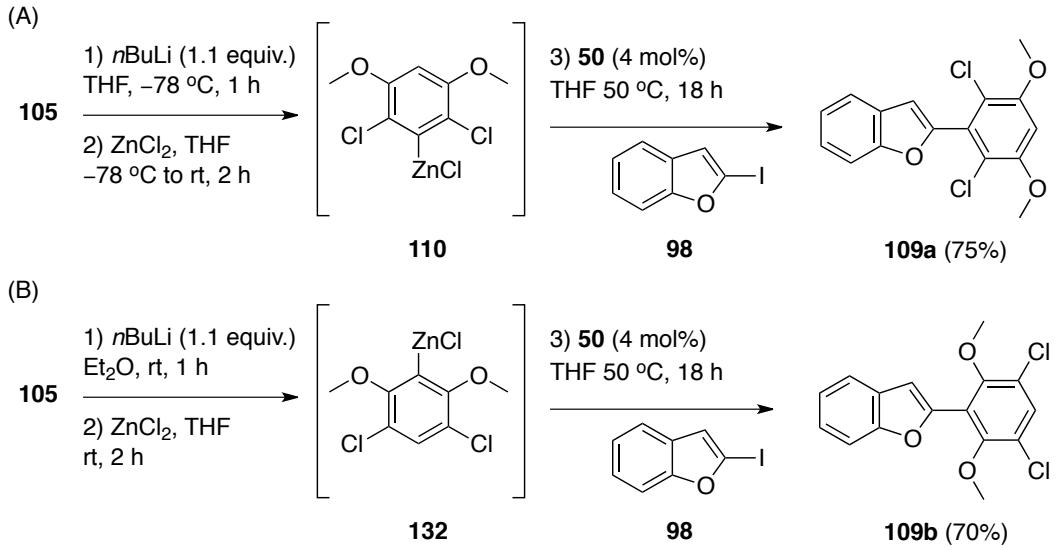

Scheme 25: Regioselective Negishi cross-coupling reaction of **105** in ether and THF.

4.4 Conclusion

In conclusion, a protocol for the regioselective formation of the 6-lithio devivative of 1,3-dichloro-4,6-dimethoxybenzene (**105**) by DoM with *n*BuLi in THF was developed. While reported in the literature as a direct deprotonation at C6, a series of time-course and labelling studies has revealed that deprotonation rather occurs exclusively at C3 and isomerizes to C6. However, when DoM was performed in Et_2O, deprotonation again occurred selectively at C6, but now zero isomerzation occurs and electrophilic capture produces the regioisomer of that produced in THF. Labeling studies revealed that deuterium has a dramatic kinetic isotope effect (KIE) that suppresses not only the original DoM reaction at C3 when deuterium is present there but also suppresses isomerization to C6 when the label is at that site. Computational studies determined that the C6-lithio species (**106**) is the thermodynamically more stable carbanion and that templated deprotonation at C3 is the kinetically more favourable process leading to carbonion **126**.

Calculations also suggest that the unusually large DIE observed (>99:1) with compound **125** is most likely a result of tunneling since the calculations predicted a normal DIE of 7.9 under the reaction conditions (Table 17). The utlility of these selective reactions in synthesis was also demonstrated in two reactions: nucleophilic addition to aldehydes and Negishi coupling (Table 20 and Scheme 25, respectively).

CHAPTER 5: Experimental procedures

5.1 General Experimental

All necessary reagents were purchased from Sigma-Aldrich or Alfa Aesar and were used without further purification, unless otherwise stated. Anhydrous solvents were purchased from Sigma-Aldrich or Fisher Scientific, and handled under argon. THF and Et_2O were distilled over sodium-benzophenone under an atmosphere of argon prior to use. Organolithium reagents were titrated by the method reported by Nielsen and coworkers prior to use.[130] Technical grade pentane, hexane, heptane, diethyl ether, ethyl acetate, and dichloromethane were used without further purification. $CDCl_3$, DMSO-d^6, CD_3CN, CD_3OD, and C_6D_6 were purchased from Sigma-Aldrich and Cambridge isotopes. Thin Layer Chromatography (TLC) was performed on EMD 60 F_{254} pre-coated glass plates and spots were visualized using UV light (254 nm), phosphomolybdic acid, p-anisaldehyde, potassium permanganate, or ceric ammonium molybdate stains. Column chromatography purifications were carried out using the flash technique on EMD silica gel 60 (230 - 400 mesh). Nuclear Magnetic Resonance (NMR) spectra were recorded on Bruker AV 300 MHz, AV 400 MHz, and DRX 600 MHz spectrometers. The chemical shifts (δ) for all ^1H spectra are reported in parts per million (ppm) and referenced to the residual proton signal of the deuterated solvent; coupling constants are expressed in Hertz (Hz). ^{13}C-NMR spectra were referenced to the carbon signals of the deuterated solvent. The ^2H-NMR spectra were recorded at 400 MHz, using acetone-d^6 (2.05 ppm) as the external standard. The ^{19}F-NMR spectra were recorded at 376 MHz, using trichlorofluoromethane as the standard. The ^{11}B-NMR spectra were recorded at 96 MHz,

using borontrifluoride etherate as the standard. The following abbreviations are used to describe signal shape; s = singlet, d = doublet, t = triplet, dd= double of doublets, q = quartet, and m = multiplet, b = broad.

Previously uncharacterized compounds were assigned by 1D and 2D NMR spectroscopy on either Bruker AV 400 or DRX 600 NMR spectrometers. Connectivity was determined using ^{1}H-^{1}H COSY, ^{1}H-^{13}C HSQC and ^{1}H-^{13}C HMBC while assignment of the *E/Z* stereochemistry was completed by evaluating the proton interactions at the vinylic center using 2D ^{1}H-^{1}H gradient NOESY spectroscopy. Quantitative proton NMR spectroscopy was completed using a relaxation delay of 5 times the longest T_1 value of the integrated protons of interest. The *E/Z* components of sample **89a** were overlapped in the 1D ^{1}H spectrum at 600 MHz and the *E/Z* ratio was determined using the volume integration of the 2D ^{1}H-^{13}C HSQC pulse program as provided by the Bruker pulse program library. Although Q-HSQC[1] has been developed for quantitative NMR, the proton resonances used in the *E/Z* isomer ratio determination all had similar $^{1}J_{13C\text{-}1H}$ coupling values, T_1 values and chemical shifts. This volume integration HSQC method was found to be accurate to within 3% error by comparing the resolvable proton integrations and the 2D HSQC volumes of the other *E/Z* isomers.

Gas chromatography (GC) was performed on a Varian Series GC/MS/MS 4000 System. High Resolution Mass Spectrometry (HRMS) analysis was performed by the McMaster Regional Centre for Mass Spectrometry in Hamilton, Ontario and at the Mass Spectrometry and Proteomics Services Unit, Queens University in Kingston, Ontario. High Pressure Liquid Chromatography (HPLC) was performed on an Agilent

Technologies 1200 Series system using a C-18 analytical column (15 cm, 4.6 mm i.d., particle size: 5 μ). Melting points were determined using a Fisher-John melting point apparatus and are uncorrected. All reactions were performed with flame-dried or oven-dried glassware under an atmosphere of argon unless stated otherwise.

5.2 Preparation of Isoprenylated Arene Regioisomers 68a and 68b (Scheme 9).

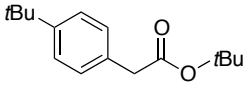

64

Synthesis of *tert*-butyl 2-(4-*tert*-butylphenyl)acetate (64). Compound **64** was prepared according to a procedure reported by Hartwig and coworkers.[131] In a glovebox, a 10 mL round-bottom flask equipped with a magnetic stir bar was charged with carbene precursor *SIPr* (156.6 mg, 0.4 mmol, 2 mol%), Pd_2dba_3 (366.3 mg, 0.4 mmol, 2 mol%), and LiHMDS (7.70 g, 46 mmol, 2.3 equiv.). The flask was capped with a rubber septum and removed from the glove box. Aryl bromide **62** (4.26 g, 20.0 mmol, 1 equiv.) was added *via* syringe, followed by distilled toluene and the mixture was stirred vigorously for 10 min at rt. Then, tert-butyl acetate **63** (2.55 g, 22 mmol, 1.1 equiv.) was added *via* syringe and the heterogenous reaction mixture was stirred overnight at rt. Saturated aqueous NH_4Cl was added to quench the reaction. The mixture was extracted with Et_2O (3x) and the pooled organic layers were washed with brine, dried over anhydrous $MgSO_4$, filtered, and the solvent removed *in vacuo*. The residue thus obtained was purified by flash chromatography on silica gel (2/95 EtOAc/hexane, R_f = 0.57) yielding **64** (3.97 g, 80%) as a yellow oil. ^{1}H-NMR for (300 MHz, $CDCl_3$) δ 7.37 (d, J = 8.4 Hz, 2H), 7.24 (d, J = 8.4 Hz, 2H), 3.54 (s, 2H), 1.49 (s, 9H), 1.35 (s, 9H); ^{13}C-NMR for (100 MHz, $CDCl_3$) δ 171.1, 149.5, 131.5,

128.7, 125.3, 80.6, 41.9, 34.3, 31.2, 278.0. Spectral data were in accordance with those reported in literature.[131]

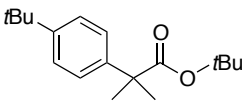

69

Synthesis of *tert*-butyl 2-(4-*tert*-butylphenyl)-2-methylpropanoate (69). Compound **69** was prepared according to a procedure modified from Baudoin and co-workers.[132] *n*BuLi (48 mL of a 2.4 M solution in hexane, 20 mmol) was added drop-wise *via* syringe to a stirred solution of N-diisopropylamine (3.1 mL, 22 mmol) in dry THF (20 mL) at –78 °C. The mixture was stirred for 15 min at -78 °C and a solution of **64** (1.24 g, 5 mmol) in THF (9 mL) was added via syringe dropwise. After stirring for an additional 30 min period, MeI (1.6 mL, 25 mmol) was added. After the mixture was warmed to rt, saturated aqueous NH_4Cl was added to quench the reaction. The mixture was extracted with Et_2O (3x) and the pooled organic layers were washed with brine, dried over anhydrous $MgSO_4$, filtered, and the solvent removed *in vacuo*. The residue was dissolved in THF (9 mL) and the above deprotonation-methylation sequence was repeated again using LDA (1.4 mL, 10 mmol) in THF (10 mL) and MeI (0.8 mL, 12.5 mmol), followed by the same work-up procedure. The residue thus obtained was purified by flash chromatography on silica gel (2/98 EtOAc/hexane, $R_f = 0.65$) yielding **64** (1.05 g, 76%) as a yellow oil. ^{1}H-NMR (400 MHz, $CDCl_3$) δ 7.34 (d, J = 8.4 Hz, 2H), 7.28 (d, J = 8.4 Hz, 2H), 1.54 (s, 6H), 1.42 (s, 9H), 1.33 (s, 9H); ^{13}C-NMR (75 MHz, $CDCl_3$) δ 176.1, 148.9, 142.2, 125.2, 124.9, 80.2, 46.6, 34.3, 31.3, 27.8, 26.6; HRMS (EI) [M^+] calcd. for $C_{18}H_{28}O_2$, 276.2089; found 276.2099.

General Procedure for the Synthesis of 65 and 70 by Lithium Aluminum Hydride Reduction: An oven dried 100 mL round-bottom flask equipped with a magnetic stir bar was charged with Lithium Aluminium Hydride (LAH) (1.5 equiv.) and then evacuated and backfilled with Ar (3x). Dry THF was then added via syringe and the mixture was cooled to 0 °C for 5 min. Next, a solution of the aryl tert-butyl ester (**64** or **69**) (1 equiv.) in dry THF was added dropwise *via* syringe to a stirred solution of LAH. The 0 °C ice bath was removed and the resulting heterogenous reaction mixture was warmed to rt and stirred vigorously. The progress of the reaction was monitored by TLC. Upon consumption of starting material, the mixture was cooled to 0 °C and quenched in the following order using dropwise addition: diluted with Et_2O, H_2O, 15% NaOH, and H_2O. The mixture was stirred at 0 °C for 10 min, the ice bath was removed and the mixture was stirred for an additional 30 min at rt. The mixture was extracted with Et_2O (3x) and the pooled organic layers were washed with brine, dried over anhydrous $MgSO_4$, filtered, and the solvent removed *in vacuo*. The residue thus obtained was purified by flash chromatography on silica gel.

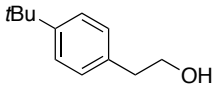

65

2-(4-*tert*-butylphenyl)ethanol (65). Following the general procedure on a 7.0 mmol scale, 1.11 g (88%) of **65** were obtained following silica gel flash chromatography (5/95 Et_2O/pentane, R_f = 0.1) as a yellow oil. ^{1}H-NMR (400 MHz, $CDCl_3$) δ 7.46 (d, J = 8.4 Hz, 2H), 7.28 (d, J = 8.0 Hz, 2H), 3.88 (t, J = 6.8 Hz, 2H), 3.07 (bs, 1H), 2.93 (t, J = 6.8 Hz, 2H) 1.45 (s, 9H); ^{13}C-NMR (100 MHz, $CDCl_3$) δ 149.1, 135.6, 128.7, 125.4, 63.5, 38.7, 34.4, 31.4. Spectral data were in

accordance with those reported in literature.[133]

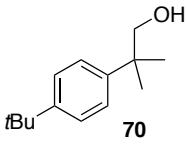

70

2-(4-*tert*-butylphenyl)-2-methylpropan-1-ol (70). Following the general procedure on a 9.4 mmol scale, 1.65 g (85%) of **70** were obtained following silica gel flash chromatography (5/95 Et_2O/pentane, R_f = 0.16) as a white solid. Mp: 114-117°C (lit. mp: 116-119°C);[134] ^{1}H-NMR (300 MHz, $CDCl_3$) δ 7.38 (d, J = 8.6 Hz, 2H), 7.33 (d, J = 8.6 Hz, 2H), 3.62 (s, 2H), 1.35 (s, 6H), 1.34 (s, 9H); ^{13}C-NMR (100 MHz, $CDCl_3$) δ 148.9, 143.0, 125.9, 125.3, 73.2, 39.7, 34.3, 31.3, 25.3. Spectral data were in accordance with those reported in literature.[133]

General Procedure for the Synthesis of 66 and 71 by IBX Oxidation: In air, a Biotage 2-5 mL microwave vial equipped with a stir bar was charged with the alcohol (1 equiv.) and then evacuated and backfilled with Ar (3x). Dry acetonitrile (C = 0.2 M) was added via syringe, followed by IBX (1.2 equiv.), and acetic acid (1.2 equiv.). The reaction mixture was stirred vigorously at room temperature. The progress of the reaction was monitored by TLC. After completion of the reaction, $NaHCO_3$ was added to the mixture. The resulting mixture was passed through a short path of silica gel using EtOAc as the eluent. The solvent was removed *in vacuo* and the residue thus obtained was purified by flash chromatography on silica gel.

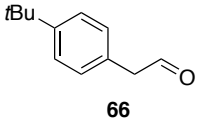

66

2-(4-(*tert*-butyl)phenyl)acetaldehyde (66). Following the general procedure on a 1.0 mmol scale, 133.9 mg (76%) of **66** were obtained

following silica gel flash chromatography (2/98 EtOAc/hexane, R_f = 0.45) as a clear, colourless oil. ^{1}H-NMR (400 MHz, $CDCl_3$) δ 9.77 (t, *J* = 2.4 Hz, 1H), 7.42 (d, *J* = 8.0 Hz, 2H), 7.19 (d, *J* = 8.0 Hz, 2H), 3.68 (d, *J* = 2.4, 2H), 1.35 (s, 9H); ^{13}C-NMR (100 MHz, $CDCl_3$) δ 199.5, 150.3, 129.2, 128.6, 125.8, 60.3, 34.4, 31.2; HRMS (EI) [M^+] calcd. for $C_{12}H_{16}O$, 176.1201; found 176.1188.

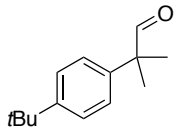

71

2-(4-(*tert*-butyl)phenyl)acetaldehyde (71). Following the general procedure on a 1.0 mmol scale, 122.6 mg (60%) of **71** were obtained following silica gel flash chromatography (5/95 EtOAc/hexane, R_f = 0.4) as a white solid. Mp: 108-111°C; ^{1}H-NMR (400 MHz, $CDCl_3$) δ 9.54 (s, 1H), 7.43 (d, *J* = 8.6 Hz, 2H), 7.24 (d, *J* = 8.6 Hz, 2H), 1.49 (s, 6H), 1.36 (s, 9H); ^{13}C-NMR (100 MHz, $CDCl_3$) δ 201.6, 150.9, 134.1, 127.2, 125.8, 68.7, 34.7, 31.3, 23.4; HRMS (EI) [M^+] calcd. for $C_{14}H_{20}O$, 204.1514; found 204.1514.

General Procedure for the Synthesis of 68a and 68b by a Wittig reaction. *n*BuLi (2.4 M solution in hexanes, 1.3 equiv.) was added slowly *via* syringe to a stirred solution of triphenylphosphonium iodide **67** or **72** (1.3 equiv.) in THF (10 mL) at 0 °C. The mixture was stirred for 30 min at 0 °C and then a solution of aldehyde **66** or **71** (1 equiv.) in THF was added drop-wise *via* syringe, whereupon the mixture was allowed to warm to rt and stirred for 12 h. The mixture was then diluted with hexanes, filtered through a pad of celite, and transferred to a separatory funnel where it was washed with brine, dried over anhydrous $MgSO_4$, filtered, and the solvent removed *in vacuo*. The residue thus obtained

was purified by flash chromatography on silica gel.

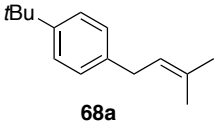

68a

1-(*Tert*-butyl)-4-(3-methylbut-2-en-1-yl)benzene (68a). Following the general procedure on a 3.2 mmol scale, 303.7 mg (62.5%) of **68a** were obtained following silica gel flash chromatography (heptane, R_f = 0.52) as a clear, colourless oil. ^{1}H-NMR (400 MHz, $CDCl_3$) δ 7.37 (d, *J* = 8.0 Hz, 2H), 7.18 (d, *J* = 8.0 Hz, 2H), 5.44-5.39 (m, 1H), 3.50 (d, *J* = 6.6, 2H), 1.80 (s, 3H), 1.78 (s, 3H), 1.37 (s, 9H); ^{13}C-NMR (100 MHz, $CDCl_3$) δ 148.4, 138.2, 132.3, 127.9, 125.2, 123.3, 34.3, 33.8, 31.4, 25.7, 17.8; HRMS (EI) [M^+] calcd. for $C_{15}H_{22}$, 202.1722; found 202.1726.

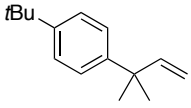

68b

1-(*Tert*-butyl)-4-(2-methylbut-3-en-2-yl)benzene (68b): Following the general procedure on a 0.65 mmol scale, 71.1 mg (70%) of **68b** were obtained following silica gel flash chromatography (heptane, R_f = 0.52) as a clear, colourless oil. ^{1}H-NMR (400 MHz, $CDCl_3$) δ 7.35 (d, *J* = 8.8 Hz, 2H), 7.30 (d, *J* = 10.8 Hz, 2H), 6.06 (dd, *J* = 17.6 and 10.8 Hz, 1H), 5.10-5.03 (m, 2H), 1.42 (s, 6H), 1.34 (s, 9H); ^{13}C-NMR (100 MHz, $CDCl_3$) δ 148.3, 148.1, 145.3, 125.6, 124.8, 110.3, 40.6, 34.1, 31.3, 28.1. HRMS (EI) [M^+] calcd. for $C_{15}H_{22}$, 202.1722; found 202.1726.

5.3 Preparation of 3,3-Disubstituted Allylpinacol Boronic Acid Ester Derivatives

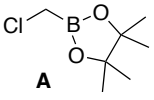

A

Synthesis of 2-(chloromethyl)-4,4,5,5-tetramethyl-1,3,2- dioxaborolane (A). A stirred solution of 2-isopropoxy-4,4,5,5-tetramethyl-1,3,2-dioxaborolane (8.5 mL, 41.6 mmol) and chloroiodomethane (3.3 mL, 45.8 mmol) in

anhydrous THF (40 mL) was cooled to –78°C. *n*BuLi (18.8 mL, 45.8 mmol, 2.44 M in hexanes) was then added drop-wise and after stirring for 30 min chlorotrimethylsilane (6.4 mL, 49.9 mmol) was added drop-wise. After 10 min at –78°C the flask was removed from the cooling bath and the contents were allowed to stir at rt for 24 h. H_2O (50 mL) was added and the mixture extracted with Et_2O (2x). The pooled organic layers were washed with brine, dried over anhydrous $MgSO_4$, filtered, and the solvent removed *in vacuo*. The crude product was purified by flash chromatography (gradient: 2% → 5% EtOAc/hexanes, R_f = 0.32 in 5/95 EtOAc/hexanes) providing **A** as a clear, light-yellow oil (6.59 g, 89.7%). ^{1}H-NMR (400 MHz, $CDCl_3$) δ 2.99 (s, 1H), 1.31 (s, 12H); ^{13}C-NMR (100 MHz, $CDCl_3$) δ 84.6, 24.7, 12.33. ^{11}B-NMR (128 MHz, $CDCl_3$) δ: 31.7. Spectra were in accordance with those reported in the literature.[135]

General Procedure for the Synthesis of Allylpinacol Boronic Acid Ester Derivatives. The derivatives were prepared according to a procedure modified from Aggarwal *et al*.[135] *t*BuLi (0.72M in pentane, 2.2 equiv.) was added slowly to a stirred solution of the corresponding vinyl iodide (1 equiv.) in dry Et_2O (12 mL) at –78°C. After 45 min at this temperature, the mixture was cooled to –110°C using a liquid N_2/pentane bath after which chloromethylboronate **A** (1.5 equiv.) was then added. After 30 min the cooling bath was removed and the mixture was stirred at rt for 3 h, after which it was cooled to 0°C and quenched by the addition of 10 mL of saturated aqueous NH_4Cl. The mixture was extracted with Et_2O (2x) and the pooled organic layers were washed with brine, dried

over anhydrous $MgSO_4$, filtered, and the solvent removed *in vacuo*. The crude product was purified by flash chromatography.

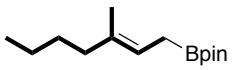

60d

(*E*)-4,4,5,5-tetramethyl-2-(3-methylhept-2-en-1-yl)-1,3,2-dioxaborolane (60d). Following the general procedure on a 3.2 mmol scale, 609.8 mg (80%) of **60d** was obtained following flash chromatography using Florosil (pentane, R_f = 0.5 in 5/95 Et_2O/pentane) as a clear, light-yellow oil. ^{1}H-NMR (400 MHz, $CDCl_3$) δ 5.24 (m, 1H), 1.99 (t, *J* = 7.4 Hz, 2H), 1.64-1.60 (m, 2H), 1.58 (s, 3H), 1.39-1.25 (m, 4H), 1.25 (s, 12H), 0.89 (s, 3H); ^{13}C-NMR (75 MHz, $CDCl_3$) δ 135.3, 118.2, 82.9, 39.5, 30.2, 24.7, 22.2, 15.7, 13.9, 17.8. ^{11}B-NMR (96 MHz, $CDCl_3$) δ: 33.2. Spectral data are in accordance with those reported in the literature.[136]

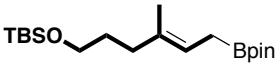

60e

(*E*)-*tert*-butyldimethyl((4-methyl-6-(4,4,5,5-tetramethyl-1,3,2-dioxaborolan-2-yl)hex-4-en-1-yl)oxy)silane (60e). Following the general procedure on a 1.6 mmol scale, 300.5 mg (53%) of **60e** was obtained following silica gel flash chromatography (pentane, R_f = 0.5 in 5/95 Et_2O/pentane) as a clear, colourless oil. ^{1}H-NMR (400 MHz, $CDCl_3$) δ 5.26 (m, 1H), 3.59 (t, *J* = 6.8 Hz, 2H), 2.03 (t, *J* = 7.2 Hz, 2H), 1.65-1.62 (m, 4H), 1.60 (s, 3H), 1.26 (s, 12H), 1.91 (s, 9H), 0.06 (s, 6H); ^{13}C-NMR (75 MHz, $CDCl_3$) δ 134.5, 123.4, 82.8, 62.7, 30.2, 35.7, 25.8, 24.6, 18.2, 15.5, 11.7, -5.4; ^{11}B-NMR (96 MHz, $CDCl_3$) δ 33.0; HRMS (EI) [M^+H^+] calcd. for $C_{19}H_{40}BO_3Si$, 355.2839; found 355.2841.

5.4 Regioselective Suzuki-Miyaura Cross-Coupling of Prenylboronic Acid Pinacol Ester Derivatives (Table 6 and 7).

General Regioselective Suzuki-Miyaura Coupling Procedure: In air, a Biotage 2-5 mL microwave vial equipped with a stir bar was charged with *Pd-PEPPSI-IPent* (**53**) (2 mol%), boronic ester (0.75 mmol, 1.5 equiv.), and aryl halide (0.5 mmol, 1 equiv.) at rt. The vial was sealed with a septum, evacuated (0.1 mmHg) and purged with argon (3x). Alternatively, if the aryl halide was a liquid at rt, it was added via syringe after purging with argon. THF (2 mL) was then added followed by 5M KOH (2.5 mmol, 4 equiv.), and the reaction vial was heated in an oil bath to 70°C for 24 hr. The reaction mixture was cooled to rt, extracted with Et_2O (3x), and the pooled organic layers washed with brine, dried over anhydrous $MgSO_4$, filtered, and the solvent removed *in vacuo*. The crude product was purified by flash chromatography.

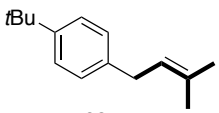

68a

1-(*Tert*-butyl)-4-(3-methylbut-2-en-1-yl)benzene (68a). Following the general coupling procedure, 82.5 mg of **68a/68b** (97:3, α:γ isomer) were obtained following silica gel flash chromatography (heptane, $R_f = 0.52$) as a clear, colourless oil (81% yield). The spectra for the major α–isomer are the same as those reported above, under *General Procedure for the synthesis of isoprenylated arene regioisomers **68a** and **68b** by a Wittig reaction (Section 1.2 above)*.

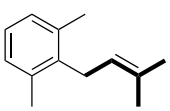
74

1,3-Dimethyl-2-(3-methylbut-2-en-1-yl)benzene (74). Following the

general coupling procedure, 65.0 mg of **74** (>99:1, α:γ isomer) were obtained following silica gel flash chromatography (heptane, R_f =0.35) as a clear, colourless oil (75% yield). The spectra for the major α–isomer are included here. ^{1}H-NMR (400 MHz, $CDCl_3$) δ 7.08 (s, 3H), 5.10-5.06 (m, 1H), 3.40 (d, *J* = 6.4 Hz, 2H), 2.37 (s, 6H), 1.86 (s, 3H), 1.77 (s, 3H); ^{13}C-NMR (100 MHz, $CDCl_3$) δ 138.2, 136.3, 131.6, 128.0, 125.7, 122.0, 28.2, 25.6, 20.0, 17.9. Spectral data for the major isomer were in accordance with those reported in the literature.[137]

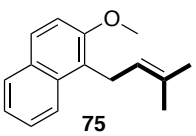

75

2-Methoxy-1-(3-methylbut-2-en-1-yl)naphthalene (75). Following the general coupling procedure, 108.4 mg of **75** (>99:1, α:γ isomer) were obtained following silica gel flash chromatography (hexanes, R_f = 0.15) as a white solid (96% yield). Mp.: 28-30°C. The spectra for the major α–isomer are included here. ^{1}H-NMR (300 MHz, $CDCl_3$) δ 8.03 (d, *J* = 8.4 Hz, 1H), 7.86 (d, *J* = 8.1 Hz, 1H), 7.80 (d, *J* = 9.0 Hz, 1H), 7.55, (t, *J* = 7.8 Hz, 1H), 7.41, (t, *J* = 7.4 Hz, 1H), 7.34 (d, *J* = 9.0 Hz, 1H), 5.33-5.29 (m, 1H), 4.00 (s, 3H), 3.89 (d, *J* = 6.6 Hz, 2H), 1.98 (s, 3H), 1.77 (s, 3H); ^{13}C-NMR (75 MHz, $CDCl_3$) δ 154.1, 133.1, 131.5, 129.4, 128.5, 127.6, 126.2, 123.7, 123.4, 123.2, 113.8, 56.8, 25.7, 24.1, 18.1; HRMS (EI) [M^+] calcd. for $C_{16}H_{18}O$, 226.1358; found 226.1361.

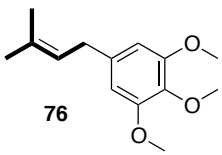

76

1,2,3-Trimethoxy-5-(3-methylbut-2-en-1-yl)benzene (76). Following the general coupling procedure, 92.6 mg of **76** (>99:1, α:γ

isomer) were obtained following silica gel flash chromatography (5/95 Et_2O/hexanes, R_f = 0.3) as a clear, yellow oil (78% yield). The reduced product, i.e., 1,2,3-trimethoxybenzene (14%) co-chromatographed with **79**. The spectra for the major α–isomer are included here. ^{1}H-NMR (400 MHz, $CDCl_3$) δ 6.42 (s, 2H), 5.35-5.32 (m, 1H), 3.86 (s, 6H), 3.84 (s, 3H), 3.31 (d, *J* = 7.2, 2H), 1,78 (s, 3H), 1.74 (s, 3H); ^{13}C-NMR (75 MHz, $CDCl_3$) δ 153.0, 137.5, 135.9, 132.6, 122.9, 105.0, 60.7, 55.9, 34.5, 25.6, 17.7; HRMS (EI) [M^+] calcd. for $C_{14}H_{20}O_3$, 236.1412; found 236.1420.

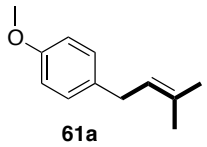
61a

1-Methoxy-4-(3-methylbut-2-en-1-yl)benzene (61a). Following the general coupling procedure, 75.8 mg of **61a** (>99:1, α:γ isomer) were obtained following silica gel flash chromatography (2/98 Et_2O/pentane, R_f = 0.36) as a clear, yellow oil (86% yield). The spectra for the major α–isomer are included here. ^{1}H-NMR (300 MHz, $CDCl_3$) δ 7.16 (d, *J* = 8.4 Hz, 2H), 6.90 (d, *J* = 8.7 Hz, 2H), 5.41-5.38 (m, 1H), 3.84 (s, 3H), 3.36 (d, J = 7.5 Hz, 2H), 1.82 (s, 3H), 1.79 (s, 3H); ^{13}C-NMR (75 MHz, $CDCl_3$) δ 157.7, 133.9, 132.1, 129.1, 123.6, 113.8, 55.2, 33.4, 25.7, 17.8. Spectral data for the major and minor isomers were in accordance with those reported in literature.[138,139]

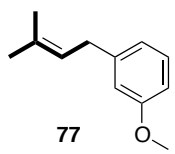
77

1-Methoxy-3-(3-methylbut-2-en-1-yl)benzene (77). Following the general coupling procedure, 68.7 mg of **77** (>99:1, α:γ isomer) were obtained following silica gel flash chromatography (2/98 Et_2O/pentane, R_f = 0.45) as a clear, yellow oil (78% yield). The spectra for the major α–isomer are included here. ^{1}H-

NMR (400 MHz, $CDCl_3$) δ 7.25 (t, *J* = 7.8 Hz, 1H), 6.83 (d, *J* = 7.6 Hz, 1H), 6.79 (s, 1H), 6.78 (d, *J* = 7.6 Hz, 1H), 5.40-5.36 (m, 1H), 3.84 (s, 3H), 3.38 (d, J = 7.2 Hz, 2H), 1.80 (s, 3H), 1.77 (s, 3H); ^{13}C-NMR (100 MHz, $CDCl_3$) δ 159.8, 143.4, 132.6, 129.2, 122.9, 120.7, 114.0, 110.8, 55.0, 34.3, 25.7, 17.7; HRMS (EI) [M^+] calcd. for $C_{12}H_{16}O$, 176.1201; found 176.1197.

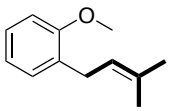
78

1-Methoxy-2-(3-methylbut-2-en-1-yl)benzene (78). Following the general coupling procedure, 81.3 mg of **78** (>99:1, α:γ isomer) were obtained following silica gel flash chromatography (2/98 Et_2O/pentane, R_f = 0.5) as a clear, yellow oil (92% yield). The spectra for the major α–isomer are included here. ^{1}H-NMR (400 MHz, $CDCl_3$) δ 7.26-7.21 (m, 2H), 6.98-6.90 (m, 2H), 5.41-5.37 (m, 1H), 3.90 (s, 3H), 3.40 (d, *J* = 7.2 Hz, 2H), 1.82 (s, 3H), 1.79 (s, 3H); ^{13}C-NMR (75 MHz, $CDCl_3$) δ 157.3, 132.4, 130.1, 129.3, 126.9, 122.6, 120.4, 110.2, 55.3, 28.5, 25.8, 17.8. Spectral data for the major isomer were in accordance with those reported in literature.[92]

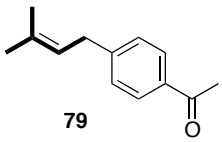
79

1-(4-(3-Methylbut-2-en-1-yl)phenyl)ethanone (79). Following the general coupling procedure, 39.5 mg of **79** (>99:1, α:γ isomer) were obtained following silica gel flash chromatography (5/95 Et_2O/pentane, R_f = 0.25) as a clear, yellow oil (42% yield). The spectra for the major α–isomer are included here. ^{1}H-NMR (300 MHz, $CDCl_3$) δ 7.90 (d, *J* = 8.1 Hz, 2H), 7.28 (d, *J* = 8.1 Hz, 2H), 5.35-5.30 (m, 1H), 3.41 (d, *J* = 7.2 Hz, 2H), 2.60 (s, 3H), 1.78 (s, 3H) 1.74 (s, 3H); ^{13}C-NMR (100 MHz, $CDCl_3$) δ 197.7, 147.6, 134.8, 133.5, 128.4, 128.4, 121.9, 34.3, 26.5, 25.6, 17.8.

Spectral data for the major isomer were in accordance with those reported in literature.[44]

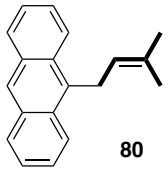

80

9-(3-Methylbut-2-en-1-yl)anthracene (80). Following the general coupling procedure, 72.6 mg of **80** (>99:1, α:γ isomer) were obtained following silica gel flash chromatography (5/95 EtOAc/heptane, R_f = 0.42) as a yellow solid (59% yield). Mp: 78-80°C. The spectra for the major α–isomer are included here. ^{1}H-NMR (300 MHz, $CDCl_3$) δ 8.40 (s, 1H), 8.30 (d, *J* = 8.7 Hz, 2H), 8.06 (d, *J* = 5.1, 2H), 7.56 (m, 4H), 5.36-5.32 (m, 1H), 4.37 (d, *J* = 6.0 Hz, 2H), 2.08 (s, 3H), 1.77 (s, 3H); ^{13}C-NMR (100 MHz, $CDCl_3$) δ 134.0, 131.6, 131.6, 129.6, 129.1, 125.7, 125.4, 124.8, 124.6, 123.6, 27.1, 25.6, 18.3; HRMS (ESI) [M^+] calcd. for $C_{19}H_{18}$, 246.1409; found 246.1418.

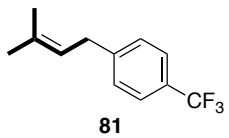

81

1-(3-Methylbut-2-en-1-yl)-4-(trifluoromethyl)benzene (81). Following the general coupling procedure, 54.7 mg of **81** (>99:1, α:γ isomer) were obtained following silica gel flash chromatography (heptane: R_f = 0.8) as a clear, colourless oil (51% yield). The spectra for the major α–isomer are included here. ^{1}H-NMR (300 MHz, $CDCl_3$) δ 7.55 (d, *J* = 8.1 Hz, 2H), 7.30 (d, *J* = 8.1 Hz, 2H), 5.35-5.31 (m, 1H), 3.42 (d, *J* = 7.2 Hz, 2H), 1.79 (s, 3H), 1.75 (s, 3H); ^{13}C-NMR (100 MHz, $CDCl_3$) δ: 145.8, 133.5, 128.5, 128.0 (q, *J* = 32 Hz), 125.1 (q, *J* = 4 Hz), 124.5 (q, *J* = 270 Hz), 121.9, 34.0, 25.6, 17.7; ^{19}F-NMR (376 MHz, $CDCl_3$) δ -62.2; HRMS (EI) [M^+] calcd. for $C_{12}H_{13}F_3$, 214.0969; found 214.0961.

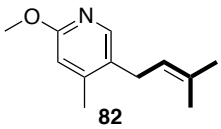

82

2-Methoxy-4-methyl-5-(3-methylbut-2-en-1-yl)pyridine (82). Following the general coupling procedure, 82.1 mg of **82** (>99:1, α:γ isomer) were obtained following silica gel flash chromatography (5/95 Et_2O/pentane, R_f = 0.25) as a clear, yellow oil (83% yield). The spectra for the major α–isomer are included here. ^{1}H-NMR (300 MHz, $CDCl_3$) δ 7.87 (s, 1H), 6.53 (s, 1H), 5.19-5.15 (m, 1H), 3.89 (s, 3H), 3.21 (d, J = 6.9 Hz, 2H), 2.23 (s, 3H), 1.73 (s, 3H), 1.72 (s, 3H); ^{13}C-NMR (100 MHz, $CDCl_3$) δ 162.9, 148.4, 145.7, 132.8, 128.7, 121.9, 111.1, 53.0, 28.7, 25.6, 19.0, 17.7; HRMS (EI) [M^+] calcd. for $C_{12}H_{17}NO$, 191.1310; found 191.1203.

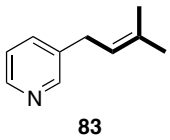

83

3-(3-Methylbut-2-en-1-yl)pyridine (83). Following the general coupling procedure, 34.9 mg of **83** (>99:1, α:γ isomer) were obtained following silica gel flash chromatography (20/80 EtOAc/hexanes, R_f = 0.23) as a clear, yellow oil (47% yield). The spectra for the major α–isomer are included here. ^{1}H-NMR (300 MHz, $CDCl_3$) δ 8.44-842 (m, 2H), 7.48-7.46 (m, 1H), 7.21-7.17 (m, 1H), 5.32-5.26 (m, 1H), 3.34 (d, J = 7.2 Hz, 2H), 1.76 (s, 3H), 1.7 (s, 3H); ^{13}C-NMR (100 MHz, $CDCl_3$) δ: 149.8, 147.1, 136.9, 135.6, 133.6, 123.1, 121.7, 31.4, 25.6, 17.7. Spectral data for the major isomer were in accordance with those reported in literature.[137]

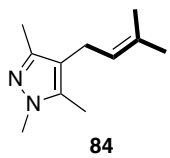

84

1,3,5-Trimethyl-4-(3-methylbut-2-en-1-yl)-1*H*-pyrazole (84). Following the general coupling procedure, 87.6 mg of **84** (>99:1, α:γ isomer) were obtained following silica gel flash chromatography (20/80 EtOAc/hexanes, R_f = 0.1) as a clear, yellow oil (98% yield). The spectra for the major

α–isomer are included here. ^{1}H-NMR (300 MHz, $CDCl_3$) δ 5.09-5.04 (m, 1H), 3.69 (s, 3H), 3.02 (d, J = 7.2 Hz, 2H), 2.15 (s, 3H), 2.14 (s, 3H), 1.73 (s, 3H), 1.69 (s, 3H); ^{13}C-NMR (100 MHz, $CDCl_3$) δ 145.3, 135.6, 130.5, 123.2, 115.3, 35.5, 25.4, 22.4, 17.6, 11.7, 9.4; HRMS (EI) [M^+] calcd. for $C_{11}H_{18}N_2$, 178.1470; found 178.1474.

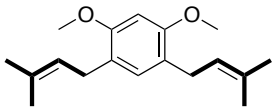

85

1,5-Dimethoxy-2,4-bis(3-methylbut-2-en-1-yl)benzene (85). Following the general coupling procedure, 132.9 mg of **85** (>99:1, α:γ isomer) were obtained following silica gel flash chromatography (5/95 Et_2O/pentane, R_f = 0.25) as a clear, colourless oil (95% yield). The spectra for the major α–isomer are included here. ^{1}H-NMR (300 MHz, $CDCl_3$) δ 6.90 (s, 1H), 6.48 (s, 1H), 5.31 (t, J = 7.2 Hz, 2H), 3.84 (s, 6H), 3.27 (d, J = 7.2 Hz, 4H), 1.75 (s, 12H); ^{13}C-NMR (75 MHz, $CDCl_3$) δ: 156.1, 131.7, 130.1, 123.3, 122.0, 95.6, 55.7, 27.8, 25.8, 17.7; HRMS (EI) [M^+] calcd. for $C_{18}H_{26}O_2$, 274.1933; found 274.1926.

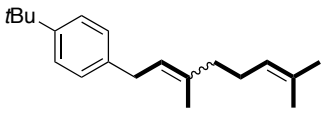

89a

1-(*tert*-butyl)-4-(3,7-dimethylocta-2,6-dien-1-yl)benzene (89a). Following the general coupling procedure, 124.3 mg of **89** (>99:1, α:γ isomer, **89a** *E/Z* = 80/20) were obtained following silica gel flash chromatography (heptane, R_f = 0.7) as a clear, colourless oil (92% yield). The spectra for the major α–isomer are included here. *E*-isomer ^{1}H-NMR (600 MHz, $CDCl_3$) δ 7.35 (d, J = 7.8 Hz, 2H), 7.17 (d, J = 8.4 Hz, 2H, 5.41-5.38 (m, 1H), 5.17-5.15 (m, 1H), 3.38 (d, J = 7.2 Hz, 2H), 2.21-2.15 (m, 2H), 2.12-2.09 (m, 2H), 1.76 (s, 3H), 1.74 (s, 3H), 1.65 (s, 3H), 1.36 (s, 12H); ^{13}C-NMR (155 MHz, $CDCl_3$) δ 148.4,

138.7, 135.9, 131.5, 127.9, 125.2, 124.2, 123.1, 39.7, 34.3, 33.5, 31.4, 26.6, 25.8, 17.7, 16.1. *Z*-isomer ^{1}H-NMR (600 MHz, $CDCl_3$) δ 7.35 (d, *J* = 7.8 Hz, 2H), 7.17 (d, *J* = 8.4 Hz, 2H, 5.41-5.38 (m, 1H), 5.21-5.19 (m, 1H), 3.38 (d, *J* = 7.2 Hz, 2H), 2.21-2.15 (m, 2H), 2.12-2.09 (m, 2H), 1.79 (s, 3H), 1.74 (s, 3H), 1.67 (s, 3H), 1.36 (s, 12H); ^{13}C-NMR (155 MHz, $CDCl_3$) δ 148.4, 138.7, 135.9, 131.6, 127.9, 125.2, 124.1, 123.9, 34.3, 33.5, 31.9, 31.4, 26.6, 25.8, 23.5, 17.7; HRMS (EI) [M^+] calcd. for $C_{20}H_{30}$, 270.2348; found 270.2341.

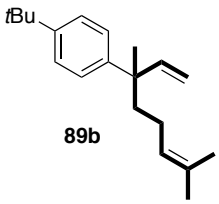

89b

1-(*tert*-butyl)-4-(3,7-dimethylocta-1,6-dien-3-yl)benzene (89b). Following the general coupling procedure, except using $Pd(PPh_3)_4$ as the catalyst, 125.5 mg of **89** (>20/80, α:γ isomer, **89a** *E/Z* = 80/20) were obtained following silica gel flash chromatography (heptanes, R_f = 0.7) as a clear, colourless oil (93% yield). The spectra for the major γ–isomer are included here. ^{1}H-NMR (400 MHz, $CDCl_3$) δ 7.34 (d, *J* = 8.8 Hz, 2H), 7.27 (d, *J* = 8.8 Hz, 2H), 6.10-6.03 (dd, *J* = 17.2 and 10.8 Hz, 2H), 5.13-5.06 (m, 2H), 1.91-1.75 (m, 4H), 1.69 (s, 3H), 1.58 and 1.55 (s, 3H), 1.40 (s, 3H), 1.34 (s, 9H); ^{13}C-NMR (100 MHz, $CDCl_3$) δ 148.3, 146.9, 144.3, 131.1, 126.1, 124.8, 124.7, 111.4, 43.8, 41.0, 34.2, 31.3, 25.6, 24.7, 23.3, 17.5; HRMS (EI) [M^+] calcd. for $C_{20}H_{30}$, 270.2348; found 270.2342.

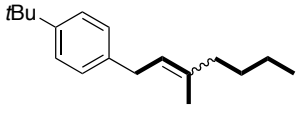

90a

1-(*tert*-butyl)-4-(3-methylhept-2-en-1-yl)benzene (90a). Following the general coupling procedure, 97.3 mg of **90**

(>99:1, α:γ isomer, **90a** *E/Z* = 80/20) were obtained following silica gel flash chromatography (heptanes, R_f = 0.8) as a clear, colourless oil (80% yield). The spectra for the major α–isomer are included here. *E*-isomer ^{1}H-NMR (600 MHz, $CDCl_3$) δ 7.36 (d, *J* = 7.8 Hz, 2H), 7.17 (d, *J* = 7.8 Hz, 2H), 5.39-5.36 (m, 1H), 3.37 (d, *J* = 5.7 Hz, 2H), 2.07 (t, *J* = 7.5 Hz, 2H), 1.74 (s, 3H), 1.48-1.42 (m, 2H), 1.39-1.32 (m, 2H), 1.30 (s, 12H), 0.97-0.93 (m, 3H); ^{13}C-NMR (75 MHz, $CDCl_3$) δ 148.4, 138.8, 136.5, 127.9, 125.2, 122.8, 39.4, 34.3, 33.6, 31.4, 30.2, 22.4, 16.11, 14.03; *Z*-isomer ^{1}H-NMR (600 MHz, $CDCl_3$) δ 7.36 (d, *J* = 7.8 Hz, 2H), 7.17 (d, *J* = 7.8 Hz, 2H), 5.39-5.36 (m, 1H), 3.37 (d, *J* = 5.7 Hz, 2H), 2.18 (t, *J* = 7.5 Hz, 2H), 1.77 (s, 3H), 1.48-1.42 (m, 2H), 1.39-1.32 (m, 2H), 1.30 (s, 12H), 0.97-0.93 (m, 3H); ^{13}C-NMR (75 MHz, $CDCl_3$) δ 148.4, 138.5, 136.4, 128.5, 124.8, 123.6, 34.4, 33.5, 31.6, 31.4, 30.4 23.5, 22.8, 14.1; HRMS (EI) [M^+] calcd. for $C_{18}H_{28}$, 244.2191; found 244.2183.

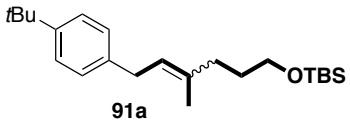

91a

***tert*-butyl((6-(4-(*tert*-butyl)phenyl)-4-methylhex-4-en-1-yl)oxy)dimethylsilane (91a).** Following the general coupling procedure, 70.3 mg of **91** (>99:1, α:γ isomer, **91a** *E/Z* = 80/20) were obtained following silica gel flash chromatography (2/98 Et_2O/pentane, R_f = 0.3) as a clear, colourless oil (76% yield). The spectra for the major α–isomer are included here. *E*-isomer ^{1}H-NMR (400 MHz, $CDCl_3$) δ 7.30 (d, *J* = 8.1 Hz, 2H), 7.11 (d, *J* = 8.1 Hz, 2H), 5.39-5.35 (m, 1H), 3.61 (t, *J* = 6.4 Hz, 2H), 3.33 (d, *J* = 7.5 Hz, 2H), 2.11-2.06 (m, 2H), 1.73 (s, 3H), 1.71-1.64 (m, 2H), 1.31 (s, 9H), 0.91 (s, 9H), 0.058 (s, 6H); ^{13}C-NMR (75 MHz, $CDCl_3$) δ 148.5, 138.7, 135.7, 127.9, 125.2, 123.3, 62.9, 35.9, 34.33, 33.7, 31.4,

31.1, 26.0, 18.4, 16.1, -5.3. *Z*-isomer ^{1}H-NMR (400 MHz, $CDCl_3$) δ 7.30 (d, *J* = 8.1 Hz, 2H), 7.18 (d, *J* = 8.1 Hz, 2H), 5.40-5.34 (m, 1H), 3.61 (t, *J* = 6.4 Hz, 2H), 3.35 (d, *J* = 7.0 Hz, 2H), 2.21-2.17 (m, 2H), 1.75 (s, 3H), 1.71-1.64 (m, 2H), 1.31 (s, 9H), 0.91 (s, 9H), 0.058 (s, 6H); ^{13}C-NMR (75 MHz, $CDCl_3$) δ 148.5, 138.7, 135.8, 128.5, 124.9, 124.1, 62.9, 36.8, 34.3, 33.5, 31.4, 31.1, 26.0, 23.4, 18.4, -5.3; HRMS (EI) [M^+] calcd. for $C_{23}H_{40}OSi$, 360.2848; found 360.2837.

5.5 Preparation of 2-arylbenzofurans 109a and 111.

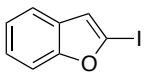

98

Synthesis of 6-methoxybenzofuran (98). To a stirred solution of benzofuran (1.18 g, 10 mmol, 1 equiv) in anhydrous Et_2O (20 mL) under an argon atmosphere at −78°C was added slowly *t*BuLi (8.8 mL, 1.7M in pentane, 15 mmol, 1.5 equiv.) via syringe. The mixture was stirred for 1 hr and a solution of I_2 (3.81 g, 15 mmol, 1.5 equiv) in dry ether (30 mL) at −78°C. The mixture was stirred for another 1 hr, allowed to warm to rt, diluted with saturated aqueous NH_4Cl, and extracted with Et_2O. The organic solution was washed with $Na_2S_2O_3$ and water, dried over Na_2SO_4, and dried in vacuo. The residue was purified using silica gel flash chromatography (heptane, R_f = 0.5) to afford **7b** as a yellow oil (2.15 g, 88 %). ^{1}H-NMR (400 MHz, $CDCl_3$) δ 7.54-7.48 (m, 2H), 7.23 (m, 2H), 6.98 (s, 1H); ^{13}C-NMR (100 MHz, $CDCl_3$) δ 158.1, 129.1, 124.1, 123.0, 119.6, 117.1, 110.7, 95.8. Spectral data were in accordance with those reported in literature.[140]

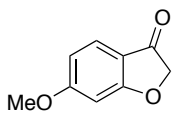

100

Synthesis of 6-methoxybenzofuranone (100). In air, a 10 mL

microwave vial equipped with a stir bar was charged with 6-hydroxy-3-coumaranone **99** (0.525 g, 3.5 mmol, 1 equiv.) and anhydrous K_2CO_3 (0.967 g, 7 mmol, 2 equiv.) at rt. The vial was sealed with a septum and purged with argon (3x). Anhydrous DMF (5.5 mL) was added via syringe, followed by methyl iodide (0.4 mL, 6.3 mmol, 1.8 equiv.) and the mixture was allowed to stir for 5 min at rt. The vial was exposed to microwave heating for 20 min at 100 °C. The reaction vessel was allowed to cool to rt. Chilled distilled water (~10 mL) was then added to the reaction mixture allowing precipitation of the crystals. The mixture was extracted with Et_2O, dried with $MgSO_4$, and dried in vacuo. The crude product was purified on silica gel by flash chromatography (20/80 EtOAc/hexanes, Rf = 0.2) providing **100** as a yellow solid (0.56 g, 97 %). Mp: 120–123°C (lit. mp: 122–124°C)[141]; ^{1}H-NMR (400 MHz, $CDCl_3$) δ 7.59 (d, J = 10.4 Hz, 1H), 6.67 (dd, J = 2.0, 8.8 Hz, 1H), 6.57 (d, J = 2.0 Hz, 1H), 4.56 (s, 2H), 3.91 (s, 3H); ^{13}C-NMR (100 MHz, $CDCl_3$) δ 197.4, 176.4, 168.1, 125.0, 114.2, 111.6, 102.7, 96.2, 75.4, 55.8. Spectral data were in accordance with those reported in literature.[141]

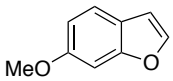

101

Synthesis of 6-methoxybenzofuran (101). This compound was prepared according to a procedure modified from Anderson and co-workers.[142] To a stirred solution of **100** (0.524 g, 3.19 mmol, 1 equiv) in EtOH (12 mL) and CH_2Cl_2 (4 mL) was added $NaBH_4$ (67 mg, 1.77 mmol, 0.55). The mixture was stirred at rt overnight after which time 1M HCl (13 mL) was added. The product was extracted with Et_2O (2 x 15 mL) and the combined organic layers were washed with brine (20 mL), dried with $MgSO_4$, and dried in vacuo. The residue was purified using silica gel flash

chromatography (2/98 EtOAc/hexanes, R_f = 0.2) to afford **101** as a colourless oil (0.357 g, 75 %). ^{1}H-NMR (400 MHz, $CDCl_3$) δ 7.56 (d, J =2.0 Hz, 1H), 7.48 (d, J = 8.4 Hz, 1H), 7.07 (s, 1H), 6.91 (dd, J = 2.0, 10 Hz, 1H), 6.72 (s, 1H), 3.88 (s, 3H); ^{13}C-NMR (100 MHz, $CDCl_3$) δ 157.9, 155.8, 143.9, 121.0, 120.5, 111.8, 106.8, 95.8, 55.6. Spectral data were in accordance with those reported in literature.[143]

Synthesis of 2-iodo-6-methoxybenzofuran (102).

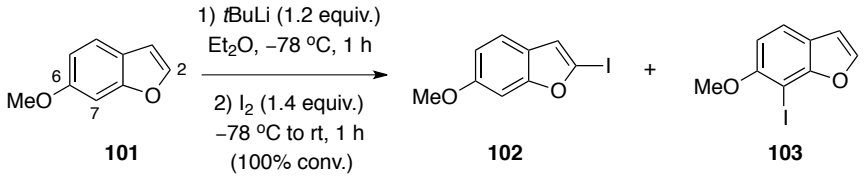

This compound was prepared according to a procedure modified from Zhang and Larock.[140] To a stirred solution of **101** (0.185 g, 1.25 mmol, 1 equiv) in anhydrous Et_2O (2.5 mL) under an argon atmosphere at -78°C was added slowly *t*BuLi (0.81 mL, 1.7M in pentane, 1.37 mmol, 1.1 equiv.) via syringe. The mixture was stirred for 1 hr and a solution of I_2 (0.35 g, 1.37 mmol, 1.1 equiv) in dry ether (3.75 mL) was added at −78°C. The mixture was stirred for another 1 hr, allowed to warm to rt, diluted with saturated aqueous NH_4Cl, and extracted with Et_2O. The organic solution was washed with $Na_2S_2O_3$ and water, dried over Na_2SO_4, and dried in vacuo to give the crude mixture of iodinated species in 93.6 % total yield (ratio **102**:**103** = 6:1). Compounds **102** and **103** were separated using HP silica gel flash chromatography (heptane) to afford firstly 2-iodo isomer **102** (5/95 Et_2O/heptane, Rf = 0.15) as a white solid (0.20 g, 58%). Mp: 95–99°C; ^{1}H-NMR (400 MHz, $CDCl_3$) δ 7.39 (d, J =8.8 Hz, 1H), 7.03 (d, J = 1.6 Hz, 1H), 6.89 (m,

2H), 3.86 (s, 3H); ^{13}C-NMR (150 MHz, $CDCl_3$) δ: 158.9, 157.8, 122.6, 119.7, 112.1, 95.5, 93.0, 65.9, 55.7. Anal. Calcd. for $C_{17}H_{16}O_4$: C, 71.82; H, 5.67; O, 22.51. Found: C, 71.14; H, 5.74. The second fraction gave the 7-iodo isomer **103** (5/95 Et_2O/heptane, Rf = 0.13) as a light yellow oil (0.031 g, 9%). ^{1}H-NMR (400 MHz, $CDCl_3$) δ: 7.64 (d, J =1.6 Hz, 1H), 7.49 (d, J = 8.4 Hz, 1H), 6.86 (m, 2H), 3.98 (s, 3H); ^{13}C-NMR (150 MHz, $CDCl_3$) δ: 156.6, 156.5, 144.9, 121.2, 121.1, 107.9, 107.3, 67.0, 57.8.

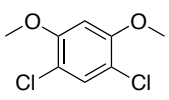

105

Synthesis of 1,5-dichloro-2,4-dimethoxybenzene (105). Compound **105** was prepared according to a procedure reported by Mikriyannis *et. al*.[144] A 100 mL round-bottom flask equipped with a magnetic stir bar was charged with 4,6-dichloro-1,3-benzene-diol (1.00 g, 5.6 mmol, 1 equiv.) and crushed anhydrous K_2CO_3 (1.94 g, 14.0 mmol, 2.5 equiv.) then evacuated and backfilled with Ar (3x). Anhydrous DMF (20 mL) was added *via* syringe, followed by methyl iodide (0.80 mL, 12.3 mmol, 2.2 equiv.) and the mixture was stirred vigorously for 5 h at rt. Chilled H_2O was then added to the reaction mixture causing precipitation of the product. The mixture was extracted with Et_2O (3x) and the pooled organic layers were washed successively with water and brine, then dried over anhydrous $MgSO_4$, filtered, and the solvent removed *in vacuo*. Decolourlizing with charcoal and filtering through a pad of silica gel yielded **105** as white crystals (1.05 g, 90 %). Mp: 113–115 °C (119 °C lit.)[105]; ^{1}H-NMR (400 MHz, $CDCl_3$) δ 7.37 (s, 1H), 6.55 (s, 1H), 3.93 (s, 6H); ^{13}C-NMR (75 MHz, $CDCl_3$) δ 154.4, 130.4, 113.9, 97.6, 56.4. Spectral data were in accordance with those reported in the literature.[105]

General Procedure for the Preparation of Aryl Boronic Acid (107a) and Pinacol Ester (107b): *n*BuLi (2.4 M in hexanes, 1.2 equiv.) was added drop-wise to a stirred solution of the **105** (1.0 equiv.) in dry THF at –78 °C. After stirring for 1 hour the boron electrophile (5 equiv.) was added. After the mixture was warmed to rt, the reaction was quenched by dropwise addition of 1M HCl, acidifying to pH ~ 2-4. Alternatively, if the boron electrophile was 2-isopropoxy-4,4,5,5-tetramethyl-1,3,2-dioxaborolane (*i*Pr-O-Bpin), saturated aqueous NH_4Cl was added to quench the reaction. The mixture was extracted with Et_2O (3x) and the pooled organic layers were washed with brine, dried over anhydrous $MgSO_4$, filtered, and the solvent removed *in vacuo*. The crude product was purified by recrystallization from Et_2O/pentane.

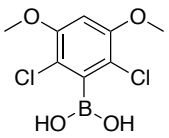

108a

2,6-dichloro-3,5-dimethoxyphenylboronic acid (108a). Using the general lithiation procedure on a 1 mmol scale, 160.1 mg (64%) of **108a** were obtained following recrystallization from Et_2O/pentane as a white solid. Mp: 265–270°C (decomp.); ^{1}H-NMR (400 MHz, DMSO-d_6) δ 8.51 (s, 2H), 6.82 (s, 1H), 3.88 (s, 6H); ^{13}C-NMR (75 MHz, DMSO-d_6) δ 154.3, 140.7, 114.1, 98.4, 56.9; ^{11}B-NMR (96 MHz, $CDCl_3$) δ: -38.9; HRMS (EI) [M^+] calcd. for $C_8H_9BCl_2O_4$, 249.9971; found 249.9954.

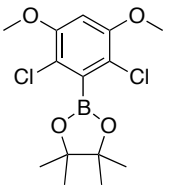

108b

2,6-dichloro-3,5-dimethoxyphenylpinacolboronic ester (108b). Using the general lithiation procedure on a 5 mmol scale, 1.21 g (72%) of **108b**

were obtained following recrystallization from Et_2O/pentane as an off-white solid. Mp: 161–163°C; ^{1}H-NMR (400 MHz, $CDCl_3$) δ 6.52 (s, 1H), 3.87 (s, 6H), 1.42 (s, 12H); ^{13}C-NMR (100 MHz, $CDCl_3$) δ 154.1, 133.3, 116.5, 98.6, 84.9, 56.4, 24.6; ^{11}B-NMR (96 MHz, $CDCl_3$) δ 30; HRMS (EI) [M^+] calcd. for $C_{14}H_{19}BCl_2O_4$, 332.0753; found 332.0737.

General Procedure for the Negishi Cross-Coupling Reaction: Compounds **109a** and **111** were prepared according to a procedure modified from Buchwald and Milne.[107] *n*BuLi (2.4 M in hexanes, 1.8 equiv.) was added drop-wise to a stirred solution of **105** (1.5 equiv.) in dry THF (C = 0.30 M) at –78 °C. After stirring for 1 h, $ZnCl_2$ (2.25 equiv.) dissolved in THF (C = 0.75 M) was added to the reaction mixture. After 30 min at –78 °C, the cooling bath was removed and the mixture was stirred at rt for 1.5 h. *Pd-PEPPSI-IPr* (4 mol%) and 2-iodobenzofurans **98** or **102** (1 equiv.) dissolved in THF (C = 0.4 M) were then added to the mixture and the flask was heated in an oil bath to 50 °C for 18 h. The reaction mixture was cooled to rt, diluted with saturated aqueous NH_4Cl, extracted with Et_2O (3x), and the pooled organic layers washed with brine, dried over anhydrous $MgSO_4$, filtered, and the solvent removed *in vacuo*. The crude product was purified by flash chromatography.

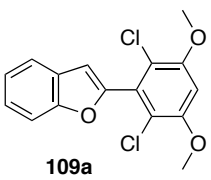

109a

2-(2,6-dichloro-3,5-dimethoxyphenyl)benzofuran (109a). Following the general Negishi cross-coupling procedure on a 2.0 mmol scale, 485 mg (75%) of **109a** were obtained following silica gel flash

chromatography (5% → 20% Et_2O/pentane gradient; R_f = 0.17 in 10/90 Et_2O/pentane) as a white solid. Mp: 195–198 °C; ^{1}H-NMR (400 MHz, $CDCl_3$) δ 7.68 (d, *J* = 8.0 Hz, 1H), 7.58 (d, *J* = 8.0 Hz, 1H), 7.36 (t, *J* = 7.2 Hz, 1H), 7.30 (t, *J* = 7.2 Hz, 1H), 6.90 (s, 1H), 6.71 (s, 1H), 3.99 (s, 6H); ^{13}C-NMR (100 MHz, $CDCl_3$) δ 154.8, 154.5, 149.9, 131.1, 128.1, 124.4, 122.8, 121.2, 116.1, 111.4, 108.1, 98.4, 56.6; HRMS (EI) [M^+] calcd. for $C_{16}H_{12}Cl_2O_3$ 322.0163; found 322.0167.

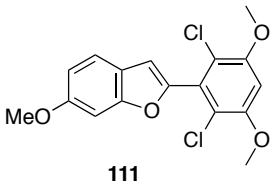

111

2-(2,6-dichloro-3,5-dimethoxyphenyl)-6-methoxybenzofuran (111). Following the general Negishi cross-coupling procedure on a 0.115 mmol scale, 34.1 mg (84%) of **111** were obtained following silica gel chromatography (5% → 25% Et_2O/pentane gradient, R_f = 0.12 in 5/95 Et_2O/pentane) as a white solid. Mp: 201–203°C; ^{1}H-NMR (400 MHz, $CDCl_3$) δ: 7.53 (d, *J* = 8.6 Hz, 1H), 7.11 (d, *J* = 1.8 Hz, 1H), 6.93 (dd, *J* = 8.5, 2.3 Hz, 1H), 6.82 (s, 1H), 6.69 (s, 1H), 3.99 (s, 1H), 3.89 (s, 3H); ^{13}C-NMR (100 MHz, $CDCl_3$) δ 158.1, 155.8, 154.5, 148.8, 131.2, 121.4, 121.3, 116.2, 112.1, 108.0, 98.3, 95.7, 56.6, 55.6. HRMS (EI) [M^+] calcd. for $C_{17}H_{14}Cl_2O_4$, 352.0269; found 352.0266.

5.6 Attempted Preparation of Isoprenylated Natural Products – cathafuran A (58) and lakoochin A (59).

General Procedure for the Regioselective Suzuki-Miyaura Cross-Coupling Reaction: In air, a Biotage 2-5 mL microwave vial equipped with a stir bar was charged with *Pd-PEPPSI-IPent* (**53**) (6 mol%), boronic ester **60a** or **60b** (0.75 mmol, 3.0 equiv.),

and 2-arylbenzofuran **109** or **111** (0.25 mmol, 1 equiv.) at rt. The vial was sealed with a septum, evacuated (0.1 mmHg) and purged with argon (3x). THF (0.5 mL) was then added followed by 7M KOH (2.0 mmol, 8 equiv.), and the reaction vial was heated in an oil bath to 70°C for 24 hr. The reaction mixture was cooled to rt, extracted with Et_2O (3x), and the pooled organic layers washed with brine, dried over anhydrous $MgSO_4$, filtered, and the solvent removed *in vacuo*. The crude product was first purified by flash chromatography.

Model Reaction - Synthesis of 2-(3,5-dimethoxy-2,6-bis(3-methylbut-2-en-1-yl)phenyl)benzofuran (114).

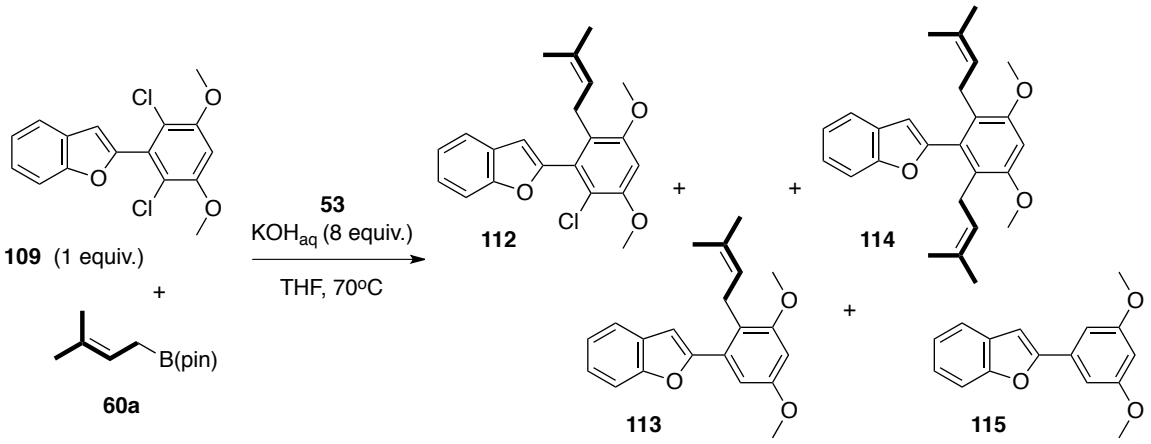

Following the general Suzuki-Miyaura cross-coupling procedure on a 0.25 mmol scale, compound **114** (>99:1, α:γ isomer) was produced along with three side products (**112**, **113**, **115**). The crude reaction was first purified by flash chromatography (0% → 10% Et_2O/pentane gradient), separating compound **112** from **113** and **114**. The fraction containing the mixture of compounds **113** and **114** was further purified by HPLC (C-18 analytical column, eluent: 50% → 0% H_2O/MeCN, flow rate: 1 mL/min). All of the compounds isolated are characterized below.

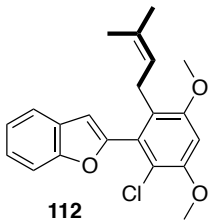

112

2-(2-chloro-3,5-dimethoxy-6-(3-methylbut-2-en-1-yl)phenyl)benzofuran (112). White solid (16.3 mg, 18%). Note: not enough material was isolated to obtain a melting point. R_f = 0.22 in 5/95 Et_2O/pentane. The spectra for the major α–isomer are included here. ^{1}H-NMR (400 MHz, $CDCl_3$) δ 7.64 (d, *J* = 7.6 Hz, 1H), 7.53 (d, *J* = 8.0 Hz, 1H), 6.76 (s, 1H), 6.66 (s, 1H), 5.08-5.05 (m, 1H), 3.96 (s, 3H), 3.90 (s, 3H), 3.27 (d, *J* = 6.8 Hz, 2H), 1.60 (s, 3H), 1.41 (s, 3H); ^{13}C-NMR (100 MHz, $CDCl_3$) δ 156.6, 154.6, 153.7, 151.8 131.2, 131.0, 128.3, 124.8, 123.9, 122.5, 122.5, 120.8, 114.8, 111.1, 107.1, 97.9, 56.4, 55.8, 26.6, 25.5, 17.4; HRMS (EI) [M^+] calcd. for $C_{21}H_{21}ClO_3$, 356.1179; found 356.1192.

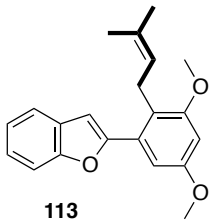

113

2-(3,5-dimethoxy-2-(3-methylbut-2-en-1-yl)phenyl)benzofuran (113). Clear, colourless oil. R_f = 0.44 in 5/95 Et_2O/pentane. HPLC retention time = 15.4 min. The spectra for the major α–isomer are included here. ^{1}H-NMR (600 MHz, $CDCl_3$) δ 7.61 (d, *J* = 7.2 Hz, 1H), 7.53 (d, *J* = 8.4 Hz, 1H), 7.31 (t, *J* = 7.7 Hz, 1H), 7.25 (t, *J* = 7.5 Hz, 1H), 6.88 (d, *J* = 2.4 Hz, 1H), 6.86 (s, 1H), 6.54 (d, *J* = 2.4 Hz, 1H), 5.19-5.18 (m, 2H), 3.87 (s, 6H), 3.86 (s, 6H), 3.51 (d, *J* = 6.6 Hz, 2H), 1.71 (s, 6H); ^{13}C-NMR (150 MHz, $CDCl_3$) δ 159.0, 158.6, 155.6, 154.6 131.4, 131.3, 129.1, 124.1, 123.7, 122.7, 121.8, 120.9, 111.1, 105.3, 104.6, 99.6, 55.8, 55.5 26.0, 25.8, 18.0; HRMS (EI) [M^+] calcd. for $C_{21}H_{22}O_3$, 322.1569; found 322.1157.

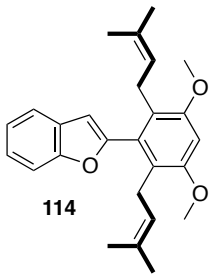

114

2-(3,5-dimethoxy-2,6-bis(3-methylbut-2-en-1-yl)phenyl)benzofuran (114): Clear, colourless oil. R_f = 0.42 in 5/95 Et_2O/pentane. HPLC retention time = 13.6 min. The spectra for the major α–isomer are included here. ^{1}H-NMR (600 MHz, $CDCl_3$) δ 7.59 (d, *J* = 7.8 Hz, 1H), 7.48 (d, *J* = 8.4 Hz, 1H), 7.27-7.24 (m, 2H), 6.63 (s, 1H), 6.62 (s, 1H), 5.09-5.07 (m, 2H), 3.87 (s, 6H), 3.14 (d, *J* = 7.2 Hz, 4H), 1.58 (s, 6H), 1.37 (s, 6H); ^{13}C-NMR (150 MHz, $CDCl_3$) δ 156.4, 154.8, 154.2, 131.8, 130.3, 128.9, 123.6, 123.2, 122.5, 120.7, 111.2, 106.5, 106.5, 97.4, 55.9, 26.6, 25.7, 17.6; HRMS (EI) [M^+] calcd. for $C_{26}H_{30}O_3$, 390.2195; found 390.2213.

Synthesis of methylated cathafuran A.

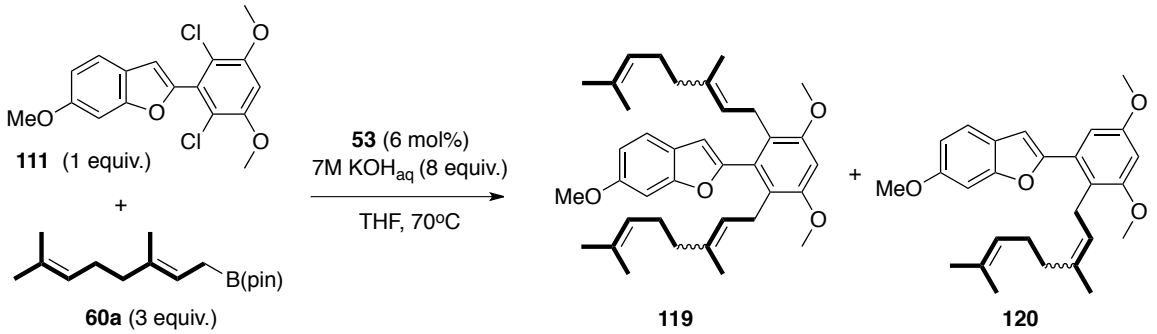

Following the general Suzuki-Miyaura cross-coupling procedure on a 0.25 mmol scale, compounds **119** and **120** (>99:1, α:γ isomer) were produced. The crude reaction was purified by flash chromatography (50% → 75% toluene/hexanes gradient), yielding 61.2 mg (45%) of compound **119** (**119a** *E/E* = 70%, **119b** *E/Z* = 30%). Compound **120** was obtained alongside some other unknown impurity (34.7 mg, 33%), therefore the olefin

geometry for **120** could not be determined. The spectra for the major α–isomer for compound **119** are described below.

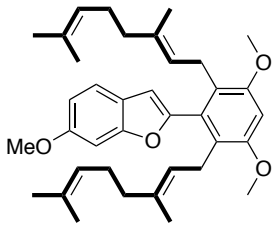

119a

E/E-isomer ^{1}H-NMR (600 MHz, $CDCl_3$) δ 7.46 (d, *J* = 8.5 Hz, 1H), 7.00 (s, 1H), 6.86 (dd, *J* = 8.5 Hz, 1H), 6.60 (s, 1H), 6.53 (s, 1H), 5.10-5.08 (m, 2H), 5.06-5.04 (m, 2H), 3.86 (s, 6H), 3.85 (s, 3H), 3.16 (d, *J* = 6.6 Hz, 4H), 2.00-1.96 (m, 4H), 1.89-1.86 (m, 4H), 1.65 (s, 6H), 1.57 (s, 6H), 1.38 (s, 6H); ^{13}C-NMR (150 MHz, $CDCl_3$) δ 157.5, 156.4, 155.8, 153.2, 133.8, 132.1, 131.0, 124.6, 123.7, 123.3, 122.2, 120.7, 111.5, 106.3, 97.3, 95.9, 55.9, 55.7, 39.7, 26.7, 26.4, 25.6, 17.6, 15.8.

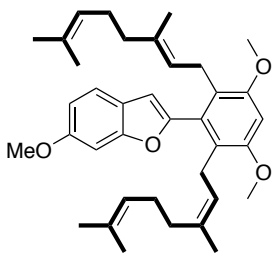

E/Z-isomer ^{1}H-NMR (600 MHz, $CDCl_3$) δ 7.46 (d, *J* = 8.5 Hz, 1H), 7.00 (s, 1H), 6.86 (dd, *J* = 8.5 Hz, 1H), 6.60 (s, 1H), 6.53 (s, 1H), 5.10-5.08 (m, 1H), 5.06-5.04 (m, 2H), 54.97-4.94 (m, 1H), 3.86 (s, 6H), 3.85 (s, 3H), 3.16 (d, *J* = 6.6 Hz, 4H), 2.00-1.96 (m, 4H), 1.89-1.84 (m, 4H), 1.65 (s, 6H), 1.58 (s, 3H), 1.57 (s, 3H), 1.50 (s, 3H), 1.38 (s, 3H); ^{13}C-NMR (150 MHz, $CDCl_3$) δ 157.5, 156.4, 155.8, 153.2, 134.3, 133.8, 132.1, 131.0, 124.6 (two overlapping signals), 124.3, 123.7, 123.3, 122.2, 120.7, 111.5, 106.3, 97.3, 95.9, 55.9, 55.7, 39.7, 31.8, 26.7, 26.4, 25.6, 23.4, 17.6, 17.5, 15.8; HRMS (EI) [M^+] calcd. for $C_{37}H_{48}O_4$, 556.3553; found 556.3539.

Attempted Double Demethylation of compound 85.

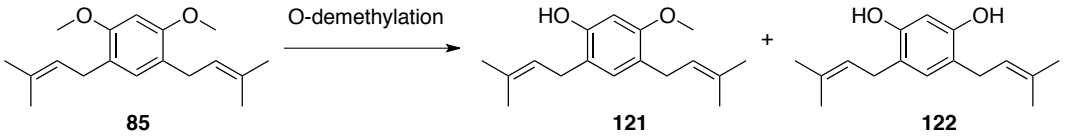

85 **121** **122**

*n*BuLi (2.07 M in hexanes, 4.0 equiv.) was added drop-wise to a stirred solution of diphenylphosphine (0.35 mL, 2.01 mmol, 4.0 equiv.) in dry THF (2.5 mL) at 0 °C and the reaction was stirred for 1 h. In a separate flame-dried Biotage 2-5 mL microwave vial was prepared a solution of **85** (137.2 mg, 0.5 mmol, 1 equiv.) in dry THF (1 mL). This solution was added to the freshly prepared lithium diphenylphosphanide dropwise via syringe. After the addition was complete the reaction was first warmed to room temperature and then heated to 70 °C for 18 h. The reaction mixture was then cooled to room temperature and extracted with Et_2O (3x). The pooled organic layers were washed with brine, dried over anhydrous $MgSO_4$, filtered, and the solvent removed *in vacuo*. The residue obtained contained a mixture of **121** and **122** 45:55 ratio). Compounds **121** and **122** were separated using silica gel flash chromatography (10% → 50% ether/pentane gradient) to afford firstly **121 (**R_f = 0.8 in 50/50 Et_2O/pentane) as a colourless oil (17.2 mg, 13%). ^{1}H-NMR (400 MHz, $CDCl_3$) δ 6.82 (s, 1H), 6.35 (s, 1H), 5.34-5.27 (m, 2H), 5.14 (s, 1H), 3.79 (s, 3H), 3.29 (d, *J* = 7.2 Hz, 2H), 3.29 (d, *J* = 7.2 Hz, 2H), 1.81 (s, 3H), 1.79 (s, 3H), 1.75 (s, 3H), 1.72 (s, 3H); ^{13}C-NMR (100 MHz, $CDCl_3$) δ 156.5, 153.1, 134.3, 131.8, 130.3, 123.0, 122.4, 121.9, 117.6, 99.4, 55.4, 29.3, 27.7, 25.8, 25.7, 17.7, 17.6; HRMS (EI) [M^+] calcd. for $C_{18}H_{26}O_2$, 260.1776; found 260.1768. The second fraction gave the **122** (R_f = 0.31, in 50/50 Et_2O/pentane) and an unknown impurity as an orange oil. ^{1}H-NMR (400 MHz, $CDCl_3$) δ 6.80 (s, 1H), 6.35 (s, 1H), 5.33-5.30 (m, 2H),

5.05 (bs, 1H), 3.28 (d, J = 7.2 Hz, 4H) 1.79 (s, 12H); ^{13}C-NMR (100 MHz, $CDCl_3$) δ 153.5, 134.2, 130.7, 122.4, 118.5, 103.6, 29.1, 25.7, 17.7; HRMS (EI) [M^+] calcd. for $C_{16}H_{22}O_2$, 246.1620; found 246.1618.

5.7 Regioselective DoM of Compound 105.

General Procedures for the DoM of 105 at C6 (i.e., Between the Two Chlorides). Synthesis of compounds 107, 123, 127, 128, and 129: *n*BuLi (2.4 M in hexanes, 1.2 equiv.) was added drop-wise to a stirred solution of the **105** (1.0 equiv.) in dry THF at –78 °C. After stirring for 1 hour the electrophile was added. After the mixture was warmed to rt, saturated aqueous NH_4Cl was added to quench the reaction. The mixture was extracted with Et_2O (3x) and the pooled organic layers were washed with brine, dried over anhydrous $MgSO_4$, filtered, and the solvent removed *in vacuo*. Alternatively, if the electrophile was I_2 the organic layers were washed with $Na_2S_2O_3$ prior to washing with brine. The crude product was purified by flash chromatography.

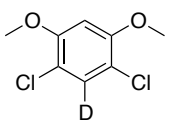

107

2,4-dichloro-3-deuterium-1,5-dimethoxybenzene (107). Following the general procedure on a 3 mmol scale, 0.4993 g (80%) of **107** were obtained following silica gel flash chromatography (10% ether/pentane; R_f = 0.17 (10% ether/pentane)) as light-yellow crystals. Mp: 110–112 °C; ^{1}H-NMR (400 MHz, $CDCl_3$) δ 6.55 (s, 1H), 3.93 (s, 6H); ^{13}C-NMR (75 MHz, $CDCl_3$) δ 154.4, 130.1 (t, J = 25 Hz), 113.8, 97.6, 56.4; ^{2}H-NMR (61.4 MHz, $CHCl_3$) δ: 6.36 (s, 1^{2}H); HRMS (EI) [M^+] calcd. for $C_8H_7DCl_2O_2$ 206.9964; found 206.9957.

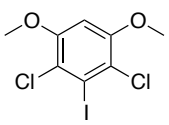

123

2,4-dichloro-3-iodo-1,5-dimethoxybenzene (123). Following the general procedure on a 5 mmol scale, 1.50 g (90%) of **123** were obtained following silica gel flash chromatography (5% → 20% ether/pentane gradient, R_f = 0.12 (10% ether/pentane)) as white crystals. Mp: 170–172 °C; ^{1}H-NMR (400 MHz, $CDCl_3$) δ 6.62 (s, 1H), 3.94 (s, 6H); ^{13}C-NMR (100 MHz, $CDCl_3$) δ 154.1, 119.8, 106.1, 97.2, 56.6; HRMS (EI) [M^+] calcd. for $C_8H_7Cl_2IO_2$ 331.8868; found 331.8879.

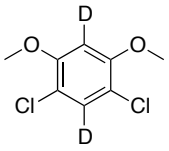

127

1,3-dichloro-2,5-deuterium-4,6-dimethoxybenzene (127). Using **125** as the starting material and following the general procedure on a 2.5 mmol scale, 0.455 g (87%) of **127** were obtained following silica gel flash chromatography (0% → 10% ether/pentane gradient; R_f = 0.20 (10% Ether/pentane)) as a white solid. Mp: 107–109 °C; ^{1}H-NMR (600 MHz, $CDCl_3$) δ 3.93 (s, 6H); ^{13}C-NMR (150 MHz, $CDCl_3$) δ 154.5, 130.2 (t, J = 25.5 Hz), 113.9, 97.4 (t, J = 25.5 Hz), 56.5; ^{2}H-NMR (61.4 MHz, $CHCl_3$) δ 6.36 (s, 1^2H), 5.54 (s, 1^2H); HRMS (EI) [M^+] calcd. for $C_8H_6D_2Cl_2O_2$ 208.0027; found 208.0034.

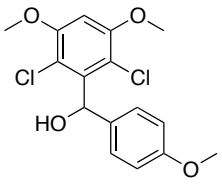

128

(2,6-dichloro-3,5-dimethoxyphenyl)(4-methoxyphenyl)meth-anol (128). Following the general procedure on a 0.25 mmol scale, 75.3 mg (88%) of **128** were obtained following silica gel flash chromatography (5% → 20% ethyl acetate/hexanes gradient, R_f = 0.13 (20% ethyl acetate/hexanes)) as a white solid. Mp: 131–133 °C; ^{1}H-NMR (400 MHz, $CDCl_3$) δ 7.22

(d, J = 8.8 Hz, 2H), 6.86 (d, J = 9.8 Hz, 2H), 6.66 (d, J = 11.2 Hz, 1H), 6.59 (s, 1H), 3.94 (s, 6H), 3.80 (s, 3H), 3.63 (J = 11.2 Hz, 1H); ^{13}C-NMR (100 MHz, $CDCl_3$) δ 158.6, 154.7, 139.2, 133.4, 126.6, 114.5, 113.5, 96.5, 72.5, 56.5, 55.1.

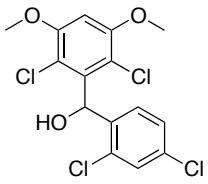

129

(2,6-dichloro-3,5-dimethoxyphenyl)(2,4-dichlorophenyl)meth- anol (129). Following the general procedure on a 0.25 mmol scale, 76.1 mg (80%) of **129** were obtained following silica gel flash chromatography (5% → 30% ethyl acetate/hexanes gradient, R_f = 0.22 (20% ethyl acetate/hexanes)) as a white solid. Mp: 175–177 °C; ^{1}H-NMR (400 MHz, $CDCl_3$) δ 7.54 (d, J = 8.4 Hz, 1H), 7.37 (d, J = 2.0 Hz, 1H), 7.24 (dd, J = 9.2 and 2.0 Hz, 1H), 6.72 (d J = 9.2 Hz, 1H), 6.60 (s, 1H), 3.95 (s, 6H), 3.16 (d, J = 9.2 Hz, 1H); ^{13}C-NMR (100 MHz, $CDCl_3$) δ 154.7, 137.0, 136.9, 133.8, 133.3, 130.1, 129.5, 126.3, 115.1, 98.6, 71.0, 56.5.

General Procedures for the DoM of Compound 105 at C3 (i.e., Between the Two Methoxy Groups). Synthesis of compounds 124, 125, 130, and 131: *n*BuLi (2.4 M in hexanes, 1.2 equiv.) was added drop-wise to a stirred solution of the **105** (1.0 equiv.) in dry Et_2O at rt. After stirring for 30 min., the electrophile was added. After an additional 30 min., the reaction mixture was quenched with saturated aqueous NH_4Cl. The mixture was extracted with Et_2O (3x) and the pooled organic layers organics were washed with brine, dried over anhydrous $MgSO_4$, filtered, and the solvent removed *in vacuo*. Alternatively, if the electrophile was I_2 the organic layers were washed with $Na_2S_2O_3$ prior to washing with brine. The crude product was purified by flash chromatography.

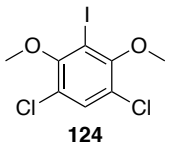

124

1,5-dichloro-3-iodo-2,4-dimethoxybenzene (124). Following the general procedure on a 5 mmol scale, 1.09 g (66%) of **124** were obtained following silica gel flash chromatography (0% → 5% ether/pentane gradient; R_f = 0.76 (5% ether/pentane)) as a light-yellow solid. Mp: 40–42 °C; ^{1}H-NMR (400 MHz, $CDCl_3$) δ 7.46 (s, 1H), 3.88 (s, 6H); ^{13}C-NMR (100 MHz, $CDCl_3$) δ 155.5, 130.8, 123.3, 92.1, 60.6; HRMS (EI) [M^+] calcd. for $C_8H_7Cl_2IO_2$ 331.8868; found 331.8859.

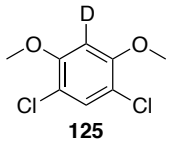

125

1,5-dichloro-3-deuterium-2,4-dimethoxybenzene (125). Following the general procedure on a 5 mmol scale, 0.78 g (75%) of **125** were obtained following silica gel flash chromatography (10% ether/pentane; R_f = 0.16 (10% ether/pentane)) as an off-white solid. Mp: 107–109 °C; ^{1}H-NMR (400 MHz, $CDCl_3$) δ 7.38 (s, 1H), 3.93 (s, 6H); ^{13}C-NMR (100 MHz, $CDCl_3$) δ 154.4, 130.4, 113.8, 97.3 (t, J = 24 Hz), 56.4; ^{2}H-NMR (61.4 MHz, $CHCl_3$) δ: 5.54 (s, 1^{2}H); HRMS (EI) [M^+] calcd. for $C_8H_7DCl_2O_2$ 206.9964; found 206.9970.

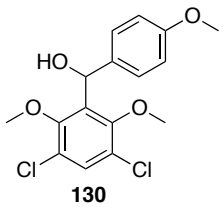

130

(3,5-dichloro-2,6-dimethoxyphenyl)(4-methoxyphenyl)meth- anol (130). Following the general procedure on a 0.25 mmol scale, 68.5 mg (80%) of **130** were obtained following silica gel flash chromatography (5% ethyl acetate/hexanes, R_f = 0.16 (5% ethyl acetate/hexanes)) as a colourless oil. ^{1}H-NMR (400 MHz, $CDCl_3$) δ 7.41 (s, 1H), 7.26 (d, J = 8.8 Hz, 2H), 6.89 (d, J = 8.8 Hz,

2H), 6.14 (d, *J* = 11.6 Hz, 1H), 3.90 (d, *J* = 11.6 Hz, 1H), 3.81 (s, 3H), 3.61 (s, 3H); ^{13}C-NMR (100 MHz, $CDCl_3$) δ 158.6, 153.1, 136.2, 134.2, 130.3, 126.3, 123.7, 113.5, 69.0, 61.3, 55.1.

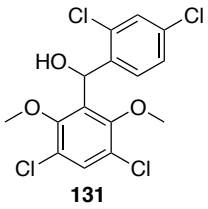

131

(3,5-dichloro-2,6-dimethoxyphenyl)(2,4-dichlorophenyl)methanol (131). Following the general procedure on a 0.25 mmol scale, 76.8 mg (80%) of **131** were obtained following silica gel flash chromatography (5% → 10% ethyl acetate/hexanes gradient, R_f = 0.25 (10% ethyl acetate/hexanes)) as a colourless oil. ^{1}H-NMR (400 MHz, $CDCl_3$) δ 7.63 (d, *J* = 8.4 Hz, 1H), 7.42 (s, 1H), 7.36 (d, *J* = 2.0 Hz, 1H), 7.33–7.31 (m, 1H), 6.34 (d, *J* = 8.6 Hz, 1H), 3.68 (s, 6H), 3.23 (d, *J* = 8.6 Hz, 1H); ^{13}C-NMR (100 MHz, $CDCl_3$) δ 153.5, 139.1, 133.5, 132.5, 131.3, 131.0, 129.2, 128.7, 126.8, 123.7, 67.0, 61.3.

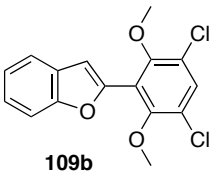

109b

Synthesis of 2-(3,5-dichloro-2,6-dimethoxyphenyl)benzofuran (109b). *n*BuLi (2.4 M in hexanes, 1.8 equiv.) was added drop-wise to a stirred solution of **105** (0.31 g, 1.5 mmol, 1.5 equiv.) in dry THF (5 mL, C = 0.30 M) at rt. After stirring for 1 h $ZnCl_2$ (0.31 g, 2.25 mmol, 2.25 equiv.) dissolved in THF (3 mL) was added to the reaction mixture and the mixture was further stirred for 2.0 h. *Pd-PEPPSI-IPr* (54.3 mg, 0.08 mmol, 4 mol%) and 2-iodobenzofuran (**98**) (0.49 g, 1.0 mmol, 1 equiv.) dissolved in THF (4 mL) were then added to the mixture and the flask was heated in an oil bath to 50 °C for 18 h. The reaction mixture was cooled to rt, diluted with saturated aqueous NH_4Cl, extracted with Et_2O (3x), and the

pooled organic layers washed with brine, dried over anhydrous $MgSO_4$, filtered, and the solvent removed *in vacuo*. The crude product was purified by flash chromatography (0% → 5% Et_2O/pentane gradient; R_f = 0.65 in 5/95 Et_2O/pentane) to yield 194 mg (70%) of **109b** as a light-yellow solid. Mp: 81–84 °C; ^{1}H-NMR (400 MHz, $CDCl_3$) δ 7.69 (d, *J* = 8.0 Hz, 1H), 7.60 (d, *J* = 8.0 Hz, 1H), 7.54 (s, 1H), 7.38 (t, *J* = 7.2 Hz, 1H), 7.32 (t, *J* = 7.2 Hz, 1H), 7.14 (s, 1H), 3.75 (s, 6H); ^{13}C-NMR (100 MHz, $CDCl_3$) δ 154.8, 153.9, 147.6, 131.1, 128.3, 124.6, 124.2, 122.9, 121.9, 121.2, 111.3, 108.7, 61.3; HRMS (EI) [M^+] calcd. for $C_{16}H_{12}Cl_2O_3$ 322.0163; found 322.0168.

CHAPTER 6 - References

1. For recent reviews, see: (a) Williams, R. M.; Stocking, E. M.; Sanz-Cervera, J. F.; *Top.*

1. For recent reviews, see: (a) Williams, R. M.; Stocking, E. M.; Sanz-Cervera, J. F.; *Top.*

Curr. Chem. **2000**, 97–173; (b) Li, S. *Nat. Prod. Rep.* **2010**, *27*, 57–78.

2. Mori, K.; Waku, M.; Sakakibara, M. *Tetrahedron* **1985**, *41*, 2825–2830.

3. Krohn, K.; Ngadjui, T. B.; Kapche, G. W. F. D.; Yapna, D. B.; Zareem, S.; Moustafa, M. Y.; Choudhary, M. I.; Kouam, F. S.; Khan, N. S. *J Nat. Prod.* **2006**, *69*, 229–233.

4. Fukui, H.; Feroj Hassan, A. F. M.; Ueoka, T.; Kyo, M. *Phytochemistry* **1998**, *47*, 1037–1039.

5. Wang, X. C.; Feng, J.; Huang, F.; Fan, Y. S.; Wang, Y. Y. ; Cao, L. Y.; Wen, P. W. *Biol. Pharm. Bull.* **2009**, *32*, 1565–1570.

6. Yazaki, K.; Sasaki, K.; Tsurumaru, Y. *Phytochemistry* **2009**, *70*, 1739–1745.

7. (a) Botta, B.; Delle Monache, G.; Menendez, P.; Boffi, A. *Trends Pharmacol. Sci.* **2005**, *26*, 606–608; (b) Botta, B.; Vitali, A.; Menendez, P.; Misiti, D.; Delle Monache, G. *Curr. Med. Chem.* **2005**, *12*, 717–739.

8. (a) Dandapani, S.; Marcaurelle, L. A.; *Curr. Opin. Chem. Biol.* **2010**, *14*, 362–370; (b) Ganesan, A. *Curr. Opin. Chem. Biol.* **2008**, *12*, 306–317.

9. (a) Lovering, F.; Bikker, J.; Humblet, C. *J. Med. Chem.* **2009**, *52*, 6752–6756; (b) Lovering, F. *Med. Chem. Commun*. **2013**, *4*, 515–519.

10. (a) Tello, M.; Kuzuyama, T.; Heide, L.; Noel, J. P.; Richard, S. B. *Cell. Mol. Life Sci.* **2008**, *65*, 1459–1463; (b) Dewick, P. M. *Nat. Prod. Rep.* **1997**, *14*, 111–144; (c) Balibar,

C. J.; Howard-Jones, A. R.; Walsh, C. T. *Nat. Chem. Biol.* **2007**, *3*, 584–592.

11. For a recent review on Friedel-Crafts (FC) alkylation involving FC-type allylations, see: Rueping, M.; Boris, J. N. *Beilstein Journal of Organic Chemistry* **2010**, *6*, No. 6.

12. Kodomari, M.; Nawa, S.; Miyoshi, T. *J. Chem. Soc., Chem. Commun.* **1995**, 1895–1896.

13. Min, J.-H.; Lee, J.-S.; Yang, J.-D.; Koo, S. *J. Org. Chem.* **2003**, *68*, 7925–7927.

14. (a) Gillman, H.; Bebb, R. *J. Am. Chem. Soc.* **1939**, *61*, 109–112; (b) Wittig, G.; Fuhrman, G. *Chem. Ber.* **1940**, *75*, 1197–1218.

15. Snieckus, V. *Chem. Rev*. **1990**, *90*, 879–933.

16. Neighbors, J. D.; Salnikova, M. S.; Wiemer, D. F. *Tetrahedron Letters* **2005**, *46*, 1321–1324.

17. Neighbors, J. D.; Salnikova, M. S.; Beutler, J. A.; Wiemer, D. F. *Bioorg. Med. Chem.* **2006**, *14*, 1771–1784.

18. (a) Beutler, J. A.; Shoemaker, R. H.; Johnson, T.; Boyd, M. R. *J. Nat. Prod.* **1998**, *61*, 1509–1512; (b) Beutler, J. A.; Jato, J.; Cragg, G. M.; Boyd, M. R. *Nat. Prod. Lett.* **2000**, *14*, 399–404.

19. (a) Kharasch, M. S.; Fields, E. K. *J. Am. Chem. Soc*. **1941**, *63*, 2316–2320; (b) Kharasch, M. S.; Fuchs, C. F. *J. Am. Chem. Soc*. **1943**, *65*, 504–507.

20. Johansson Seechurn, C. C. C.; Kitching, M. O.; Colacot, T. J.; Snieckus, V. *Angew. Chem Int. Ed.* **2012**, *51*, 5062–5085.

21. *Metal-catalyzed cross-coupling reactions*, 2nd ed.; de Meijere, A., Diederich, F. Eds.; Wiley: New York, 2004.

22. Trost, B. M.; Van Vranken, D. L. *Chem. Rev.* **1996**, *96*, 395–422; and references cited therein.

23. Tsuji, J.; Takahashi, H.; Morikawa, M. *Tetrahedron Lett.* **1965**, *49*, 4387–4388.

24. Hartwig, J. F. *The Organometallic Chemistry of the Transition Metals: From Bonding to Catalysis*; University Science: Sausalito, CA: **2010**.

25. Trost, B. M.; Hung, M.-H. *J. Am. Chem. Soc.* **1984**, *106*, 6837–6839.

26. For selected reviews on the η^3-η^1-η^3 isomerization of allyl palladium complexes, see: (a) ref. 22; (b) Pregosin, P. S.; Salzmann, R. *Coord. Chem. Rev.* **1996**, *155*, 35–68.

27. (a) Åkermark, B.; Hansson, S.; Vitagliano, A. *J. Am. Chem. Soc.* **1990**, *112*, 4587–4588; (b) Sjögren, M.; Hansson, S.; Åkermark, B.; Vitagliano, A. *Organometallics*, **1994**, *13*, 1963–1971; (c) Trost, B. M. *Acc. Chem. Res.* **1996**, *29*, 355–364.

28. Trost, B. M.; Fullerton, T. J. *J. Am. Chem. Soc.* **1973**, *95*, 292–294.

29. Trost, B. M.; Van Vranken, D. L.; Bingel, C. *J. Am. Chem. Soc.* **1992**, *114*, 9327–9343.

30. Miyashita, A.; Yasuda, A.; Takaya, H.; Toriumi, K.; Ito, T.; Souchi, T.; Noyori, R. *J. Am. Chem. Soc.* **1980**, *102*, 7932–7934.

31. Trost, B. M.; Strege, P. E. *J. Am. Chem. Soc.* **1977**, *99*, 1649–1651.

32. Hayashi, T. *Pure & Appl. Chem.*, **1988**, *60*, 7–12.

33. (a) von Matt, P.; Pfalz, A. *Angew. Chem., Int. Ed. Engl.* **1993**, *32,* 566–569; (b) Sprinz, J.; Helmchen, G. *Tetrahedron Lett.* **1993**, *34,* 1769–1773; (c) Dawson, G. J.; Frost, C. G.; Williams, J. M. J.; Coote, S. J. *Tetrahedron Lett.* **1993**, *34,* 3149–3150.

34. Hayashi, T.; Konishi, M.; Yokota, K.; Kumada, M. *J. Chem. Soc., Chem. Commun.*

1981, 313–314.

35. Matsushita, H.; Negishi, E. *J. Chem. Soc., Chem. Commun.* **1982**, 160–161.

36. Echavarren, A. M.; Tueting, D. R.; Stille, J. K. *J. Am. Chem. Soc.* **1988**, *110*, 4039–4041.

37. Pigge, F. C *Synthesis* **2010**, *11*, 1745–1762; and references therein.

38. Lou, Y.-R. *Comprehensive Handbook of Chemical Bond Energies*, CRC Press, Boca Raton, FL, **2007**.

39. For Pd-catalyzed reactions with allylfluorosilanes, see: (a) Hatanaka, Y.; Ebina, Y.; Hiyama, T. *J. Am. Chem. Soc.* **1991**, *113*, 7076–7077; (b) Hatanaka, Y.; Goda, K.; Hiyama, T. *Tetrahedron Lett.* **1994**, *35*, 6511–6514.

40. For Pd-catalyzed reactions with allylstannanes, see: (a) Echavarren, A. M.; Stille, J. K. *J. Am. Chem. Soc.* **1987**, *109*, 5478–5486; (b) Farina, V.; Krishnan, B. *J. Am. Chem. Soc.* **1991**, *113*, 9585–9595; (c) Obora, Y.; Tsuji, Y.; Kobayashi, M.; Kawamura, T. *J. Org. Chem.* **1995**, *60*, 4647–4649; (d) Takaoka, S.; Nakade, K.; Fukuyama, Y. *Tetrahedron Lett.* **2002**, 43, 6919–6923; (e) Takemura, S.; Hirayama, A.; Tokunaga, J.; Kawamura, F.; Inagaki, K.; Hashimoto, K.; Nakata, M. *Tetrahedron Lett.* **1999**, *40*, 7501–7505; (f) Mattson, A. E.; Scheidt, K. A. *J. Am. Chem. Soc.* **2007**, *129*, 4508–4509; (g) Takaoka, S.; Takaoka, N.; Minoshima, Y.; Huang, J.-M.; Kubo, M.; Harada, K.; Hioki, H.; Fukuyama, Y. *Tetrahedron* **2009**, *65*, 8354–8361.

41. For Pd-catalyzed reactions with allylboron derivatives, see: (a) Yamamoto, Y.; Takada, S.; Miyaura, N. *Chem. Lett.* **2006**, *35*, 704–705; (b) Yamamoto, Y.; Takada, S.; Miyaura, N. *Chem. Lett.* **2006**, *35*, 1368–1369; (c) Yamamoto, Y.; Takada, S.; Miyaura,

N. *Organometallics* **2009**, 28, 152–160; (d) Sebelius, S.; Olsson, V. J.; Szabó, K. J. *J. Am. Chem. Soc.* **2005**, *127*, 10478–10479; (e) Olsson, V. J.; Sebelius, S.; Selander, N.; Szabó, K. J. *J. Am. Chem. Soc.* **2006**, *128*, 4588–4589; (f) Sebelius, S.; Olsson, V. J.; Wallner, O. A.; Szabó, K. *J. J. Am. Chem. Soc.* **2006**, *128*, 8150–8151; (h) For a publication on secondary allylic boronic esters, see: Glasspoole, B. W.; Ghozati, K.; Moir, J. M.; Crudden, C. M. *Chem. Commun.* **2012**, *48*, 1230–1232.

42. (a) Tsuji, T.; Yorimitsu, H.; Oshima, K. *Angew. Chem., Int. Ed.* **2002**, *41*, 4137–4139; (b) Ohmiya, H.; Tsuji, T.; Yorimitsu, H.; Oshima, K. *Chem.-Eur. J.* **2004**, *10*, 5640–5648.

43. Xu, Z.; Negishi, E.-I. *Org. Lett.* **2008**, *10*, 4311–4314.

44. Lee, P. H.; Sung, S.-Y.; Lee, K. *Org. Lett.* **2001**, *3*, 3201–3204.

45. Yamamoto, Y.; Maruyana, R. *J. Org. Chem.* **1983**, *48*, 1564–1565.

46 .Yang, Y.; Mustard, T. J.; Cheong, P. H.; Buchwald, S. L. *Angew. Chem., Int. Ed.* **2013**, *52*, 14098–14102.

47. (a) Tolman, C. A. *J. Am. Chem. Soc*. **1970**, *92*, 2953–2956; (b) Tolman, C. A. *J. Am. Chem. Soc.* **1970**, *92*, 2956–2965.

48. Tolman, C. A. *Chem. Rev.* **1977**, *77*, 313–348.

49. Freixa, Z.; van Leeuwen, P. W. N. M. *Dalton Trans.* **2003**, 1890–1901.

50. Negishi, E.-i, Takahashi, T.; Akiyoshi, K. *J. Orgomet. Chem.* **1987**, *334*,181–194.

51. Housecroft, C. E; Sharpe, A. G. *Inorganic Chemistry,* Pearson Prentice Hall, **2008.**

52. Tolman, C. A. *J. Am. Chem. Soc.* **1970**, *92*, 2953–2955.

53. Hayashi, T.; Konishi, M.; Kumada, M. *Tetrahedron Lett.* **1979**, 1871–1874.

54. Brown, J. M.; Guiry, P. J. *Inorg. Chim. Acta.* **1994**, *220*, 249–259.

55. Negishi, E.-i.; *Handbook of Organopalladium Chemistry for Organic Synthesis*; Wiley-Interscience: New York, **2002**.

56. Birkholz, M.-N.; Freixa, Z.; van Leeuwen, P. W. N. M. *Chem. Soc. Rev*., **2009**, *38*, 1099–1118.

57. Littke, A. F.; Fu, G. C. *Angew. Chem. Int. Ed*. **1998**, *37*, 3387–3388.

58. For a review of the Buchwald family of dialkybiaryl phosphines, see: Martin, R.; Buchwald, S. M. *Acc. Chem. Res.* **2008**, *41*, 1461–1473.

59. QPhos ligand: (a) Shelby, Q.; Kataoka, N.; Mann, G.; Hartwig, J. F. *J. Am. Chem. Soc.* **2000**, *122*, 10718–10719; JosiPhos ligand: (b) Shen, Q.; Shekhar, S.; Stambuli, J. P.; Hartwig, J. F. *Angew. Chem. Int. Ed.* **2005**, *44*, 1371–1375; (c) Alvaro, E.; Hartwig, J. F. *J. Am. Chem. Soc.* **2009**, *131*, 7858–7868.

60. See: (a) Organ, M. G.; Chass, G. A.; Fang, D.-C.; Hopkinson, A. C.; Valente, C. *Synthesis* **2008**, *17*, 2776–2797; and (b) references 1-4 therein.

61. (a) Wanzlick, H. W. *Angew. Chem. Int. Ed*. **1962**, *1*, 75–80; (b) Wanzlick, H. W.; Schönherr, H. J. *Angew. Chem. Int. Ed*. **1968**, *7*, 141–142.

62. Öfele, K.; *J. Organomet. Chem*. **1968**, *12*(3), 42–43.

63. Arduengo, A.J. III; Harlow, R.L.; Kline, M. *J. Am. Chem. Soc*. **1991**, *113*, 361–363.

64. Herrmann, W. A.; Elison, M.; Fischer, J.; Köcher, C.; Artus, G. R. J. *Angew. Chem. Int. Ed*. **1995**, *34*, 2371–2374.

65. Fortman, G. C.; Nolan, S. P. *Chem. Soc. Rev.* **2011**,*40*, 5151–5169.

66. Arduengo, A. J. III; Krafczyk, R.; Schmutzler, R. *Tetrahedron* **1999**, *55*, 14523–14534.

67. Altenhoff, G.; Würtz, S.; Glorius, F. *Tetrahedron Lett*. **2006**, *47*, 2925–2928.

68. Organ, M. G.; Çalimsiz, S.; Sayah, M.; Hoi, K. H.; Lough, A.J. *Angew. Chem. Int. Ed.* **2009**, *48*, 2383–2387.

69. Berthon-Gelloz, G.; Siegler, M. A.; Spek, A. L.; Tinant, B.; Reek, J. N. H.; Markó, I. E. *Dalton Trans*. **2010**, *39*, 1444–1446.

70. Meiries, S.; Speck, K.; Cordes, D. B.; Slawin, A. M. Z.; Nolan, S. P. *Organometallics* **2013**, *32*, 330−339.

71. Zhang, Y.; César, V; Lavigne, G. *Eur. J. Org. Chem.* **2015**, 2042–2050.

72. (a) Chianese, A. R.; Li, X.; Janzen, M. C.; Faller, J. W.; Crabtree, R. H. *Organometallics* **2003**, *22*, 1663–1667; (b) Chianese, A. R.; Kovacevic, A.; Zeglis, B. M.; Faller, J. W.; Crabtree, R. H. *Organometallics* **2004**, *23*, 2461–2468.

73. Kelly III, R. A.; Clavier, H.; Giudice, S.; Scott, N. M.; Stevens, E. D.; Bordner, J.; Samardjiev, I.; Hoff, C. D.; Cavallo, L.; Nolan, S. P. *Organometallics* **2008**, *27*, 202–210.

74. Hillier, A. C.; Sommer, W. J.; Yong, B. S.; Peterson, J. L.; Cavallo, L.; Nolan, S. P. *Organometallics* **2003**, *22*, 4322–4326.

75. (a) Frohlich, N.; Pidun, U.; Stahl, M.; Frenking, G. *Organometallics* **1997**, *16*, 442–448; (b) Chen, H.; Justes, D. R.; Cooks, R. G. *Org. Lett.* **2005**, *7*, 3949–3952.

76. Organ, M. G.; Avola, S.; Dubovyk, I.; Hadei, N.; Kantchev, E. A. B.; O'Brien, C. J.; Valente, C. *Chem. Eur. J.* **2006**, *12*, 4749–4755.

77. Valente, C.; Baglione, S.; Candito, D.; O'Brien, C. J.; Organ, M. G. *Chem. Commun.*

2008, 735–736.

78. Organ, M. G.; Abdel-Hadi, M.; Avola, S.; Hadei, N.; Nasielski, J.; O'Brien, C. J.; Valente, C. *Chem. Eur. J.* **2007**, *13*, 150–157.

79. Organ, M. G.; Abdel-Hadi, M.; Avola, S.; Dubovyk, I.; Hadei, N.; Kantchev, E. A. B.; O'Brien, C. J.; Valente, C. *Chem. Eur. J.*, **2008**, *14*, 2443–2452.

80. O'Brien, C. J.; Kantchev, E. A. B.; Valente, C.; Hadei, N.; Chass, G. A.; Lough, A. L.; Hopkinson, A. C.; Organ, M. G. *Chem. Eur. J.* **2006**, *12*, 4743–4748.

81. For a review on the development of the second generation of *Pd-PEPPSI* complexes, see: Valente, C.; Çalimsiz, S.; Hoi, K. H.; Mallik, D.; Sayah, M.; Organ, M. G. *Angew. Chem. Int. Ed*. **2012**, *51*, 3314–3332.

82. Altenhoff, G.; Goddard, R.; Lehmann, C. W.; Glorius, F. *J. Am. Chem. Soc.* **2004,** *126*, 15195–15201.

83. (a) Çalimsiz, S.; Sayah, M.; Mallik, D.; Organ, M. G. *Angew. Chem. Int. Ed.* **2010**, *49*, 2014–2017; (b) Çalimsiz, S.; Organ, M. G. *Chem. Commun.* **2011**, *47*, 5181–5183; (c) McCann, L. C.; Hunter, H. N.; Clyburne, J. A. C.; Organ, M. G. *Angew. Chem. Int. Ed.* **2012**, *51*, 7024–7024; (d) McCann, L.; Organ, M. G. *Angew. Chem. Int. Ed.* **2014**, *53*, 4386–4389.

84. Farmer, J. L.; Hunter, H. N.; Organ, M. G. J. Am. Chem. Soc. 2012, 134, 17470–174473.

85. Dowlut, M.; Mallik, D.; Organ, M. G. *Chem. Eur. J.* **2010**, *16*, 4279–4283.

86. (a) Hoi, K.H.; Çalimsiz, S.; Froese, R. D. J.; Hopkinson, A. C.; Organ, M. G. *Chem. Eur. J.* **2011**, *17*, 3086–3090; (b) Hoi, K.H.; Çalimsiz, S.; Froese, R. D. J.; Hopkinson, A.

C.; Organ, M. G. *Chem. Eur. J.* **2012**, *18*, 145–51.

87. Sayah, M.; Organ, M. G. *Chem. Eur. J.* **2011**, *17*, 11719–11722.

88. (a) Pompeo, M.; Froese, R. D. J.; Hadei, N.; Organ, M. G. *Angew. Chem. Int. Ed.* **2012**, *51*, 11354–11357; (b) Atwater, B.; Chandrasoma, N.; Mitchell, D.; Rodriguez, M. J.; Pompeo, M.; Froese, R. D. J.; Lough, A. J.; Organ, M. G. *Angew. Chem. Int. Ed.* **2015**, *54*, 9502–9506.

89. Dutheuil, G.; Selander, N.; Szabó, K. J.; Aggarwal, V. K. *Synthesis* **2008**, 2293–2297.

90. Ni, G.; Zhang, Q.-J.; Zheng, Z.-F.; Chen, R.-Y.; Yu, D.-Q. *J. Nat. Prod.* **2009**, *72*, 966–968.

91. Puntumchai, A.; Kittakoop, P.; Rajviroongit, S.; Vimuttipong, S.; Likhitwitayawuid, K.; Thebtaranonth, Y. *J. Nat. Prod.* **2004**, *67*, 485–486.

92. Gerbino, D. C.; Mandolesi, S. D.; Schmalz, H.-G.; Podestá, J. C. Eur. J. Org. Chem. 2009, 3964–3972.

93. In ref. 41b, Miyaura and co-workers reported unanticipated α-selectivity when coupling 4- and 2-bromoanisoles.

94. Jørgensen, M.; Lee, S.; Liu, X.; Wolkowski, J. P.; Hartwig, J.F. *J. Am. Chem. Soc.* **2002**, *124*, 12557–12565.

95. For a recent report explaining the unexpected activity of *Pd-PEPPSI* complexes coupling electrophiles with multiple halogens, see: Larrosa, I.; Somoza, C.; Banquy, A.; Goldup, S. M. *Org. Lett.* **2011**, *13*, 146–149.

96. For the preparation of allylboronates **60b** and **60c** see: (a) see ref 89; (b) Zhang, P.; Roundtree, I. A.; Morken, J. P. *Org. Lett.* **2012**, *14*, 1416–1419; For the preparation of **60d** and **60e** see Chapter 5.

97 . For the preparation of 4,4,5,5-tetramethyl-2-(2-methylbut-3-en-2-yl)-1,3,2-dioxaborolane **60f**, see: (a) Hoffmann, R. W.; Wolff, J. J. *Chem. Ber.* **1991**, *124*, 563–569; (b) Clary, J.W.; Rettenmaier, T.J.; Snelling, R.; Bryks, W; Banwell, J.; Wipke, W.T.; Singaram, B., *J. Org. Chem.* **2011**, *76*, 9602–9610.

98. Yang, Y.; Buchwald, S. L. *J. Am. Chem. Soc.* **2013**, *135*, 10642–10645.

99. Shi, Y.-Q.; Nomura, T.; Fukai, T. *Filoterapia* **2007**, *78*, 617–618; and references therein.

100. (a) Charoenlarp, P.; Radomyos, P.; Harinasuta, T. *Southeast Asian J. Trop. Med. Public Health* **1981**, *12*, 568–570; (b) Charoenlarp, P.; Radomyos, P.; Bunnag, D. *J. Med. Assoc. Thai* **1989**, *72*, 71–73.

101. Mann, I. S.; Widdowson, D. A. *Tetrahedron* **1991**, *47*, 7991–18000.

102. Mann, I. S.; Widdowson, D. A. *Tetrahedron* **1991**, 7981–7990.

103. For changes in regioselectivity by the inclusion of TMEDA as an additive, see: a) Slocum, D. W.; Book, G.; Jennings, C. A. *Tetrahedron Lett.* **1970**, *11*, 3443–3445; b) Slocum, D. W.; Jennings, C. A. *J. Org. Chem.* **1976**, *41*, 3653–3664.

104. Newman, S. G.; Aureggi, V.; Bryan, C. S.; Lautens, M. *Chem. Commun.* **2009**, 5236–5238.

105. Kraus, G. A.; Zeng, Y. *Synthetic Communications* **2000**, *30*, 2133–2141.

106. Sekiguchi, Y.; Okubo, T.; Shibata, T.; Abe, K.; Yamamoto, S.; Kashiwa, S. **2008**, WO/2008/018639.

107. Milne, J. E.; Buchwald, S. L. *J. Am. Chem. Soc.* **2004**, *126*, 13028–13032.

108. Krasovskiy, A.; Knochel, P. *Synthesis*, **2006**, *5*, 890–891.

109. Hwu, J. R.; Tsay, S.-C. *J. Org. Chem.*, **1990**, *55*, 5987–5991.

110. Cvengroš, J.; Neufeind, S.; Becker, A.; Schmalz, H.-G., **2008**, *13*, 1993–1998.

111. Chae, J., *Arch Pharm Res*, **2008**, *31*, 305–309.

112. Frey, L. F.; Marcantonio, K. M.; Chen, C.-Y.; Wallace, D. J.; Murry, J. A.; Tan, L.; Chen, W.; Dolling, U. H.; Grabowski, E. J. J., *Tetrahedron*, **2003**, *59*, 6363–6373.

113. Roberts, J. D.; Curtin, D. Y. *J. Am. Chem. Soc.* **1946**, *68*, 1658–1660.

114. For selected examples of studies on DMG, see: (a) Beak, P.; Brown, R. A. *J. Org. Chem.* **1982**, *47*, 34–46; (b) Gant, T. G.; Myers, A. I. *Tetrahedron* **1994**, *50*, 2297–2360.

115. For review on DoM, see: (a) Gschwend, H. W.; Rodriguez, H. R. *Org. Reac.* **1979**, *26*, 1–360; (b) Beak, P.; Snieckus, V. *Acc. Chem. Res.* **1982**, *15*, 306–312; (c) ref. 121.

116. Hay, D. R.; Song, Z.; Smith, S. G.; Beak, P. *J. Am. Chem. Soc.* **1998**, *110*, 8145–8153.

117. Clayden, J. *Organolithiums: Selectivity for Synthesis*, Pergamon, **2002**.

118. Anctil, E. J.-G.; Sniekus, V. *J. Organomet. Chem.* **2002**, *653*, 150–160.

119. (a) Shiina, K.; Brennan, T.; Gilman, H. *J. Organomet. Chem.* **1968**, *11-15*, 471–477; (b) Kress, T. H.; Leanna, M. R. *Synthesis* **1988**, 803 –805; (c) Iwao, M. *J. Org. Chem.* **1990**, *55*, 3622–3627.

120. Shimano, M.; Meyers, A. I. *J. Am. Chem. Soc.* **1994**, *116*, 10815–10816.

121. Clayden, J.; Pink, J. H.; Westlund, N.; Wilson, F. X. *Tetrahedron Lett.* **1998**, *39*, 8377–8380.

122. Source of values of tetrahydrofuran and Et2O (diethyl ether), see: http:// depts.washington.edu/eooptic/linkfiles/dielectric_chart[1].pdf.

123. For computational details please see: Farmer, J. L.; Froese, R. D. J.; Lee-Ruff, E.; Organ, M. G. *Chem. Eur. J.* **2015**, *21*, 1888–1893.

124. Chadwick, S. T.; Rennels, R. S.; Rutherford, J. L.; Collum, D. B. *J. Am. Chem. Soc.* **2000**, *122*, 8640–8647.

125. van Eikema Hommes, N. J. R.; Schleyer, P. V. R. *Tetrahedron* **1994**, *50*, 5903–5916.

126. (a) Brunton, G.; Griller, Barclay, L. R. C.; Ingold, C. U. *J. Am. Chem. Soc.* **1976**, *98*, 6803–6811; (b) Brunton, G.; Gray, J. A.; Griller, D.; Barclay, L. R. C.; Ingold, K. U. *J. Am. Chem. Soc.* **1978**, *100*, 4197–4200.

127. Hammerschmidt, F.; Schmidt, S. *Eur. J. Org. Chem.* **2000**, 2239–2245.

128. Vedejs, E.; Little, J. *J. Am. Chem. Soc.* **2002**, *124*, 748–749.

129. Wood, M. F.; Bissiriou, S.; Lowe, C.; Norrish, A. M.; Senechal, K.; Windeatt, K. M.; Coles, S. J.; Hursthouse, M. *Org. Biomol. Chem.* **2010**, *8*, 4653–4665.

130. Burchat, A. F.; Chong, J. M.; Nielson, N. *J. Organomet. Chem.* **1997**, *542*, 281−283.

131. Hama, T.; Ge. S.; Hartwig, J. F. *J. Org. Chem.* **2013**, *78*, 8250–8266.

132. Rousseaux, S.; Davi, M.; Sofack-Kreutzer, J.; Pierre, C.; Kefalidis, C. E.; Clot, E.; Fagnou, K.; Baudoin, O. *J. Am. Chem. Soc.* **2010**, *132*, 10706–10716.

133. Bodnar, B. S.; Vogt, P. F. *J. Org. Chem.* **2009**, *74*, 2598–2600.

134. Johnson, R. A.; Hall, C. S.; Krueger, W. C.; Murray, H. C *Bioorganic Chemistry* **1973**, *2*, 99–110.

135. Dutheuil, G.; Webster, M. P.; Worthington, P. A.; Aggarwal, V. K. *Angew. Chem. Int. Ed.* **2009**, *48*, 6317–6519.

136. Hoffmann, R. W.; Schlapbach, A. Leibigs Ann. Chem. 1990, 1243–1248.

137. Iwasaki, M.; Yorimitsu, H.; Oshima, K. *Bull. Chem. Soc. Jpn.* **2009**, *82*, 249–253.

138. **61a** α-isomer: Malkov, A. V.; Davis, S. L.; Baxendale, I. R.; Mitchell, W. L.; Kocovsky, P. J. *J. Org. Chem.* **1999**, *64*, 2751–2764.

139. **61b** γ-isomer: Mayer, M.; Czaplik, W. M.; von Wangelin, A. J. *Advanced Synthesis and Catalysis*. **2010**, *13*, 2147–2152.

140. Larock, R. C.; Zhang, H. *J. Org. Chem*, **2002**, *67*, 7048–7056.

141. Laczkowski, K. Z.; Pakulski, M. M.; Krzeminski, M. P.; Parasuraman, J.; Zaidlewicz, M. *Tetrahedron: Asymmetry* **2008**, *19*, 788–795.

142. Anderson, J. C.; Denton, R. M.; Hickin, h. G.; Wilson, C. *Tetrahedron.* **2004**, *60*, 2327–2335.

143. Sun, N.; Huang, P.; Wang, Y.; Mo, W.; Hu, B.; Shen, Z.; Hu, X. *Tetrahedron* **2015**, *71*, 4835–4841.

144. Mikriyannis, A.; Nikas, S. P.; Alapafuja, S. O.; Shukla, V. G. **2009**, WO2009/052319.

PART II: ROOM TEMPERATURE, ADDITIVE-FREE CARBON-SULFUR COUPLING USING NOVEL NHC-Pd COMPLEXES

CHAPTER 1 – Introduction

1.1. The Importance of Carbon–Sulfur (C–S) Bonds

Thioethers are structural motifs found in many important compounds that are employed in a number of fields, ranging from biology (e.g., methionine, biotin) and medicine (e.g., BenPen, Amoxil, Singulair, Cymbalta, Evista, Actos) to materials science (e.g., polyphenylene sulfide). Additionally, thioethers can serve as useful precursors to more highly oxidized sulfur-containing functional groups, such as sulfoxides and sulfones,[1] which are key structural elements in a number of highly potent active pharmaceutical ingredients used to treat cancer, HIV, and Alzheimer's disease.[2] Given the importance of thioethers, a significant amount of research has gone into developing synthetic methods to facilitate the selective formation of C–S bonds.

While alkyl thioethers can be prepared readily by nucleophilic substitution bimolecular (S_N2) reactions, the same reaction at an sp^2-carbon centre, to generate aromatic thioethers, is far less trivial. Traditional methods, such as the reaction of aromatic compounds with sulfur, nucleophilic aromatic substitution (S_NAr) reactions of activated aryl halides with substituted thiophenols, and the reaction of electrophilic sulfur with nucleophilic organometallic reagents (e.g., organolithium or organomagnesium reagents) were once commonly employed routes for accessing aryl sulfides.[3] Unfortunately, many of these reactions require forcing conditions, are

limited in their scope, and suffer from the formation of disulfides and other sulfur-containing side products, leading to disappointing yields.[4]

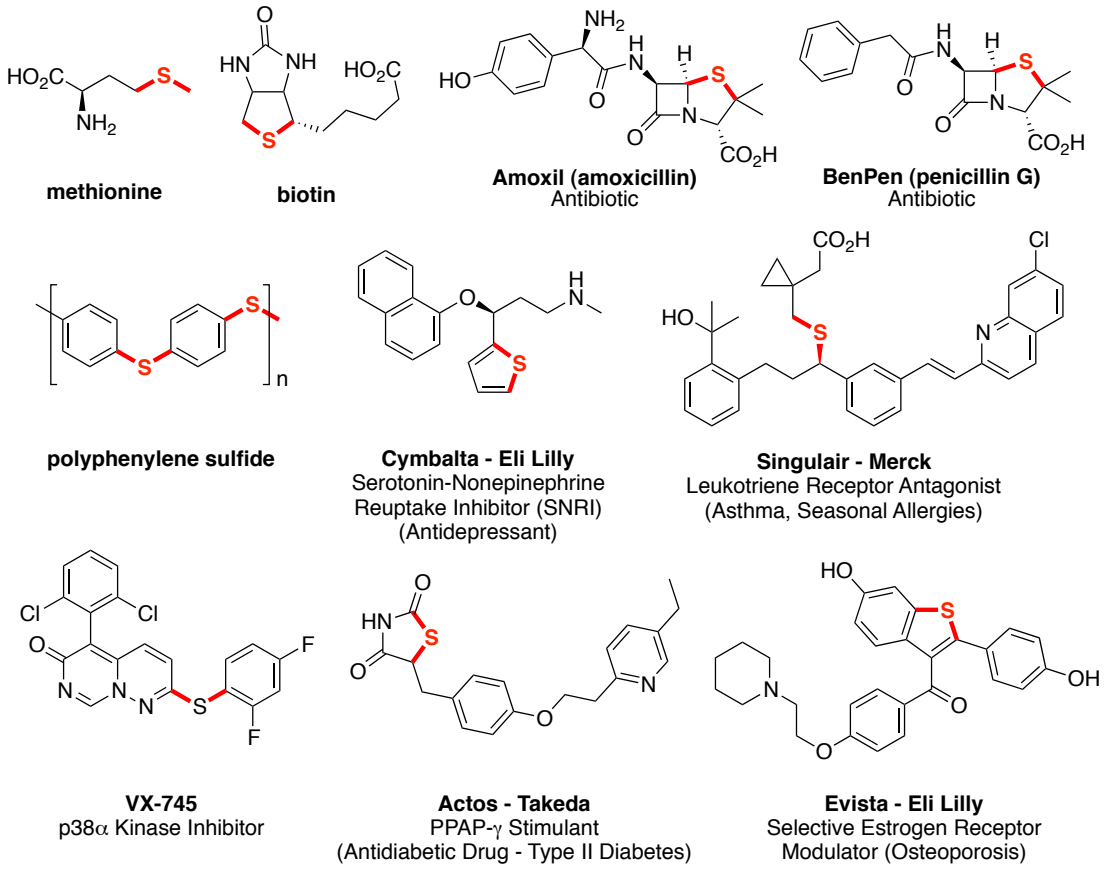

Figure 1: Selected examples of sulfur-containing compounds present in nature, polymers, and marketed drugs.

More recently, transition metal-catalyzed cross-coupling of thiols with aryl halides has emerged as a more mild and general protocol for the formation of C–S bonds and has greatly facilitated access to more highly functionalized aryl thioethers.[5] While this transformation has been successfully catalyzed by Fe,[6] Co,[7] Ni,[8] and Cu,[9] Pd has

undoubtedly become the metal of choice due to its ability to couple a wide array of substrates under the mildest conditions, i.e., low temperatures and low catalyst loading.[10] Reviews discussing metal catalyzed C–S bond forming reactions have been published,[11] however, only advances made in C–S coupling involving palladium will be reviewed in this thesis.

1.2. Pd-Catalyzed Aryl Sulfination Reactions

The mechanism for Pd-catalyzed sulfination has been thoroughly investigated by Hartwig and co-workers and is thought to proceed through the same elementary steps (i.e., oxidative addition (OA), transmetallation (TM) or ligand exchange, and reductive elimination (RE)) as other cross-coupling reactions (Scheme 1).[12] The only difference is that for the transmetallation step, a thiolate anion replaces an organometallic reagent as the nucleophile. While substantial progress has been made in the Pd-catalyzed formation of C–C, C–N, and C–O bonds, fewer advances have been made in generating efficient protocols for the formation of C–S bonds. The main reason for this is the ability of sulfur species, such as thiolates (RS^-), to act as catalyst poisons by moving Pd^{II} intermediates off the catalytic cycle into thiolate-derived resting states (Scheme 1, resting states **A**, **B**, and **C**).[12,13] Over the years, several catalyst systems have been developed to address this problem, with a few notable examples described below.

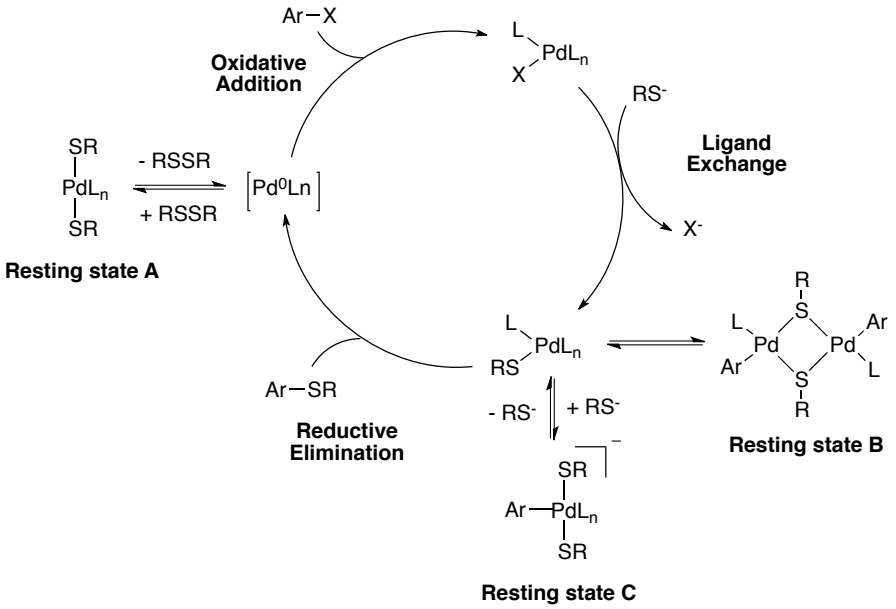

Scheme 1: Putative catalytic cycle for Pd-catalyzed aryl sulfinations.

The first example of Pd-catalyzed aryl sulfination was reported by Migita and co-workers in 1978, who demonstrated that the coupling of aryl bromides and iodides to both aryl and alkylthiols could proceed in the presence of 10 mol% [$Pd(PPh_3)_4$] (Equation 1).[14] This method provided access to the corresponding thioethers in moderate to good yields, however it required high reaction temperatures (100°C), high catalyst loadings, long reaction times, and was unsuccessful with aryl chlorides.

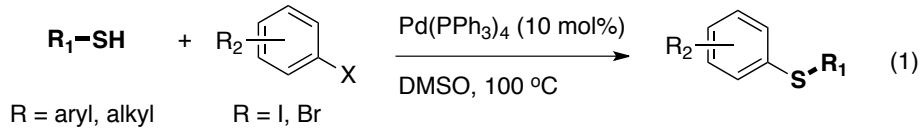

Following Migita's report, efforts to improve the selectivity, efficiency, and substrate scope of these cross-coupling reactions have largely focussed on the development of improved catalyst systems and the search for new ancillary ligands. Since ancillary ligands are responsible for transmitting key steric and electronic properties to the

metal centre that are essential for enabling catalysis, much can be learned about each elementary step within the catalytic cycle by varying these ligands. For a more in depth discussion on ancillary ligands see Part 1, Chapter 1, Section 1.4.

1.2.1. Aryl Sulfinations with Phosphine Ligands

Until recently, bidentate phosphines have been the most widely used ancillary ligands in Pd-catalyzed sulfination reactions.[10b-c, 15] Unlike their monodentate counterparts,[16] bidentate phosphines are resistant to displacement from Pd by nucleophilic thiolate anions. This was demonstrated in a 2006 report by Murata and Buchwald, in which various monodentate and bidentate phosphine ligands were evaluated in the cross-coupling of 4-bromoanisole with thiophenol and *tert*-butylthiol.[15b] Whereas all of the bulky monodentate phosphine ligands were found to be ineffective, the majority of the bidentate ligands screened were active, with 1,1'-bis(diisopropylphosphino)ferrocene (DiPPF) giving the best results for both aryl and alkylthiols. The $Pd(OAc)_2$/DiPPF catalyst system was found to couple a variety of electronically deactivated and sterically hindered aryl halides with primary, secondary, and tertiary alkylthiols as well as aromatic thiols (Figure 2). Furthermore, DiPPF was the first ligand reported to facilitate coupling of unactivated aryl chlorides with a variety of thiols in high yields, albeit at high temperatures ($\geq$ 100°C).

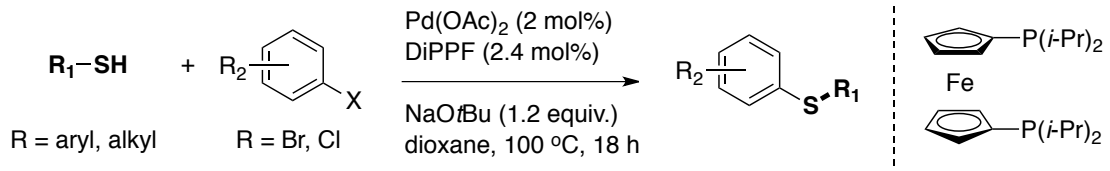

Figure 2: Pd-catalyzed C–S bond formation using a $Pd(OAc)_2$/DiPPF catalyst system.

Perhaps the most efficient bisphosphine ligand reported to date for C–S coupling is the ferrocene-based Josiphos ligand (CyPF-*t*-Bu) described by Hartwig and co-workers.[3b,10c,12,13,17] Combining this bulky, strongly coordinating bidentate ligand with Pd salts (i.e., $Pd(OAc)_2$, $Pd(dba)_2$) generates long-lived Pd complexes which are capable of coupling a number of functionalized aryl halides with both aryl and alkylthiols, even at very low catalyst loadings (down to 0.001 mol%) (Scheme 2). Hartwig and co-workers attribute the high reactivity of the Josiphos-ligated catalyst system to the strong coordinating ability of the ligand, which prevents the formation of anionic or bridging thiolate complexes (Resting States B and C, Scheme 1). Furthermore, the stronger electron donating nature of the Josiphos ligand, relative to arylphosphines, helps promote oxidative addition while the enhanced steric topography enables facile reductive elimination.[13] It should be noted that while this catalyst system was found to couple di-*ortho*-substituted aryl bromides with aryl thiols, the aryl chloride equivalents failed to give any cross-coupled product, even at elevated temperatures (≥ 100 °C).

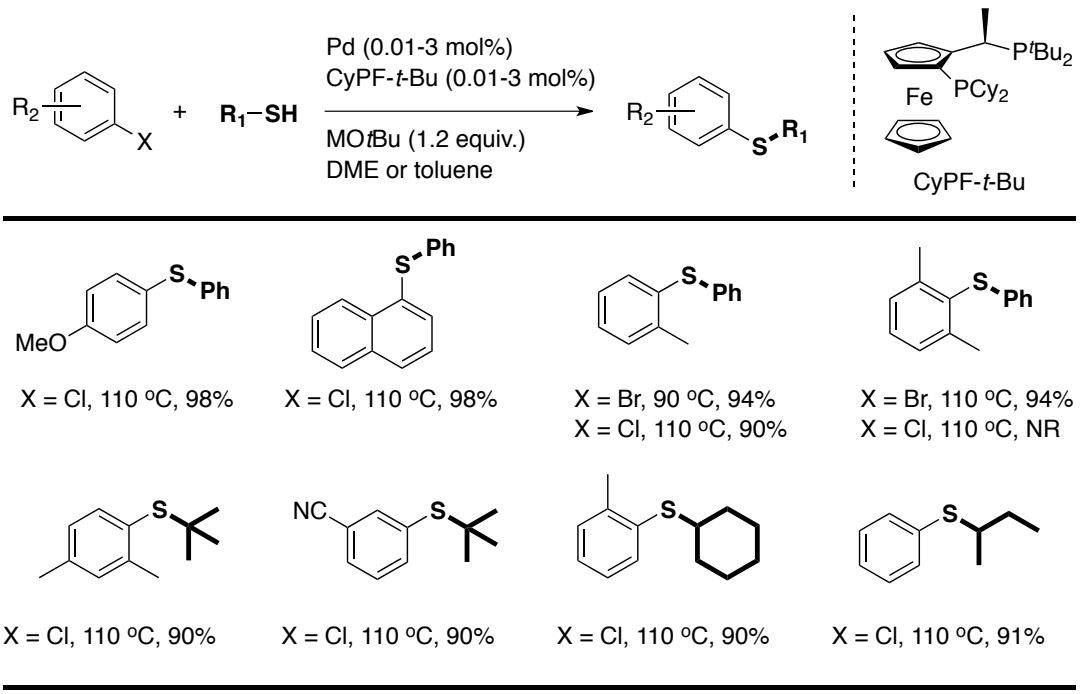

Scheme 2: Coupling of aryl halides with thiols using Hartwig's Josiphos-ligated catalyst system.

Mechanistic investigations with isolated Pd complexes also revealed that, while the overall reaction requires temperatures of 110 °C to reach completion, each step in the catalytic cycle proceeds at 25 °C or lower.[12] These results suggest that the resting state of the reaction lies off the catalytic cycle, leading the authors to propose resting states **A**, **B**, and **C** shown in Scheme 1. Therefore, to improve the reaction outcome for this transformation, designing ligands that help keep the catalyst on cycle or help shift the equilibrium away from the non-productive resting states is essential.

Despite the important advances made with phosphine ligands, the majority of these catalyst systems still require temperatures in excess of 100 °C to achieve

acceptable conversions to product and are much less effective when electronically deactivated and/or sterically hindered aryl chlorides are employed as coupling partners. Further, many state-of-the-art phosphine ligands are relatively labile which can have a negative impact on the reaction outcome, especially when the steric topography around the metal centre is crucial for the reaction outcome. More recently, N-heterocyclic carbenes (NHC) ligands have demonstrated to be an effective alternative to phosphine ligands in many C–C and C–X cross-coupling reactions. Since NHCs are significantly more donating than even the most electron-rich phosphines,[18] they are less likely to dissociate from the metal centre leading to better reaction outcomes. However, the use of NHC ligands in C–S coupling has been less explored relative to phosphine ligands.

1.2.2. Aryl Sulfinations with N-heterocyclic carbene (NHC) Ligands

Liu and co-workers reported the first example of an NHC ligand being used in Pd-catalyzed sulfination in 2010. Three complexes were prepared (**1 – 3**) and evaluated for their activity in C-S cross-coupling chemistry (Scheme 3).[19] The mixed phosphine-NHC complex [(*SIEt*)Pd(PPh_3)Cl_2] (**2**) was identified as the most active pre-catalyst and was shown to effectively couple a variety of aryl iodides and bromides with aryl thiols using 2 mol% catalyst and KO*t*Bu base in toluene at 110 °C. Complex **2** showed high activities in coupling both deactivated aryl iodides and bromides with various aryl thiols, however poor yields were obtained with alkyl thiols. Furthermore, aryl chlorides were found to be unreactive under the developed conditions.

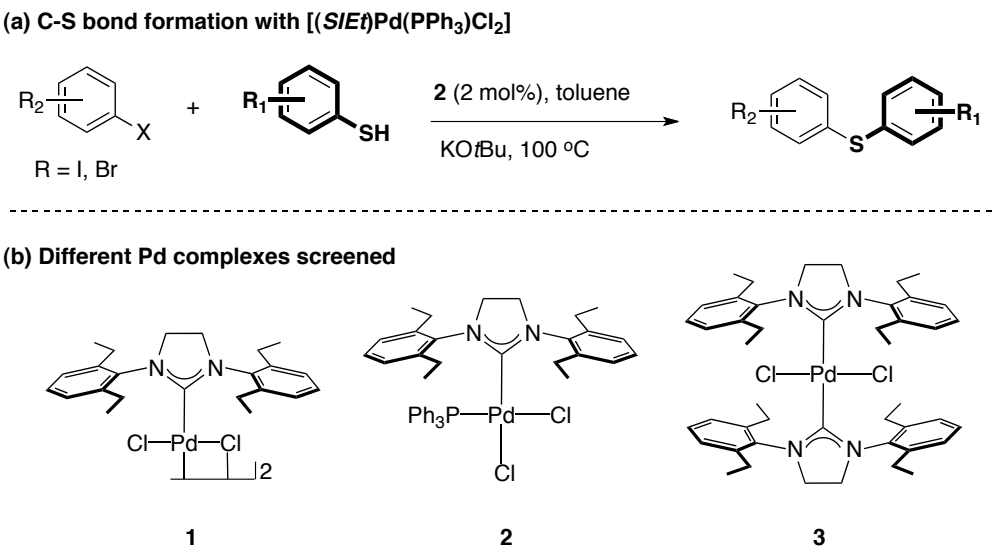

Scheme 3: (a) C–S bond formation with mixed phosphine-NHC complex [(*SIEt*)Pd(PPh_3)Cl_2] (**2**) and other Pd-NHC complexes.

Since aryl chlorides are more readily available and much less expensive than their bromide or iodide counterparts, the development of catalyst systems capable of efficiently coupling these substrates is highly desirable. In 2011, Sayah and Organ disclosed the first low-temperature Pd-catalyzed protocol to prepare C–S bonds.[20] The authors reported *Pd-PEPPSI-IPent* (**4**, 2 mol%) to be highly effective in sulfination chemistry, coupling a range of (hetero)aryl bromides and chlorides with aryl and alkyl thiols at or near ambient temperatures using KO*t*Bu as the base (Scheme 4). Interestingly however, it was found that catalyst turnover at these temperatures could only be achieved if **4** was pre-heated to 80 °C in the presence of a reducing agent, such as LiO*i*Pr (20 mol%) prior to addition of the thiol.

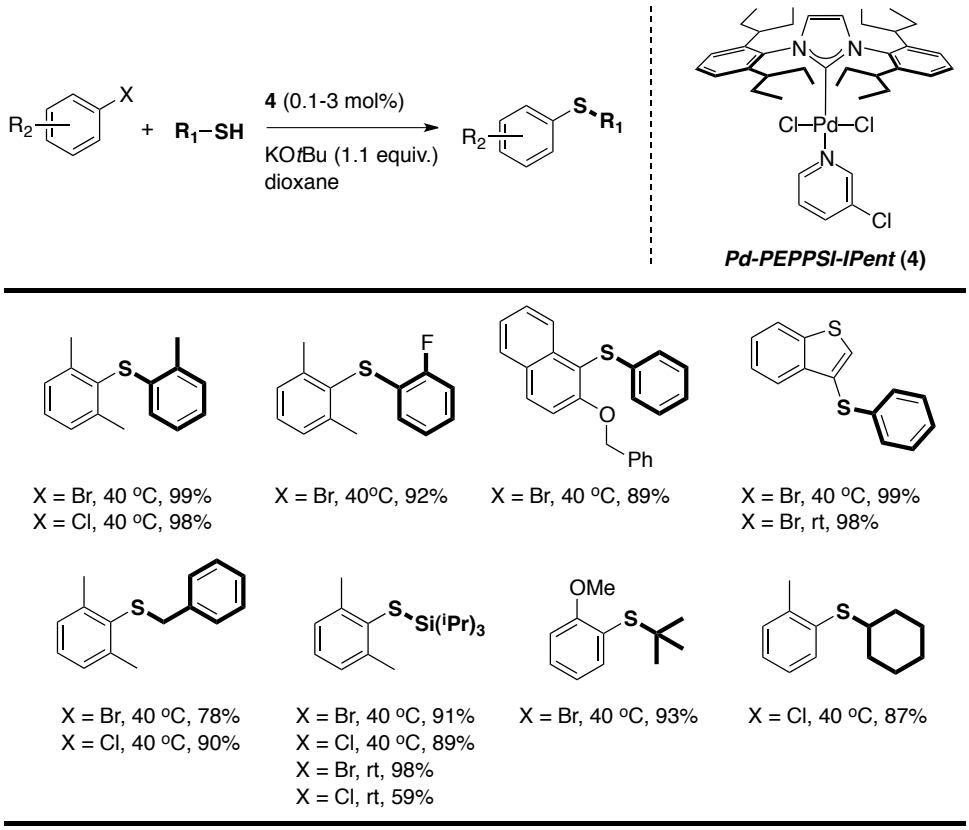

Scheme 4: Pd-catalyzed aryl sulfination with *Pd-PEPPSI-IPent* (**4**).

While pre-catalyst activation for *Pd-PEPPSI* complexes has been demonstrated to occur readily at or near ambient temperature in various C-C[21,22,23] and C-N[24] bond forming reactions, the mechanism by which Pd^{II} is reduced to Pd^0 in aryl sulfinations is less clear. In 2013, Organ and co-workers investigated the mechanism of pre-catalyst activation with different *Pd-PEPPSI* complexes in the absence of exogenous activators such as LiO*i*Pr.[25] In this study, substituents on the pyridine ligand and the NHC backbone were varied systematically to determine their effect on catalyst activation using the coupling of thiophenol (**6**) with sterically hindered 2-bromo-1,3-dimethylbenzene (**5**) as the model reaction. They found that

increasing the bulk of the pyridine ligand as well as installing chlorines on the backbone of the NHC significantly lowered the activation temperature, presumably by increasing the rate of disulfide RE (i.e., going from complex **17** to **20** in Figure 3). *Pd-PEPPSI-IPent*^{Cl}*-o-picoline* (**15**) was identified as the best catalyst system, giving near quantitative conversion to aryl thioether **7** at 40 °C (Scheme 5). Under the same reaction conditions, *Pd-PEPPSI-IPent* (**4**) required 80 °C for the reaction to go to completion (Entry not shown in Scheme 5).

During the course of their mechanistic investigations, Organ and co-workers also found that dithiolate complex (**17**) forms rapidly and quantitatively under the reaction conditions, which, in the absence of LiO*i*Pr or excess base, decomposes to inactive tri-palladium complex (**19**) rather than undergoing reductive elimination (RE) of dithiane and entering the catalytic cycle as **20**. Heating complex **17** also failed to bring active catalyst back on cycle and only NHC salt **18** was isolated, indicating that RE of the NHC with a *cis*-thiolate is more kinetically favourable than formation of **20**. Interestingly, these studies also revealed that *in situ* generated KO*i*Pr is key for *Pd-PEPPSI* catalyzed sulfination.[26] Since the solubility of potassium thiolates in toluene is low relative to other alkali metal thiolates, the use of potassium alkoxide bases is essential to minimize the concentration of thiolate in solution, thus minimizing the formation of unproductive Pd-thiolate resting states (Figure 3, **17**-**19**). Further, while *tert*-butoxide was not capable of bringing about active catalysis of tri-palladium resting state **19** isopropoxide was able to do so. It was suggested that isopropoxide was suitably small enough to penetrate and attack this highly hindered

complex, which ultimately led to monomeric complex **20** via RE of the resultant disulfide, and catalysis ensues. [27]

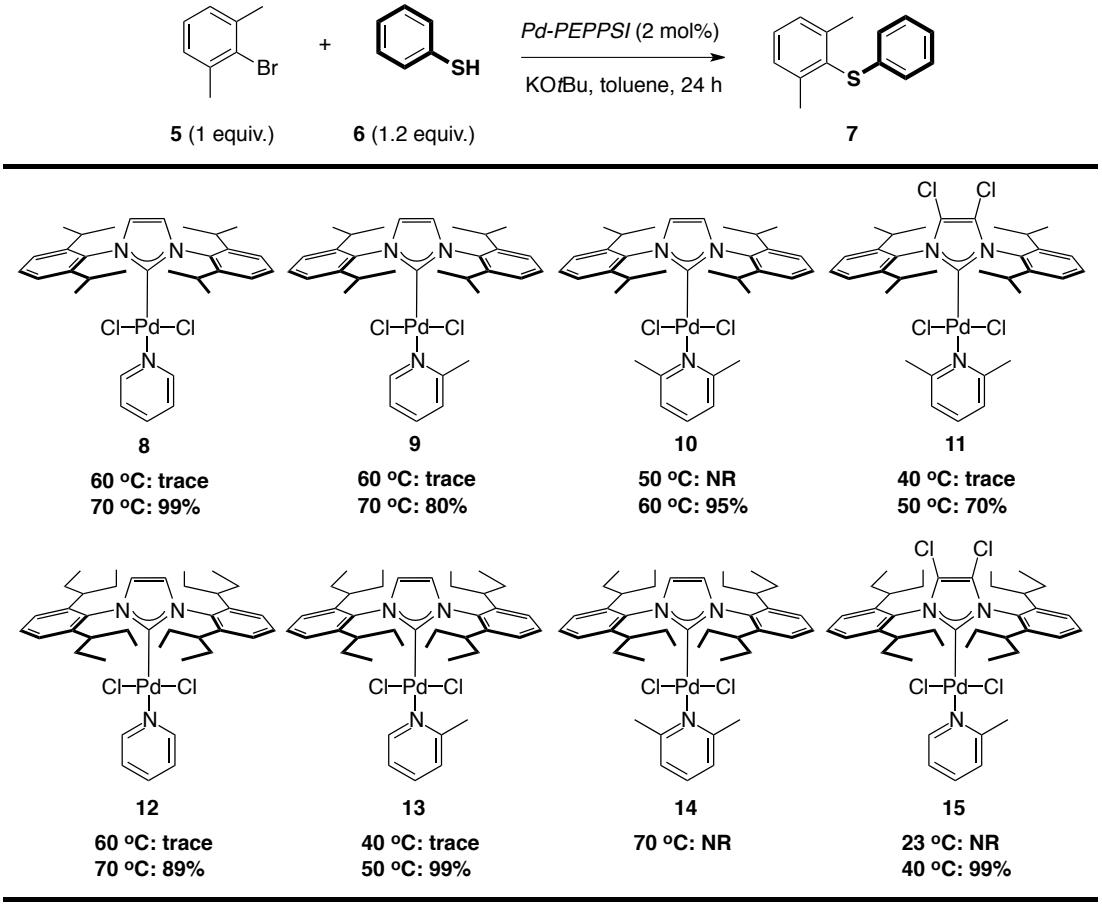

Scheme 5: Sulfination of 2-bromo-1,3-dimethylbenzene (**5**) with thiophenol (**6**) using various *Pd-PEPPSI* complexes without activators at different temperatures. (NR = no reaction).

As a result of their newfound mechanistic insight, Sayah and Organ demonstrated that **15** could be used to couple a range of (hetero)aryl sulfides with sterically hindered aryl chlorides and bromides to produce a wide variety of thioethers (Scheme 6). Of special note, tetra-*ortho*-substituted thioethers could be prepared for the first time at or near ambient temperatures without the need for cumbersome pre-

activation protocols.

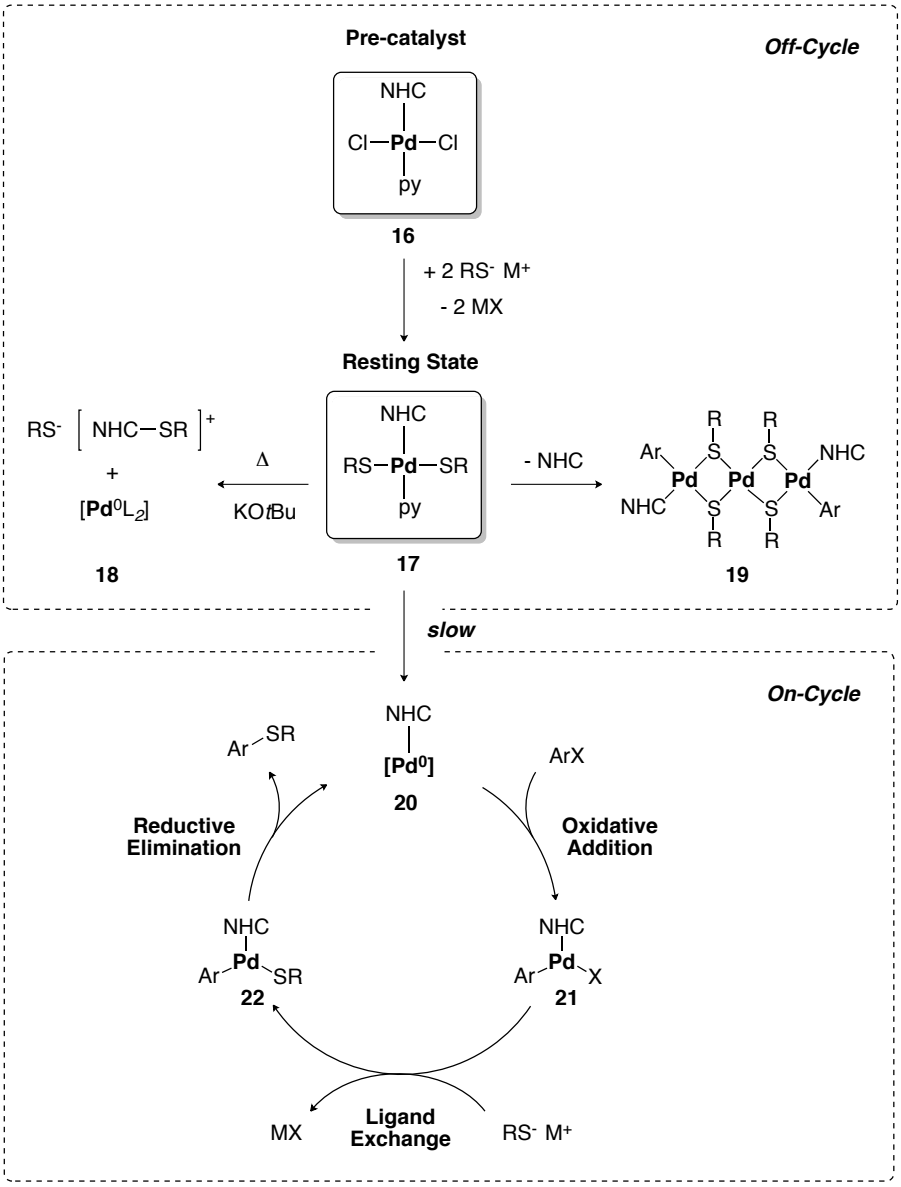

Figure 3: Supposed mechanism of C–S coupling with Pd–PEPPSI pre-catalysts.

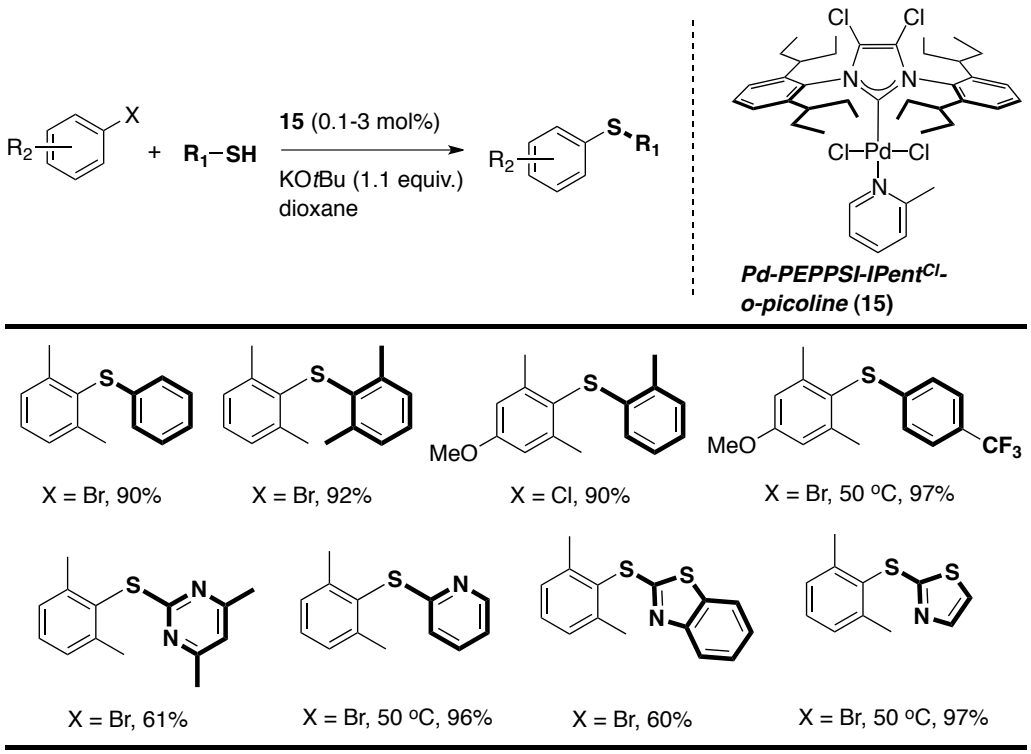

Scheme 6: Coupling of sterically and electronically deactivated aryl halides and thiols at room temperature using *Pd-PEPPSI-IPent-o-picoline* (**15**).

Following the pioneering work by Organ and co-workers, Nolan and Bastug also reported that other well-defined, NHC-Pd complexes were competent catalysts in C–S cross-coupling chemistry. Specifically, [Pd(*IPr*^{*OMe})(cin)Cl] (**23**) was found to be an efficient catalyst, coupling a number of challenging aryl halides with aliphatic and aromatic thiols at low catalyst loadings (0.1 mol% - 3 mol%) (Scheme 7).[28] Although these reactions could be performed in the absence of any additives or external activators that are sometimes needed to activate NHC-Pd catalysts (*vide infra*), extended reaction times and temperatures in excess of 100 °C were still necessary to achieve full conversion to product.

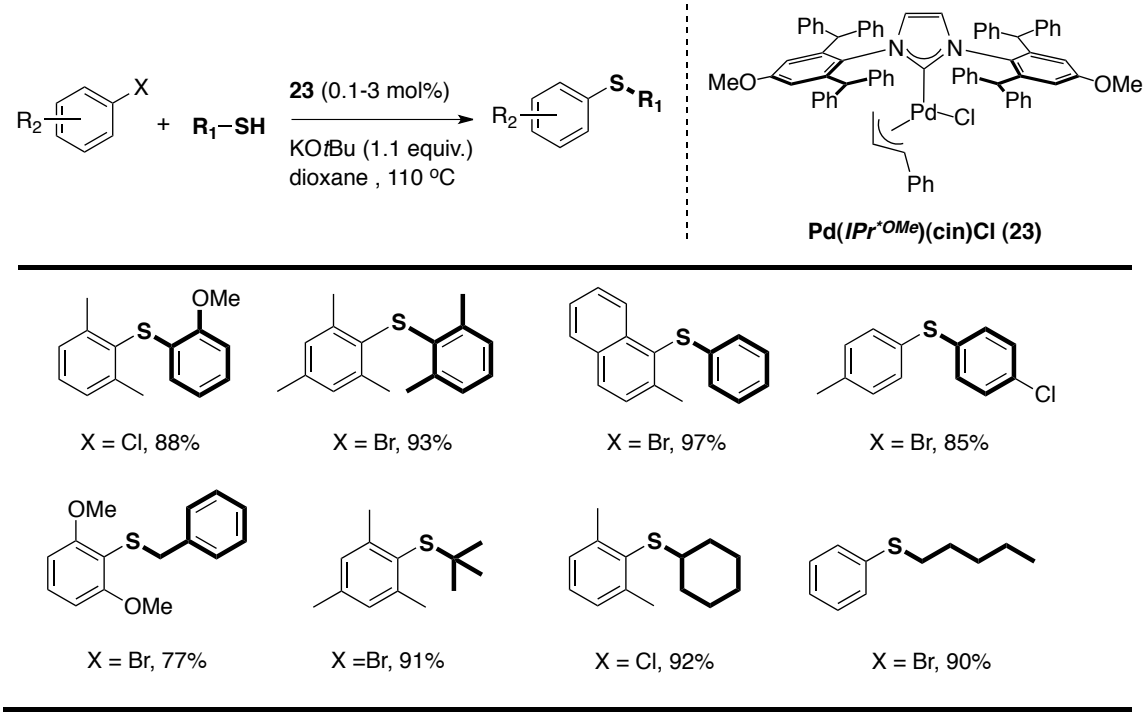

Scheme 7: Pd-catalyzed sulfination using [Pd(*IPr*^{*OMe})(cin)Cl] (**23**).

1.3. Plan of Study

Advances in ligand design have clearly had a major impact on Pd-catalyzed sulfination reactions, generating highly active catalysts that can efficiently form challenging C–S bonds under mild conditions. Among these catalyst systems, Pd-*PEPPSI-IPent-o-picoline* (**15**) has proven to be the most effective, coupling highly deactivated thiols with sterically and electronically deactivated aryl halides at or near room temperature. While the heightened activity of **15** obviated the need for cumbersome pre-activation steps required for *Pd-PEPPSI-IPent* (**4**), external additives (LiO*i*Pr) or non-commecially available bases (KO*i*Pr) were still needed to facilitate low temperature sulfination of challenging aryl halides. Consequently, the

aim of this project is to design alternative and more readily activated NHC-based pre-catalysts that will avoid unproductive off-cycle resting states, thus eliminating the need for exogenous activators or complicated pre-activation steps.

During the Organ group's work on aryl amination using *Pd-PEPPSI* complexes, it was discovered that the use of secondary amines, such as morpholine, in conjunction with alkoxides, such as KO*t*Bu, resulted in rapid pre-catalyst activation relative to when weaker bases, such as Cs_2CO_3, were employed.[24b] In the absence of KO*t*Bu, ^{1}H-NMR analysis revealed quantitative displacement of the pyridine ligand by morpholine, forming [(*NHC*)$PdCl_2$(morpholine)] complexes. We believe that, in the presence of KO*t*Bu, these complexes are rapidly reduced to Pd(0) ostensibly after deprotonation, β-hydride elimination (BHE), and reductive elimination (RE). In light of these observations, it was wondered if these *trans*-ligated morpholine complexes could themselves be used as pre-catalysts for additive-free C–S coupling. Thus, a number of [(*NHC*)$PdCl_2$(morpholine)] complexes were prepared and their activity in aryl sulfination was evaluated.

CHAPTER 2 – Synthesis and Evaluation of [(*NHC*)$PdCl_2$(morpholine)] Complexes in C–S Cross-Coupling

2.1. Preparation of [(NHC)$PdCl_2$(morpholine)] Complexes

The study began with the preparation of a number of [(*NHC*)$PdCl_2$(morpholine)] complexes (**26a**–**26e**) using the general approach outlined in Scheme 8.[29]

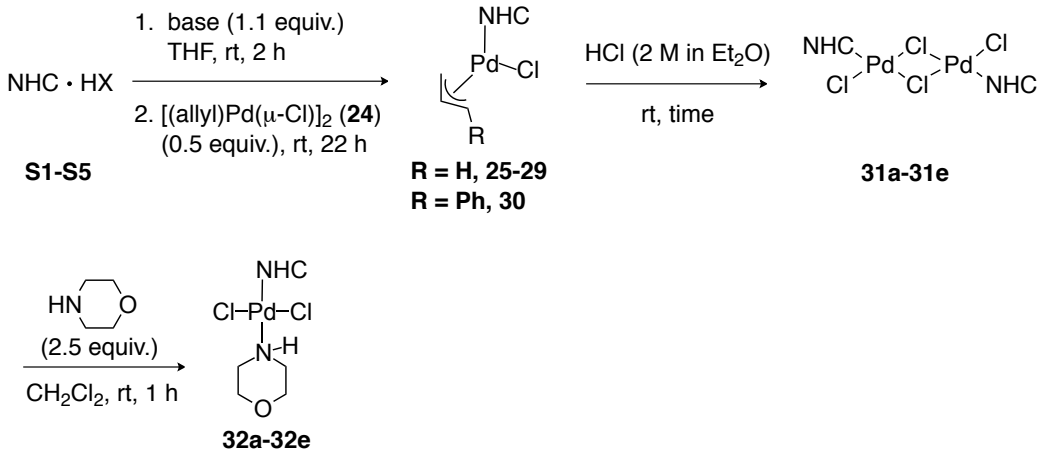

Scheme 8: Synthesis of [(*NHC*)$PdCl_2$(morpholine)] complexes **32a**–**32e**.

[Pd(*NHC*)(η^3-allyl)Cl] complexes (**25–30**) were prepared according to the procedure of Nolan and co-workers.[30] Treatment of NHC salts (**S1–S5**) with a slight excess of base (KO*t*Bu or LiHMDS) in THF generated the free carbene *in situ*, which, followed by the addition of Pd-dimer [(allyl)Pd(μ–Cl)]$_2$ (**24**), afforded [Pd(*NHC*)(η^3-allyl)Cl] complexes (**25–30**) (Scheme 9).

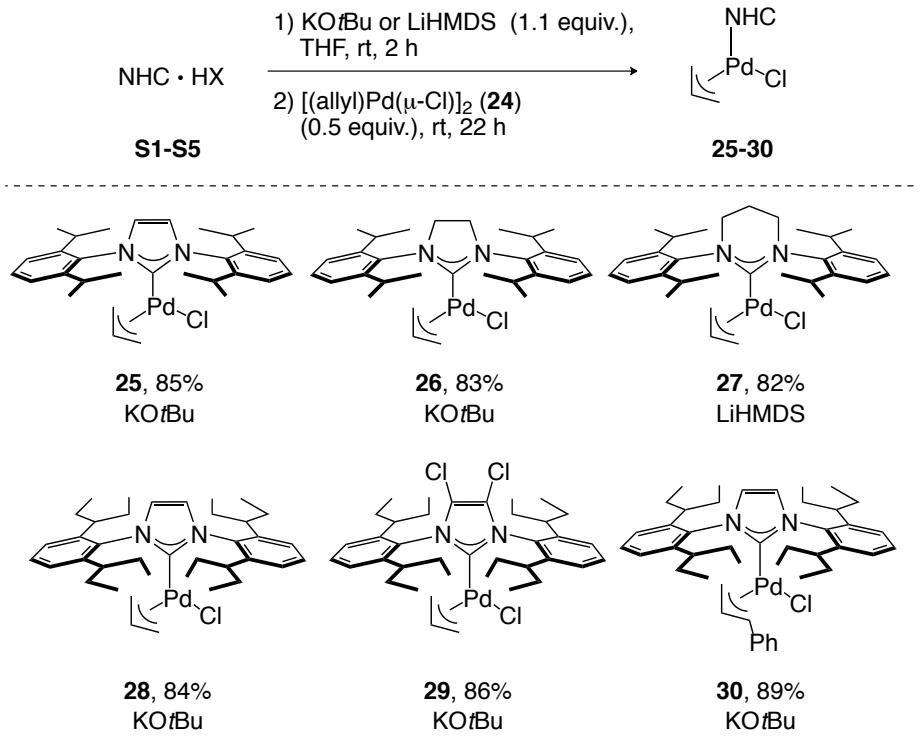

Scheme 9: Synthesis of [Pd(*NHC*)(η3-allyl)Cl] (**25-30**).

Next, stirring complexes **25–29** with ethereal HCl resulted in the formation of chloro-bridged dimers **31a–31e**, which were used in the next step without any further purification.[31] Lastly, treating complexes **31a–31e** with a slight excess of morpholine in dichloromethane furnished complexes that appeared clean by ^{1}H- and ^{13}C-NMR spectroscopy after simple filtration through a plug of neutral alumina (Scheme 10). Complexes **32a–32e** were fully characterized by ^{1}H and ^{13}C NMR spectroscopy and HRMS.

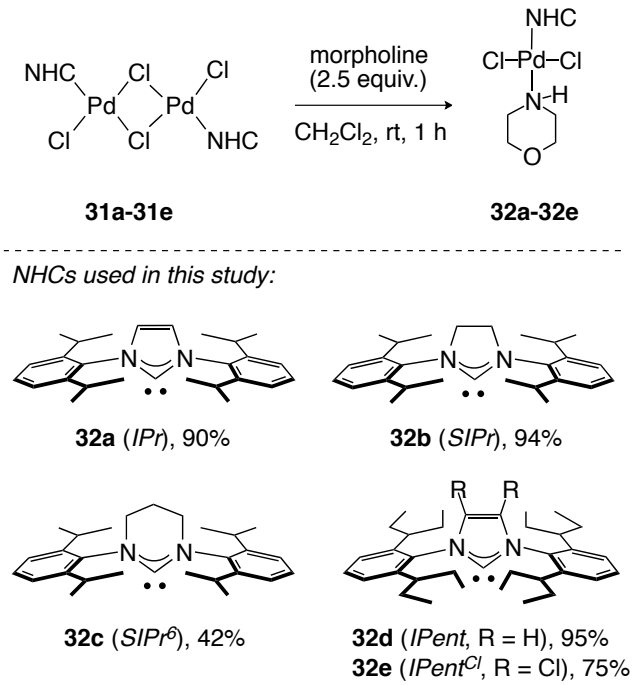

Scheme 10: Preparation of [(*NHC*)$PdCl_2$(morpholine)] complexes.

The structural features of these [(*NHC*)$PdCl_2$(morpholine)] complexes were analyzed by X-ray crystallography, with **32d** chosen as a representative complex. Crystals of **32d** suitable for X-ray diffraction were grown by slow diffusion of pentane into a concentrated dichloromethane solution. As seen in Figure 4, the morpholine ligand is oriented *trans* to the *NHC*, in a slightly distorted square-planar geometry. The nitrogen N3 and chlorine Cl2, attached to the palladium and the hydrogen H(N3) from the morpholine ligand, are all in the same plane, perpendicular to the *NHC* ring. Hydrogen-bonding (H-bonding) between the morpholine ligand and one of the chlorines attached to the Pd was also detected.[32] This H-bonding is considered to be intramolecular since the H–Cl distance between Cl2 and H(N3) (2.60 Å) is shorter than the sum of the van der Waals radii for H and Cl atoms (2.95 Å).[33] In addition to

this N(H)−Cl intramolecular interaction, a weak intermolecular C(H)−O (2.39 Å) interaction was also observed between carbon C(2), hydrogen (2A), and oxygen (1) (Figure 4). This hydrogen bonding is below the sum of the van der Waals radii of H and O (2.72 Å),[32] and links the molecules into chains along the [010] plane in the solid state.[34]

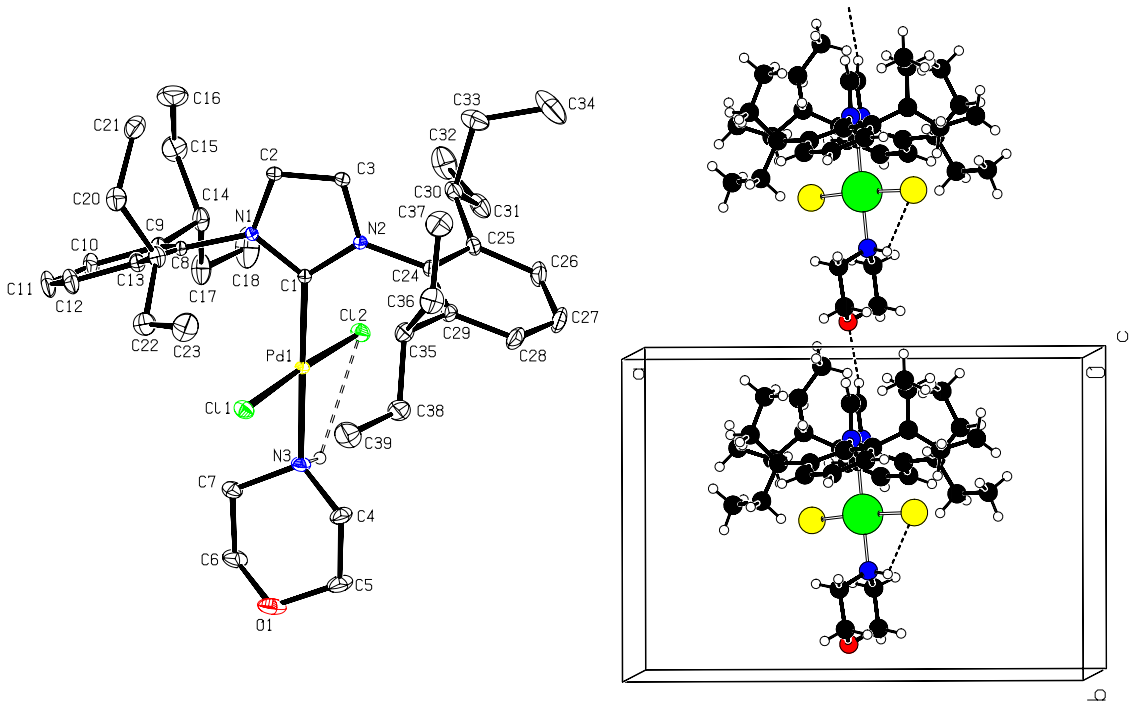

Figure 4: (a) The molecular structure of **32d** with ellipsoids drawn at the 30% level (CCDC–1017466).[34] Hydrogen atoms are not shown; (b) Part of the crystal structure of **32d** with hydrogen bonds shown as dashed lines. The weak intermolecular C**–**H···O hydrogen bonds link molecules forming chains along the b axis (i.e., the [010] plane).

2.2. Evaluation of [(NHC)PdCl$_2$(morpholine)] Complexes

In order to determine how readily these new pre-catalysts activate, complex **32a** was dissolved in toluene and treated with 3 molar equivalents of KO*t*Bu in the

presence of 2-(2-chlorophenyl)pyridine (**33**) (Equation 2). In this study, **32a** was chosen as a representative complex since salient structural features could be more easily identified by ^{1}H-NMR spectroscopy relative to other NHC ligand counterparts. After only 5 minutes at ambient temperature, 75% conversion to the corresponding trapped complex **28** was observed, indicating reduction to Pd(0).

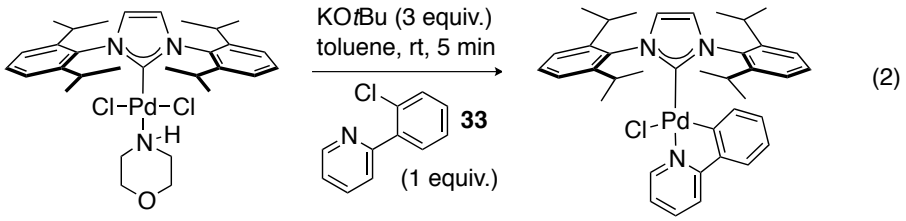

32a **34** (2)

With a better understanding of the time-frame of catalyst activation, complexes **32a-e** were then evaulated in the challenging Migita coupling of sterically hindered oxidative addition partner 2-chloro-1,3-dimethylbenzene (**35**) with thiophenol (**6**) (Table 1). Each complex was stirred for 5 minutes at ambient temperature in the presence of KO*t*Bu prior to the addition of thiophenol to ensure catalyst activation. A distinct colour change from deep purple to light yellow was generally observed during this time, which is indicative of successful catalyst activation.

Evaluation of NHCs based on the IPr core was first investigated. Assuming all pre-catalysts were equally activated, backbone saturation (i.e., *IPr* vs. *SIPr*) had only a minimal effect on catalyst activity (Table 1, entries 1 and 2), whereas the use of complex **32c**, which contains an "expanded ring" tetrahydropyrimidin-2-ylidine-derived NHC ligand (*SIPr*[6]) improved catalytic activity, turning over at nearly twice the rate of its imidazol-2-ylidine (*IPr*) analogue (Entry 1 vs 3). Expanding the ring of

the NHC ligand projects the N-aryl substituents more closely towards the metal coordination sphere, creating a more sterically congested Pd centre, which has been shown to facilitate reductive elimination in various cross-coupling reactions and to help keep the catalyst on-cycle in aryl sulfinations; both of which could explain the jump in reactivity.[35]

Table 1: Comparison of [(*NHC*)$PdCl_2$(morpholine)] pre-catalysts with other NHC–Pd^{II} pre-catalysts in the sulfination of 2-chloro-1,3-dimethylbenzene with thiophenol.[a]

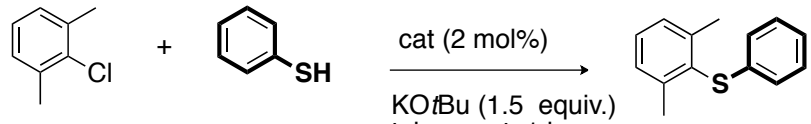

35 (1 equiv.) **6** (1.2 equiv.) **7**

Entry	Pre-catalyst	Conv. (%)[b]	Yield (%)[c]
1	**32a** (*IPr*)	26	25
2	**32b** (*SIPr*)	35	33
3	**32c** (*SIPr*^{6})	60	50
4	**32d** (*IPent*)	96	95
5	**32e** (*IPent*^{Cl})	50	46
6	*Pd-PEPPSI-IPent* (**4**)	0	0
7	[Pd(*IPent*)(η^3-allyl)Cl] (**28**)	50	46
8	[Pd(*IPent*)(η^3-cinnamyl)Cl] (**30**)	47	39

[a] Reactions were performed on a 0.25 mmol scale at a concentration of 0.125 M. [b] Percent conversion to product was determined by ^{1}H-NMR spectroscopic analysis of the crude reaction mixture. [c] Yields are reported on isolated products following silica gel chromatography.

Switching to complex **32d**, which features the yet bulkier *IPent* NHC, resulted in a significant jump in catalyst activity (Entry 4). Again, assuming all pre-catalysts were equally activated, these results suggest that increasing the steric bulk around the metal centre improves catalyst activity, which is consistent with trends previously reported by our group.[20,25] Surprisingly however, switching to complex **32e**, which features the backbone chlorinated *IPent*^{Cl} NHC, resulted in a significant reduction in catalytic

activity (Entry 5). While the reason for the lower overall performance of **32e** is not clear, it is suspected that it is most likely linked to pre-catalyst activation. Previous studies have shown that once activated, *IPent*^{Cl} is perhaps the most active Pd-NHC complex yet created,[25,27] hence the problem most likely lies off-cycle in catalyst activation.

While the exact mechanism by which these *trans*-ligated morpholine complexes are reduced to Pd(0) is not known, the Organ group has proposed that deprotonation of morpholine, followed by BHE and RE affords the active catalyst (Scheme 11a). From previous work in the Organ group on secondary alkyl Negishi coupling, it was shown that BHE is slower with *IPent*^{Cl} than *IPent* due to the increased steric bulk around then Pd-centre.[21f] The chlorine atoms on the backbone of the NHC in *IPent*^{Cl} push the N-aryl groups closer to the metal coordination sphere, destabilizing the 4-centred transition state (TS) required of BHE more than the 3-centred TS of RE (Scheme 11b). This could explain the difference in reactivity between complexes **32d** and **32e,** in that *IPent*^{Cl} would be slower to activate than *IPent* since the rate of BHE is slower with the *IPent*^{Cl} ligand. This would also imply that BHE is the rate-limiting step in the catalyst activation process since the Organ groups previous work shows RE to be faster with IPent^{Cl} relative to IPent.

a) Catalyst activation pathway

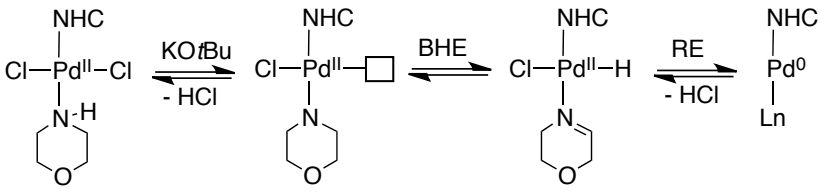

b) Transitions States for Reductive Elimination (RE) and Beta-Hydride Elimination (BHE)

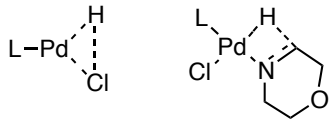

3-centred TS RE **4-centred TS BHE**

Scheme 11: a) Proposed catalyst activation pathway; b) Reductive Elimination (RE) and Beta-Hydride Elimination (BHE) transitions states.

To better understand the difference in reactivity between complexes **32d** and **32e**, both activation and reaction parameters were systematically varied for the couping of aryl chloride **35** to thiophenol **6** (Table 2). Keeping the activation time the same (5 min.) while increasing the reaction time from 1 h to 2 h resulted in a significant increase in conversion to product for **26e** (Entries 2 and 3). Next, increasing the activation time from 5 min. to 10 min. while keeping the reaction time the same also seemed to significantly improve the reaction outcome, leading to excellent conversion in 1 h (Entries 2 and 4). Lastly, heating the reaction to 40 °C again significantly improved the catalytic activity of complex **32e** (Entry 5).

Table 2: Comparison of **32d** and **32e** in the sulfination of 2-chloro-1,3-dimethylbenzene with thiophenol.[a]

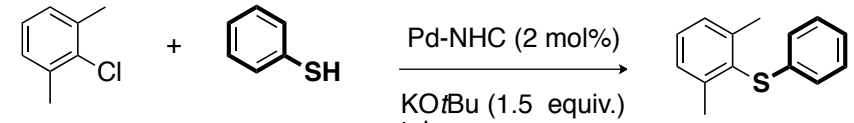

35 (1 equiv.) **6** (1.2 equiv.) **7**

Entry	Temp. (°C)	Activation time (min)	Pre-catalyst	Reaction Time	Yield (%)[b]
1	25	5	**32d**	1	95
2	25	5	**32e**	1	46
3	25	5	**32e**	2	92
4	25	10	**32e**	1	81
5	40	5	**32e**	1	86
6	25	0	**32d**	24	97

[a] Reactions were performed on a 0.25 mmol scale at a concentration of 0.125M. [b] Yields are reported on isolated products following silica gel chromatography.

These results are consistent with the hypothesis that complex **32e** activates more slowly than **32d** under the standard reaction conditions (Entries 1 and 2). However, this can be overcome by either extending the pre-activation time or reaction time, or by elevating the temperature to 40 °C. Nevertheless, complex **32d** was chosen for further study as this complex complex activates faster than **32e**, leading to faster reaction times and allowing the use of lower temperatures. Lastly, to demonstrate the importance of catalyst activation on the overall rate of product formation, a reaction was performed in which the pre-activation step was removed. In other words, thiol **6** was added to the reaction mixture alongside aryl chloride **35** and KO*t*Bu at the beginning of the reaction. This resulted in a significant decrease in catalytic activity, requiring 24 hours to reach full conversion to product (Entry 6). The decrease in

catalytic activity is believed to be due to the morpholine ligand now having to compete with a 60-fold excess of thiolate in order for catalyst activation to occur.

Having established **32d** to be the most readily activated morpholine-derived pre-catalyst, leading to the best conversion to product under our sulfination conditions, complex **32d** was next screened against other well-defined NHC-Pd(II) pre-catalysts reported to activate readily under similar conditions.[31,36] As expected, *Pd-PEPPSI-IPent* (**4**) failed to show any activity in the absence of external activators at ambient temperature (Table 1, Entry 6). Both [Pd(*IPent*)(η^3-allyl)Cl] (**28**) and [Pd(*IPent*)(η^3-cinnamy)Cl] (**30**) complexes led to only 50% and 30% conversion to product, respectively (Table 1, entries 7 and 8). These results were not surprising considering that, while similar Pd–π–allyl complexes (e.g., complex **23**, Scheme 7) have been shown to activate readily in the presence of *tert*-butoxide, the reported activation times are typically much longer.[31]

2.3. Substrate Scope Study in Aryl Sulfination with [(IPent)PdCl$_2$(morpholine)] (32d)

With optimization complete, **32d** was evaluated in the aryl sulfination of a variety of (hetero)aryl halides with both aryl and alkyl thiols. First, the reaction of thiophenol **6** with various aryl and (hetero)aryl halides (Table 3, **7**, **36**-**42**) was studied. The reactions proceeded smoothly under the conditions outlined in Table 3, regardless of the steric or electronic character of the oxidative addition partners, with many reactions going to completion in just 1-2 h. In general, completion of the reaction mixtures was monitored visually since addition of potassium thiolate

produces a heterogenous mixture that gradually becomes homogenous as the reaction proceeds to produce the thioether product.

Table 3: Sulfination of sterically and electronically deactivated oxidative addition partners with aryl sulfide partners.[a,b]

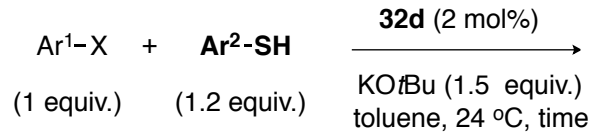

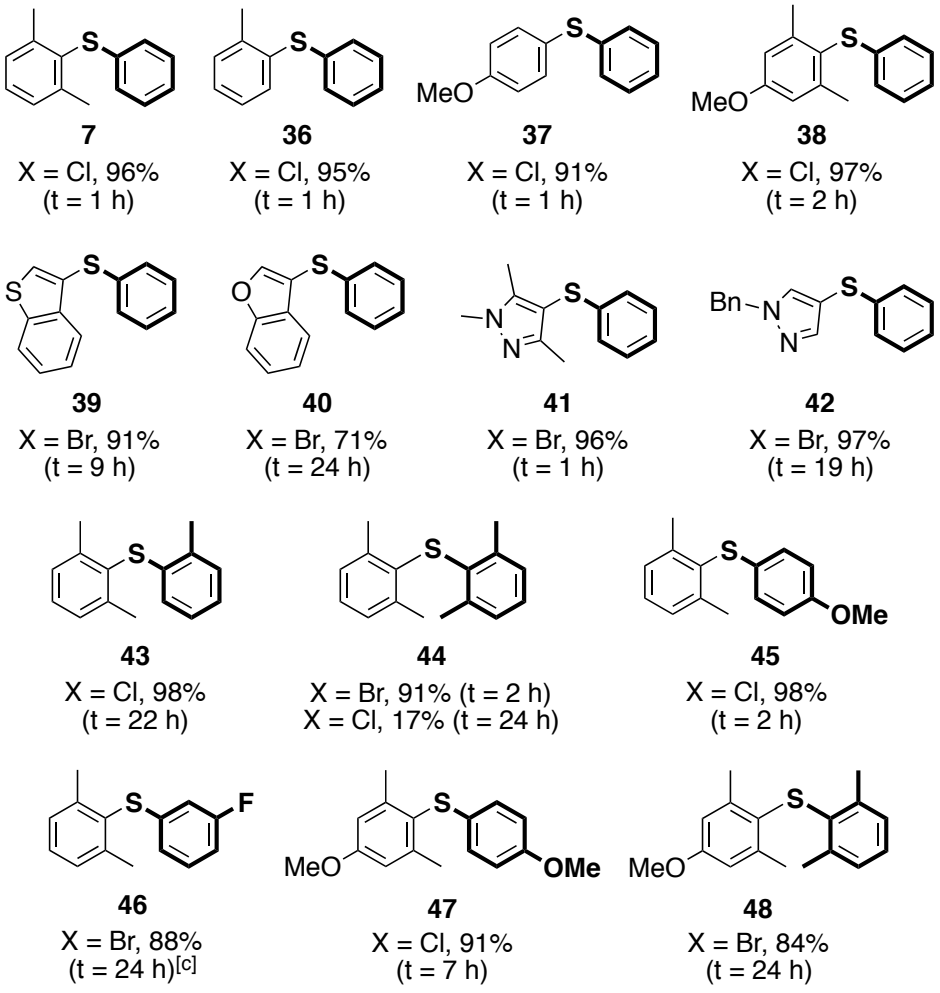

[a] Reactions were performed on a 0.25 mmol scale at a concentration of 0.125M. [b] Yields are reported on isolated products following silica gel chromatography and are averaged over two runs. [c] The potassium thiolate was used instead of the thiol under the same reaction conditions.

With thiophenol **6** demonstrating good reactivity, attention was then focused on coupling different aromatic thiols with sterically encumbered, electron rich aryl halides (Table 3, **43**-**48**). Sterically encumbered aryl sulfides were well tolerated, with 1,3-dimethylthiophenol leading to tetra-othro-substituted products **44** and **48** in high yields within 24 hours or less. Interestingly, in the formation of **44,** changing the halide of the oxidative addition partner from chloride to bromide significantly reduced the reaction time and improved the yield of the reaction. The reason why aryl bromides couple more efficiently than their chloride counterparts in sulfination chemistry is still not well understood. Hartwig and and co-workers have proposed that oxidative addition (OA) across the aryl bromide bond occurs more readily than the aryl chloride for aryl sulfination reactions catalyzed by the Josiphos-ligated catalysts system.[17] However, for complex **32d** and other Pd-PEPPSI compexes, RE is believed to be the rate-determining step (RDS) in this transformation and not OA, thus the reason for why aryl bromides couple better than aryl chlorides cannot be rationalize at this time. Further, the rate of catalyst turnover appears to depend more on the steric and electronic properties of the sulfide rather than the aryl halide, generally requiring longer reaction times for both electron deficient and sterically encumbered sulfides (**7** vs **43** and **7** vs **46**). For example, when 2-chlorotoluene was treated with 2,6-dimethylbenzenethiol under the same reaction conditions described in Table 3, only 30% of product **43** could be isolated (Equation 3). This result is consistent with the idea that RE is the RDS in C-S cross-coupling catalyzed by **32d**.

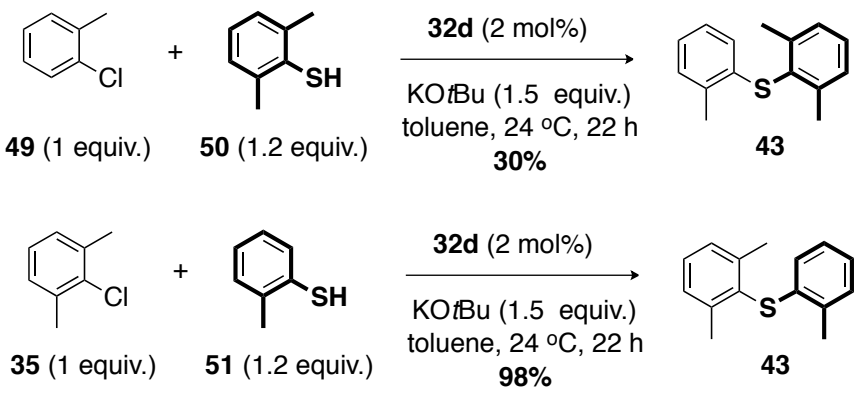

Scheme 12: Investigating the steric effects of the oxidative addition partner and the nucleophile on C–S bond formation catalyzed by **32d**.

Having demonstrated excellent reactivity of **32d** with the thiophenol derivatives, attention was then focused on non-aromatic thiols as these substrates have been described in the literature to be more challening to couple due to a slower RE step relative to aryl thiols.[37] As shown in Table 4, the coupling reactions proceeded well with primary (e.g., **52**, **57**), secondary (e.g., **53**, **58**), tertiary (e.g.,**54**, **60**), and benzylic (e.g., **55**, **59**) thiols with hindered and deactivated aryl halides. Hindered triisopropylsilyl(TIPS)-protected thiol were also found to couple with ease under these mild conditions (e.g., **56**, **61**). As reported by Hartwig and co-workers, this method serves as a convenient way to access aryl thiols, after deprotection of the TIPS moiety, that are otherwise not readily available.[3b] Since aryl thiols are prone to oxidation, they readily decompose if not properly stored under an inert atmosphere and consequently, there are a limited number of aryl thiols commercially available.

Table 4: Sulfination of sterically and electronically deactivated oxidative addition partners with alkyl sulfide partners.[a,b]

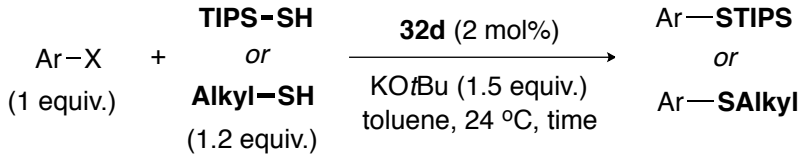

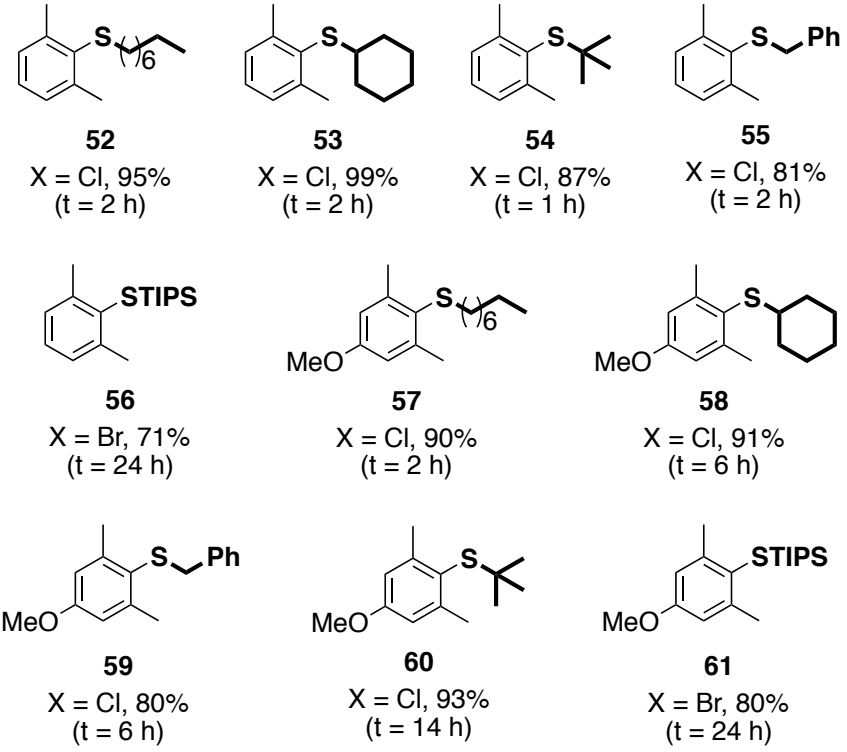

[a] Reactions were performed on a 0.25 mmol scale at a concentration of 0.125M. [b] Yields are reported on isolated products following silica gel chromatography and are averaged over two runs.

2.4. Effects of Disulfide and Oxygen in Aryl Sulfination Reactions

During these investigations, it was noticed that some aryl thiols failed to couple under the developed reaction conditions. Upon ^{1}H-NMR spectroscopic analysis, varying amounts of disulfide contaminants were noticed in some of the aryl thiol reagents, specifically in those that failed to give any cross-coupled product. For

example, in the case of **46** (Table 3), initially no cross-coupled product was observed when the free thiol was used. However, when the disulfide-free potassium salt was prepared and subjected to the same reaction conditions, excellent conversion to product **46** was achieved. The Organ group[20,25,27] and others[13,38] have previously shown that the active Pd(0) species can oxidatively add across the S–S bond of disulfides, forming persistent [$Pd^{II}(SAr)_2$] complexes (e.g., complex **17** in Figure 3). For NHC complexes, in the absence of external reducing agents such as LiO*i*Pr, these resting states cannot be broken down to re-enter the catalytic cycle, even at elevated temperatures (refer to Figure 3). Therefore, in the case of **46**, the presence of disulfide (20-30 mol %) was thought to be the reason as to why intially no reaction was observed. To demonstrate the deleterious effect that even a catalytic amount of disulfide can have on this transformation, aryl chloride **35** and thiophenol **6** were coupled in the presence of 1,2-diphenyldisulfide (5 mol %) (Equation 3). After 24 hours, only trace amounts of product **7** were detected.

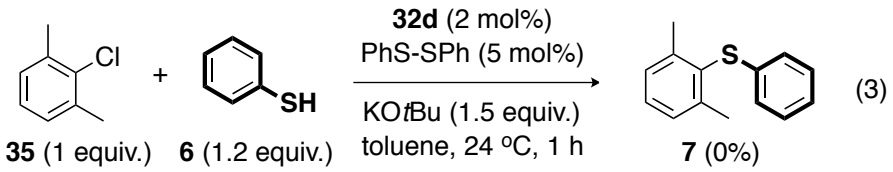

(3)

As mentioned previously, aerobic oxidation of thiols and thiolate anions is known to occur quite readily.[39] In this study, it was believed that the disulfide poisoning effects observed with morpholine-derived complexes **32a-e** and with the entire family of *Pd-PEPPSI* pre-catalysts in sulfination applications could also explain the heightened sensitivity of this reaction to dissolved oxygen.[20,25,27] For

instance, during the optimization studies it was observed that when the reaction solvent was not degassed via the freeze-pump-thaw method, the reaction outcome was poorly reproducible and that extended reaction times were required to achieve acceptable conversions to product. A similar poisoning effect was noted recently by Pfizer process chemists during the optimization of the commercial manufacturing route of Axitinib.[40] In that study, low-level disulfide impurities, originating from aerobic oxidation of the nucleophilic thiol, were observed to significantly inhibit catalyst activity. However, the authors report that this difficulty could be overcome by the addition of solid reducing agents, such as Zn metal, or by making the headspace inert by charging with an inert gas, such as nitrogen.

2.5. Conclusion

In summary, a series of new NHC-Pd^{II} pre-catalysts (**32a-e**) featuring a *trans*-oriented morpholine ligand (relative to the *NHC*) were successfully synthesized and characterized. Replacing the pyridine ligand with morpholine was shown to help facilitate rapid reduction of the Pd^{II} pre-catalyst to Pd^{0}, thus improving the performance of NHC-based pre-catalysts in cross-coupling reactions where pre-catalyst activation is difficult. Complexes **32a-e** were evaluated in aromatic sulfination and [(*IPent*)$PdCl_2$(morpholine)] **32d** was identified as the most readily activated, thus the most reactive under the developed reaction conditions. Under the optimized conditions, **32d** was shown to effectively couple a wide substrate scope including deactivated aryl halides with aryl, alkyl, and silyl thiols at ambient temperature. More importantly, the need for additives, external activators, or

cumbersome pre-activation steps were not necessary to activate the catalysts. Mechanistic studies revealed that these complexes are rapidly reduced to the active NHC-Pd^0 species under the reaction conditions, thus avoiding the formation of deleterious off-cycle Pd^{II}-thiolate resting states known to occur with other common NHC-Pd^{II} pre-catalysts. These results place morpholine-derived **32d** among the most readily activated NHC-based pre-catalysts yet reported for sulfination chemistry.

CHAPTER 3 – Experimental Procedures

3.1. General Experimental

All reagents were purchased from Sigma-Aldrich or Alfa Aesar and were used without further purification, unless otherwise stated. [Pd(*IPr*)(η^3-allyl)Cl] (**25**) and [Pd(*SIPr*)(η^3-allyl)Cl] (**26**) were prepared according to literature precedents.[30] *IPent•HCl* (**S4**) and *Pd-PEPPSI-IPent* (**4**) were provided by Total Synthesis Ltd. (Toronto, Ontario). *IPent^{Cl}•HCl*[21f] (**S5**), *SIPr^6•HBr*[41] and *SIPr^6•HBF$_4$*[42] (**S3**) were prepared according to literature precedents. Toluene (HPLC grade, cat 123161) was purchased from Fisher Scientific, degassed via three cycles of freeze-pump-thaw, and stored in the glovebox. $CDCl_3$, C_6D_6, and DMSO-d^6 were purchased from Sigma-Aldrich. All reaction vials (screw-cap threaded, caps attached, 15x45 mm) were purchased from Fisher Scientific. Thin Layer Chromatography (TLC) was performed on EMD 60 F_{254} pre-coated glass plates and spots were visualized using UV light (254 nm) and ceric ammonium molybdate or potassium permanganate stains. Column chromatography purifications were carried out using the flash technique on EMD silica gel 60 (230 - 400 mesh) and on aluminum oxide, activated, neutral, Brockmann I (150 mesh).[43] Nuclear Magnetic Resonance (NMR) spectra were recorded on Bruker AV 300 MHz and AV 400 MHz spectrometers at 25 °C, with the exception of **27**, which was recorded at 75 °C. The chemical shifts (δ) for all ^{1}H spectra are reported in parts per million (ppm) and referenced to the residual proton signal of the

deuterated solvent; coupling constants are expressed in Hertz (Hz). ^{13}C-NMR spectra were referenced to the carbon signals of the deuterated solvent. The ^{19}F–NMR was recorded at 376 MHz, using trifluorotoluene (-63.72 ppm) as the standard. The following abbreviations are used to describe multiplicity: s = singlet, d = doublet, t = triplet, q = quartet, sept = septet, dd = doublet of doublets, td = triplet of doublets, qd = quartet of doublets, m = multiplet, and b = broad. For ^{13}C APT NMR spectra, quaternary carbons and carbons with an even number of attached protons produce a positive (+) signal whereas peaks with a negative (-) signal arise from carbons attached to an odd number of protons. High Resolution Mass Spectrometry (HRMS) analysis was performed by the Mass Spectrometry and Proteomics Services Unit at Queens University in Kingston, Ontario. Melting points were determined using a Fisher-Johns melting point apparatus and are uncorrected. Unless otherwise indicated, all experiments were conducted under an atmosphere of dry argon in oven-dried or flame-dried glassware using standard Schlenk techniques.

3.2. General Procedure for the Preparation of [Pd(NHC)(η^3-allyl)Cl] Complexes (25–30)

In a glovebox, a round-bottom flask equipped with a magnetic stir bar was charged with base (KO*t*Bu or LiHMDS) (1.1 equiv.) after which it was taken out of the glovebox and charged with *NHC•HX* (1 equiv.) in air. The flask was evacuated and backfilled with Ar (x3) then THF (11.5 mL) was added. After stirring for 2 h at rt, [(η^3-R-allyl)Pd(μ-Cl)]$_2$ (0.5 equiv.) was added in one shot under a cone of Ar. After 22 h, the heterogeneous suspension was diluted with Et_2O then filtered through a pad

of silica gel, washing the filter cake copiously with Et_2O. The filtrate was concentrated to yield a yellow/orange oil that solidified after sonication with pentane. Washing with cold pentane furnished pure complexes **25 – 30**.

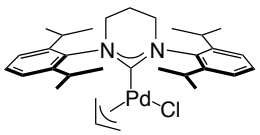

27

[Pd(*SIPr*^{6})(η^3-allyl)Cl] (27): Using *SIPr*^{6}•*HBF*$_4$ (**S3**) and LiHMDS following the general procedure, 469.6 mg (82%) of **27** were isolated as a light-yellow solid. Mp: 185–189°C (decomp.); ^{1}H-NMR (400 MHz, C_6D_6, 75°C) δ 7.26 – 7.23 (m, 7H), 4.44 – 4.34 (m, 1H), 3.91 – 3.82 (m, 4H), 3.62 (d, *J* = 7.2 Hz, 1H), 3.47 – 3.44 (m, 4H), 2.56 (d, *J* = 13.2 Hz, 1H), 2.03 – 2.00 (m, 2H), 1.86 (d, *J* = 6.4 Hz, 1H), 1.62 (d, *J* = 5.6 Hz, 12H), 1.25 (d, *J* = 7.2 Hz, 12H); ^{13}C-NMR (100 MHz, C_6D_6, 75°C) δ 214.9, 147.4, 146.6, 146.1, 143.7, 128.4, 124.4, 124.0, 112.3, 70.0, 49.6, 49.2, 28.9, 28.4, 26.6, 26.4, 24.2, 23.6, 20.5; HRMS (EI) [M^+] calcd. for $C_{31}H_{45}N_2PdCl$ 586.2306; found 586.2327.

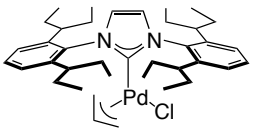

28

[Pd(*IPent*)(η^3-allyl)Cl] (28): Using *IPent*•*HCl* (**S4**) and KO*t*Bu following the general procedure, 861.4 mg (84%) of **28** were isolated as a light-yellow solid. Mp: 173–175°C (decomp.); ^{1}H-NMR (400 MHz, C_6D_6) δ 7.32 (t, *J* = 8.0 Hz, 2H), 7.16 (d, *J* = 8.0 Hz, 2H), 6.76 (s, 2H), 4.73 (sept, *J* = 6.8 Hz, 1H), 4.02 (d, *J* = 7.2 Hz, 1H), 3.02 (d, *J* = 13.6, 1H), 2.97 – 2.90 (m, 3H), 2.69 – 2.68 (m, 2H), 2.31 – 2.29 (m, 2H), 2.19 – 2.12 (m, 2H), 1.90 – 1.78 (m, 4H), 1.69 – 1.46 (m, 9H), 1.23 (bs, 12H), 0.86 (m, 12H); ^{13}C-NMR (100 MHz, C_6D_6) δ 184.5 (+), 144.3 (+), 144.0 (+), 137.9 (+), 128.9 (-),

125.2 (-), 124.8 (-), 124.1 (-), 113.3 (-), 72.3 (+), 48.9 (+), 41.8 (-), 41.5 (-), 28.2 (+), 28.0 (+), 27.6 (+), 27.4 (+), 13.2 (-), 12.7 (-), 11.7 (-), 11.0 (-); HRMS (EI) [M^+] calcd. for $C_{38}H_{57}N_2PdCl$ 682.3245; found 682.3273.

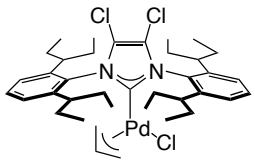

29

[Pd(*IPent*^{Cl})(η^3-allyl)Cl] (**29**): Using *IPent*^{Cl}•*HCl* (**S5**) and KO*t*Bu following the general procedure Following the general procedure, 741.7 mg (86%) of **29** were isolated as a light-yellow solid. ^{1}H-NMR (400 MHz, C_6D_6) δ 7.33 (t, *J* = 7.6 Hz, 2H), 7.18 (d, *J* = 8.0 Hz, 4H), 4.78 – 4.67 (m, 1H), 4.10 (d, *J* = 7.2 Hz, 1H), 3.07 (d, *J* = 13.2 Hz, 1H), 2.97 (m, 2H), 2.85 – 2.78 (m, 3H), 2.30 – 2.08 (m, 4H), 1.90 (sept, *J* = 7.6 Hz, 4H), 1.77 – 1.70 (m, 9H), 1.20 (q, *J* = 6.8 Hz, 12H), 0.95 (t, *J* = 7.3 Hz, 12H); ^{13}C-NMR (100 MHz, C_6D_6) δ 186.7, 144.4, 144.1, 135.0, 129.4, 126.0, 125.6, 119.7, 113.6, 73.2, 52.1, 41.5, 41.4, 27.1, 26.9, 26.2, 25.9, 25.8, 25.7, 12.1, 11.8, 11.2, 11.0. Spectral data were in accordance with those reported in literature.[21f]

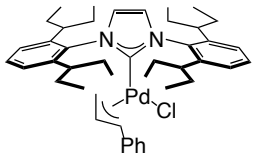

30

[Pd(*IPent*)(η^3-cinnamyl)Cl] (**30**): Using *IPent*•*HCl* (**S4**) and KO*t*Bu following the general procedure, 252.3 mg (89%) of **30** were isolated as a light-yellow solid. Mp: 138–141°C; ^{1}H-NMR (400 MHz, $CDCl_3$) δ 7.42 (t, *J* = 7.6 Hz, 2H), 7.20 – 7.10 (m, 11H), 5.24 – 5.16 (m, 1H), 4.43 (d, *J* = 13.2 Hz, 1H), 2.56 (bs, 4H), 2.08 – 2.03 (m, 4H), 1.83 – 1.76 (m, 4H), 1.74 – 1.61 (m, 5H), 1.56 – 1.46 (m, 4H), 1.02 (t, *J* = 7.0 Hz, 12H), 0.76 (t, *J* = 7.4 Hz, 12H); ^{13}C-NMR (100 MHz, $CDCl_3$) δ 181.7 (+), 143.8 (+), 137.7 (+), 129.0 (-

), 128.3 (-), 127.3 (-), 126.7 (-), 124.9 (-), 124.4 (-), 108.4 (-), 91.6 (-), 45.5 (+), 41.7 (-), 28.0 (+), 27.4 (+), 12.9 (-), 11.4 (-); HRMS (EI) [M^+] calcd. for $C_{44}H_{61}N_2PdCl$ 586.2306; found 586.2327. Spectral data were in accordance with those reported in literature although the melting point was previously unreported.[44]

3.3. General Procedure for the Preparation of [(NHC)PdCl$_2$(morpholine)] Complexes (32a–32e)

A solution of [Pd(*NHC*)(η^3-allyl)Cl] [(**25– 29**) (1 equiv.) in HCl (2 M in Et_2O, 1 mL per 0.1 mmol of complex) was stirred under a static atmosphere of Ar, during which time an orange solid precipitated from the reaction mixture. After the indicated time, the solvent was then removed yielding crude **31a** – **31e** as orange solids, which were then suspended in CH_2Cl_2 (2 mL per 0.5 mmol complex). The suspension was charged with morpholine (2.5 equiv.) and the resulting solutions were allowed to stir at rt for the indicated time. The solvent was then evaporated and the residue purified via filtration through a plug of neutral alumina with CH_2Cl_2 to yield pure [(*NHC*)PdCl(morpholine)] complexes (**32a** – **32e**).

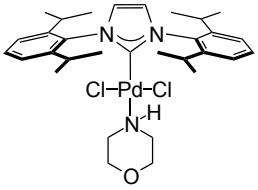

32a

[(*IPr*)PdCl$_2$(morpholine)], 32a (Scheme 10): Following the general procedure (t = 1 h), 521.6 mg (91%) of **32a** were isolated as a light-yellow solid. Mp: 153–155°C (lit. mp: 150-151°C);[45] ^{1}H-NMR (300 MHz, $CDCl_3$) δ 7.53 (t, *J* = 7.5 Hz, 2H), 7.37 (d, *J* = 7.5 Hz, 4H), 7.11 (s, 2H), 3.63 (dd, *J* = 12.0, 3.0 Hz, 2H), 3.30 – 3.26 (td, *J* = 12, 1.8 Hz, 2H), 3.14 – 2.99 (m, 6H), 2.52 – 2.41 (m, 3H), 1.47 (d, *J* =

6.8 Hz, 12H), 1.11(d, *J* = 6.8 Hz, 12H); ^{13}C-NMR (75 MHz, $CDCl_3$) δ 157.0, 146.6, 135.0, 130.1, 124.8, 123.8, 67.6, 47.0, 28.7, 26.2, 23.01. Spectral data were in accordance with those reported in literature.[45]

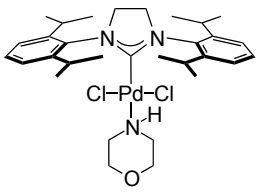

32b

[(*SIPr*)PdCl$_2$(morpholine)], 32b (Scheme 10): Following the general procedure (t = 3 h), 418.0 mg (94%) of **32b** were isolated as a light-yellow solid. Mp: 181–183°C; ^{1}H-NMR (400 MHz, $CDCl_3$) δ 7.44 (t, *J* = 7.8 Hz, 2H), 7.31 (d, *J* = 7.8 Hz, 4H), 4.04 (s, 4H), 3.60 (dd, *J* = 12.0, 2.2 Hz, 2H), 3.53 – 3.43 (m, 4H), 3.23 (t, *J* = 12.0 Hz, 2H), 3.00 (qd, *J* = 12.8, 3.2 Hz, 2H), 2.44 (d, *J* = 13.6 Hz, 2H), 2.35 (t, *J* = 12.0 Hz, 1H), 1.54 (d, *J* = 6.4 Hz, 12H), 1.25 (d, *J* = 6.8 Hz, 12H); ^{13}C-NMR (100 MHz, $CDCl_3$) δ 187.7 (+), 147.7 (+), 135.4 (+), 129.4 (-), 124.3 (-), 67.8 (+), 53.5 (+), 46.6 (+), 28.7 (-),26.8 (-), 24.0 (-); HRMS (ESI) $[M+H]^+$ calcd. for $C_{31}H_{47}Cl_2N_3OPd$ 654.2209; found 654.2189.

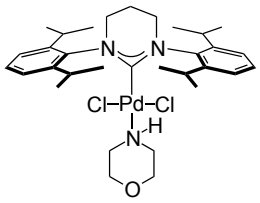

32c

[(*SIPr*^{6})PdCl$_2$(morpholine)], 32c (Scheme 10): Following the general procedure (t = 3 h), 14.7 mg (42%) of **32c** were isolated as a light-yellow solid. Mp: 240–245°C (decomp); ^{1}H-NMR (400 MHz, $CDCl_3$) δ 7.40 (t, *J* = 7.6 Hz, 2H), 7.31 (d, *J* = 7.6 Hz, 4H), 3.71 (t, *J* = 5.8 Hz, 4H), 3.57 – 3.47 (m, 6H), 3.13 (td, *J* = 12.0, 1.6 Hz, 2H), 2.80 (qd, *J* = 12.0, 3.2 Hz, 2H), 2.36 – 2.30 (m, 2H), 2.12 – 2.01 (m, 3H), 1.55 (d, *J* = 6.4 Hz, 12H), 1.21 (d, *J* = 6.8 Hz, 12H); ^{13}C-NMR (100 MHz, $CDCl_3$) δ 185.3

(+), 147.4 (+), 141.6 (+), 129.1 (-), 124.1 (-), 67.7 (+), 51.0 (+), 46.4 (+), 29.1 (-), 27.2 (-) 24.0 (-), 21.0 (+); HRMS (ESI) $[M+H]^+$ calcd. for $C_{32}H_{49}Cl_2N_3OPd$ 668.2365; found 668.2389.

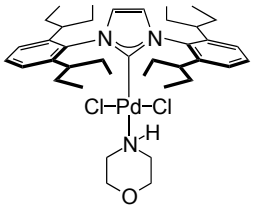

32d

[(*IPent*)$PdCl_2$(morpholine)], 32d (Scheme 10): Following the general procedure (t = 1 h), 345.9 mg (95%) of **32d** were isolated as a light-yellow solid. Mp: 260–265°C (decomp.); ^{1}H-NMR (400 MHz, $CDCl_3$) δ 7.46 (t, *J* = 7.6 Hz, 2H), 7.25 (d, *J* = 7.6 Hz, 4H), 7.03 (s, 2H), 3.63 (dd, *J* = 12.0, 2.8 Hz, 2H), 3.25 (t, *J* = 11.4 Hz, 2H), 3.06 (qd, *J* 12, 2.8 Hz, 2H), 2.70 – 2.63 (m, 4H), 2.52 (d, *J* = 12.0 Hz, 3H), 2.15 – 2.05 (m, 4H), 1.90 – 1.80 (m, 4H), 1.57 – 1.49 (m, 8H), 1.09 (t, *J* = 7.2 Hz, 12H), 0.77 (t, *J* = 7.2 Hz, 12 H); ^{13}C-NMR (100 MHz, $CDCl_3$) δ 155.4, 144.5, 136.5, 129.0, 125.1, 67.8, 47.0, 41.1, 28.5, 27.0, 12.9, 11.0; HRMS (ESI) $[M+H]^+$ calcd. for $C_{39}H_{61}N_3OCl_2Pd$ 764.3314; found 764.3341.

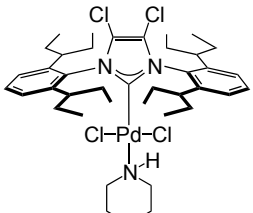

32e

[(*IPent*^{Cl})$PdCl_2$(morpholine)] 32e (Scheme 10): Following the general procedure (t = 1 h), 540.0 mg (75%) of **32e** were isolated as a light-yellow solid. Mp: 177–180°C; ^{1}H-NMR (400 MHz, $CDCl_3$) δ 7.51 (t, *J* = 7.8 Hz, 2H), 7.29 (d, *J* = 7.8 Hz, 4H), 3.62 (dd, *J* = 12.0 Hz, 2.4 Hz, 2H), 3.25 (t, *J* = 12.0 Hz, 2H), 3.07 (qd, 12.6, 3.2 Hz, 2H), 2.81 – 2.80 (m, 4H), 2.68 (t, *J* = 12.0 Hz, 1H), 2.49 (d, *J* = 13.2 Hz, 2H), 2.03 – 1.86 (m, 8 Hz), 1.71 – 1.61 (m, 4 H), 1.54 – 1.43 (m, 4H), 1.12 (t, *J* = 7.6 Hz,

12H), 0.83 (t, J = 7.2 Hz, 12H); ^{13}C-NMR (100 MHz, $CDCl_3$) δ 159.1 (+), 145.1 (+), 133.4 (+), 129.6 (-), 126.2 (-), 120.8 (-), 67.7 (+), 47.1 (+), 40.8 (-), 27.4 (+), 26.5 (+), 12.6 (-), 10.8 (-); HRMS (ESI) $[M+H]^+$ calcd. for $C_{39}H_{59}N_3OCl_4Pd$ 832.2519; found 832.2559.

3.4. Activation Study

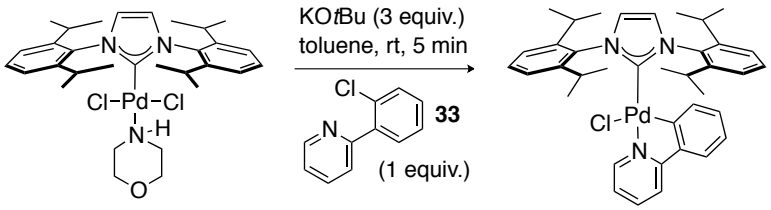

32a **34**
75% conv. (73%)

In a glovebox, an oven-dried 1 dram vial equipped with a magnetic stir bar was charged with **32a** (41.1 mg, 0.06 mmol, 1 equiv.) and KO*t*Bu (20.2 mg, 0.18 mmol, 3.0 equiv.). The vial was sealed with a Teflon-lined screw cap and a solution of 2-(2-chlorophenyl)pyridine 33**7**) (11.9 mg, 0.063 mmol, 1.05 equiv.) in toluene (1.0 mL) was added. The resulting heterogeneous mixture was stirred vigorously for 5 min. The reaction was then taken out of the glovebox, diluted with CH_2Cl_2, filtered through a plug of SiO_2 eluting with 10% MeOH/CH_2Cl_2, and concentrated *in vacuo*. The residue thus obtained was purified by flash chromatography on silica gel (20/80 Et_2O/pentane, R_f = 0.06) yielding **34** (36.1 mg, 73%) as a light-yellow solid. Mp: 280–285°C (decomp.) (lit. mp: 278-284°C, decomp.)[46]; ^{1}H-NMR (400 MHz, $CDCl_3$) δ 9.30 (d, J = 5.6 Hz), 7.56 (t, J = 8.0 Hz, 1H), 7.45 (d, J = 8.0 Hz, 1H), 7.39 (t, J = 7.6 Hz, 2H), 7.32 (t, J = 7.6 HZ, 3H), 7.28 (s, 2H), 7.18 (d, J = 8.0 Hz, 2H), 6.99 –

6.88 (m, 3H), 6.74 (d, J = 7.6 Hz, 1H), 3.7 – 3.23 (m, 4H), 1.51 (d, J = 6.4 Hz, 6H), 1.19 (d, J = 6.4 Hz, 6H), 1.06 (d, J = 6.8 Hz, 6H), 0.81 (d, J = 6.8 Hz, 6H); ^{13}C-NMR (100 MHz, $CDCl_3$) δ 178.8 (+), 164.3 (+), 155.7 (+), 150.0 (-), 147.7 (+), 146.4 (+), 144.9 (+), 137.7 (-), 137.5 (-), 135.9 (+), 129.9 (-), 128.9 (-), 124.9 (-), 124.2 (-), 124.0 (-), 123.1 (-), 122.7 (-), 121.4 (-), 117.3 (-), 29.0 (-), 28.5 (-), 26.5 (-), 26.2 (-), 23.2 (-), 22.9 (-). Spectral data were in accordance with those reported in literature.[47]

3.5. Preparation of Potassium 3-fluorobenzenethiolate (62)

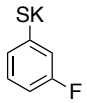

62

In the glovebox, a 50 mL round-bottom flask equipped with a magnetic stir bar was charged with KO*t*Bu (1.99 g, 17.8 mmol, 1.0 equiv.) after which it was sealed with a rubber septum and removed from the glovebox. THF (17 mL) was added *via* syringe and to the resulting turbid solution was added 3-fluorobenzenethiol (1.5 mL, 17.8 mmol, 1.0 equiv.) dropwise *via* syringe. After stirring for 30 min., the white heterogeneous suspension was allowed to stand for 1 h. The solvent was withdrawn via syringe and the resulting white solid was washed with Et_2O (20 mL x 3). Drying under high vacuum for 16 h yielded 2.05 g of **62** (70%) as a white solid. Mp: 68–73°C; ^{1}H-NMR (400 MHz, DMSO-d^6) δ 7.80 (d, J = 7.5 Hz, 1H), 7.70 (m, 1H), 6.63 (m, 1H), 6.15 (m, 1H); ^{13}C-NMR (100 MHz, DMSO-d^6) δ 163.7 (d, J = 8.0 Hz), 162.1 (d, J = 239.0 Hz), 129.6, 127.2 (d, J = 10.0 Hz), 118.5 (d, J = 17.0 Hz), 102.8 (d, J = 21.0 Hz); ^{19}F-NMR (376 MHz, DMSO-d^6) δ -117.4 (m, 1F); HRMS (ESI) $[M-K]^-$ calcd. for C_6H_4FS 127.0017; found 127.0013.

3.6. General Cross-Coupling Procedure.

In a glovebox, an oven-dried 1 dram vial equipped with a magnetic stir bar was charged with **32d** (3.8 mg, 0.005 mmol, 2 mol%) and KO*t*Bu (44.3 mg, 0.375 mmol, 1.5 equiv.). The vial was sealed with a Teflon-lined screw cap and the aryl halide (0.25 mmol, 1 equiv.) and toluene (2 mL) were injected in rapid succession. Alternatively, if the aryl halide was a solid it was added to the vial before the addition of toluene. The resulting mixture was stirred for 5 min. to ensure pre-catalyst activation, during which time a colour change from dark blue to brown/yellow was observed. The thiol (0.3 mmol, 1.2 equiv.) was then added dropwise over the course of 1 min. and the suspension was stirred at ambient temperature until judged complete by TLC analysis. The reaction was quenched by the addition of aqueous 1M NaOH (1 mL) and the resulting biphasic mixture stirred vigorously for 5 min. The organic layer was removed and the aqueous layer was extracted with Et_2O (x3). The combined organic extracts were washed with brine (x1), dried over anhydrous Na_2SO_4, filtered through a short plug of silica gel, and concentrated *in vacuo*. Alternatively, in the case of TIPS-protected thiols, the reaction was directly filtered through a plug of celite, eluted with ether, and then concentrated *in vacuo*. The residue thus obtained was purified by flash chromatography to yield pure thioether.

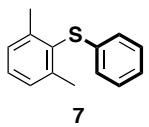

7

(2,6-Dimethylphenyl)(phenyl)sulfane, 7 (Table 3): Following the general procedure (t = 1 h), 51.4 mg of **7** (96%) were isolated by flash chromatography (hexanes, R_f = 0.3) as a clear, colourless oil. ^{1}H-NMR (400 MHz,

$CDCl_3$) δ 7.31 – 7.21 (m, 5H), 7.11 (t, *J* = 7.4 Hz, 1H), 6.99 (d, *J* = 7.4 Hz, 2H), 2.49 (s, 6H); ^{13}C-NMR (100 MHz, $CDCl_3$) δ 143.9 (+), 138.0 (+), 130.5 (+), 129.3 (-), 128.9 (-), 128.5 (-), 125.6 (-), 124.6 (-), 21.8 (-). Spectral data were in accordance with those reported in literature.[17]

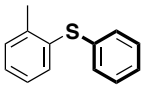

36

Phenyl(*o*-tolyl)sulfane, 36 (Table 3): Following the general procedure (t = 1 h), 47.7 mg of **36** (95%) were isolated by flash chromatography (hexanes, R_f = 0.4) as a light-yellow solid. Mp: 40–43°C; ^{1}H-NMR (400 MHz, $CDCl_3$) δ 7.35 – 7.16 (m, 9H), 2.42 (s, 3H); ^{13}C-NMR (100 MHz, $CDCl_3$) δ 140.0 (+), 136.2 (+), 133.8 (+), 133.0 (-), 130.6 (-), 129.6 (-), 129.1 (-), 127.9 (-), 126.7 (-), 126.3 (-), 20.6 (-). Spectral data were in accordance with those reported in literature although the melting point was previously unreported.[17]

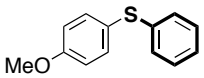

37

(4-Methoxyphenyl)(phenyl)sulfane, 37 (Table 3): Following the general procedure (t = 1 h), 49.4 mg of **37** (91%) were isolated by flash chromatography (5/95 Et_2O/pentane, R_f = 0.49) as an orange oil. ^{1}H-NMR (400 MHz, $CDCl_3$) δ 7.46 (d, *J* = 8.6 Hz, 2H), 7.29 – 7.16 (m, 5H), 6.94 (d, *J* = 8.6 Hz, 2H), 3.86 (s, 3H); ^{13}C-NMR (100 MHz, $CDCl_3$) δ 159.8 (+), 138.6 (+), 135.3 (-), 128.9 (-), 128.2 (-), 125.7 (-), 124.3 (+), 114.9 (-), 55.3 (-). Spectral data were in accordance with those reported in literature.[28]

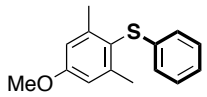

38

(4-Methoxy-2,6-dimethylphenyl)(phenyl) sulfane, 38 (Table 3): Following the general procedure (t = 2 h), 59.3 mg of **38** (97%) were isolated by flash chromatography (5/95 Et_2O/pentane, R_f = 0.75) as a yellow solid. Mp: 57–58°C; ^{1}H-NMR (300 MHz, $CDCl_3$) δ 7.22 (t, *J* = 7.5 Hz, 2H), 7.09 (t, *J* = 7.5 Hz, 1H), 6.94 (d, *J* = 7.8 Hz, 2H), 6.78 (s, 2H), 3.85 (s, 3H), 2.44 (s, 6H); ^{13}C-NMR (100 MHz, $CDCl_3$) δ 160.0 (+), 145.5 (+), 138.7 (+), 128.8 (-), 125.1 (-), 124.4 (-), 121.3 (+), 113.9 (-), 55.1 (-), 22.0 (-). Spectral data were in accordance with those reported in literature although the melting point was previously unreported.[28]

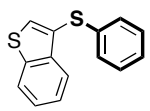

39

3-(Phenylthio)benzo[*b*]thiophene, 39 (Table 3): Following the general procedure (t = 9 h), 55.2 mg of **39** (91%) were isolated by flash chromatography (pentane, R_f = 0.35) as an off-white solid. Mp: 36–38°C; ^{1}H-NMR (300 MHz, $CDCl_3$) δ 7.94 (d, *J* = 8.0 Hz, 1H), 7.87 (d, *J* = 6.4 Hz, 1H), 7.60 (s, 1H), 7.46 – 7.40 (m, 2H), 7.28 – 7.16 (m, 5H); ^{13}C-NMR (100 MHz, $CDCl_3$) δ 139.9 (+), 138.8 (+), 136.5 (+), 132.0 (-), 128.9 (-), 127.4 (-), 125.7 (-), 124.9 (-), 124.7 (-), 123.9 (+), 123.0 (-), 122.8 (-). Spectral data were in accordance with those reported in literature although the melting point was previously unreported.[48]

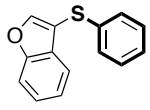

40

3-(Phenylthio)benzofuran, 40 (Table 3): Following the general procedure (t = 24 h), 40.0 mg of **40** (71%) were isolated by flash chromatography (heptane, R_f = 0.2) as a light-yellow solid. Mp: 45–47°C; ^{1}H-NMR

(400 MHz, $CDCl_3$) δ 7.89 (s, 1H), 7.58 (d, *J* = 8.0 Hz, 1H), 7.50 (d, *J* = 7.6 Hz, 1H), 7.38 (t, *J* = 7.8 Hz, 1H), 7.29 – 7.24 (m, 5H), 7.19 – 7.14 (m, 1H); ^{13}C-NMR (100 MHz, $CDCl_3$) δ 155.7 (+), 148.8 (-), 136.0 (+), 129.0 (-), 128.1 (+), 127.2 (-), 125.8 (-), 125.1 (-), 123.4 (-), 120.4 (-), 111.9 (-), 110.4 (+); HRMS (EI) [M^+] calcd. for $C_{14}H_{10}OS$ 226.0452; found 226.0460.

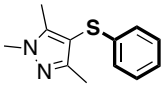

41

1,3,5-Trimethyl-4-(phenylthio)-1*H*-pyrazole, 41 (Table 3): Following the general procedure (t = 1 h), 52.6 mg of **41** (96%) were isolated by flash chromatography (20/80 EtOAc/hexane, R_f = 0.22) as a yellow oil. ^{1}H-NMR (400 MHz, $CDCl_3$) δ 7.20 (t, *J* = 7.8 Hz, 2H), 7.07 (d, *J* = 7.8 Hz, 1H), 6.98 (d, *J* = 8.0 Hz, 2H), 3.80 (s, 3H), 2.25 (s, 3H), 2.21 (s, 3H); ^{13}C-NMR (100 MHz, $CDCl_3$) δ 151.7 (+), 143.8 (+), 138.7 (+), 128.8 (-), 125.2 (-), 124.7 (-), 103.6 (+), 36.6 (-), 11.9 (-), 10.0 (-). Spectral data were in accordance with those reported in literature.[20]

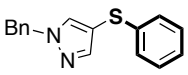

42

1-Benzyl-4-(phenylthio)-1*H*-pyrazole, 42 (Table 3): Following the general procedure (t = 19 h), 64.9 mg of **42** (97%) were isolated by flash chromatography (10/90 Et_2O/pentane, R_f = 0.24) as a yellow solid. Mp: 55–57°C; ^{1}H-NMR (400 MHz, $CDCl_3$) δ 7.69 (s, 1H), 7.57 (s, 1H), 7.43 – 7.25 (m, 3H), 7.30 – 7.23 (m, 4H), 7.15 (d, *J* = 6.8 Hz, 3H), 5.36 (s, 2H); ^{13}C-NMR (100 MHz, $CDCl_3$) δ 145.0 (-), 138.9 (+), 135.8 (+), 134.6 (-), 129.0 (-), 128.9 (-), 128.4 (-),

127.9 (-), 126.2 (-), 125.4 (-), 107.8 (+), 56.6 (-); HRMS (EI) [M^+] calcd. for $C_{16}H_{14}N_2S$ 266.0878; found 266.0871.

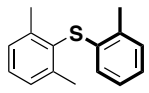

43

(2,6-Dimethylphenyl)(*o*-tolyl)sulfane, 43 (Table 3): Following the general procedure (t = 22 h), 56.0 mg of **43** (98%) were isolated by flash chromatography (pentane, R_f = 0.69) as a white solid. Mp: 82–85°C (lit. mp: 78–80°C)[19a]; ^{1}H-NMR (400 MHz, $CDCl_3$) δ 7.32 – 7.19 (m, 4H), 7.06 – 6.96 (m, 2H), 6.46 (d, *J* = 7.6 Hz, 1H), 2.50 (s, 3H), 2.46 (s, 6H); ^{13}C-NMR (100 MHz, $CDCl_3$) δ 144.0 (+), 137.0 (+), 134.8 (+), 130.5 (+), 129.9 (-), 129.1 (-), 128.4 (-), 126.4 (-), 124.3 (-), 124.1 (-), 21.7 (-), 20.0 (-). Spectral data were in accordance with those reported in literature.[49]

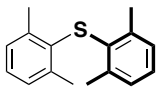

44

Bis(2,6-dimethylphenyl)sulfane, 44 (Table 3): Following the general procedure (t = 2 h), 54.7 mg of **44** (91%) were isolated by flash chromatography (heptane, R_f = 0.41) as a white solid. Mp: 77–79°C (lit. mp: 81–82°C)[19a]; ^{1}H-NMR (400 MHz, $CDCl_3$) δ 7.09 – 7.01 (s, 6H), 2.23 (s, 12H); ^{13}C-NMR (100 MHz, $CDCl_3$) δ 140.4 (+), 134.3 (+), 128.4 (-), 126.9 (-), 21.7 (-). Spectral data were in accordance with those reported in literature.[50]

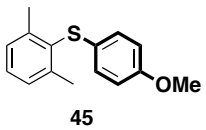

45

(2,6-Dimethylphenyl)(4-methoxyphenyl) sulfane, 45 (Table 3): Following the general procedure (t = 2 h), 60.2 mg of **45** (98%) were isolated by flash chromatography (pentane, R_f = 0.14) as an off-white solid. Mp:

50–52°C; ^{1}H-NMR (400 MHz, $CDCl_3$) δ 7.24 – 7.17 (m, 3H), 6.94 (d, *J* = 9.0 Hz, 2H), 6.77 (d, *J* = 9.0 Hz, 2H), 3.76 (s, 3H), 2.45 (s, 6H); ^{13}C-NMR (100 MHz, $CDCl_3$) δ 157.5 (+), 143.5 (+), 131.8 (+), 128.9 (-), 128.6 (+), 128.4 (-), 127.9 (-), 114.6 (-), 55.3 (-), 21.9 (-); HRMS (EI) [M^+] calcd. for $C_{15}H_{16}OS$ 244.0922; found 244.0931.

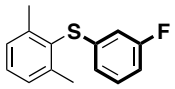

46

(2,6-Dimethylphenyl)(3-fluorophenyl)sulfane, 46 (Table 3): Following the general procedure (t = 24 h), 51.1 mg of **46** (88%) were isolated by flash chromatography (pentane, R_f = 0.45) as a clear, colourless oil. ^{1}H-NMR (400 MHz, $CDCl_3$) δ 7.31 – 7.14 (m, 4H), 6.81 – 6.76 (m, 2H), 6.59 (d, *J* = 7.6 Hz, 1H), 2.46 (s, 6H); ^{13}C-NMR (100 MHz, $CDCl_3$) δ 163.2 (+, d, *J* = 246 Hz), 143.9 (+), 140.6 (+, d, *J* = 8.0 Hz), 130.1 (-, d, *J* = 8.0 Hz) 129.7 (-), 129.6 (+), 128.6 (-), 121.1 (-, d, *J* = 2.0 Hz), 112.5 (-, d, *J* = 24.0 Hz), 111.5 (-, d, *J* = 21.0 Hz), 21.7 (-); ^{19}F-NMR (376 MHz, $CDCl_3$) δ -112.6 (m, 1F). Spectral data were in accordance with those reported in literature.[20]

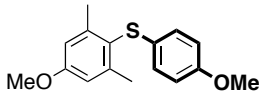

47

(4-Methoxy-2,6-dimethylphenyl)(4-methoxyphenyl) **sulfane, 47** (Table 3): Following the general procedure (t = 7 h), 62.2 mg of **47** (91%) were isolated by flash chromatography (5/95 Et_2O/pentane, R_f = 0.36) as a white solid. Mp: 67–68°C; ^{1}H-NMR (400 MHz, $CDCl_3$) δ 6.90 (d, *J* = 8.8 Hz, 2H), 6.78 – 6.74 (m, 4H), 3.82 (s, 3H), 3.76 (3H), 2.43 (s, 6H); ^{13}C-NMR (100 MHz, $CDCl_3$) δ 159.9 (+), 157.3 (+), 145.3 (+), 129.4 (+), 127.3 (-), 122.7 (+), 114.7

(-), 113.9 (-), 55.4 (-), 55.2 (-), 22.2 (-); HRMS (EI) [M^+] calcd. for $C_{16}H_{18}O_2S$ 274.1028; found 274.1034.

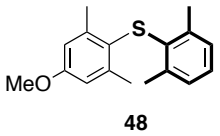

48

(2,6-dimethylphenyl)(4-methoxy-2,6-dimethylphenyl)sulfane, **48** (Table 3): Following the general procedure (t = 24 h), 56.9 mg of **48** (84%) were isolated by flash chromatography (5/95 Et_2O/pentane, R_f = 0.61) as a yellow solid. Mp: 71–73°C (lit. mp: 63–65°C)[19c]; ^{1}H-NMR (400 MHz, $CDCl_3$) δ 7.07 – 7.00 (m, 3H), 6.62 (s, 2H), 3.78 (s, 3H), 2.25 (s, 12H); ^{13}C-NMR (100 MHz, $CDCl_3$) δ 158.4 (+), 142.1 (+), 140.2 (+), 134.8 (+), 128.5 (-), 126.6 (-), 125.3 (+), 113.9 (-), 55.1 (-), 22.0 (-), 21.7 (-). Spectral data were in accordance with those reported in literature.[26]

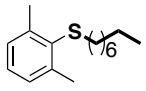

52

((2,6-Dimethylphenyl)(octyl)sulfane, 52 (Table 4): Following the general procedure (t = 2 h), 59.5 mg of **52** (95%) were isolated by flash chromatography (pentane, R_f = 0.54) as a clear, colourless oil. ^{1}H-NMR (400 MHz, $CDCl_3$) δ 7.12 (s, 3H), 2.66 (t, *J* = 7.4 Hz, 2H), 2.57 (s, 6H), 1.59 – 1.52 (m, 2H), 1.41 – 1.28 (m, 10H), 0.90 (t, *J* = 6.6 Hz, 3H); ^{13}C-NMR (100 MHz, $CDCl_3$) δ 143.0 (+), 134.0 (+), 127.9 (-, two overlapping signals), 35.4 (+), 31.8 (+), 29.9 (+), 29.2 (+, two overlapping signals), 28.9 (+), 22.6 (+), 22.1 (-), 14.1 (-); HRMS (EI) [M^+] calcd. for $C_{16}H_{26}S$ 250.1755; found 250.1763.

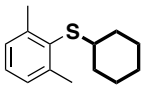

53

Cyclohexyl(2,6-dimethylphenyl)sulfane, 53 (Table 4): Following the general procedure (t = 2 h), 54.6 mg of **53** (99%) were isolated by flash chromatography (pentane, R_f = 0.51) as an off-white solid. Mp: 38–40°C; ^{1}H-NMR (400 MHz, $CDCl_3$) δ 7.13 (s, 3H), 2.89 – 2.82 (m, 1H), 2.57 (s, 6H), 1.88 – 1.85 (m, 2H), 1.79 – 1.75 (m, 2H), 165-1.61 (m, 1H), 1.47-1.38 (m, 5H); ^{13}C-NMR (100 MHz, $CDCl_3$) δ 143.4 (+), 133.1 (+), 127.9 (-, two overlapping signals), 47.4 (-), 33.7 (+), 26.2 (+), 25.8 (+), 22.4 (-); HRMS (EI) [M^+] calcd. for $C_{14}H_{20}S$ 220.1286; found 220.1293.

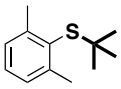

54

***tert*-Butyl(2,6-dimethylphenyl)sulfane**, **54** (Table 4): Following the general procedure (t = 1 h), 42.3 mg of **54** (87%) were isolated by flash chromatography (pentane, R_f = 0.50) as a clear, colourless oil. ^{1}H-NMR (400 MHz, $CDCl_3$) δ 7.15 (s, 3H), 2.60 (s, 6H), 1.31 (s, 9H); ^{13}C-NMR (100 MHz, $CDCl_3$) δ 145.2 (+), 132.2 (+), 128.3 (-), 127.9 (-), 49.2 (+), 31.6 (-), 23.1 (-). Spectral data were in accordance with those reported in literature.[17]

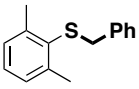

55

Benzyl(2,6-dimethylphenyl)sulfane, 55 (Table 4): Following the general procedure (t = 2 h), 46.0 mg of **55** (81%) were isolated by flash chromatography (pentane, R_f = 0.3) as a clear, colourless oil. ^{1}H-NMR (400 MHz, $CDCl_3$) δ 7.25 – 7.24 (m, 3H), 7.17 – 7.09 (m, 5H), 3.82 (s, 2H), 2.42 (s, 6H); ^{13}C-NMR (100 MHz, $CDCl_3$) δ 143.6 (+), 138.5 (+), 132.8 (+), 128.8 (-), 128.5 (-), 128.3

(-), 128.0 (-), 126.9 (-), 39.8 (+), 21.8 (-). Spectral data were in accordance with those reported in literature.[16]

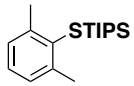

56

((2,6-Dimethylphenyl)thio)triisopropylsilane, 56 (Table 4): Following the general procedure (t = 24 h), 55.3 mg of **56** (71%) were isolated by flash chromatography using neutral Al_2O_3 (pentane, R_f = 0.44) as a yellow oil. ^{1}H-NMR (400 MHz, $CDCl_3$) δ 7.05 (s, 3H), 2.54 (s, 6H), 1.29-1.18 (m, 3H), 1.05 (d, *J* = 7.2 Hz, 18H); ^{13}C-NMR (100 MHz, $CDCl_3$) δ 143.4 (+), 131.0 (+), 127.8 (-), 126.6 (-), 23.6 (-), 18.5 (-), 14.1 (-). Spectral data were in accordance with those reported in literature.[20]

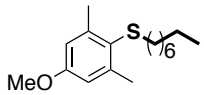

57

((4-Methoxy-2,6-dimethylphenyl)(octyl) sulfane, 57 (Table 4): Following the general procedure (t = 2 h), 63.1 mg of **57** (90%) were isolated by flash chromatography (5/95 Et_2O/pentane, R_f = 0.65) as a yellow oil. ^{1}H-NMR (400 MHz, $CDCl_3$) δ 6.68 (s, 2H), 3.79 (s, 3H), 2.60 (t, *J* = 7.4 Hz, 2H), 2.54 (s, 6H), 1.57 – 1.50 (m, 2H), 1.40 – 1.27 (m, 10H), 0.91 (t, *J* = 6.8 Hz, 3H); ^{13}C-NMR (100 MHz, $CDCl_3$) δ 159.0 (+), 144.6 (+), 125.2 (+), 113.5 (-), 55.1 (-), 35.8 (+), 31.8 (+), 29.8 (+), 29.3 (+), 29.2 (+), 29.0 (+), 22.7 (+), 22.4 (-), 14.1 (-); HRMS (EI) [M^+] calcd. for $C_{17}H_{28}OS$ 280.1861; found 280.1872.

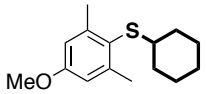

58

Cyclohexyl(4-methoxy-2,6-dimethylphenyl) sulfane, 58 (Table 4): Following the general procedure (t = 6 h), 52.7 mg of **58** (91%) were isolated by flash chromatography (pentane, R_f = 0.17) as a yellow solid. Mp: 52–53°C; ^{1}H-NMR (400 MHz, $CDCl_3$) δ 6.68 (s, 2H), 3.79 (s, 3H), 2.79 – 2.72 (m, 1H), 2.53 (s, 6H), 1.86 – 1.74 (m, 4H), 1.62 – 1.60 (m, 1H), 1.42 – 1.37 (m, 5H); ^{13}C-NMR (100 MHz, $CDCl_3$) δ 158.9 (+), 144.9 (+), 124.2 (+), 113.3 (-), 55.0 (-), 47.6 (-), 33.5 (+), 26.2 (+), 25.8 (+), 22.6 (-); HRMS (EI) [M^+] calcd. for $C_{15}H_{22}OS$ 250.1391; found 250.1383.

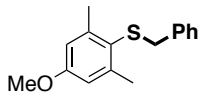

59

Benzyl(4-methoxy-2,6-dimethylphenyl) sulfane, 59 (Table 4): Following the general procedure (t = 6 h), 51.9 mg of **59** (80%) were isolated by flash chromatography (5/95 Et_2O/pentane, R_f = 0.53) as a light-yellow oil. ^{1}H-NMR (400 MHz, $CDCl_3$) δ 7.2-7.23 (m, 3H), 7.08 – 7.06 (m, 2H), 6.65 (s, 2H), 3.80 (s, 3H), 3.75 (s, 2H), 2.36 (s, 6H); ^{13}C-NMR (100 MHz, $CDCl_3$) δ 159.3 (+), 145.2 (+), 138.5 (+), 128.8 (-), 128.2 (-), 126.8 (-), 123.9 (-), 113.4 (-), 55.1 (-), 40.2 (+), 22.0 (-); HRMS (EI) [M^+] calcd. for $C_{16}H_{18}OS$ 258.1078; found 258.1087.

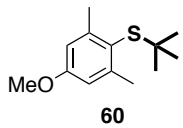

60

(*tert*-Butyl(4-methoxy-2,6-dimethylphenyl) sulfane, **60** (Table 4): Following the general procedure (t = 14 h), 51.2 mg of **60** (93%) were isolated by flash chromatography (5/95 Et_2O/pentane, R_f = 0.55) as a yellow oil. ^{1}H-NMR (400 MHz, $CDCl_3$) δ 6.71 (s, 2H), 3.80 (s, 3H), 2.57 (s, 6H), 128 (s, 9H); ^{13}C-NMR (100 MHz, $CDCl_3$) δ 159.1 (+), 146.7 (+), 123.6 (+), 113.4 (-), 55.0 (-), 48.8

(+), 31.5 (-), 23.4 (-); HRMS (EI) [M^+] calcd. for $C_{13}H_{20}OS$ 224.1235; found 224.1227.

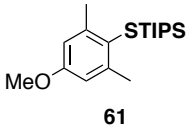

61

Triisopropyl((4-methoxy-2,6-dimethyl phenyl)thio)silane, 61 (Table 4): Following the general procedure (t = 24 h), 66.2 mg of **61** (82%) were isolated by flash chromatography using neutral Al_2O_3 (2/98 Et_2O/pentane, R_f = 0.42) as a clear, colourless oil. ^{1}H-NMR (400 MHz, $CDCl_3$) δ 6.64 (s, 2H), 3.77 (s, 3H), 2.51 (s, 6H), 1.29 – 1.18 (m, 3H), 1.06 (d, *J* = 7.2 Hz, 18H); ^{13}C-NMR (100 MHz, $CDCl_3$) δ 158.1 (+), 144.3 (+), 121.5 (+), 113.5 (-), 55.1 (-), 23.8 (-), 18.5 (-), 14.0 (-); HRMS (EI) [M^+] calcd. for $C_{18}H_{32}OSSi$ 324.1943; found 324.1935.

CHAPTER 4 – References

1. (a) Rayner, C. M. in *Advances in Sulfur Chemistry, Vol. 2, JAI Press, Greenwich,* CT, **2000**; (b) Solladie, G. *Comprehensive Organic Synthesis Vol. 6* (Eds.: Trost, B. M.; Fleming, I.), Pergamon Press, Oxford (UK), **1991**, p. 113–170.

2. (a) Otzen, T.; Wempe, E. G.; Kunz, B.; Bartels, R.; Lehwark-Yvetot, G.; Hänsel, W.; Schaper, K.-J.; Seydel, K. J. *J. Med. Chem.* **2004**, *47*, 240–253. (b) Wang, Y.; Chackalamannil, S.; Hu, Z.; Clader, J. W.; Greenlee, W.; Billard, W.; Binch III, G.; Crosby, G.; Ruperto, V.; Duffy, R. A.; McQuade, R.; Lachowicz, *Bioorg. Med. Chem. Lett.* **2000**, *10*, 2247–2250; (c) Sun, Z.-Y.; Botros, E.; Su, A.-D.; Kim, Y.; Wang, E.; Baturay, N. Z.; Kwon, C.-H. *J. Med. Chem.* **2000**, *43,* 4160–4168.

3. (a) J. R. Campbell, *J. Org. Chem.* **1964**, *29*, 1830–1833; (b) M. A. Fernández-Rodríguez, J. F. Hartwig, *Chem. Eur. J.* **2010**, *16*, 2355–2359 and references therein.

4. (a) Dougherty, G.; Hammond, P. D. *J. Am. Chem. Soc.* **1935**, *57*, 117–118; (b) Glass, H. B.; Reid, E. E. *J. Am. Chem. Soc.* **1929**, *51*, 3428–3430.

5. (a) Beletskaya, I. P.; Ananikov V. P. in *Catalyzed Carbon-Heteroatom Bond Formation* (Ed.: Yudin, A. K.), Wiley-VCH, Weinheim (Germany), 2011, pp. 69–118; (b) Eichman, C. C.; Stambuli, J. P. *Molecules* **2011**, *16*, 590–608.

6. (a) Correa, A.; Carril, M.; Bolm, C. *Angew. Chem. Int. Ed.* **2008**, *47*, 2880–2883; (b) Buchwald, S. L.; Bolm, C. *Angew. Chem. Int. Ed.* **2009**, *48*, 5586-5587.

7. Wong, Y.-C.; Jayanth, T. T.; Cheng, C.-H. *Org. Lett.* **2006**, *8*, 5613–5616.

8. (a) Cristau, H.J.; Chabaud, B.; Chene, A.; Christol, H. *Synthesis* **1981**, 892–894; (b) Percec, V.; Bae, J.Y.; Hill, D.H. *J. Org. Chem.* **1995,** *60*, 6895–6903; (c) Takagi, K. *Chem. Lett.* **1987**, 2221–2224; (d) Baldovino-Pantaleon, O.; Hernandez-Ortega, S.; Morales-Morales, D. *Adv. Synth. Catal.* **2006,** *348*, 236–242; (e) Jammi, S.; Barua, P.; Rout, L.; Saha, P.; Punnlyamurthy, T. *Tetrahedron Lett.* **2008,** *49*, 1484–1487; (f) Zhang, Y.G.; Ngeow, K.C.; Ying, J.Y. *Org. Lett.* **2007,** *9*, 3495–3498.

9. (a) Herrero, M. T.; SanMartin, R.; Domínguez, E. *Tetrahedron* **2009**, *65*, 1500–1503; (b) Zhang, S.; Zhang, D.; Liebeskind, L. S. *J. Org. Chem.* **1997**, *62*, 2312–2313; (c) Liebeskind, L. S.; Yang, H.; Li, H. *Angew. Chem. Int. Ed.* **2009**, *48*, 1417–1421; *Angew. Chem.* **2009**, *121*, 1445–1449; (d) Yu, Y.; Srogl, J.; Liebeskind, L. S. *Org. Lett.* **2004**, *6*, 2631 –2634; (e) Yu, Y.; Liebeskind, L. S. *J. Org. Chem.* **2004**, *69*, 3554–3557.

10. (a) Migita, T.; Shimizu, T.; Asami, Y.; Shiobara, J.; Kato, Y.; Kosugi, M. *Bull. Chem. Soc. Jpn.* **1980**, *53*, 1385–1389; (b) Itoh, T.; Mase, T. *Org. Lett.* **2004**, *6,* 4587–4590; (c) Fernández-Rodríguez, M. A.; Shen, Q.; Hartwig, J. F. *J. Am. Chem. Soc.* **2006**, *128*, 2180–2181; (d) Mispelaere-Canivet, C.; Spindler, J.-F.; Perrio, S.; Beslin, P. *Tetrahedron* **2005**, *61*, 5253–5259.

11. Bichler, P.; Love, J. A. in C–X Bond Formation (Eds.: Vigalok, A.), Springer, Heidelberg (Germany), **2010**, pp. 39–64.

12. Alvaro, E.; Hartwig, J. F. *J. Am. Chem. Soc.* **2009**, *131*, 7858–7868.

13. Fernández-Rodríguez, M. A.; Shen, Q.; Hartwig, J. F. *Chem. Eur. J.* **2006**, *12*, 7782–7796.

14. Kosugi, M.; Shimizu, T.; Migita, T. *Chem. Lett.* **1978**, 13–14.

15. For a selection of catalyst systems that make use of bidendate phosphines in sulfination chemistry, see: (a) Gao, G.-Y.; Colvin, A. J.; Chen, Y.; Zhang, X. P. *J. Org. Chem.* **2004,** *69*, 8886–8892; (b) Murata, M.; Buchwald, S. L. *Tetrahedron* **2004**, *60*, 7397–7403; (c) Li, G. Y.; Zheng, G.; Noonan, A. F. *J. Org. Chem.* **2001**, *66*, 8677–8681; (d) Li, G. Y. *Angew. Chem. Int. Ed.* **2001**, *40*, 1513–1516; *Angew. Chem.* **2001**, *113*, 1561–1564; (e) Schopfer, U.; Schlapbach, A. *Tetrahedron* **2001**, *57*, 3069–3073; (f) Zheng, N.; McWilliams, J. C.; Fleitz, F. J.; Armstrong, J. D.; Volante, R. P. *J. Org. Chem.* **1998**, *63*, 9606–9607; (g) Ciattini, P. G.; Morera, E.; Ortar, G. *Tetrahedron Lett.* **1995**, *36*, 4133–4136.

16. For an example of a monodendate phosphine used in C–S coupling, see: Eichman, C. C.; Stambuli, J. P. *J. Org. Chem.* **2009**, *74*, 4005–4008.

17. Fernández-Rodríguez, M. A.; Hartwig, J. F. *J. Org. Chem.* **2009**, *74*, 1663–1672.

18. Kelly III, R. A.; Clavier, H.; Giudice, S.; Scott, N. M.; Stevens, E. D.; Bordner, J.; Samardjiev, I.; Hoff, C. D.; Cavallo, L.; Nolan, S. P. *Organometallics* **2008**, *27*, 202–210.

19. Fu, C.–F.; Liu, Liu, Y.–H.; Peng, S.–M.; Liu, S.–Z. *Tetrahedron* **2010**, *66*, 2119–2122.

20. Sayah, M.; Organ, M. G. *Chem. Eur. J.* **2011**, *17*, 11719–11722.

21. For Negishi reactions catalyzed by *Pd-PEPPSI* complexes, see: (a) Organ, M. G.; Avola, S.; Dubovyk, I.; Hadei, N.; Kantchev, E. A. B.; O'Brien, C. J.; Valente, C. *Chem. Eur. J.* **2006**, *12*, 4749-4755; (b) Achonduh, G. T.; Hadei, N.; Valente, C.;

Avola, S.; O'Brien, C. J.; Organ, M. G. *Chem. Commun.* **2010**, *46*, 4109-4111; (c) Çalimsiz, S.; Sayah, M.; Mallik, D.; Organ, M. G. *Angew. Chem.* **2010**, *122*, 2058-2061; *Angew. Chem., Int. Ed.* **2010**, *49*, 2014-2017; (d) Valente, C.; Belowich, M. E.; Hadei, N.; Organ, M. G. *Eur. J. Org. Chem*. **2010**, 4343; (e) Çalimsiz, S.; Organ, M. G. *Chem. Commun.* **2011**, *47*, 5181-5183; (f) Pompeo, M.; Hadei, N.; Froese, R. D. J.; Organ, M. G. *Angew. Chem.* **2012**, *124*, 11516-11519; *Angew. Chem. Int. Ed.* **2012**, *51*, 11354–11357.

22. For Suzuki-Miyaura reactions catalyzed by *Pd-PEPPSI* complexes, see: (a) O'Brien, C. J.; Kantchev, E. A. B.; Valente, C.; Hadei, N.; Chass, G. A.; Lough, A.; Hopkinson, A. C.; Organ, M. G. *Chem. Eur. J.* **2006**, *12*, 4743; (b) Organ, M. G.; Çalimsiz, S.; Sayah, M.; Hoi, K. H.; Lough, A. J. *Angew. Chem.* **2009**, *121*, 2419–2423 *Angew. Chem., Int. Ed.* **2009**, *48*, 2383-2387.

23. For Stille-Migita reactions catalyzed by *Pd-PEPPSI* complexes, see: Dowlut, M.; Mallik, D.; Organ, M. G. *Chem. Eur. J.* **2010**, *16*, 4279-4283.

24. (a) Hoi, K. H.; Çalimsiz, S.; Froese, R. D. J.; Hopkinson, A. C.; Organ, M. G. *Chem. Eur. J.* **2011**, *17*, 3086-3090; (b) Hoi, K. H.; Çalimsiz, S.; Froese, R. D. J.; Hopkinson, A. C.; Organ, M. G. *Chem. Eur. J.* **2012**, *18*, 145-151; (c) Pompeo, M.; Farmer, J. L; Froese, R. D. J.; Organ, M. G. *Angew. Chem.* **2014**, *126*, 3287-3290.

25. Sayah, M.; Lough, A. J.; Organ, M. G. *Chem. Eur. J.* **2013**, *19*, 2749–2756.

26. Sayah, M.; Organ, M. G. *Chem. Eur. J.* **2013**, *19*, 16196–16199.

27. For the complete mechansim of *PEPPSI* pre-catalyst activation in sulfination, see ref. 26.

28. Bastug, G.; Nolan S. P. *J. Org. Chem.* **2013**, *78*, 9303–9308.

29. For recent work on NHC–Pd complexes bearing *trans*-ligated secondary and tertiary amines, see: (a) Chen, M.-T.; Vicic, D. A.; Chain, W. J.; Turner, M. L.; Navarro, O. *Organometallics* **2011**, *30*, 6770–6773; (b) Guest, D.; Chen, M.-T.; Tizzard, G. J.; Coles, S. J.; Turner, M. L.; Navarro, O. *Eur. J. Inorg. Chem.* **2014**, 2200–2203; (c) Gallop, C. W. D.; Chen, M.-T.; Navarro, O. *Org. Lett.* **2014**, *16*, 3724 –3727.

30. Viciu, M. S.; Germaneau, R. F.; Navarro-Fernandez, O.; Stevens, E. D.; Nolan, S. P. *Organometallics* **2002**, *21,* 5470–5472.

31. Jensen, D. R.; Sigman, M. S. *Org. Lett.* **2003**, *5*, 63-65

32. For other examples of an intramolecular hydrogen bonding in a Pd complex, see: (a) Andrieu, J.; Camus, J.-M.; Dietz, J.; Richard, P.; Poli, R. *Inorg. Chem.* **2001**, *40*, 1597 – 1605; (b) ref. 26a.

33. Bondi, A. *J. Phys. Chem.* **1964**, *68*, 441–451.

34. For the crystal structure of **32d** and key structural information (e.g., bond distances), see Farmer, J. L.; Pompeo, M.; Lough, A. J.; Organ, M. G. *Chem. Eur. J.* **2014**, *20*, 15790-15798 (Supporting Information). CCDC-1017466 (**32d**) contains the supplementary crystallographic data for this paper. These data can be obtained free of charge from The Cambridge Crystallographic Data Centre via www.ccdc.cam.ac.uk/data_request/cif.

35. Dunsford, J. J.; Cavell, K. J.; Kariuki, B. M. *Organometallics* **2012**, *31*, 4118–

4121. The precent buried volume, %VBur steric parameter for *SIPr* and *SIPr*[6] Gold (I) complexes of the general formula [Au(*NHC*)Cl] found in this study were 47 and 50.8, respectively.

36. For applications and mechanistic analysis involving various [Pd(*NHC*)(allyl)Cl] complexes, see: (a) ref. 30.; and (b) Marion, N.; Navarro, O.; Mei, J.; Stevens, E. D.; Scott, N. M.; Nolan, S. P. *J. Am. Chem. Soc.* **2006**, *128*, 4101–4111.

37. Hartwig, J. F. *Inorg. Chem.* **2007**, *46*, 1936–1947.

38. (a) Zanella, R.; Ros, R.; Grazian, M. *Inorg. Chem.* **1973**, *12*, 2736–2738; (b) Louie, F.; Hartwig, J. F. *J. Am. Chem. Soc.* **1995**, *117*, 11598–11599.

39. Witt, D. *Synthesis* **2008**, *16*, 2491–2509.

40. Chekal, B. P.; Guinness, S. M.; Lillie, B. M.; McLaughlin, R. W.; Palmer, C. W.; Post, R. F.; Sieser, J. E.; Singer, R. A.; Sluggett, G. W.; Vaidyanathan, R.; Withbroe, G. J. *Org. Process Res. Dev.* **2014**, *18*, 266–274.

41. Kolychev, E. L.; Portnyagin, I. A.; Shuntikov, V. V.; Khrustalev, V. N.; Nechaev, M. S. *J. Organomet. Chem.* **2009**, *694*, 2454–2462.

42. Iglesias, M.; Beestra, D. J.; Knight, J. C.; Ooi, L.-L.; Stasch, A.; Coles, S.; Male, L.; Hursthouse, M. B.; Cavell, K. J.; Dervisi, A.; Fallis, I. A. *Organometallics*, **2008**, *27*, 3279–3289.

43. Still, W. C.; Kahn, M.; Mitra, A. *J. Org. Chem*, **1978**, *43*, 2923–2925.

44. Meiries, S.; Le Duc, G.; Chartoine, A.; Collado, A.; Speck, K.; Arachchige, K. S. A.; Slawin, A. M. Z.; Nolan, S. P. *Chem. Eur. J.* **2013**, *19*, 17358–17368.

45. Wang, Z.-Y.; Chen, G.-Q.; Shao, L.-X.; *J. Org. Chem.* **2012,** *77*, 6608–6614.

46. Nasieiski, J.; Hadei, N.; Achonduh, A.; Kantchev, E. A. B.; O'Brien, C. J.; Lough, A.; Organ, M. G. *Chem. Eur. J.* **2010**, *16*, 10844–10853.

47. Günay, M. E.; Özdemir, N.; Ulusoy, M.; Uçak, M.; Dinçer, M.; Çetinkaya, B. *J. Organomet. Chem.* **2009**, *694*, 2179–2184.

48. Mori, T.; Nishimura, T.; Yamamoto, T.; Doi, I.; Miyazaki, E.; Osaka, I.; Takimiya, K. *J. Am. Chem. Soc.* **2013**, *135*, 13900–13913.

49. Abd-El-Aziz, A. S.; Lee, C. C.; Prórko, A.; Sutherland, R. G. *J. Organomet. Chem.* **1988**, *348*, 95–107.

50. Grilli, S.; Lunazzi, L.; Mazzant, A. *J. Org. Chem.* **2001**, *66*, 4444–4446.